



Advances in Magnetics 2020-21, June 13-16, 2021

BOOK of ABSTRACTS

IEEE Advances in Magnetics 2020-21 - Programme

(rev 12 Jun)

Sunday, June 13

14.00 - 14.15	opening
14.15 - 14.30	tutorial 1 Moya (chair F. Albertini)
14.30 - 14.45	
14.45 - 15.00	
15.00 - 15.15	tutorial 2 Finocchio (chair M. Carpentieri)
15.15 - 15.30	
15.30 - 15.45	

Monday, June 14

8:45 - 9:00	Spintronics, multiferroics and voltage control of magnetism (A) (chair: C. Rinaldi)	Fontcuberta (I)	Materials for Energy (A) (chair: N. Dempsy)	Sepehri-Amin (I)	Non destructive tests (chair: A. Tamburrino)	Reboud (I)		
9:00 - 9:15								Capineri
9:15 - 9:30				Kaşpar			Suess (I)	Kyrgiazoglou
9:30 - 9:45				Haykal			Podmiljsak	Ducharme
9:45 - 10:00				Brambilla			Herper	Ciriani
10:00 - 10:15				Cosset-Cheneau				
10:15 - 10:30				Finco			break	break
10:30 - 10:45				break				
10:45 - 11:00				POSTERS			POSTERS	POSTERS
11:00 - 11:15				chair: D. Ortega			chair: C. de Julian	chair: M. Madami
11:15 - 11:30		BioMagnetism and Biomedical appl		Materials for Energy	Spin waves & Magnonics			
11:30 - 11:45				ENG-P01 : P30	SPW-P01 : P14			
11:45 - 12:00		BIO-P01 : P17			SKY-P01 : P09			
12:00 - 12:15								
12:15 - 12:30								
12:30 - 12:45		lunch						
12:45 - 13:00								
13:00 - 13:15								
13:15 - 13:30								
13:30 - 13:45		Plenary 1 - Jungwirth (chair: R. Bertacco)						
13:45 - 14:00								
14:00 - 14:15	BioMagnetism and Biomedical appl (A) (chair: O. Bottauscio)	Iglesias	Materials for Energy (B) (chair: P. Tiberto)	Palmero (I)	Skyrmions (A) (chair: N. Reyren)	Bernand-Mantel (I)		
14:15 - 14:30								Uzdin
14:30 - 14:45				Manzin			Quondam Antonio	Sassi
14:45 - 15:00				Ortega			Sangregorio	Fillion
15:00 - 15:15				Bonato			Maltoni	
15:15 - 15:30				Telling			Bhat	break
15:30 - 15:45		break		break				
15:45 - 16:00	Magnetic Levitation (A) (chair: A. Musolino / L. Sani)	Lomonova (I)	Materials for Energy (C) (chair: D. Suess)	de Julian Fernandez (I)	Recording & Sensors (A) (chair: G. Varvara)	Makarov (I)		
16:00 - 16:15								Laureti
16:15 - 16:30				Radman			Deledda	Baraduc
16:30 - 16:45				Rudnev			Tiberto (I)	Ortner
16:45 - 17:00				Tortella			Ala	Cantoni
17:00 - 17:15				Gruber			Dobák	Pereira
17:15 - 17:30		Gutierrez			Drózdź			
17:30 - 17:45					Maspero			
17:45 - 18:00								

- BIO • Biomagnetism and biomedical applications
- REC • Magnetic recording, magnetic memories and sensors
- ENG • Magnetic materials for energy applications
- SPW • Spin waves and magnonics
- SMU • Spintronics, multiferroics and voltage control of magnetism
- SOT • Spin-orbit torque
- SKY • Skyrmions

Tuesday, June 15

8:45 - 9:00	Spin Orbit Torque (A) (chair: J.M. George)	Krishnia (I)	Magnetic Levitation (B) (chair: L. Sani / A. Musolino)	Mazaauric			
9:00 - 9:15				D'Ovidio			
9:15 - 9:30				Godinho	Geçer		
9:30 - 9:45				Tacchi	Wang		
9:45 - 10:00				Pizzini (I)	Sundukov		
10:00 - 10:15					break		
10:15 - 10:30				break	break		
10:30 - 10:45							
10:45 - 11:00				POSTERS		POSTERS	
11:00 - 11:15				chairs: S. Laureti - A. Tamburrino		chair: M. Coisson	
11:15 - 11:30		Spin Orbit Torque	SOT-P01 : P05	Adv. Meas & FORC & Artificial Intelligence O.			
11:30 - 11:45		Recording & Sensors	REC-P01 : P08	AMT-P01 : P08			
11:45 - 12:00		Levitation	LEV-P01 : P17	FRC-P01 : P04			
12:00 - 12:15		N.D.T.	NDT-P01 : P03	AIO-P01 : P05			
12:15 - 12:30							
12:30 - 12:45		lunch					
12:45 - 13:00							
13:00 - 13:15							
13:15 - 13:30	Spin Orbit Torque (B) (chair: G. Finocchio)	Haney (I)	Spinwaves & Magnonics (A) (chair: G. Gubbiotti)	Kim (I)	FORC (chair: A. Stancu)	Ruta (I)	
13:30 - 13:45						Demokritov (I)	Gross (I)
13:45 - 14:00				Tomasello (I)		van Dijken	Brückl
14:00 - 14:15				Basso (I)		Petti	Stoleriu
14:15 - 14:30				Malagò		Filimonov	Breth
14:30 - 14:45				Della Ventura		break	Visscher
14:45 - 15:00		break		break			
15:00 - 15:15							
15:15 - 15:30		Plenary 2 - Datta (chair: G. Finocchio)					
15:30 - 15:45							
15:45 - 16:00							
16:00 - 16:15	Macroscale model & Devices (B) (chair: C. Visone)	Flatau (I)	Skyrmions (B) (chair: R. Tomasello)	Hug (I)	BioMagnetism & Biomedical appl (B) (chair: P. Ravazzani)	Cardoso de Freitas (I)	
16:15 - 16:30						Bessarab	Beklemisheva
16:30 - 16:45				Koprivica		Kechrakos	Leliaert (I)
16:45 - 17:00				Slimani			Baumgarten
17:00 - 17:15				Faba			
17:15 - 17:30							
17:30 - 17:45							
17:45 - 18:00							

- MIC • Mathematical modeling and micromagnetics
- DEV • Macroscale modeling of magnetic and multif. materials and devices
- FRC • FORC-based identification techniques
- AMT • Advanced measurement techniques
- NDT • Electromagnetic non-destructive testing
- LEV • Magnetic levitation and bearings, el. machines and other e.m. devices
- AIO • Artificial intelligence, optimization and inverse problems

Wednesday, June 16

8:45 - 9:00	Spintronics, multiferroics and voltage control of magnetism (B) (chair: J. Fontcuberta)	Akerman (I)	Recording & Sensors (B) (chair: F. Casoli)	Garello (I)	Advanced Measurements (chair: E. Hristofolou)	Finco		
9:00 - 9:15							Bachar	
9:15 - 9:30				Miyahara			Sepehri-Amin	Passeri (I)
9:30 - 9:45				Yusupov			Meo	Wiekhorst
9:45 - 10:00				Attané			Carva	Sannidhi
10:00 - 10:15				Shan			Avilés-Félix	break
10:15 - 10:30				Zahedinejad			break	break
10:30 - 10:45				break				
10:45 - 11:00				POSTERS				
11:00 - 11:15				chair: R. Bertacco			Ktena (I)	
11:15 - 11:30		Spintronics, multiferroics ...	SMU-P01 : P18		Harmon (I)			
11:30 - 11:45		MathMod & Micro	MIC-P01 : P09		Kowalik			
11:45 - 12:00		MacroMod & Dev	DEV-P01 : P09					
12:00 - 12:15								
12:15 - 12:30								
12:30 - 12:45		lunch						
12:45 - 13:00								
13:00 - 13:15								
13:15 - 13:30		Awards & closing ceremony						
13:30 - 13:45								
13:45 - 14:00	Spinwaves & Magnonics (B) (chair: S. Tacchi)	Schmidt (I)	Mathmodeling & Micromagnetics (A) (chair: m. d'Aquino)	Schrefl (I)	Materials for Energy (D) (chair: M. Solzi)	Buchelnikov		
14:00 - 14:15							Tahkhsa	
14:15 - 14:30				Madami (I)			Berkov	Coisson
14:30 - 14:45				Bunkov			Behbahani	Hong
14:45 - 15:00				Gerevenkov			Ferrero	break
15:00 - 15:15				Fulara			Kulesh	
15:15 - 15:30		break		Legut				
15:30 - 15:45				break				
15:45 - 16:00								
16:00 - 16:15	Spintronics, multiferroics ... (C) (chair: G. Schmidt)	Rinaldi	Mathmodel & Micromag (B) (chair: V. Puliafito)	Muratov (I)	Materials for Energy (E) (chair: S. Fabbri)	Kitanovski (I)		
16:15 - 16:30							Fontana	
16:30 - 16:45				Kozioł-Rachwał			Berkov	Aliev
16:45 - 17:00				Harknett			Vantaraki	Chicco
17:00 - 17:15				Fagiani			Sanchez-Tejerina	Dall'Olio
17:15 - 17:30				Ślęzak				
17:30 - 17:45								
17:45 - 18:00								

Monday, June 14

8:45 - 9:00	Spintronics, multiferroics and voltage control of magnetism (A) (chair: C. Rinaldi)	Fontcuberta (I)	Materials for Energy (A) (chair: N. Dempsey)	Sepehri-Amin (I)	Non destructive tests (chair: A. Tamburrino)	Reboud (I)		
9:00 - 9:15								Capineri
9:15 - 9:30		Kašpar				Suess (I)		Kyrgiazoglou
9:30 - 9:45		Haykal				Podmiljsak		Ducharne
9:45 - 10:00		Brambilla				Herper		Ciriani
10:00 - 10:15		Cosset-Cheneau						
10:15 - 10:30		Finco		break		break		
10:30 - 10:45		break						
10:45 - 11:00		POSTERS		POSTERS		POSTERS		
11:00 - 11:15		chair: D. Ortega		chair: C. de Julian		chair: M. Madami		
11:15 - 11:30		BioMagnetism and Biomedical appl		Materials for Energy		Spin waves & Magnonics		
11:30 - 11:45				ENG-P01 : P30		SPW-P01 : P14		
11:45 - 12:00		BIO-P01 : P17				Skyrmions		
12:00 - 12:15						SKY-P01 : P09		
12:15 - 12:30								
12:30 - 12:45		lunch						
12:45 - 13:00								
13:00 - 13:15								
13:15 - 13:30								
13:30 - 13:45		Plenary 1 - Jungwirth (chair: R. Bertacco)						
13:45 - 14:00								
14:00 - 14:15	BioMagnetism and Biomedical appl (A) (chair: O. Bottauscio)	Iglesias	Materials for Energy (B) (chair: P. Tiberto)	Palmero (I)	Skyrmions (A) (chair: N. Reyren)	Bernand-Mantel (I)		
14:15 - 14:30		Marquina				Quondam Antonio		Uzdin
14:30 - 14:45		Manzin				Sangregorio		Sassi
14:45 - 15:00		Ortega				Maltoni		Fillion
15:00 - 15:15		Bonato				Bhat		
15:15 - 15:30		Telling						break
15:30 - 15:45		break		break				
15:45 - 16:00	Magnetic Levitation (A) (chair: A. Musolino / L. Sani)	Lomonova (I)	Materials for Energy (C) (chair: D. Suess)	de Julian Fernandez (I)	Recording & Sensors (A) (chair: G. Varvaro)	Makarov (I)		
16:00 - 16:15								Laureti
16:15 - 16:30		Radman				Deledda		Baraduc
16:30 - 16:45		Rudnev				Tiberto (I)		Ortner
16:45 - 17:00		Tortella						Cantoni
17:00 - 17:15		Gruber				Ala		Pereira
17:15 - 17:30		Gutierrez				Dobák		Drózdź
17:30 - 17:45						Maspero		
17:45 - 18:00								

Tuesday, June 15

8:45 - 9:00	Spin Orbit Torque (A) <i>(chair: J.M. George)</i>	Krishnia (I)	Magnetic Levitation (B) <i>(chair: L. Sani / A. Musolino)</i>	Mazauric		
9:00 - 9:15				D'Ovidio		
9:15 - 9:30		Godinho		Geçer		
9:30 - 9:45		Tacchi		Wang		
9:45 - 10:00		Pizzini (I)		Sundukov		
10:00 - 10:15						
10:15 - 10:30		break		break		
10:30 - 10:45						
10:45 - 11:00		POSTERS			POSTERS	
11:00 - 11:15		<i>chairs: S. Laureti - A. Tamburrino</i>			<i>chair: M. Coisson</i>	
11:15 - 11:30		Spin Orbit Torque	SOT-P01 : P05		Adv. Meas & FORC & Artificial Intelligence O.	
11:30 - 11:45		Recording & Sensors	REC-P01 : P08		AMT-P01 : P08	
11:45 - 12:00					FRC-P01 : P04	
12:00 - 12:15		Levitation	LEV-P01 : P17		AIO-P01 : P05	
12:15 - 12:30		N.D.T.	NDT-P01 : P03			
12:30 - 12:45		lunch				
12:45 - 13:00		lunch				
13:00 - 13:15		lunch				
13:15 - 13:30	Spin Orbit Torque (B) <i>(chair: G. Finocchio)</i>	Haney (I)	Spinwaves & Magnonics (A) <i>(chair: G. Gubbiotti)</i>	Kim (I)	FORC <i>(chair: A. Stancu)</i>	Ruta (I)
13:30 - 13:45						Demokritov (I)
13:45 - 14:00	Tomasello (I)			van Dijken		Brückl
14:00 - 14:15	Macro model & Devices (A) <i>(chair: S. Quondam)</i>	Basso (I)		Petti		Stoleriu
14:15 - 14:30		Malagò		Filimonov		Breth
14:30 - 14:45		Della Ventura		break	Visscher	
14:45 - 15:00						
15:00 - 15:15		break		break		
15:15 - 15:30		Plenary 2 - Datta <i>(chair: G. Finocchio)</i>				
15:30 - 15:45		Plenary 2 - Datta <i>(chair: G. Finocchio)</i>				
15:45 - 16:00		Plenary 2 - Datta <i>(chair: G. Finocchio)</i>				
16:00 - 16:15		Plenary 2 - Datta <i>(chair: G. Finocchio)</i>				
16:15 - 16:30	Macroscale model & Devices (B) <i>(chair: C. Visone)</i>	Flatau (I)	Skyrmions (B) <i>(chair: R. Tomasello)</i>	Hug (I)	BioMagnetism & Biomedical appl (B) <i>(chair: P. Ravazzani)</i>	Cardoso de Freitas (I)
16:30 - 16:45		Koprivica		Bessarab		Beklemisheva
16:45 - 17:00		Slimani		Kechrakos		Leliaert (I)
17:00 - 17:15		Faba				Baumgarten
17:15 - 17:30						
17:30 - 17:45						
17:45 - 18:00						

Wednesday, June 16

8:45 - 9:00	Spintronics, multiferroics and voltage control of magnetism (B) (chair: J. Fontcuberta)	Akerman (I)	Recording & Sensors (B) (chair: F. Casoli)	Garello (I)	Advanced Measurements (chair: E. Hristofolou)	Finco		
9:00 - 9:15							Bachar	
9:15 - 9:30		Miyahara				Sepehri-Amin		Passeri (I)
9:30 - 9:45		Yusupov				Meo		Wiekhorst
9:45 - 10:00		Attané				Carva		Sannidhi
10:00 - 10:15		Shan				Avilés-Félix		break
10:15 - 10:30		Zahedinejad		break		break		
10:30 - 10:45	break				Advanced Meas. & Artificial Intel (chairs: M. Coisson - G. Lozito)	Ktena (I)		
10:45 - 11:00	POSTERS							
11:00 - 11:15	<i>chair: R. Bertacco</i>							
11:15 - 11:30	Spintronics, multiferroics ...		SMU-P01 : P18				Harmon (I)	
11:30 - 11:45							Kowalik	
11:45 - 12:00	MathMod & Micro		MIC-P01 : P09					
12:00 - 12:15	MacroMod & Dev		DEV-P01 : P09					
12:15 - 12:30								
12:30 - 12:45	lunch							
12:45 - 13:00								
13:00 - 13:15								
13:15 - 13:30	Awards & closing ceremony							
13:30 - 13:45								
13:45 - 14:00	Spinwaves & Magnonics (B) (chair: S. Tacchi)	Schmidt (I)	Mathmodeling & Micromagnetics (A) (chair: m. d'Aquino)	Schrefl (I)	Materials for Energy (D) (chair: M. Solzi)	Buchelnikov		
14:00 - 14:15							Tahkhsa	
14:15 - 14:30		Madami (I)				Berkov		Coisson
14:30 - 14:45						Behbahani		Hong
14:45 - 15:00		Bunkov				Ferrero		break
15:00 - 15:15		Gerevenkov				Kulesh		
15:15 - 15:30	Fulara		Legut			Kitanovski (I)		
15:30 - 15:45	break					Fontana		
15:45 - 16:00					Materials for Energy (E) (chair: S. Fabbri)	Aliev		
16:00 - 16:15	Rinaldi	Mathmodel & Micromag (B) (chair: V. Puliafito)	Muratov (I)			Chicco		
16:15 - 16:30	Kozioł-Rachwał			Berkov			Dall'Olio	
16:30 - 16:45	Harknett			Vantaraki				
16:45 - 17:00	Fagiani			Sanchez-Tejerina				
17:00 - 17:15	Ślęzak							
17:15 - 17:30								
17:30 - 17:45								
17:45 - 18:00								

Session: **Biomagnetism and biomedical applications**

Sub-session A **Monday, June 14 -- 14.00-15.30** **Virtual room 1**

ID code	Presenting	Authors	Title	Type
BIO-A01	Oscar Iglesias	Oscar Iglesias	Aggregates and dipolar interactions in nanoparticle assemblies for hyperthermia	Oral
BIO-A02	Clara Marquina	Teobaldo E. Torres, Enio Lima Jr., M. Pilar Calatayud, Beatriz Sanz, Alfonso Ibarra, Rodrigo Fernández-Pacheco, Álvaro. Mayoral, Clara Marquina, M. Ricardo Ibarra and Gerardo F. Goya	Relevance of Brownian relaxation as power absorption mechanism in magnetic hyperthermia	Oral
BIO-A03	Alessandra Manzin	A. Manzin, R. Ferrero, G. Barrera, F. Celegato, M. Coisson, P. Tiberto	Design and in silico modelling of magnetic nanodisks for hyperthermia applications	Oral
BIO-A04	Daniel Ortega	Irene Rubia-Rodríguez, Luca Zilberti, Alessandro Arduino, Oriano Bottauscio, Mario Chiampì, Daniel Ortega	Evaluation of passive implants as an exclusion criterion in magnetic hyperthermia	Oral
BIO-A05	Marta Bonato	Marta Bonato, Emma Chiaramello, Serena Fiocchi, Gabriella Tognola, Paolo Ravazzani, Marta Parazzini	Use of stochastic approaches in 5G scenario for EMF exposure assessment	Oral
BIO-A06	Neil D. Telling	Maneea E. Sharifabad, Rémy Soucaille, Robert J. Hicken, and Neil D. Telling	A magneto-optical microscope for investigating magnetisation dynamics of nanoparticles under hyperthermia conditions	Oral

Sub-session B **Tuesday, June 15 -- 16.15 - 17.45** **Virtual room 3**

BIO-I-B1	S. Cardoso de Freitas	S. Cardoso de Freitas, P. Ribeiro, M. Neto, M. Silva, P. Ribeiro, R. Ferreira, P.P. Freitas	Strategies for biometric parameters readout using magnetic fields	Invited
BIO-B01	A. V. Beklemisheva	A. V. Beklemisheva, A. A. Gurevich, L. V. Panin	Magnetophoresis, sedimentation, and diffusion of dia- and paramagnetic particles in gradient magnetic field from ferromagnetic microwire systems	Oral
BIO-I-B2	J. Leliaert	J. Leliaert, A. Coene, M. Liebl, D. Eberbeck, U. Steinhoff, F. Wiekhorst	When noise becomes data: characterizing magnetic nanoparticles using thermal noise magnetometry	Invited
BIO-B02	Daniel Baumgarten	Veronica Gonella, Daniel Baumgarten	Investigation of influences on vessel constriction in magnetic drug targeting using a numerical model of a branched vessel	Oral

Session: **Magnetic recording, magnetic memories and sensors**

Sub-session A **Monday, June 14 -- 15.45-18.00**

ID code	Presenting	Authors	Title	Type
REC-I-A1	D. Makarov	D. Makarov	Advances in compliant magnetic field sensorics	Invited
REC-A01	Sara Laureti	S. Laureti, G. Varvaro, M. Hassan, C. Rinaldi, S. Varotto, G. Barucca, O. Lik, N. Schmidt and M. Albrecht	SAF-based perpendicular magnetized GMR spin-valves on flexible substrates	Oral
REC-A02	Claire Baraduc	S. Dounia, S. Teresi, J. Alvarez-Hérault, L. Lombard, J.R. Childress, I.L. Prejbeanu, C. Baraduc	Control of Chirality and hysteresis in asymmetric vortex-based TMR sensors	Oral
REC-A03	Michael Ortner	Michael Ortner, Perla Malagó	Application of the magnetostatic method of moments for computationally efficient magnet system design	Oral
REC-A04	Matteo Cantoni	M. Cantoni, L. Nessi, C. Rinaldi, R. Bertacco	Magnetic characterization of free-standing membranes for spin polarimetry	Oral
REC-A05	M. J. Pereira	M. J. Pereira, J. S. Amaral, N. J. O. Silva, V. S. Amaral, F. Albertini, F. Casoli	Transformation temperature mapping and distribution of locally induced phase transformations in Ni-Mn-Ga thin films	Oral
REC-A06	P. Drózd	P. Drózd, M. Ślęzak, W. Janus, M. Szpytma, H. Nayyef, A. Kozioł-Rachwał, K. Freindl, D. Wilgocka Ślęzak, J. Korecki, T. Ślęzak	Driving the polar spin reorientation transition of ultrathin ferromagnets with antiferromagnetic-ferromagnetic phase transition of nearby FeRh alloy film	oral
REC-A07	Simone Cucurullo	Federico Maspero, Simone Cucurullo, Riccardo Bertacco	Frequency-modulated MEMS magnetometer using magnetic flux concentrators and permanent magnets	oral

Sub-session B **Wednesday, June 16 -- 08.45-10.15**

REC-I-B1	Kevin Garello	K. Garello, B. Dieny, R.C. Sousa, G. Prenat, I.L. Prejbeanu	MRAM adoption in microelectronics: status and perspectives	Invited
REC-B01	H. Sepehri-Amin	H. Sepehri-Amin, W. Zhou, Y. Sakuraba, C. Abert, D. Suess, K. Hono	Realizing oscillation of all-in-plane spin-torque-oscillator for microwave assisted magnetic recording	Oral
REC-B02	Andrea Meo	Andrea Meo, Roy. W. Chantrell, Phanwadee Chureemart, Jessada Chureemart	Effect of intermixing on HAMR dynamics in exchange spring media	Oral
REC-B04	K. Carva	K. Carva, K. Uhlířová, P. Baláž, I. Turek, F. Mácá, J. Kudrnovský, V. Drchal	Phase stability and finite temperature magnetism of novel antiferromagnet CuMnAs	Oral
REC-B05	L. Avilés-Félix	L. Avilés-Félix, A. Olivier, G. Li, C. Davies, L. Álvaro-Gómez, M. Rubio-Roy, S. Auffret, A. Kirilyuk, Th. Rasing, L. Buda-Prejbeanu, R. Sousa, B. Dieny and I. L. Prejbeanu	All-optical switching in FeCoB/Ta/(Tb/Co)N electrodes for the development of ultrafast magnetic tunnel junctions	Oral

Session: **Magnetic materials for energy applications**

Sub-session A **Monday, June 14 -- 08.45-10.15**

ID code	Presenting	Authors	Title	Type
ENG-I-A1	H. Sepehri-Amin	H. Sepehri-Amin, I. Dirba, Xin Tang, A. K. Srinithi, T. Ohkubo, K. Hono	Development of high coercivity SmFe12-based permanent magnets	Invited
ENG-I-A2	D. Suess	Dieter Suess	3D printing of isotropic and anisotropic hard magnets	Invited
ENG-A01	Benjamin Podmiljsak	Benjamin Podmiljsak, Spomenka Kobe, Carlo Burkhardt, Antje Lehmann	Is a circular economy ecosystem for NdFeB-type magnets feasible	Oral
ENG-A03	Heike C. Herper	Heike C. Herper, Olle Eriksson	Predicting new rare earth lean permanent magnets by computational design -- the challenge of the 4f electrons	Oral

Sub-session B **Monday, June 14 -- 14.00-15.30**

ENG-I-B1	Ester Palmero	Ester M. Palmero, Daniel Casaleiz, Javier de Vicente, Alberto Bollero	Developing alternative permanent magnets: from the synthesis of tuned composites to additive manufacturing	Invited
ENG-B01	Simone Quondam Antonio	Simone Quondam Antonio, Francesco Riganti Fulginei, Antonino Laudani, Antonio Faba, Andrea Di Schino, Ermanno Cardelli	Hysteresis modelling for 3D printed FeSi magnetic cores	Oral
ENG-B02	Claudio Sangregorio	Beatrice Muzzi, Alberto López-Ortega, Martín Albino, Michele Petrecca, Claudia Innocenti, Giovanni Bertoni, César de Julián Fernández, Claudio Sangregorio	Exchange coupled magnetic nanoheterostructures with enhanced energy product	Oral
ENG-B03	Pierfrancesco Maltoni	Pierfrancesco Maltoni, Tapati Sarkar, Gaspare Varvaro, Gianni Barucca, Davide Peddis, Roland Mathieu	Controlling magnetic coupling in hard-soft oxide nanocomposites	Oral
ENG-B04	Farooq H. Bhat	Farooq H. Bhat, Ghazala Anjum	Structural and electronic properties of cobalt doped NdMnO3	Oral

Sub-session C **Monday, June 14 -- 15.45-17.30**

ENG-I-C1	Cesar de Julian Fernandez	César de Julián Fernández, Durgamadhhab Mishra, Michele Petrecca, M. Albino, Anna Zink Eikeland, Marian Stingaciu, Riccardo Cabassi, J. Guzmán-Mínguez, Fulvio Bolzoni, Franca Albertini, Beatrice Muzzi, Blac Belec, Adrian Quesada, T. Schliesch, Mogens Christensen, Petra Jenus, Stefano Deledda, Claudio Sangregorio	hexaferrite nanoparticles for new magnets	Invited
ENG-C01	Stefano Deledda	Durgamadhhab Mishra, Marian Stingaciu, Riccardo Cabassi, Fulvio Bolzoni, Franca Albertini, Claudio Sangregorio, Michele Petrecca, Mogens Christensen, Anna Zink Eikeland, Stefano Deledda, César de Julián Fernández	Investigation of high coercivity in Al and Cr substituted strontium hexaferrites (SrFe12O19) by x-ray, neutron diffraction and magnetic measurements	Oral
ENG-I-C2	Paola Tiberto	Paola Tiberto	Magnetic ferrites: a tunable system for innovative applications	Invited
ENG-C02	G. Ala	G. Ala, G. Giglia, A. Imburgia, R. Miceli, P. Romano, F. Viola, S. Quondam Antonio, H. P. Rimal	EMI soft ferrite filters design for power conversion systems applications	Oral
ENG-C03	S. Dobák	S. Dobák, C. Ragusa, C. Beatrice, F. Fiorillo	Magnetic losses in amorphous and nanocrystalline alloys up to 1 GHz: an analytical approach	Oral

Session: **Spintronics, multiferroics and voltage control of magnetism**

Sub-session A Monday, June 14 -- 08.45-10.30

ID code	Presenting	Authors	Title	Type
SMU-I01	J. Fontcuberta	H. B. Vasili, D. Pesquera, M. Valvidares, P. Gargiani, E. Pellegrin, F. Bondino, E. Magnano, A. Barla, J. Fontcuberta	In-operando adjustable orbital polarization in nickelate perovskites	Invited
SMU-A01	Zdeněk Kašpar	Zdeněk Kašpar, Miloslav Surýnek, Jan Zubáč, Filip Křížek, Vít Novák, Tomáš Jungwirth and Kamil Olejník	High resistive unipolar switching in thin film antiferromagnet CuMnAs	Oral
SMU-A02	Angela Haykal	Angela Haykal, Johanna Fischer, Waseem Akhtar, Aurore Finco, Jean-Yves Chaudreau, Daniel Sando, Cécile Carrétéro, Nicolas Jaouen, Manuel Bibes, Michel Viret, Stephane Fusil, Vincent Garcia, Vincent Jacques	A journey into the antiferromagnetic spin textures of BiFeO ₃	Oral
SMU-A03	A. Brambilla	A. Brambilla, A. Lodesani, A. Picone, A. Calloni, M. S. Jagadeesh, G. Bussetti, G. Vinai, G. Panaccione, L. Duò, M. Finazzi, F. Ciccacci	Magnetic properties of self-assembled Co and Ni porphyrins in Fe-based spinterfaces	Oral
SMU-A04	M. Cosset-Cheneau	M. Cosset-Cheneau, L. Vila, G. Zahnd, D. Gusakova, A. Marty, and J.-P. Attané	Measurement of the spin relaxation anisotropy in 3d ferromagnets	Oral
SMU-A05	A. Finco	S. Chouaieb, A. Finco, F. Fabre, W. Akhtar, A. Haykal, A. Hrabec, A. Thiaville, S. Rohart, M. Belmeguenai, M. S. Gabor, G. Rana, L. Prejbeanu, O. Boule and V. Jacques	All-optical imaging of magnetic skyrmions with a scanning-NV magnetometer	Oral

Sub-session B Wednesday, June 16 -- 08.45-10.30

SMU-I-B1	J. Akerman	Johan Akerman, Mohammad Zahedinejad, Ahmad A. Awad, Shreyas Muralidhar, Roman Khymyn, Himanshu Fulara, Hamid Mazraati, Mykola Dvornik	Voltage controlled mutual synchronization in spin Hall nano-oscillator arrays	Invited
SMU-B01	Shin Miyahara	Shin Miyahara	Anomalous electroactive magnetic excitations in frustrated magnets	Oral
SMU-B02	Roman Yusupov	Roman Yusupov, Igor Yanilkin, Amir Gumarov, Andrey Petrov, Airat Kiliamov, Alexander Rodionov, Sergey Nikitin, Lenar Tagirov	Synthesis, magnetic properties and inhomogeneities in Pd _{1-x} Fe _x alloy ultrathin epitaxial films	Oral
SMU-B03	J. P. Attané	P. Noel, C. Thomas, F. Trier, D. C. Vaz, Y. Fu, A. Johansson, B. Haas, P-H. Jouneau, S. Gambarelli, B. Göbel, F. Bruno, G. Singh, S. McKeown-Walker, L. M. Vicente-Arche, J. Bréhin, S. Fusil, V. Garcia, A. Sander, S. Valencia, P. Bruneel, M. Vivek, M. Gabay, N. Bergeal, F. Baumberger, H. Okuno, A. Fert, A. Barthélémy, I. Mertig, T. Meunier, P. Ballet, L. Vila, M. Bibes, and J. P. Attané	Spin to charge conversion in the topological insulator HgTe and in STO-based two-dimensional electron gas	Oral
SMU-B04	Guangcun Shan	Guangcun Shan, Xin Li	A comparative study of GMI effect calculation for magnetic thin film via theoretical deduction and machine learning	Oral
SMU-B05	Mohammad Zahedinejad	Mohammad Zahedinejad, H. Fulara, S. Fukami, S. Kanaib, H. Ohno, J. Åkerman	Memristors make unruly spin Hall nano-oscillators synchronize and remember.	Oral

Sub-session C Wednesday, June 16 -- 16.00-17.15

SMU-C01	C. Rinaldi	S. Varotto, L. Nesi, F. Fagiani, S. Cecchi, P. Noël, S. Petrò, A. Novati, R. Calarco, M. Cantoni, J.-P. Attané, L. Vila, M. Bibes, J. Slawinska, M. B. Nardelli, S. Picozzi, R. Bertacco, C. Rinaldi	Ferroelectric control of spin-to-charge conversion in GeTe	Oral
SMU-C02	A. Koziol-Rachwał	A. Koziol-Rachwał, J. Korecki, M. Szpytma, M. Ślęzak, P. Drózd, W. Janus, H. Nayyef, M. Zając, T. Ślęzak	Beating the ordering temperature limit of FeO with antiferromagnetic proximity in FeO/CoO	Oral
SMU-C03	J. Harknett	J. Harknett, C.D.W. Cox, M.T. Greenaway, K. Morrison	The anomalous Nernst effect in Co ₂ MnSi thin film	Oral
SMU-C04	F. Fagiani	L. Nesi, F. Fagiani, A. Novati, Matteo Cantoni, Stefano Cecchi, Giovanni Vinai, Debashis Mondal, Raffaella Calarco, Silvia Picozzi, Riccardo Bertacco, Christian Rinaldi	Coexistence of topological and Rashba states in ferroelectric SnTe	Oral
SMU-C05	M. Ślęzak	M. Ślęzak, H. Nayyef, P. Drózd, W. Janus, A. Koziol-Rachwał, M. Szpytma, M. Zając, T. O. Menteş, F. Genuzio, A. Locatelli, T. Ślęzak	Field-free switching between orthogonal spin states in antiferromagnetic NiO(111) on Fe(110)	Oral

Session: **Spin-orbit torque**

Sub-session A Tuesday, June 15 -- 08.45-10.15

ID code	Presenting	Authors	Title	Type
---------	------------	---------	-------	------

SOT-I-A1	S. Krishnia	S. Krishnia, F. Ajejas, Y. Sassi, S. Collin, A. Fert, J. M. George, N. Reyren, V. Cros, H. Jaffrès	Determination of Spin-Orbit Torques in Pt / Co / Al / (Pt Ta) Skyrmion Magnetic Multilayers	Invited
SOT-A02	J. Godinho	T. Janda, J. Godinho, E. Pfiltzner, G. Ulrich, S. Reimers, Z. Šobáň, H. Reichlová, V. Novák, R. P. Campion, P. Wadley, K. W. Edmonds, S. S. Dhesi, F. Maccherozzi, R. M. Otxoa, P. E. Roy, K. Olejník, P. Němec, T. Jungwirth, B. Kaestner, J. Wunderlich	Scanning magneto-thermoelectric imaging of spin-orbit torque switching in antiferromagnetic films	Oral
SOT-A03	Silvia Tacchi	Silvia Tacchi, Weiman Lin, Baisiun Yang, Andy Paul Chen, Xiaohan Wu, Rui Guo, Shaohai Chen, Qidong Xie, Xinyu Shu, Liang Liu, Yajuan Wu, Guo Meng	Effect of the oxide termination on both the Dzyaloshinskii-Moriya interaction and the perpendicular magnetic anisotropy in BTO/CoFeB/Pt	Oral
SOT-I-A2	Stefania Pizzini	T. Gushi, M. Klug, S. Ghosh, J. Peña Garcia, J. Vogel, J.P. Attané, T. Suemasu, L. Vila and S. Pizzini	Very large domain wall velocities in Mn4N ferrimagnetic thin films	Invited

Sub-session B Tuesday, June 15 -- 13.15-14.15

SOT-I-B1	Paul Haney	Paul Haney, Fei Xue, Vivek Amin, Mark Stiles	Staggered spintronics	Invited
SOT-I-B2	Riccardo Tomasello	Riccardo Tomasello, Akshaykumar Salimath, Fengjun Zhuo, Giovanni Finocchio, Aurelien Manchon	Role of current driven torques on skyrmion motion in Antiferromagnets	Invited

Session: **Skyrmions**

Sub-session A Monday, June 14 -- 14.00-15.15

ID code	Presenting	Authors	Title	Type
SKY-I-A1	A. Bernard-Mantel	Anne Bernard-Mantel, Cyril B. Muratov, Thilo M. Simon	Theory of Néel-Bloch transition for compact magnetic skyrmions	Invited
SKY-A02	V.M. Uzdin	M.N. Potkina, I.S. Lobanov, H. Jónsson, V.M. Uzdin	Lifetime of skyrmions in the limit of infinitesimal lattice constant	Oral
SKY-A03	Yanis Sassi	Yanis Sassi, Sachin Krishnia, William Legrand, Fernando Ajejas, Sophie Collin, Karim Bouzehouane, Aymeric Vechiola, Nicolas Reyren, Vincent Cros, Albert Fert	Current induced motion of magnetic skyrmion in double injection (Pt/Co/Al/Ta)N system	Oral
SKY-A04	Charles-Elie Fillion	Charles-Elie Fillion, Raj Kumar, Aymen Fassatoui, Stefania Pizzini, Laurent Ranno, Stéphane Auffret, Isabelle Joumard, Olivier Boulle, Gilles Gaudin, Liliana Buda-Prejbeanu, Claire Baraduc, Héléne Béa	Voltage-Controlled Skyrmion Chirality Switch	Oral

Sub-session B Tuesday, June 15 -- 16.15-17.15

SKY-I-B1	Hans J. Hug	Hans J. Hug, A.-O. Mandru, O. Yildirim, M. A. Marionia	Current limits of high-resolution and quantitative magnetic force	Invited
SKY-B01	Pavel F. Bessarab	Anastasiia S. Varentcova, Stephan von Malottki, Maria N. Potkina, Grzegorz Kwiatkowski, Stefan Heinze, Pavel F. Bessarab	Toward room-temperature nanoscale skyrmions in ultrathin films	Oral
SKY-B02	Dimitris Kechrakos	Dimitris Kechrakos, Leda Tzannetou	Magnetic skyrmions on cylindrical nanotubes: Formation, stability and electrical detection	Oral

Session: **Mathematical modeling and micromagnetics**

Sub-session A Wednesday, June 16 -- 13.45-15.30

ID code	Presenting	Authors	Title	Type
MIC-I-A1	T. Schrefl	Thomas Schrefl, Alexander Kovacs, Harald Oezert, Markus Gusenbauer, Thomas G. Woodcock, Panpan Zhao	Deep learning magnetization dynamics	Invited
MIC-A01	Dmitry Berkov	Elena Semenova, Dmitry Berkov and Natalia Gorn	Comparison of various simulation methods for determination of the switching rate of magnetic nanoelements	Oral
MIC-A02	Razyeh Behbahani	Razyeh Behbahani, Martin L. Plumer, Ivan Saika-Voivod	Coarse-graining in micromagnetic simulations of dynamic hysteresis loops	Oral
MIC-A03	Riccardo Ferrero	Riccardo Ferrero, Alessandra Manzin	Cayley transform based time integration applied to a 3D micromagnetic solver	Oral
MIC-A04	Nikita A. Kulesh	Nikita A. Kulesh, Mikhail E. Moskalev, Alexander N. Gorkovenko, Ilya A. Pushkarev, Vladimir V. Vas'kovskiy, Vladimir V. Lepalovskij	Micromagnetic approach to analysis of temperature-dependent exchange bias properties of polycrystalline films	Oral

AMT-A01	Aurore Finco	Aurore Finco, Angera Haykal, Kana Tanos, Florentin Fabre, Saddam Chouaieb, Waseem Akhtar, Isabelle Robert-Philip, William Legrand, Fernando Ajejas, Karim Bouzehouane, Nicolas Reyren, Thibaut Devolder, Jean-Paul Adam, Joo-Von Kim, Vincent	Imaging non-collinear antiferromagnetic textures via single spin relaxometry	Oral
AMT-A03	Nimrod Bachar	Nimrod Bachar, Aviad Levy, Thomas Prokscha, Andreas Suter, Elvezio Morenzoni, Zaher Salman, Guy Deutscher	Kubo spins in nanoscale aluminum grains: A muon spin relaxation study	Oral
AMT-I-A1	D. Passeri	D. Passeri		Invited
AMT-A05	Frank Wiekhorst	Frank Wiekhorst, Patricia Radon, Norbert Löwa, Abdulkader Baki, Regina Bleul	Magnetic particle spectroscopy to determine the reproducibility of magnetic nanoparticle syntheses	Oral
AMT-B01	Abhinav Sannidhi	Abhinav Sannidhi, Paul W. Todd, Thomas R. Hanley	Measuring magnetophoretic mobility of single magnetic nanoparticles	Oral

Joint Session: **Advanced measurement techniques & Artificial intelligence, optimization and inverse problems**

Wednesday, June 16 -- 10.30-11.45

AMT-I-B1	A.Ktena	Aphrodite Ktena, Mehrija Hasicic, Eleni Maggiorou, Spyridon Aggelopoulos, Evangelos Hristoforou	Magnetic Permeability vs Barkhausen Noise Measurements for Magnetic NDT Applications	Invited
AIO-I01	S. Harmon	Stuart Harmon, Roberta Guilizzoni, Graeme Finch	Developing bespoke magnetic measurement solutions: an NMI perspective	Invited
AIO-A01	Marcin Kowalik	Marcin Kowalik, R. Zalecki, M. Gieburowski, J. Niewolski, W. Tokarz	The application of unsupervised learning to the AC susceptibility measurements of High-Temperature Superconductors	Oral

Session: **Electromagnetic non-destructive testing**

Monday, June 14 -- 08.45-10.15

ID code	Presenting	Authors	Title	Type
NDT-I-A1	C. Reboud	Christophe Reboud, Roberto Miorelli, Anastassios Skarlatos, Edouard Demaldent	Coupled electromagnetic models for nondestructive evaluation of materials	Invited
NDT-A01	Lorenzo Capineri	Lorenzo Capineri, Margarita Chizh, Andrey Zhuravlev, Vladimir Razevig, Sergey Ivashov, Tim, Bechtel, Pierluigi Falorni, Andrea Bulletti, Luca Bossi	Non destructive testing applications of the microwave holographic radar	Oral
NDT-A02	Athanasios Kyrgiazoglou	Athanasios Kyrgiazoglou, Theodoros Theodoulidis, Nikolaos Poulakis	Eddy current testing of ferromagnetic steel tubes under magnetization	Oral
NDT-A04	B. Ducharme	S. Zhang, A. Kita, B. Ducharme, T. Uchimoto	Eddy Current Magnetic Signature (EC-MS): Experimental tests and Simulations	Oral
NDT-A05	Cesare Ciriani	Francesco Comuzzi, Cesare Ciriani, Andrea Cernigoi, Boris Sosic	Optimized design of a "magnetic rope detector" according to UNI EN 12927-2019 standard	Oral

Session: **Magnetic levitation and bearings, electrical machines and other electromagnetic devices**

Sub-session A Monday, June 14 -- 15.45-17.30

ID code	Presenting	Authors	Title	Type
LEV-I-A1	Elena Lomonova	Elena Lomonova, Bob van Nindhuis, Helm Jansen, Bart Gysen	Multi-degree-of-freedom spherical actuator and magnetic gravity compensator – integrated solution for robotics applications	Invited
LEV-A01	Karlo Radman	Karlo Radman, Wolfgang Gruber, Hubert Mitterhofer	Free-form topology optimization for magnetic arrays of planar levitation systems	Oral
LEV-A02	Igor Rudnev	Igor A. Rudnev, Maxim A. Osipov, Alexander S. Starikovskii, Dmitriy A. Abin, Sergey V. Pokrovskii, Irina V. Anishenko, Alexey I. Podlivaev	Contactless magnetic bearing based on second generation high temperature superconducting tape	Oral
LEV-A03	Andrea Tortella	Mauro Andriollo, Simone Bernasconi, Andrea Tortella	Design Issues of a Rotating to Linear Motion Magnetic Converter for Short Distance Transport Applications	Oral
LEV-A04	Wolfgang Gruber	Wolfgang Gruber, Edmund Marth, Gerald Jungmayr	Semi-bearingless magnetic geared motor	Oral
LEV-B04	Hector Gutierrez	Hector Gutierrez, Hanri Luijten	Active levitation in multiple degrees of freedom using null-flux coils	Oral

Sub-session B Tuesday, June 15 -- 08.45-10.00

LEV-B01	Vincent Mazauric	Vincent Mazauric, Nadia Maizi	A magnetic lattice-based representation of power systems dedicated to transient stability analysis	Oral
---------	------------------	-------------------------------	--	------

LEV-B02	Gino D'Ovidio	Giovanni Lanzara, Gino D'Ovidio	Stability investigation of UAQ4 high temperature superconducting MagLev system suspension	Oral
LEV-B03	Bekir Geçer	Bekir Gecer, N.Fusun Oyman Serteller	Design and analysis of 6/4, 8/6 and 10/8 switched reluctance motors using Ansys/Maxwell and MATLAB/Simulink	Oral
LEV-B05	Qirui Wang	Qiang Liu, Qirui Wang, Zhuang Li, Heng Li, Kang Xu	Overview of the actuator of roll stabilization and steady posture	Oral
LEV-B07	Evgeny Yu Sundukov	Evgeny Yu Sundukov, Nadezhda A. Tarabukina, Veronika E. Sundukova	Transport systems with «movers» & «fellow travelers» kind suspension	Oral

Monday, June 14

Session: Biomagnetism and biomedical applications

ID code	Presenting	Authors	Title	Type
BIO-P01	Riccardo Ferrero	Riccardo Ferrero, Ioannis Androulakis, Alessandra Manzin, Gerard Van Rhoon	Design of a TEM applicator for in vitro testing of RF hyperthermia	Poster
BIO-P03	Levan P. Ichkitidze	Levan P. Ichkitidze, Mikhail V. Belodedov, Alexandr Yu. Gerasimenko, Dmitry V. Telyshev, Sergey V. Selishchev, Yanina V. Rezvantseva	Registration of Biological Molecules Using Magnetic Field Sensors	Poster
BIO-P04	Federica Celegato	Federica Celegato, Gabriele Barrera, Marco Coisson, Matteo Cialone, Riccardo Ferrero, Alessandra Manzin, Paola Rizzi, Franca Albertini, Paola Tiberto	FePd nanoparticles by solid-state dewetting for magnetic hyperthermia	Poster
BIO-P05	François Tavernier	François Tavernier, Noël Burais, Riccardo Scorretti	Numerical dosimetry of low-frequency electromagnetic fields by using reduced models of the source of the field	Poster
BIO-P06	Aaron Jaufenthaler	Aaron Jaufenthaler, Peter Schier, Thomas Middelmann, Maik Liebl, Dietmar Eberbeck, Daniel Baumgarten	Quantitative 2D magnetorelaxometry imaging of magnetic nanoparticles using optically pumped magnetometers	Poster
BIO-P07	Oriano Bottauscio	Alessandro Arduino, Oriano Bottauscio, Rüdiger Brühl, Mario Chiampi and Luca Zilberti	Hazards related to switching gradient field heating for patients carrying orthopaedic implants during MRI sessions	Poster
BIO-P09	Rikkert Van Durme	Rikkert Van Durme, A. Coene, G. Crevecoeur, L. Dupré	Maximizing local magnetic particle concentrations using dynamic optimization	Poster
BIO-P10	Evangelos Hristoforou	Maria G. Savvidou, Angelo Ferraro, Antonio Molino, Evangelos Hristoforou	Selective Magnetic Separation to concentrate bioactive compounds from microalgae	poster
BIO-P11	K. Everaert	K. Everaert, J. Leliaert, B. Van Waeyenberge, F. Wiekhorst	Thermal Noise Magnetometry of Magnetic Nanoparticle Ensembles	Poster
BIO-P17	Marta Bonato	Serena Focchi, Marta Bonato, Emma Chiaramello, Gabriella Tognola, Marta Parazzini, Paolo Ravazzani	Numerical modelling of magnetic force on human targets in magnetic targeting applications	Poster

Session: Magnetic materials for energy applications

ID code	Presenting	Authors	Title	Type
ENG-P01	Lukasz Hawelek	Lukasz Hawelek, Tymon Warski, Adrian Radon, Przemyslaw Zackiewicz, Anna Wójcik, Mariola Kądziołka-Gaweł, Aleksandra Kolano-Burian	Structure and magnetic properties of thermodynamically predicted rapidly quenched Fe85-xCuxB15 alloys	poster
ENG-P02	D. Benea	D. Benea, R. Hifian, V. Pop, O. Isnard	Investigations on the magnetic properties of the RxZr1-xFe11-xCozTic (R = Y, Gd) alloys	poster
ENG-P06	Tymon Warski	Tymon Warski, Przemyslaw Zackiewicz, Wojciech Lonski, Rafal Babilas, Aleksandra Kolano-Burian, Lukasz Hawelek	Effect of Cr addition on thermal stability, magnetic and electro-chemical properties of high induction Fe-B alloys	poster
ENG-P07	Emir Poskovic	Emir Poskovic, Luca Ferraris, Fausto Franchini, Federico Carosio, Marco Actis Grand	Quick characterization method for SMC materials for a preliminary selection	poster
ENG-P08	G. Ala	G. Ala, R. Miceli, G. Giglia, P. Romano, G. Schettino, F. Viola, S. Quondam Antonio, H. P. Rimal	LCL soft ferrite filter design for grid connected three-phase 5-levels cascaded H-Bridge inverters with MC PWM modulation techniques	poster
ENG-P09	Tatsuya Kon	Tatsuya Kon, Nobuyoshi Imaoka and Kimihiro Ozaki	Effects of fabricating conditions on the coercivity of Fe-Mn soft magnetic powders	poster
ENG-P14	Rafael Vieira	Rafael Vieira, Olle Eriksson, Torbjörn Björkman, Heike C. Herper	Magnetic properties and magnetocaloric effect of FeRh – an ab-initio study	poster
ENG-P17	Adler Gamzatov	Adler Gamzatov, A.M. Aliev, D-H. Kim, A.R. Kaul	Influence of cyclic magnetic field frequency on magnetocaloric effect in manganese's	poster
ENG-P18	Oksana Pavluchkina	Oksana Pavluchkina, Vladimir Sokolovskiy, Vasilij Buchelnikov, Mikhail Zagrebin	Structural, magnetic and electronic properties of Fe-Rh-Y (Y=Mn, Pd) compounds: ab initio study	poster
ENG-P19	Simon Nosan	Simon Nosan, Urban Tomc, Katja Klinar, Andrej Kitanovski	New concept of electromagnetic field source for magnetic refrigeration	poster
ENG-P21	Mariya Matyunina	Mariya V. Matyunina, Mikhail A. Zagrebin, Vladimir V. Sokolovskiy, Vasilij D. Buchelnikov	Magnetostriction of Fe-Ga-Z (Z=Al, Ge, Si) alloys studying by torque method	poster
ENG-P22	F. Casoli (G. Varvaro)	Francesca Casoli, Gaspare Varvaro, Simone Fabbrici, Milad Takhsa Ghahfarokhi, Federica Celegato, Paola Tiberto, Franca Albertini	Insight into the magnetization process of ferromagnetic shape memory films with twinned microstructure	poster
ENG-P23	Mikhail A. Zagrebin	Mariya V. Matyunina, Mikhail A. Zagrebin, Vladimir V. Sokolovskiy, Vasilij D. Buchelnikov	Magnetostriction of AZ phase in Fe-(Ga, Ge, Al) alloys: insights from first-principles calculations	poster
ENG-P24	Mikhail Yu. Bogush	Maxim N. Ulyanov, Sergey V. Taskaev, Dmitriy V. Gunderov, Dmitriy S. Bataev, Mikhail Yu. Bogush	Magnetic properties of HPT Fe-Ni-Al alloys	poster

ENG-P26	Maksim S. Anikin	Maksim S. Anikin, Evgeniy N. Tarasov, Dmitry S. Neznakhin, Mikhail A. Semkin, Nadezhda V. Selezneva, Aleksander V. Zinin	Variety of magnetic structures in R(Co _{0.84} Fe _{0.16}) ₂ (R = Ho, Er) systems with yttrium substituted for rare earth elements	poster
ENG-P27	Alena Vishina	Alena Vishina, Olle Eriksson, Heike C. Herper	Ab-initio study of the electronic structure and magnetic properties of Ce ₂ Fe ₁₇	poster
ENG-P30	Gabriele Barrera	Simone Lantean, Gabriele Barrera, Candido F. Pirri, Paola Tiberto, Marco Sangermano, Ignazio Roppolo, Giancarlo Rizza	3D printing of Magneto-Responsive Polymeric Materials with Tunable Mechanical and Magnetic Properties by Digital Light Processing	poster

Session: Spin waves and magnonics + Skyrmions

ID code	Presenting	Authors	Title	Type
SPW-P03	Sergey Odintsov	Sergey Odintsov, Evgeniy Beginin, Sergey Nikitov, Alexandr Sadovnikov	Spin wave beams in multilayer magnonic crystals	poster
SPW-P04	Vladislav Gubanov	Vladislav Gubanov, Alexandr Sadovnikov	Spin-wave prorogation and spatial-frequency separation in a lateral non-identical system of coupled magnonic crystals with defect zone	poster
SPW-P05	Vladislav Gubanov	Vladislav Gubanov, Yulia Gubanova, Natalia Noginova, Alexandr Sadovnikov	Anisotropy control in the meander structure of permalloy with tangential magnetization	poster
SPW-P06	Yury Bunkov	Yury Bunkov	Principles of Magnonic Qubit Formation	poster
SPW-P07	Yury Bunkov	V. I. Belotelov, Yu. M. Bunkov, A.A. Kholin, G. A. Knyazev, A. N. Kuzmichev, P. M. Vetoshko	Bose condensation of magnons in a YIG film at a magnetic field gradient.	poster
SPW-P08	L. H. F. Andrade	M. A. B. Tavares, L. H. F. Andrade, F. M. Matinaga, G. F. M. Gomes, M. M. Zapata, L. E. Fernandez-Outona, M. D. Martins	Spin dynamics in [Co ₆₀ Fe ₄₀ /Pt] ₅ multilayers investigated with femtosecond laser pulses	poster
SPW-P11	Yuri Filimonov	Yuri Khivintsev, Yuri Nikulin, Valentin Sakharov, Michail Seleznev, Alexander Kozhevnikov, Sergei Vysotskii, Yuri Filimonov	Spin pumping by MSSW in YIG/n-InSb and YIG/Pt microstructures	poster
SKY-P02	P. Robert Kotiuga	P. Robert Kotiuga	On the role of continuum models in the simulation, design and evaluation of magnetic skyrmion devices	poster
SKY-P03	Edoardo Albisetti	Edoardo Albisetti, Daniela Petti, Giacomo Sala, Silvia Tacchi, Simone Finizio, Sebastian Wintz, Jörg Raabe, Paolo Vavassori, Matteo Pancaldi, Elisa Riedo, Riccardo Bertacco	Nanopatterning multidimensional spin-textures: from magnetic domains to topological solitons	poster
SKY-P04	Max T. Birch	Max T. Birch, D. Cortés-Ortuño, L. A. Turnbull, M. N. Wilson, F. Groß, N. Träger, A. Laurensen, N. Bukin, S. H. Moody, M. Weigand, G. Schütz, H. Popescu, R. Fan, P. Steadman, J. A. T. Verezhak, G. Balakrishnan, J. C. Loudon, A. C. Twitchett-Harrison, O. Hovorka, H.	The complete picture: real-space imaging of confined magnetic skyrmion tubes	poster

Tuesday, June 15

Session: Magnetic recording & Sensors + Spin Orbit Torque + Magnetic levitation + Non destructive test

ID code	Presenting	Authors	Title	Type
SOT-P04	Vito Puliafito	Vito Puliafito, Ansa Safin, Israa Medlej, M. Carpentieri, B. Azzerboni, A. Slavin, G. Finocchio	Numerical and analytical model of an antiferromagnetic terahertz detector	Poster
SOT-P05	Ansar Safin	Ansar Safin, Sergey Nikitov, Andrei Slavin, Vasily Tiberkevich	Mutual phase locking of the nonlinear THz-frequency antiferromagnetic spin-Hall oscillators	poster
REC-P03	G. Pradhan	G. Pradhan, G. Barrera, F. Cologato, M. Coisson, P. Tiberto	Local magnetization reversal in FeGa magnetic nanostructures	poster
LEV-P01	Wang Yang	Wang Yang, Chen Dezhi, Cao Xiongxiang, Zhang Shichong	Research on the performance of DC-DC Converter based on electrical steel sheet and ferrite mixed core for medium frequency transformer	poster
LEV-P02	Xiongxiang Cao	Xiongxiang Cao, Dezhi Chen, Yang Wang, Shichong Zhang, Baodong Bai	Study on core loss of thin silicon steel medium frequency transformer	poster
LEV-P04	Dae Yong Um (Yougang Sun)	Dae Yong Um, Min Jae Kim, Ho Yeong Lee, Jung Min kim, Gwan Soo Park	Analytical Design, Analysis and Experimental Validation of Planar Induction Heating Coil for Domestic Induction Cooker	poster
LEV-P08	N.Fusun Oyman Serteller	Ozturk Tosun, N.Fusun Oyman Serteller, Vedat Topuz, Kenan Tokar	Electromagnetic Analysis Effect on Design of a Brushless DC motor	poster
LEV-P09	Andrea Marić	Andrea Marić and Ljiljana Živanov	Influence of Ferrite Sections Variation on 3D LTCC Micro-Transformer Performance	poster
LEV-P10	Valentin Mateev	Iliana Marinova, Valentin Mateev	Conical coaxial magnetic gear	poster
LEV-P11	Junqi Xu (Yougang Sun)	Chen Chen, Junqi Xu, Guobin Lin, Yougang Sun	Big Data Analysis of Signal Transfer in Levitation System of Medium and Low Speed Maglev Train	poster
LEV-P12	Valentin Mateev	Valentin Mateev, Iliana Marinova	Coaxial magnetic gear with viscose ferrofluid	poster
LEV-P13	Valentin Mateev	Valentin Mateev, Iliana Marinova	Coaxial magnetic gear torque control	poster
LEV-P17	Guobin Li (Yougang Sun)	Yougang Sun, Junqi Xu, Lijun Rong, Wen Ji, Guobin Li	Levitation Robust control for magnetic levitation system of maglev vehicle with time-delay	poster
NDT-P01	A. Tamburrino	L. Ferrigno, M. Laracca, A. Tamburrino, S. Ventre, A. Sardellitti	Thickness measurements using Eddy current techniques	poster

NDT-P02	B. Ducharne	H. S. Nguedjang, Y. A. Tene Deffo, P. Tsafack, B. Ducharne, M.A. Raulet, L. Morel	Printed magnetic needle probes sensor, embedding magnetic state monitoring	poster
NDT-P03	Chang Geun Heo	Chang Geun Heo, Gwan Soo Park	Effect of external metal shape and distance on signal in magnetic flux leakage type non-destructive testing	poster

Session: **Advanced measurement techniques + FORC + Artificial Intelligence Optimization**

ID code	Presenting	Authors	Title	Type
AMT-P01	Chiaki Uyeda	Chiaki Uyeda, Hiroki Fukuyama, Keiji Hisayoshi, Kentaro Terada	Observation of field-induced motions of a single diamagnetic particle to study the structure of individual nano-size particle	poster
AMT-P02	Keiji Hisayoshi	Keiji Hisayoshi, Chiaki Uyeda, Kentaro Terada	Translation of interstellar solids induced by Nd magnetic circuit	poster
AMT-P04	Gabriele Barrera	Marco Coisson, Wilhelm Hüttenes, Matteo Cialone, Gabriele Barrera, Federica Celegato, Paola Rizzi, Zoe Barber, Paola Tiberto	Measurement of thin film magnetostriction using field-dependent atomic force microscopy	poster
AMT-P05	Riccardo Cabassi	Riccardo Cabassi and Fulvio Bolzoni	Characterization of polycrystalline permanent magnets with the Singular Point Detection technique	poster
AMT-P06	S. Pütter	S. Pütter, S. Mattau, A. Koutsoubas, P. Schöffmann, A. Syed Mohd, K. Zherenkov, E. Babcock, Z. Salhi, A. Ioffe, T. Brückel	Revealing magnetic properties of thin films utilizing polarized neutrons	poster
AMT-P07	Tommaso Lapucci	Tommaso Lapucci, Luigi Troiano, Carlo Carobbi, Lorenzo Capineri	Soft and hard iron compensation without sensor motion for the compasses of an operational towed hydrophone array	poster
FRC-P01	Alexandru Stancu	Alexandru Stancu, Laurentiu Stoleriu	Nonmonotonic xyFORCs in two-phase magnetic systems	poster
FRC-P03	Valeria Kolesnikova	V. Kolesnikova, M. Rivas, I. Baraban, JC Martinez-Garcia, M. Gorshenkov, V. Rodionova	Engineering of magnetization reversal processes in multiphase microwires by interplay of magnetostatic and magnetoelastic anisotropy	Poster
AIO-P01	Antonino Laudani	Salvatore Coco, Antonino Laudani	Machine learning estimation of the effective permeability of mixture for magnetic shielding	Poster
AIO-P02	Antonino Laudani	Salvatore Coco, Antonino Laudani	A neural spatial mapping of magnetic fields for exposure surveys	Poster
AIO-P03	Francesco Riganti Fulginei	Antonino Laudani, Gabriele Maria Loxito, Francesco Riganti Fulginei, Alessandro Salvini	Comparative analysis between feed-forward and recurrent neural networks for simulating magnetic scalar hysteresis	Poster
AIO-P04	Francesco Riganti Fulginei	Antonino Laudani, Valentina Lucaferri, Francesco Riganti Fulginei, Alessandro Salvini	Identification of Hysteresis Play Model from measurement data by means of Continuous Flock of Starlings Optimization algorithm	Poster
AIO-P05	Riccardo Scorretti	Riccardo Scorretti, Fabien Sixdenier	An analytical formula to identify the parameters of the energy-based hysteresis model	Poster
AIO-P06	Valentina Lucaferri	Valentina Lucaferri, Mauro Parodi, Francesco Riganti Fulginei, Alessandro Salvini	Parallel Neural Networks system for dynamic magnetic hysteresis modelling	poster

Wednesday, June 16

Session: **Spintronics, multiferroics and voltage control of magnetism + Math model. & Micromagnetics + Macroscale model. & Devices**

ID code	Presenting	Authors	Title	Type
SMU-P01	E. F. Pinzón-Escobar	E. F. Pinzón-Escobar, G. Alvarez, A. Esparza-García, H. Montiel	Comparative electric transport behavior between Co-rich soft magnetic heterostructures	poster
SMU-P03	Aleksei V. Shestakov	Aleksei V. Shestakov, M.A. Cherosov, M.I. Ibragimova, R.M. Eremina	Features in the field dependence of the Hall constant Mn _{0.135} Hg _{0.865} Te	poster
SMU-P04	Daniil R. Baigutlin	Vasily D. Buchelnikov, Vladimir V. Sokolovskiy, Olga N. Miroshkina, Daniil R. Baigutlin, Mikhail A. Zagrebin, Bernardo Barbiellini, Erkki Lähderanta	Switching metal-to-half-metal behavior in Heusler alloy	poster
SMU-P08	Jan Zubáč	Jan Zubáč, Zdeněk Kašpar, Filip Krížek, Vit Novák, Kamil Olejník, Tomáš Jungwirth	Switching of antiferromagnetic CuMnAs by ultrashort electrical pulses	poster
SMU-P09	Sven E. Ilse	Sven E. Ilse, Daan B. Boltje, Gisela Schütz, Eberhard Goering	X-ray resonant magnetic reflectometry (XRMR) study of the interface between ferromagnetic transition metals and MgO	poster
SMU-P10	E. F. Pinzón-Escobar	E. F. Pinzón-Escobar, H. Montiel, G. Alvarez, A. Esparza-García	Comparative magneto transport behaviour between Co-rich soft magnetic heterostructures	poster
SMU-P11	Alexander Omelyanchik	Alexander Omelyanchik, Liudmila Makarova, Irina Baraban, Karim Amirov, Marat Khairullin, Vladimir Rodionov, Nikolai Perov, Davide Peddis, and Valeria Rodionova	Synthesis of bismuth and cobalt ferrites nanoparticles for preparation of magnetoelectric nanocomposites	poster
SMU-P12	Frank Schulz	Frank Schulz, Zach Nunn, Erol Girt, Eberhard Goering	Tracing back the interlayer thickness dependence of saturation magnetization in Co/RuFe/Co sandwiches using XMCD	poster
SMU-P15	Deepika Tripathi	Deepika Tripathi, Rama Yadav, Manoj prajapat, Dhanveer Singh Rana, V.Shelke	effect of synchronized la and al substitution in bulk bismuth ferrite	poster

MIC-P01	Inna Lobanova	Inna Lobanova, Stéphane Despréaux, Stéphane Labbé	Micromagnetic modelling of hysteresis in permalloy thin films with impurities	Poster
MIC-P02	Oksana Pavlukhina	Oksana Pavlukhina, Vasilii Buchelnikov, Vladimir Sokolovskiy, Mikhail Zagrebin, Mariya Matyunina, Olga Miroskina, Danil Baigutlin	Kinetics of phase transformations in Fe-Ga alloys	Poster
MIC-P03	Vladimir Kondratyev	Vladimir Kondratyev	Self-organized critical superferromagnetic dynamics	Poster
MIC-P04	B. Ducharne	Y. A. Tene Deffo, P. Tsafack, B. Ducharne, E. Tanyi	Evaluation of inhomogeneous mechanical residual stress distribution from the experimental needle probe method and a Jiles-Atherton- Sablik based space discretized simulation tool	Poster
DEV-P04	Riccardo Scorretti	Riccardo Scorretti, Fabien Sixdenier, Atef Lekdim	Static Hysteresis modelling of NO FeSi in rolling and transverse directions by using the energy based model	Poster
DEV-P06	Giambattista Grusso	Giambattista Grusso, Simone Quondam Antonio, Ermanno Cardelli	Modelling hysteresis phenomena in power filters: a circuit approach	poster
DEV-P07	Szymon Gontarz	Szymon Gontarz, Radoslaw Patyk, Lukasz Bohdal, Dorota Jackiewicz	Multiparameter modelling and analysis of mechanical cutting process of grain oriented silicon steel	poster



Advances in Magnetism 2020-21, June 13-16, 2021

BOOK of ABSTRACTS

Tutorials & Plenary

Abstracts can be easily browsed through the bookmarks

Multicaloric materials

Xavier Moya

Department of Materials Science, University of Cambridge

Cooling is essential for food, medicine, electronics and thermal comfort of people in houses and cars, but existing technologies for refrigeration and air-conditioning are based on the compression and expansion of gases that are harmful for the environment.

Cooling using solids is therefore attractive but thermoelectric cooling based on the Peltier effect, and optical cooling based on anti-Stokes fluorescence, are at best only ~10% efficient. By contrast, magnetocaloric, electrocaloric, and mechanocaloric cooling based on thermal changes produced in magnetically, electrically, and mechanically responsive oxides when subjected to changes in magnetic field, electric field and mechanical field promise higher efficiencies.

In this lecture, I will:

- describe the fundamentals of caloric materials from a historical perspective
- give an overview of their measuring techniques
- present recent advances on magnetocaloric, electrocaloric and mechanocaloric materials
- and describe recent developments on cooling devices that are based on these materials.

Microwave and THz detectors based on spintronic diodes

Giovanni Finocchio^a

^a Department of Mathematical and Computer Sciences, Physical Sciences and Earth Sciences -
University of Messina

Microwave detectors based on the spin-torque diode effect are among the key emerging spintronic devices. By utilizing the spin of electrons in addition to their charge, they have the potential to overcome the theoretical performance limits of their semiconductor (Schottky) counterparts. In the first part of the talk, I will discuss our recent results in the field of microwave detectors based on spin diodes.[1] Those devices realized with magnetic tunnel junctions exhibit high-detection sensitivity $>200\text{kV/W}$ at room temperature, without any external bias fields, and for low-input power (micro-Watts or lower).[2] This sensitivity, achieved taking advantage of the injection locking, is significantly larger than both biased state-of-the-art-Schottky diode detectors and other existing spintronic diodes. Another application of spintronic diodes is the electromagnetic energy harvesting. Here I will show the development of a bias-field-free spin-torque diodes that could be an efficient harvester of broadband ambient RF radiation, capable to efficiently harvest microwave powers of microWatt and below and to power a black phosphorous nanodevice. Finally, the talk will discuss the promising directions of THz detectors based on antiferromagnetic materials including their unique properties such as resonance response and tunability and the remaining challenges to face.

-
- [1] B. Fang, M. Carpentieri, X. Hao, H. Jiang, J.A. Katine, I.N. Krivorotov, B. Ocker, J. Langer, K.L. Wang, B. Zhang, B. Azzerboni, P.K. Amiri, G. Finocchio, Z. Zeng, Giant spin-torque diode sensitivity in the absence of bias magnetic field, Nat. Commun. 7 (2016). doi:10.1038/ncomms11259.
- [2] L. Zhang, B. Fang, J. Cai, M. Carpentieri, V. Puliafito, F. Garescì, P.K. Amiri, G. Finocchio, Z. Zeng, Ultrahigh detection sensitivity exceeding 10^5 V/W in spin-torque diode, Appl. Phys. Lett. 113 (2018) 102401. doi:10.1063/1.5047547.

Antiferromagnets for neuromorphics and opto-electronics

Tomas Jungwirth^{a,b}

^a Institute of Physics, Czech Academy of Sciences, Czech Republic, ^b School of Physics and Astronomy, University of Nottingham, UK

Louis Néel pointed out in his Nobel lecture that while interesting from theoretical viewpoint, antiferromagnets did not seem to have any applications. Indeed, the alternating directions of magnetic moments on individual atoms and the resulting zero net magnetization have made antiferromagnets hard to control by tools common in ferromagnets. This has hindered both the research and utility of these abundant magnetic materials. Recent studies have shown, however, that current-induced spin-orbit torque and anisotropic magnetoresistance can be used to efficiently manipulate and detect the Néel vector [1]. Bi(multi)polar switching signals in these first realizations of antiferromagnetic memories were in the fraction of a per cent scale – far from the requirements for practical applications. We will present a concept showing alternative means for unipolar electrical or optical switching, spanning a broad range from microseconds to femtoseconds, in memory devices comprising a simple film of an antiferromagnet and showing readout signals in the ~10-100% range [2]. We fabricate analog memory micro-devices with remarkably reproducible, reversible multi-level switching signals that are insensitive to magnetic fields. Our concept opens research and development directions ranging from microelectronic memory-logic components for spiking neural networks to opto-electronic memory-sensor devices with high temporal and spatial resolution.

[1] Focus on Antiferromagnetic Spintronics, Nature Physics 14 (2018).

[2] Z. Kaspar et al., <https://arxiv.org/abs/1909.09071>.

p-bit: between a bit and a q-bit

Kerem Camsari and Supriyo Datta

Purdue University, West Lafayette, IN 47907, USA

Digital computing is based on a deterministic bit with two values, 0 and 1. On the other hand, quantum computing is based on a q-bit which is a delicate superposition of 0 and 1. This talk draws attention to something in-between namely, a **p-bit** which is a robust classical entity fluctuating between 0 and 1 [1].

The concept of p-bits is of particular interest to the magnetics community because they have been implemented experimentally using stochastic magnetic tunnel junctions (s-MTJ's) fabricated with a slight modification of market-ready magnetoresistive Random Access Memory (MRAM) technology [2].

We have shown that these **p-bits** can be used as building blocks for constructing autonomous clockless **p-circuits** that can accelerate many current applications like optimization, invertible logic and machine learning [3], while providing a bridge to the emerging field of quantum computing [4].

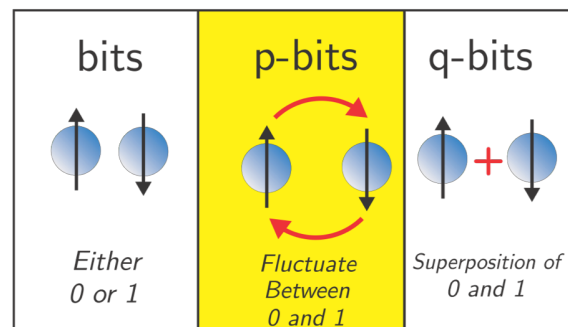


Figure 1: A p-bit is a classical entity fluctuating between 0 and 1.

[1] K.Y. Camsari et al. “p-bits for probabilistic spin logic,” *Appl. Phys. Reviews* **6**, 011305 (2019).

[2] W.A. Borders et al. “Integer Factorization using Stochastic Magnetic Tunnel Junctions,” *Nature* **573**, 390 (2019).

[3] J. Kaiser et al. “Probabilistic Circuits for Autonomous Learning: A simulation study,” *Frontiers in Computational Neuroscience*, to appear (2020).

[4] K.Y. Camsari et al. “Scalable Emulation of Sign-Problem-Free Hamiltonians with Room-Temperature p-bits,” *Physical Review Applied* **12**, 034061 (2019).



Advances in Magnetism 2020-21, June 13-16, 2021

BOOK of ABSTRACTS

Oral Sessions

Abstracts can be easily browsed through the bookmarks

Advances in Magnetics 2020-21, June 13-16, 2021

Biomagnetism and biomedical applications

Abstracts can be easily browsed through the bookmarks

Aggregates and dipolar interactions in nanoparticle assemblies for hyperthermia

Òscar Iglesias¹

¹Dpt. de Física de la Matèria Condensada and IN²UB, Facultat de Física, Universitat de Barcelona, Av. Diagonal 645, 08028 Barcelona (Spain)

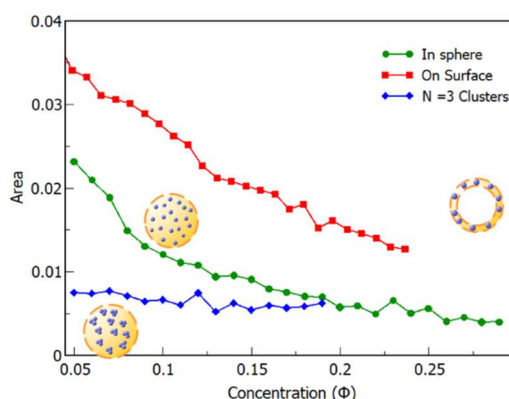
oscariglesias@ub.edu

Magnetic hyperthermia is one of the most promising biomedical applications of magnetic nanoparticles (NP) and is intended to be alternative to cancer therapies based on drug delivery and radiotherapy. It is based on the fact that magnetic NP dissipate heat when an oscillating magnetic field is applied to them in a quantity (specific absorption rate, SAR) that is closely related to the area of the hysteresis loop. The main problem in the field has become to find the suitable range of parameters that maximize SAR for a given material [1], SAR depends of course on the amplitude of the applied magnetic field and its frequency, but also on intrinsic parameters of the NP such as saturation magnetization, anisotropy, shape and size [2]. Although the role of external parameters is somehow well contrasted, there is still ongoing controversy on the role that dipolar interactions (DI) and aggregation state of the assemblies play on SAR. We will present results of Monte Carlo simulations of hysteresis loops of interacting NP assemblies in the macrospin approximation [3]. We will present first results of different regular spatial arrangements of NP, showing the influence of interparticle separation and particle size on SAR. Next, we will study the case of randomly placed NP with varying concentrations mimicking experimentally found situations [4] (inside and at the surface of liposomes/cells, clusters). It is found that formation of chain-like arrangements or assemblies with prolate shapes, lead to considerable increases in SAR due to DI.

Acknowledgements

Work supported by Spanish MINECO (MAT2015-68772-P, PGC2018-097789-B-I00), Catalan DURSI (2017SGR0598) and EU FEDER funds (Una manera de hacer Europa) also CSUC for supercomputer facilities.

- [1] S.-H. Noh, et al. *Nano Today* **13**, 61 (2017); R. Hergt et al. *Nanotechnology* **21**, 015706 (2010).
- [2] B. Mehdaoui, et al. *Phys. Rev. B* **87**, 174419 (2013); R. P. Tan et al. *Phys. Rev. B* **90**, 214421 (2014); P. Hasse and U. Nowak *Phys. Rev. B* **85**, 045435 (2012); P. V. Melenev et al. *Phys. Rev. B* **86**, 104423 (2012).
- [3] C. Martínez-Boubeta et al. *Scientific Reports* **3**, 1652 (2013).
- [4] Brollo et al., *Phys. Chem. Chem. Phys.* **20**, 17829 (2018); D. Niculaes et al., *ACS Nano* **11**, 12121 (2017)



Concentration dependence of the hysteresis loop area for different kinds of NP random assemblies.

Relevance of Brownian relaxation as power absorption mechanism in magnetic hyperthermia

Teobaldo E. Torres^a, Enio Lima Jr.^a, M. Pilar Calatayud^b, Beatriz. Sanz^b, Alfonso Ibarra^{b, c}, Rodrigo Fernández-Pacheco^{b, c}, Álvaro. Mayoral^d, Clara Marquina^{e, f}, M. Ricardo Ibarra^{b, c, e, f} and Gerardo F. Goya^{b, e, f}

^a Div. Resonancias Magnéticas, Centro Atómico de Bariloche/CONICET, Bariloche Argentina

^b Instituto de Nanociencia de Aragón (INA), Universidad de Zaragoza, Zaragoza, Spain

^c Laboratorio de Microscopias Avanzadas (LMA), Universidad de Zaragoza, Zaragoza, Spain

^d School of Physical Science and Technology, ShanghaiTech University, Pudong, Shanghai, PR China

^e Departamento de Física de la Materia Condensada, Universidad de Zaragoza, Zaragoza Spain.

^f Instituto de Ciencia de Materiales de Aragón (ICMA), Consejo Superior de Investigaciones Científicas (CSIC) - Universidad de Zaragoza, Zaragoza, Spain.

The Linear Response Theory (LRT) is a widely accepted framework to analyse the power absorption of magnetic nanoparticles for magnetic fluid hyperthermia [1, 2]. Its validity is restricted to low applied fields and/or to highly anisotropic magnetic nanoparticles. Here, we present a systematic experimental analysis and numerical calculations of the specific power absorption (SPA) by highly anisotropic cobalt ferrite magnetic nanoparticles with different average sizes and in different viscous media [3, 4]. The predominance of Brownian relaxation as the origin of the magnetic losses in these particles is established, and the changes of the SPA with the viscosity of the carrier liquid are consistent with the LRT approximation. The impact of viscosity on the SPA is relevant for the design of MNPs intended for heating the intracellular medium in *in vitro* and *in vivo* hyperthermia experiments. The combined numerical and experimental analyses presented here shed light on the underlying mechanisms that make highly anisotropic MNPs unsuitable for magnetic hyperthermia [4]. Our work includes also *in vitro* hyperthermia experiments on a culture of Co-ferrite NP-loaded cells. A detailed characterization of the intracellular distribution of the MNP has been also undertaken, by advanced microscopy tools. Besides Transmission Electron Microscopy (TEM), a study by Focused Ion Beam-Scanning Electron Microscopy (FIB-SEM) has been carried out, which has allowed the 3D reconstruction of the cells and the precise visualization of the MNP. These investigations have been completed with chemical analysis by energy-dispersive x-ray spectroscopy (EDS).

[1] R. Hergt, W. Andra, C.G. d'Ambly, I. Hilger, W.A. Kaiser, U. Richter and H.G. Schmidt, IEEE Transactions on Magnetism **34** (1998) 3745.

[2] Y.L. Raikher, V. Stepanov and R. Perzynski, Physica B-Condensed Matter **343** (2004) 262.

[3] T.E. Torres, E. Lima Jr., A. Mayoral, A. Ibarra, C. Marquina, M. R. Ibarra and G. F. Goya, J. Appl. Phys. **118** (2015) 183902.

[4] T.E. Torres, E. Lima Jr., M. P. Calatayud, B. Sanz, A. Ibarra, R. Fernández-Pacheco, A. Mayoral, C. Marquina, M. R. Ibarra and G. F. Goya, Sci. Rep. **9** (2019) 9:3992.

Design and *in silico* modelling of magnetic nanodisks for hyperthermia applications

Alessandra Manzin^a, Riccardo Ferrero^a, Marta Vicentini^{a,b}, Gabriele Barrera^a,
Federica Celegato^a, Marco Coïsson^a, Paola Tiberto^a

^a Istituto Nazionale di Ricerca Metrologica (INRIM), Torino, Italy

^b Politecnico di Torino, Torino, Italy

Magnetic nanomaterials like superparamagnetic iron oxide nanoparticles have been intensively studied for application in hyperthermia based cancer therapies. Recently, the attention has been shifted to both single- and multi-domain ferromagnetic nanostructures, because of heating efficiency improvement due to hysteresis losses [1]. Various strategies have been adopted to increase this heating contribution, such as the use of materials with high uniaxial magneto-crystalline anisotropy and the modification of nanostructure geometry. The latter has been explored focusing on nanodisks, nanorings and nanotubes, which lead to large hysteresis losses and magnetic vortex remanence state, thus reducing agglomeration effects.

Here, we focus on permalloy nanodisks, performing a parametric analysis aimed at finding the optimal size for magnetic hyperthermia, considering the Hergt-Dutz limit [2] for the selection of field frequency and amplitude. The study is carried out via micromagnetic modelling [3], also investigating the influence of nanodisk local concentration, magnetostatic interactions and relative orientation with the applied field [4].

After selecting the optimal parameters, we calculate the temperature increase induced in biological tissues, by solving the Pennes' bioheat transfer equation. The study is performed in a computational anatomical model of a mouse, changing the size of the target region, where the nanodisks are dispersed with variable dose, and its location in the body, considering different organs [5]. The figure below reports the results obtained with 150 nm diameter nanodisks, which are able to release a specific loss power of 225 W/g at 50 kHz in tissues.

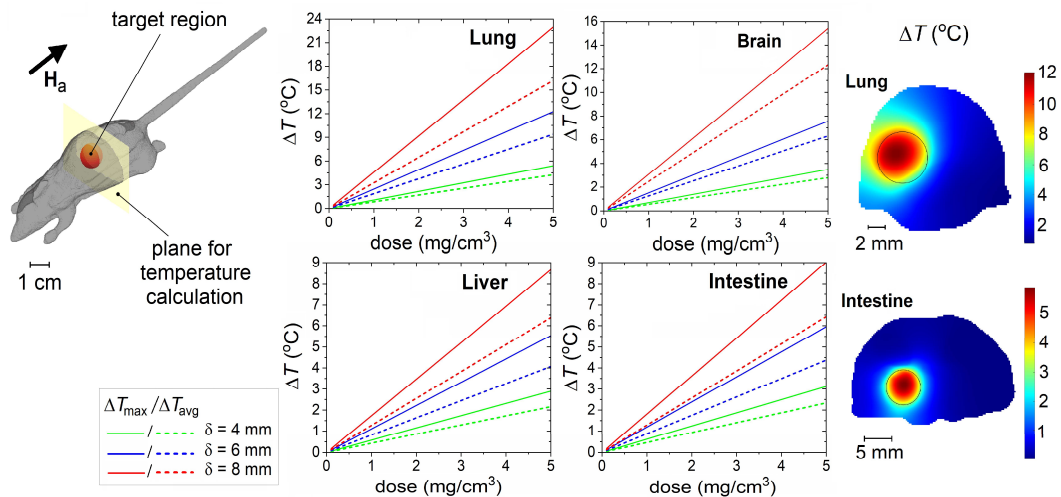


Figure 1: Left: Comparison of temperature increments reached at the heating equilibrium, by varying the mouse organ where the target region is placed, its size δ and the dose of permalloy nanodisks. Right: Maps of temperature increase for $\delta = 6$ mm and a nanodisk dose of 5 mg/cm³.

-
- [1] M. Angelakeris, *Biochimica et Biophysica Acta* **1861** (2017), 1642–1651.
 [2] R. Hergt and S. Dutz, *JMMM* **311** (2007), 187–192.
 [3] A. Manzin and R. Ferrero, *JMMM* **492** (2019), 165649
 [4] R. Ferrero et al., *Scientific Reports* **9** (2019), 6591.
 [5] A. Manzin, R. Ferrero and M. Vicentini, *submitted*.

Evaluation of passive implants as an exclusion criterion in magnetic hyperthermia

Irene Rubia-Rodríguez^a, Luca Zilberti^b, Alessandro Arduino^b, Oriano Bottauscio^b,
Mario Chiampi^b, Daniel Ortega^a

^aIMDEA Nanoscience, Faraday 9, 28049 Madrid, Spain

^bIstituto Nazionale di Ricerca Metrologica (INRiM), Strada delle Cacce 91, 10135 Turin,
Italy

Computer simulations (in silico) have complemented in vivo and in vitro experiments to develop new therapies in medicine, reducing time and costs to produce the tests. One of the treatments benefiting from in silico trials is magnetic hyperthermia, a nanotechnology-driven cancer therapy that has already been and is currently trialled in clinical settings as coadjuvant to chemotherapy and radiotherapy to successfully treat several types of tumours [1,2]. In silico trials can predict the effectiveness of a treatment and optimize it to get the best benefit/risk ratio. In turn, this improvement allows for adjusting the treatment to each case resulting in high-performance, precision therapies.

The standing safety criteria in clinical magnetic hyperthermia explicitly exclude prospective patients bearing any kind of metallic or partly metallic implants [1,3] due to their possible heating through eddy currents. This restrictive approach tends to overestimate the potential damage caused by the temperature increase of these prostheses in the presence of an alternating magnetic field, and there is an absolute lack of studies quantifying it.

In this work we use computational simulations to carefully appraise the real risk posed to potential magnetic hyperthermia patients bearing passive implants (Fig. 1), analysing both dosimetric quantities and temperature increase in the regions of interest. Different tumour and implant types, as well as treatment configurations are considered. We also study the influence of the implants on the effective magnetic field intensity at the treated area.

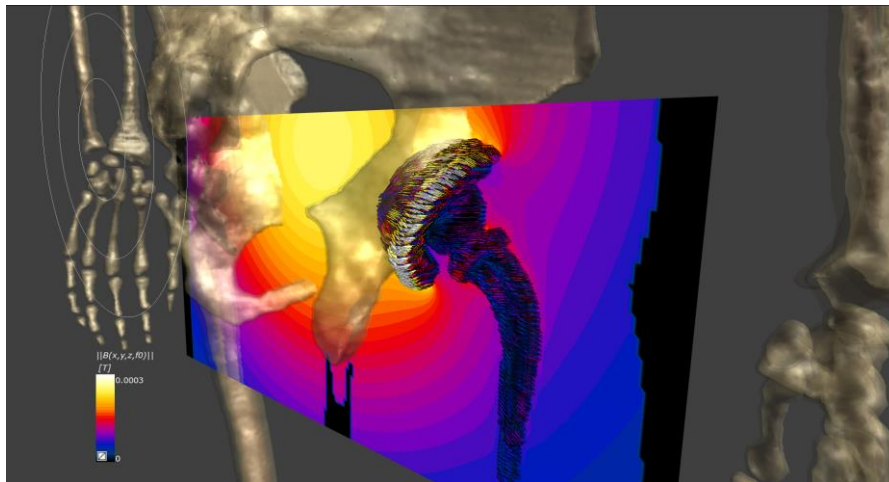


Figure 1: Possible heating of a hip implant during a magnetic hyperthermia treatment.

-
- [1] M. Johannsen et al. *Int. J. Hyperthermia* **21** (2005), 637; M. Johannsen et al. *Int. J. Hyperthermia* **23** (2007), 315; D. Ortega, Q. A. Pankhurst. in *Nanoscience: Vol. 1: Nanostructures through Chemistry* (2013), 60.
- [2] www.nocanther-project.eu
- [3] Maier-Hauff et al, *J. Neurooncol.* **103** (2011), 317.

Use of stochastic approaches in 5G scenario for EMF exposure assessment

Marta Bonato^{a,b}, Emma Chiamello^a, Serena Fiocchi^a, Gabriella Tognola^a, Paolo Ravazzani^a, Marta Parazzini^a

^a Institute of Electronics, Computer and Telecommunication Engineering, CNR, Milano, Italy

^b Department of Electronics, Information and Bioengineering, Politecnico di Milano, Italy

The upcoming development of the 5th generation mobile networks (5G) based on wireless communications will involve for the first time a wide use of the millimeter wave spectrum (30-300 GHz). Furthermore, the need of new network requirements, such as low transmission latency and data rate transmission increase, will also involve the introduction of technology innovations. Among these, the most innovative are the use 'massive' MIMO antennas and the beamforming technique, which will permit to send and receive more data simultaneously and in more efficient ways.

All these changes will lead to a new world of connectivity, which will develop the concept of future smart cities, factories and roads and will improve the users' benefits. Nevertheless, this heterogeneous network will also drastically modify the users' exposure to RF EMF in the next years and may raise questions from general public [1]. This underline the need of conducting promptly an appropriate exposure assessment considering this highly variable exposure scenarios.

The purpose of the present work is to introduce the use of stochastic dosimetry approaches as methods to face the variability of these new EMF exposure scenarios for obtaining a more complete exposure assessment. Stochastic techniques are methods that combines the classical electromagnetic computational techniques and statistics to build surrogate models for obtaining the distribution of the quantity of interest with low computational effort. Indeed, despite the progress in high performance computing, the classical computational electromagnetic techniques will still require highly time-consuming simulations for every single new specific case in order to evaluate the exposure level, because it will be necessary to take account of all the multitude of factors that characterize the highly variable 5G scenario.

Stochastic dosimetry was successfully used in previous works both at low and high frequency cases [2] and seems promising for dealing with the complexity of the emerging 5G scenarios. This statistical approach will allow providing accurate exposure assessment considering both realistic and typical exposures scenario and use cases that the new 5G networks will bring in the immediate future. In particular, the work will mainly focus on some downlink exposure cases, characterizing the exposure level changes that will occur with the introduction of the massive MIMO antennas and the beamforming technique.

[1] Recommendations, ITU-T. K-Series. "5G technology and human exposure to RF EMF." (2017).

[2] Chiamello E, Fiocchi S, Parazzini M, Ravazzani P, Wiart J. Stochastic Dosimetry for Radio-Frequency Exposure Assessment in Realistic Scenarios. In Uncertainty Modeling for Engineering Applications 2019 (pp. 89-102). Springer, Cham.

A magneto-optical microscope for investigating magnetisation dynamics of nanoparticles under hyperthermia conditions

Maneea E. Sharifabad^a, Rémy Soucaille^b, Robert J. Hicken^b, and Neil D. Telling^a,

^a School of Pharmacy and Bioengineering, Keele University, United Kingdom

^b Department of Physics and Astronomy, University of Exeter, Stocker Road, Exeter, Devon, United Kingdom

Nanoparticle-mediated magnetic hyperthermia treatment is a promising cancer therapy that enables selective heating of cancerous tissues to slow or stop tumour growth, whilst also increasing tumour sensitivity to chemotherapy and radiotherapy. The importance of magnetic hyperthermia is driving the growing interest in the development of various magnetic nanocomposites, and consequently dictates the need for development of efficient characterisation tools capable of assessing nanoparticles under relevant biological conditions.

Here we present a novel combined magneto-optical and fluorescence lifetime scanning laser microscope, which enables the study of magnetisation dynamics and magnetic hyperthermia of nanoparticles in cellular environments under hyperthermia conditions. The developed system is capable of mapping localised AC magnetic susceptibility, hysteresis and fluorescence lifetime, under magnetic fields generated at frequencies up to 1 MHz, and amplitudes of up to 50 mT (dependent on frequency). The system is able to measure both liquid samples (e.g. nanoparticle suspensions) and dry samples.

Figure 1 shows representative data from magnetic nanoparticles either immobilised on a biological membrane (Fig. 1a) or in aqueous suspension (Fig. 1b). In Fig. 1a, the distribution of the magnetic nanoparticles on the membrane was first determined by mapping the fluorescence lifetime phase signal from a fluorophore attached to the nanoparticle surface, using a frequency domain method (inset to Fig. 1). The AC hysteresis loops shown were then obtained by positioning the focused laser spot on a cluster of the nanoparticles, and demonstrate the expected variation from magnetisation relaxation at low field amplitudes, to magnetisation reversal at high field amplitudes. The AC susceptibility measured from the aqueous nanoparticle suspension is shown in Fig. 1b, and reveals a peak in the out-of-phase component of the complex AC susceptibility at a frequency of ~ 1 kHz, corresponding to Brownian relaxation of nanoparticle aggregates in the suspension. The application of the microscope to studies of cellular based magnetic hyperthermia and nanoparticle development, will be discussed.

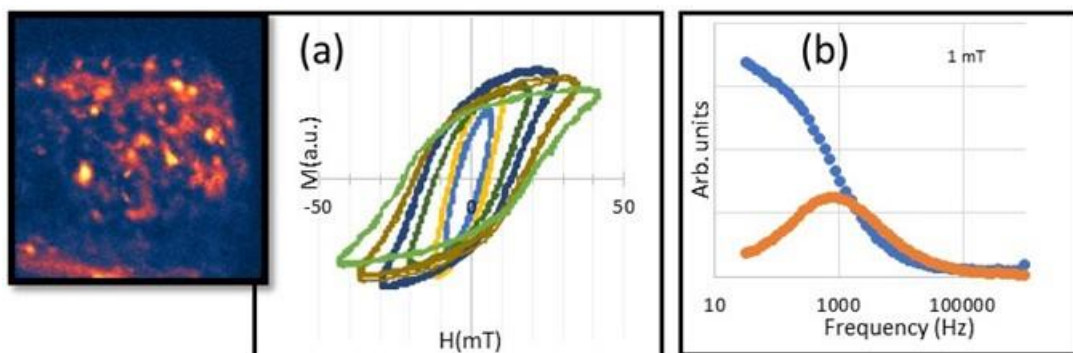


Figure 1: Example magneto-optical measurements. (a) AC hysteresis loops measured at 129 kHz from magnetite nanoparticles immobilised on a biological membrane. (b) AC susceptibility curves measured from an aqueous magnetite nanoparticle suspension (blue – in phase component, orange – out of phase component). Inset shows the fluorescence lifetime phase image from the nanoparticles measured in (a).

Strategies for biometric parameters readout using spintronic sensors

S.Cardoso^{1,2,*}, P.Ribeiro^{1,2}, M.Neto^{1,2}, M.Silva^{1,2}, P.Ribeiro^{1,2}, R.Ferreira³, P.P.Freitas^{1,3}

¹INESC-MN, Rua Alves Redol 9, 1000-029 Lisboa, Portugal

²Instituto Superior Técnico (IST), Univ. de Lisboa, Av. Rovisco Pais, 1000-029 Lisboa, Portugal

³International Iberian Nanotechnology Laboratory, Braga, Portugal

*Presenting Author: scardoso@inesc-mn.pt

Magnetoresistive (MR) sensors were driven by the technological requirements and economic progress of computers and information storage in the early 1990's, and have presently a mature level of implementation in the market. This talk will explore emerging areas related with biosensing where MR sensors have been evaluated as an alternative to other sensing technologies, including wearable devices. Our attention will be oriented towards architectures enabling the detection of sub-nanoTesla fields, for heart and brain activity monitoring, but we will also describe other biometric parameters that can be assessed using magnetic concepts, such as tactile sensors and wearable magnetic sensor devices.

We will start by describing the challenges in designing and optimizing the signal-to-noise ratio of spintronic sensors to detect magnetic fields existing in the human body (heart, brain,...). The MR materials used for reliable operation are discussed, focusing on ultrathin (~1nm) amorphous AlOx and crystalline MgO tunnel barriers, combined with soft ferromagnetic electrodes. The ultimate field detectable by a MR sensor is conditioned by the noise level, therefore particular interest has been addressed to reaching pTesla detectivities at room temperature, with high impact towards competing technologies as SQUIDS or other hybrid devices, as described in a recent roadmap from the IEEE society [1]. The microfabrication challenges are discussed, supported with the key requirements for some technological applications from biomedical [3] and robotics applications [4]. In these applications, the use of flexible interconnections enable advantageous integration in flexible interfaces of wafer-scale sensor chips with optimized performance and low cost production. Examples will be provided where spintronic sensors can detect surface topography and are useful tools in pressure sensing [2] which opens a realm of applications for tactile sensors in robotic hands.

References

- [1] Chao Zheng, et.al., "Magnetoresistive Sensor Development Roadmap (Non-Recording Applications)", IEEE Trans.Magn. 55 (4), pp. 1-30 (2019)
- [2] P.P.Freitas, R.Ferreira and S.Cardoso "Spintronic Sensors", Proceedings of the IEEE, 104 (10), pp. 1894 - 1918 (2016)
- [3] S.Cardoso, et.al, "Challenges and trends in magnetic sensor integration with microfluidics for biomedical applications", Journal of Physics D-Applied Physics, 50 (21), 213001 (2017)
- [4] Pedro Ribeiro, et.al., "Bio-inspired ciliary force sensor for robotic platforms" , IEEE Robotics and Automation Letters (RA-L) vol.2 (2), 971-976 (2017)

Magnetophoresis, sedimentation, and diffusion of dia- and paramagnetic particles in gradient magnetic field from ferromagnetic microwire systems

A. V. Beklemisheva^{a,b}, A. A. Gurevich^{a,b}, L. V. Panina^{a,b}

^a National University of Science and Technology (NUST MISIS), Moscow, 119049, Russia

^b Institute for Design Problems in Microelectronics RAS, Moscow, 124365, Russia

The use of gradient magnetic fields is one of the attractive methods for remote control of transport and diffusion of dia- and para-magnetic particles of micro and nano dimensions. This is of considerable interest for applications in miniature biochemical laboratories and medical physics. This paper proposes in a new system of micro magnets based on amorphous microwires of Co-rich composition in a glass biocompatible shell to create magnetic fields with gradients in the range of 10^3 - 10^5 T/m. Depending on the wire magnetization and their spatial arrangements, a number of magnetic energy profiles are realized, which are characterized by 2D minima located in the vicinity of wires. A camel-like energy minimum forms in the central plane between two microwires magnetized along a diameter (x-axis). In this case, a stable diamagnetic trap is possible at the height of about the wire radius as demonstrated in Fig. 1a. The microwires can be used as magnetic tweezers: two or more microwires located towards each other and magnetized along the length generate magnetic fields with strong spatial distribution. Thus, the magnetic energy of two wires located along their axis (z-axis) has a minimum in the central plane along the radius as shown in Fig. 1b. The designed magnetic field sources are interesting for cell sorting and manipulation. A minimally invasive non-contact magnetic trapping method is proposed for controlling cell movement and targeted drug delivery, which may be used in cell therapy [1-2]. The authors have obtained preliminary data on the potential use of permanent magnetic fields together with nanomaterials for cell death induction in Jurkat cell line, without human peripheral blood mononuclear cells viability inhibition.

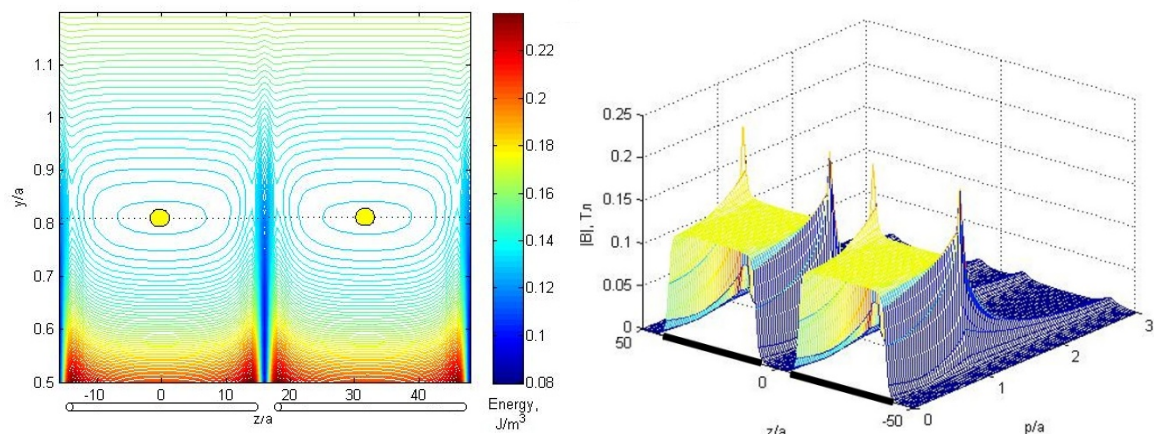


Fig.1. (a): Equipotential curves of the total energy (magnetic and gravitational) for a diamagnetic cell with the susceptibility $\chi = -10^{-5}$ in the plane ($x = 0$) for a periodic system of microwires magnetized along a diameter. Parameters for calculation: wire radius $a = 7 \mu\text{m}$, distance between the wires $d = 2a$, wire length $L = 16a$. The cell is captured by a magnetic trap over the micro wires. (b): The distribution of magnitude of magnetic field induction $|B|$ from a pair of micro wires, with longitudinal magnetization.

-
- [1] Nguyen H. P., Vy T. H. // British Journal of Applied Science & Technology 2017. 7. № 10798
[2] M. Rubio Ayala, et al//Th. Simmet. Biomaterials. (2018) 163, 174

When noise becomes data: characterizing magnetic nanoparticles using thermal noise magnetometry

J. Leliaert^a, A. Coene^a, M. Liebl^b, D. Eberbeck^b, U. Steinhoff^b, F. Wiekhorst^b,
B. Fischer^c, L. Dupré^a and B. Van Waeyenberge^a

^aGhent University, Ghent, Belgium

^bPhysikalisch-Technische Bundesanstalt, Berlin, Germany

^cHamburg University, Hamburg, Germany

In recent years, magnetic nanoparticles have attracted a lot of interest due to their appealing properties for biomedical applications. For instance, when exposed to an alternating magnetic field, they generate heat which can be used in the destruction of cancer cells. Furthermore, when equipped with a suitable coating, they can be ideal drug carriers or disease detectors. Finally, the combination of their small sizes, giving them virtually full body access, and a large magnetic moment, enabling noninvasive detection, makes them excellent candidates for use in imaging applications[1]. However, for these applications to work safely and reliably, the nanoparticle properties should be well known and their dynamic behavior should be fully understood.

Typically, magnetic nanoparticles are investigated by measuring their response to externally applied magnetic fields. For example, in magnetorelaxometry[2], the relaxation of the magnetic moment of the nanoparticles is measured after a magnetization phase in an externally applied field. However, such external excitations affect the aggregation state of the particles by e.g. inducing chain formation, and thus influence the measurement results.

We recently demonstrated the feasibility of a new approach[3], in which the noise signal resulting from the thermal switching of the nanoparticles in the absence of any external excitation is measured. With the help of SQUIDs in a magnetically shielded environment, a noise spectrum originating from the nanoparticles has been observed, and the shape of the spectrum was interpreted to estimate the properties of the nanoparticles. Here, we present thermal noise magnetometry results of several magnetic nanoparticle samples, and show the complementarity and similarity to magnetorelaxometry data of the same samples[4].

[1] Gleich, B., & Weizenecker, J. *Nature*, 435 (7046), 1214 (2005)

[2] Wiekhorst, et al. *Pharmaceutical research*, 29(5), 1189-1202 (2012)

[3] J. Leliaert, et al., *Appl. Phys. Lett.*, 107, 222401 (2015).

[4] J. Leliaert, D. Eberbeck, et al., *J. Phys. D: Appl. Phys.* 50 (8), 085004 (2017)

Investigation of influences on vessel constriction in magnetic drug targeting using a numerical model of a branched vessel

Veronica Gonella, Daniel Baumgarten

Institute of Electrical and Biomedical Engineering, UMIT – Private University for Health Sciences, Medical Informatics and Technology, Hall in Tirol, Austria

Magnetic drug targeting is a promising approach in cancer therapy, where therapeutic substances are bound to magnetic nanoparticles and directed to a target region by an external magnetic field. However, the complete understanding and accurate control of the nanoparticles' behaviour still represents a challenge. Mathematical models emulating the physical principles are a valuable tool to understand the influence of important parameters of the particles and the applied magnetic field and might provide the basis for therapy planning in the future. In this work, we investigate different influences on vessel constriction due to particle accumulations below the magnet in a simplified branched artery model.

We developed a computational fluid dynamic model to predict the transport of magnetic nanoparticles in a fluid flow under the influence of an external magnetic field. In our model, developed in COMSOL Multiphysics, the advection-diffusion equation was implemented to describe the ferrofluid mass transport and coupled to the Maxwell equations to describe the magnetic field. A two-way coupling approach [1] has been employed to consider the fluidic drag on the particles as well as the magnetic momentum transfer from the accelerated nanoparticles towards the fluid. The model was verified by reproducing the setup of experimental investigations containing a Y-branched tube and a permanent magnet in specific positions and comparing the outcome of the simulation to the experimental results [2].

In this work, the time-dependent ferrofluid behaviour was simulated using the same model and the targeting efficiency, i.e. the fraction of ferrofluid attracted to the branched tube by the magnet was computed. Magnetic field positions as well as particle concentration and properties were varied, and the respective target efficiency was studied in the resulting target maps. Figure 1 shows the simulated particle concentration for a specific magnet position (left) and the target map (right) illustrating the target efficiency for different magnet positions with the respective magnetic volume forces. We observed that the targeting efficiency increased with the magnetic fluid volume force on the ferrofluid determined by the distance of the magnet. However, bringing the magnet too close to the tube leads to a drop in the efficiency due to obstruction of the branched tube by ferrofluid being kept below the magnet.

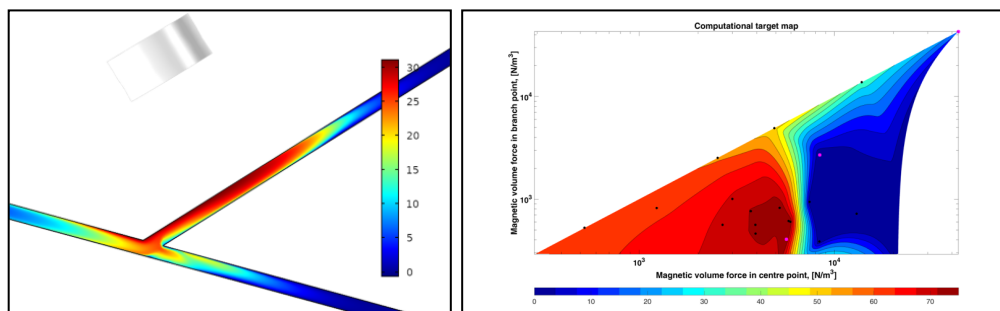


Figure 1: *Ferrofluid molar concentration distribution in the bifurcation region and in the target branch expressed in mol/m³ (left) and computational target maps showing the percentage of ferrofluid uptake in the target region (right).*

[1] Fratzl et al., *Soft Matter*. **14** (2018), 2671-2681.

[2] Gitter et al., *J. Mag. Magn. Mat.* **323** (2011), 1413-1416.

Advances in Magnetism 2020-21, June 13-16, 2021

Magnetic recording, magnetic memories and sensors

[Abstracts can be easily browsed through the bookmarks](#)

Advances in compliant magnetic field sensorics

Denys Makarov^a

^a Helmholtz-Zentrum Dresden-Rossendorf e.V., Dresden, Germany

The recent rapid advance and eagerness of portable consumer electronics stimulate the development of functional elements towards being lightweight, flexible, and wearable. Next generation flexible appliances aim to become fully autonomous and will require ultra-thin and flexible navigation modules, body tracking and relative position monitoring systems. Key building blocks of navigation and position tracking devices are magnetic field sensors.

Although there is a remarkable progress in the field of shapeable magnetoelectronics [1], until recently there was no technology available that can enable sensitivities to geomagnetic fields of 50 μT and, ultimately, magnetic fields of smaller than 1 μT in a mechanically compliant form factor. If available, these devices would contribute greatly to the realization of high-performance on-skin interactive electronics [2,3] and point of care applications [4,5].

Here, we will present technological platforms allowing to realize not only mechanically imperceptible electronic skins, which enable perception of the geomagnetic field (e-skin compasses) [6], but also enable sensitivities down to ultra-small fields of sub-50 nT [7]. We demonstrate that e-skin compasses allow humans to orient with respect to earth's magnetic field ubiquitously. Furthermore, biomagnetic orientation enables novel interactive devices for virtual and augmented reality applications. We showcase this by realizing touchless control of virtual units in a game engine using omnidirectional magnetosensitive skins (fig. 1). This concept was further extended by demonstrating a compliant magnetic microelectromechanical platform (m-MEMS), which is able to transduce both tactile (via mechanical pressure) and touchless (via magnetic field) stimulations simultaneously and discriminate them in real time [8]. Those devices are crucial for interactive electronics, human-machine interfaces, but also for the realization of smart soft robotics with highly compliant integrated feedback system as well as in medicine for physicians and surgeons

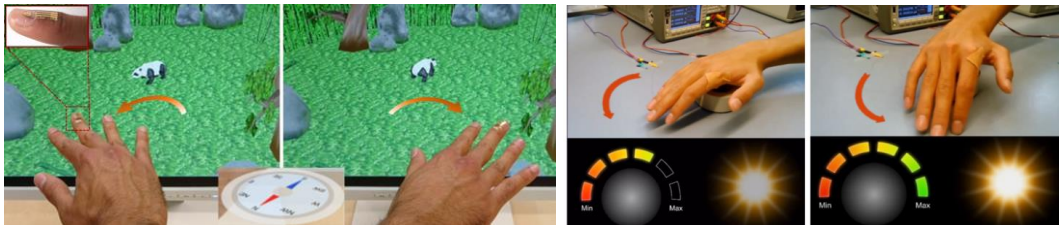


Figure 1: Magnetic skins for touchless interactive electronics: (left) Snapshots of a movie showing control of the trajectory of a virtual character (panda) by hand motion in the geomagnetic field [6]. (right) Snapshots of a movie showing the use of compliant magnetic field sensors to manipulate physical properties of virtual objects by turning a hand, e.g. dimming the intensity of light of a virtual bulb [2].

-
- [1] D. Makarov et al., *Applied Physics Reviews* **3** (2016), 011101.
 - [2] G. S. Canon Bermudez et al., *Science Advances* **4** (2018), eaao2623.
 - [3] M. Melzer et al., *Nature Communications* **6** (2015), 6080.
 - [4] G. Lin et al., *Lab Chip* **14** (2014), 4050.
 - [5] G. Lin et al., *Lab Chip* **17** (2017), 1884.
 - [6] G. S. Canon Bermudez et al., *Nature Electronics* **1** (2018), 589.
 - [7] P. N. Granell et al., *npj Flexible Electronics* **3** (2019), 3.
 - [8] J. Ge et al., *Nature Communications* (2019). doi:10.1038/s41467-019-12303-5

SAF-based perpendicular magnetized GMR spin-valves on flexible substrates

S. Laureti^a, G. Varvaro^a, M. Hassan^{a,b}, C. Rinaldi^c, S. Varotto^c, G. Barucca^b, O. Lik^d, N. Schmidt^d and M. Albrecht^d

^a Istituto di Struttura della Materia, CNR, nM2-Lab, Monterotondo Scalo (Roma), Italy

^b Università Politecnica delle Marche, Dipartimento SIMAU, Ancona, Italy

^c Department of Physics and IFN-CNR, Politecnico di Milano, Milano, Italy

^d Institute of Physics, University of Augsburg, Augsburg, Germany

Flexible electronics has received a great deal of attention over the past decades for its outstanding potential in many technological fields [1-3]. The ability to bend and adjust the shape of a device and the low weight and costs make flexible devices more advantageous than their conventional counterparts on rigid substrates. While the progress and development of longitudinal magnetized devices on non-planar substrates has been remarkable over the last years, perpendicularly magnetized structures on flexible substrates are rather unexplored despite they allow for additional functionality and improved performance.

In this work, flexible Co/Pd-based GMR spin-valve multi-stacks consisting of a [Co/Pd]_N free layer and a fully compensated [Co/Pd]_N/Ru/[Co/Pd]_N synthetic antiferromagnet reference electrode separated by a Cu spacer, were prepared both by direct deposition on polyethylene naphthalate (PEN) polymer tapes and by using a transfer-and-bonding approach exploiting the low adhesion of a gold underlayer to SiOx/Si(100) substrates [4]. The first strategy has the advantage of being a one-step process that allows for high surface coverage, being however limited to materials that do not require high processing temperatures (< 180°C). In contrast, the transfer-and-bonding approach is a more complex and multistep process, which is, on the other hand, compatible with high processing temperatures and it allows for stack transfer to arbitrary flexible substrates. As shown on Fig. 1, large-area flexible spin-valve thin film heterostructures with a GMR ratio comparable to that of conventional rigid heterostructures deposited on SiOx/Si(100) substrates were obtained. The larger GMR ratio of flexible samples on PEN tapes is due to the lower surface roughness with respect to the gold underlayer. Measurements under bending conditions also reveal the robustness of the flexible spin-valves, whose magneto-resistive properties are moderately affected even under a bending angle of 180°, thus paving the way for their integration on curved surfaces.

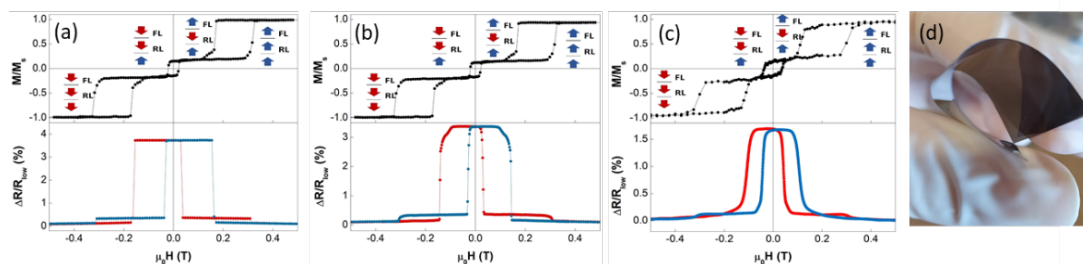


Fig.1 (a,b,c) Room temperature out-of-plane hysteresis loop and corresponding magneto-resistance response of SAF-based spin-valve on (a) rigid SiOx/Si(100) substrates (reference samples) and flexible tapes obtained by (b) direct deposition on PEN polymer tapes and (c) by using the Au-mediated transfer-and-bonding approach. (d) Representative picture of a flexible spin-valve thin film stack obtained by direct deposition on PEN tapes.

[1] Flexible Electronics. W.S. Wong and A. Salleo, Eds., Springer (2009)

[2] D. Makarov et al., Appl. Phys. Rev. 3 (2016) 011101

[3] M Melzer et al., J. Phys. D: Appl. Phys., (2020), 53, 083002

[4] G. Varvaro, M. Hassan et al., Nanoscale, (2019), 11, 21891

Control of Chirality and hysteresis in asymmetric vortex-based TMR sensors

S. Dounia^a, S. Teresi^b, J. Alvarez-Hérault^a, L. Lombard^a, J.R. Childress^a, I.L. Prejbeanu^b, C. Baraduc^b

^a Crocus-Technology, Grenoble, France

^b SPINTEC, UGA CEA CNRS, Grenoble, France

In the context of miniaturization, energy conservation, smart devices and IOT, magnetic field sensors based on magnetic tunnel junctions (MTJ) constitute an attractive choice, with small size, very high intrinsic sensitivity and low power consumption. The specific sensor response curve is determined by the magnetization configuration and hysteresis loop behavior of the soft (sensing) layer of the MTJ. A possible implementation is the vortex-based sensor, in which the junction sensing layer magnetization is in a vortex configuration at zero field, consisting of a small central core with out-of-plane magnetization and an in-plane magnetization rotating around the core with a specific chirality (clockwise or counterclockwise). Depending on the geometry, the vortex can be the natural stable micromagnetic configuration of the sensor, with the lowest energy at remanent state. This is the case for circular dots of soft ferromagnetic materials with sufficient thickness [1]. Circular vortex-state sensors typically exhibit much lower sensitivity compared to uniform-magnetization sensors, but are naturally linear and exhibit low hysteresis in a limited field range [2].

Here we use micro-magnetic simulations to study the effect of geometrical asymmetry [3] on the vortex properties, in particular on the vortex nucleation, chirality and magnetization cycle. We explore different modifications of the magnetic dot shape that ensure the control of the vortex chirality. We specifically study magnetic disk or ellipse with a cut on one side of different size and shape. Then we determine the geometrical parameters (in particular the position and size of the cut) that also allow a large nucleation field, thus leading to a quasi-linear response on a large field range. However, due to the asymmetric shape, the control of the vortex chirality is obtained at the cost of a small hysteresis: in general, the magnetization is not exactly zero at remanence. In order to reduce this hysteresis, we study magnetization at remanence for different dots with cut by varying the geometrical parameters and show that certain combination of parameters give zero magnetization at remanence. An analytical model also describes this result, obtained by micromagnetic simulations. Finally, another route to reduce hysteresis is to take advantage of magnetostatic interaction between magnetic dots within a 2D array [4]. The stray field of neighboring dots influences the vortex core position and may thus reduce the magnetization at remanence. This effect is explored for pairs of asymmetric dots at different distance and position. Our results show various means to reduce and even cancel the hysteresis.

[1] R. Cowburn et al., Phys. Rev. Lett. **83** (1999), 1042

[2] D. Suess et al., Nature Elec. **1** (2018), 362

[3] S. Agramunt-Puig et al., Appl. Phys. Lett. **104** (2014), 012407

[4] O. Sukhostavets et al., Phys. Rev. B **87** (2013), 094402

Application of the magnetostatic method of moments for computationally efficient magnet system design

Michael Ortner^a and Perla Malagó^a

^a Silicon Austria Labs GmbH, Sensor Systems, Europastraße 12, 9524 Villach, Austria

Nowadays, there is a variety of applications for permanent magnet assemblies, based on the idea that the superposition of the fields of multiple magnets results in a field of beneficial form or amplitude. Examples are Halbach arrangements [1] that generate very homogenous fields of high amplitudes, or field shaping applications [2] to achieve a desired functional form of the field for sensing purposes.

The proposal in [3] to design magnetic sensor systems based on analytical models is easily extended to design magnet systems. However, the accuracy of the analytical approximation is questionable when dealing with strongly opposing fields from multiple permanent magnets and realistic materials having $\mu_r > 1.1$ that exhibit demagnetization effects. On the other hand, a full treatment using heavy finite element (FE) simulation inhibits geometric optimization as pointed out in [3].

Here, we discuss the accuracy of the analytical approach and show that (FE) reaches its limit quickly. A method of moments implementation [4] based on point matching for construction of the demagnetization tensor is introduced as a powerful alternative for including demagnetization effects, while avoiding the usual geometry approximations in rectangular grids. It is demonstrated that with this method it is possible to find global optima for magnet systems in continuous spaces of several dimensions without referring to distributed computation, GPUs or mainframes.

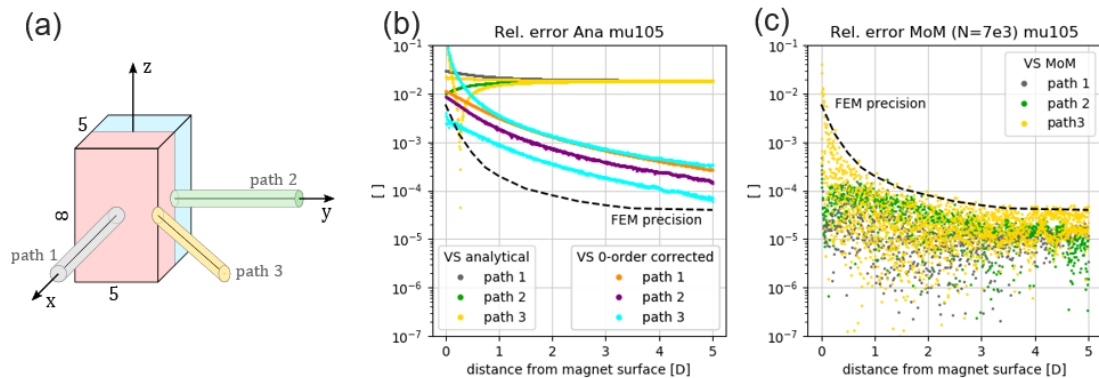


Figure: (a) Sketch of magnet and paths where field is tested. (b) Relative error of analytical models. (c) A method of moments with less than 10^4 cells undercuts a FEM with more than 10^6 elements and computes several orders of magnitude faster.

-
- [1] Bjørk, R. et al., "Optimization and improvement of Halbach cylinder design." *Journal of Applied Physics* **104.1** (2008): 013910.
 - [2] Ortner, M. et al., "Application of 3D-printed magnets for magnetic position detection systems." *IEEE sensors proceedings 2017* (pp. 1-3).
 - [3] P. Malagó et al., "Magnetic Position System Design Method Applied to Three-Axis Joystick Motion Tracking." *Sensors* **20.23** (2020): 6873.
 - [4] Chadebec, O. "A review of magnetostatic moment method." *IEEE Transactions on magnetics* **42.4** (2006): 515-520.

Magnetic characterization of free-standing membranes for spin polarimetry

M. Cantoni, L. Nessi, C. Rinaldi, R. Bertacco

PoliFab and Department of Physics, Politecnico di Milano, Italy

Arrays of free-standing magnetic membranes with nanometric thickness can be effectively employed as spin detectors of electron beams, either generated by an electron gun or photoemitted by a sample in electron spectroscopy experiments [1]. The working principle is the selective transmission of electrons with spin parallel or anti-parallel to a quantization axis defined by the direction of the magnetization of a ferromagnetic layer [2]. A proper fabrication process is needed to obtain the free-standing membranes, that must be thin, mechanically robust and self-sustaining, and yielding efficient transmission (>0.05) and spin asymmetry (~ 0.5).

The desired quantization axis (in-plane or out-of-plane) is defined using different magnetic materials and/or stacks, e.g. Co or CoFeB for the in-plane configuration and Co/Pt or CoFeB/Ta for the out-of-plane one. The whole structure, including a mechanical support layer (e.g. a graphene layer, titanium, chromium,...), the magnetic layer and a protective overlayer, cannot exceed the thickness of ten nanometers in order to guarantee a reasonable transmission of the device.

Micrometric structures with honeycomb geometry to maximise the effective area, suitable to be integrated on membranes, were fabricated by magnetron sputtering and optical lithography (see Fig. 1(a)). The CoFeB thickness and annealing temperature were optimized to achieve in-plane or out-of-plane magnetization, and fully characterized by Vibrating Sample Magnetometer, Faraday Effect and micro-Kerr effect. In Fig. 1(b) is reported the local probing, at the micrometric scale, of the magnetic properties of a structure, yielding relevant information as magnetic remanence, coercive field, and magnetic domain structure and dynamics.

Integration of this template on ultrathin graphene films (few monolayers) was then addressed, with attention to the mechanical reliability of the films during all fabrication processes. The next step of this work will be the characterization of the membrane spin filtering properties through a spin-polarized beam of low energy electrons, in order to determine the transmitted beam polarization [3] and the final figure-of-merit of the device.

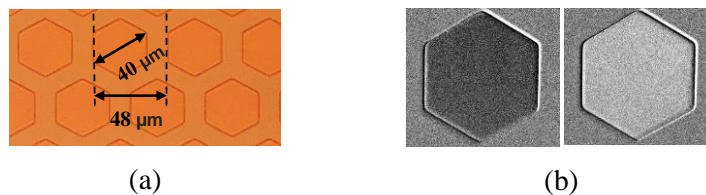


Figure 1: (a) micrometric honeycomb array of the magnetic membranes; (b) Magnetic contrast in a single membrane upon reversal of the magnetic field (in saturation conditions). Black/white colour indicates upwards/downwards magnetization, while grey colour corresponds to the non-magnetic area surrounding the membranes.

[1] Y. Lassailly et al., Phys. Rev. B **50** (1994) 13054(R)

[2] T. Övergaard et al., arXiv:1709.03838v3.

[3] M. Cantoni and R. Bertacco, Rev. Sci. Instrum. **75** (2004) 2387-2392

Transformation temperature mapping and distribution of locally induced phase transformations in Ni-Mn-Ga thin films

M. J. Pereira^a, J. S. Amaral^a, N. J. O. Silva^a, V. S. Amaral^a, F. Albertini^b, F. Casoli^b

^a CICECO – Aveiro Institute of Materials and Physics Department, Aveiro, Portugal

^b IMEM-CNR, Parma, Italy

Ni-Mn-Ga is a ferromagnetic-shape-memory alloy (FSMA) presenting two phases, austenite and martensite, the higher and lower symmetry phases, above and below the structural transformation temperature (T_M), respectively. The martensitic transformation introduces twin boundaries at the atomic level inducing almost parallel waves on the sample's surface [1-2]. We address the transformation confined in a micro/nanoscale area, with a Scanning Thermal Microscope (SThM) probe (radius ~ 100 nm, sensitivity of ~ 1 $\Omega/^\circ\text{C}$ and 50 nm spatial resolution) to locally heat, induce the transformation and determine the corresponding T_M . The probe performs as a thermal actuator and sensor in contact mode. Structural changes during transformation can be simultaneously detected by the probe's cantilever vertical deflection. This method has been previously described in further detail [3]. For comparison, we study topography changes during homogeneous heating of the sample. We report on 400 and 100 nm Ni-Mn-Ga thin films deposited on MgO substrates, illustrating the difference between both heating scenarios. When the whole film is being heated, a $2 \times 2 \mu\text{m}$ area of the 400 nm film transforms within ~ 4 K. A SThM probing of transformations, in the same area, in up to 100 contact points presents a T_M distribution interval up to 15 K (Fig. 1). Local probing of the transformation in the same point is reproducible for more than ten heatings. When the probed area is widened to about $3 \times 3 \mu\text{m}$, the T_M distribution width is further increased, reaching about 70 K, but keeping similar average value around 350 K. Mapping of T_M distributions performed in both films are presented (Fig. 1). The results are compared with information on T_M provided by magnetization vs temperature measurements. The observed differences indicate that local environmental conditions are relevant in triggering this first order transformation process. The material around the heated volume imposes different constraints to the sliding of atom planes when compared to the homogeneous heating. Also, it is known in the Ni-Mn-Ga system that, in general, 1% change in Ni content can increase T_M by up to 80 K outside the coexistence zone of magnetic and structural transformations [4]. The role of the power locally supplied to the sample through the contact point is further matter to elucidate.

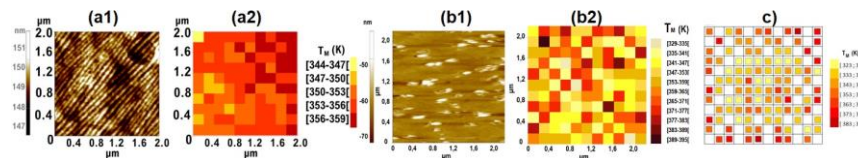


Figure 1: a1), a2) : Topography scan and T_M distribution map for a $2 \times 2 \mu\text{m}$ of 400 nm film, respectively; b1), b2) : Topography scan and T_M distribution map for a $2.2 \times 2.2 \mu\text{m}$ of 100 nm film, respectively; c) $2.2 \times 2.2 \mu\text{m}$ area of 100 nm film.

[1] Webster, P. J., Ziebeck, K. R. A., Town, S. L., Peak, M. S., *Phil. Mag. B* **49** (1984) 295.

[2] Righi, L., Albertini, F., Pareti, L. *et al.*, *Acta Materialia* **55** (2007) 5237.

[3] Pereira, M., Amaral, J. *et al.*, *Microscopy & Microanalysis* **22(6)** (2016) 1270-1280

[4] Khovaylo V. V. *et al.*, *Physical Review B* **72** (2005) 224408/1-224408/10

Driving the polar spin reorientation transition of ultrathin ferromagnets with antiferromagnetic– ferromagnetic phase transition of nearby FeRh alloy film

P. Drózdź^a, M. Ślęzak^a, W. Janus^a, M. Szpytma^a, H. Nayyef^a, A. Kozioł-Rachwał^a,
K. Freindl^b, D. Wilgocka Ślęzak^b, J. Korecki^{a,b}, T. Ślęzak^a

^a AGH University of Science and Technology, Faculty of Physics and Applied Computer Science, al. Mickiewicza 30, 30-059 Kraków, Poland

^b Jerzy Haber Institute of Catalysis and Surface Chemistry PAS, ul. Niezapominajek 8, 30-239 Kraków, Poland

Control of the spin orientation in magnetic materials is a key issue in modern spintronics. Materials with a large perpendicular magnetic anisotropy (PMA) are important from both the application and theoretical points of view, because a large PMA provides magnetization with a high thermal stability, which is necessary for high density magnetic memories.

We show an effective way to control the PMA of an ultrathin magnetic layer via indirect magnetic coupling to the FeRh layer mediated through a thin Au spacer [1]. For the PMA system we used Fe-Au monoatomic superlattices. In our experiment, structural matching of the FeRh(001) and Au(001) surfaces allowed fully epitaxial FeRh/Au/FeAu trilayers to be grown on an MgO substrate. We demonstrated that the magnetization orientation of a Fe-Au superlattices can be switched between the in-plane and out-of-plane directions by the AFM-FM phase transition in a nearby FeRh system. The observed polar spin reorientation (SRT) process of the Fe-Au spins displays the major features of a magnetic phase transition in the FeRh; namely, it is reversible and hysteretic. Accordingly, the magnetization states of the FeAu with different spin orientations can be stabilized near room temperature depending on the thermal history of the sample. This can be directly seen from comparison of PMOKE loops collected for FeAu/Au/FeRh trilayers at 280 K during cooling (blue curve) and heating (red curve) process. The hysteresis curves are characterized by a significantly different values of Kerr rotation at remanence value as shown in Fig. 1. The reported phenomenon provides a mechanism for writing information purely by the temperature change and without the external magnetic field.

The straightforward interpretation of the polar SRT process of the FeAu stack involves interlayer magnetic coupling (IMC) between the FeRh and FeAu spin systems mediated across the Au spacer. The IMC is negligible when the FeRh layer is in its AFM state and the FeAu stack displays out-of-plane magnetization originating from its intrinsic perpendicular magnetic anisotropy. When the in-plane magnetized FM phase nucleates with increasing temperature, IMC forces the rotation of the FeAu stack magnetization to the film plane.

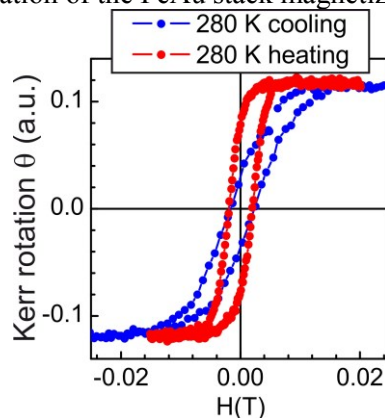


Fig. 1. The PMOKE loops collected at 280 K during cooling and heating process.

Frequency-modulated MEMS magnetometer using magnetic flux concentrators and permanent magnets

Federico Maspero^a, Simone Cuccurullo^b, Riccardo Bertacco^{a,b}

^a CNR-IFN, Politecnico di Milano, Piazza Leonardo da Vinci 32, Milano, Italia

^b Physics Department, Politecnico di Milano, Piazza Leonardo da Vinci 32, Milano, Italia

Inertial Measurement Units (IMUs) integrate an accelerometer, a gyroscope and a magnetometer to provide motion information. While accelerometers and gyroscopes are based on the MEMS (Micro-Electro-Mechanical System) technology, commercial integrated magnetometers rely on the Magneto Resistance (MR) technology due to their compact size, low cost and good performance. A MEMS magnetometer could enable a fully-MEMS IMU reducing chip size and cost, and improving performance (e.g. sensors alignment). Although several MEMS magnetometers have been proposed in the last years [1]-[3], the MR technology remains the leading one. We propose a novel frequency-modulated MEMS magnetometer inspired by the working principle of Magnetic Force Microscopy (MFM), in which the resonance frequency of a magnetized cantilever is shifted by the magnetic field gradient produced by a sample. The proposed sensor (fig. 1) comprises: i) a MEMS resonator integrating permanent magnets; ii) magnetic flux concentrators (MFCs) to shape the incoming magnetic field into a field gradient, i.e. a force gradient acting on the MEMS resonator and inducing the shift of its resonance frequency. The proposed magnetometer is compatible with industrial MEMS process. Moreover, with respect to Lorentz force magnetometers, its sensitivity does not depend on the current consumption, making the novel device a good candidate for a fully MEMS, low power, high performance IMU. Indeed, the expected power consumption and resolution of this sensors are in the order of few μW and few nT/rtHz , with large margin for process optimization. In this work, the analytical and numerical modelling of the magnetometer are presented together with preliminary experimental results. The work is part of the European FET project OXiNEMS.

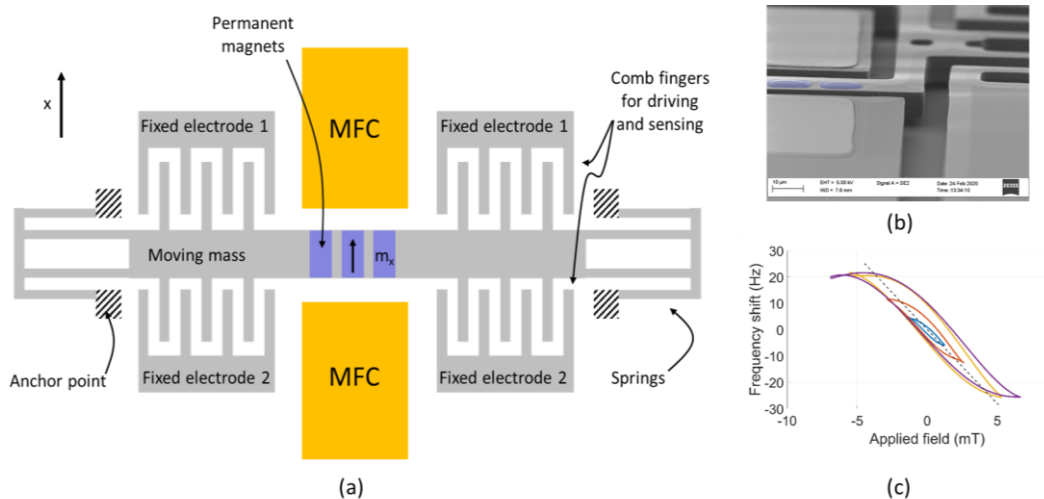


Figure 1: (a) Schematic top-view of the device; (b) SEM image of the fabricated sensor; (c) Resonance frequency shift versus applied field.

- [1] G. Laghi *et al.*, Journal of Microelectromechanical Systems, vol. 25, n. 4, 2016.
- [2] D. DiLella *et al.*, Sensors and Actuators A: Physical, vol. 86, n. 1, 2000.
- [3] Y. Hui *et al.*, Journal of Microelectromechanical Systems, vol. 24, n. 1, 2015.

MRAM adoption in microelectronics: status and perspectives

K. Garello¹, B. Dieny¹, R.C. Sousa¹, G. Prenat¹, I.L. Prejbeanu¹

¹SPINTEC, Univ. Grenoble Alpes, CEA/CNRS, F-38000 Grenoble, France

The adoption of the Spin-transfer Torque Magnetic Random Access Memory (STT-MRAM) technology by the main microelectronics industrial actors represents a major achievement of spintronics R&D. Thanks to its unique combination of assets, MRAM can be used for memory applications that other emerging non-volatile memory technologies cannot address, particularly CMOS voltage compatibility, write speed and write endurance. In fact, STT-MRAM is nowadays introduced in chips as replacement of embedded FLASH. Improving speed and power limitations of STT mechanism, Spin-orbit torque (SOT) MRAM has emerged as a credible next-generation MRAM technology targeting replacement of SRAM and offering a better footprint than CMOS-based SRAM. More advanced MRAM family concepts, based on voltage control of anisotropy (VCMA), and interconversion between spin and charge current may open the route towards ultra low power applications.

Beyond the route towards these new concepts and applications, I will introduce current MRAM technology status, discuss the many challenges that must be overcome, involving innovative materials, improved processes, and new architectural development [1]. Additionally, I will discuss the envisioned potential of MRAM for completely new computing approaches such as in-memory computing, stochastic computing or massively parallel approach as in neuromorphic architecture.

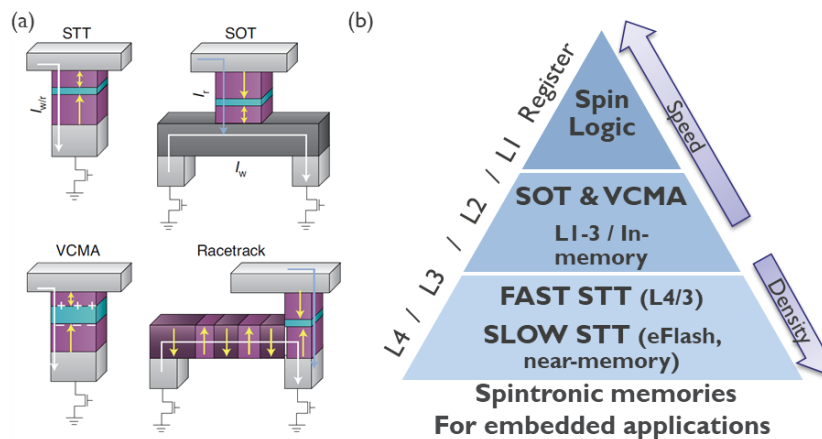


Figure: (a) Various MRAM architectures having potential to be introduced in memory hierarchy: spin transfer torque (STT), spin-orbit torque (SOT), voltage control of magnetic anisotropy (VCMA) and multibit cell based on racetrack concept, (b) Envisioned modification of the embedded memory hierarchy by spintronic solutions, possibly extending to in-memory computing and logic applications.

[1] B. Dieny et al, Opportunities and challenges for spintronics in the microelectronics industry, Nature electronics, 3, 446 (2020)

Realizing oscillation of all-in-plane spin-torque-oscillator for microwave assisted magnetic recording

H. Sepehri-Amin^a, W. Zhou^a, Y. Sakuraba^a, C. Abert^b, D. Suess^b, K. Hono^a

^a National Institute for Materials Science, Tsukuba, Japan

^b Christ Christian Doppler Laboratory, University of Vienna, Austria

Microwave assisted magnetic recording (MAMR) is considered as one of the most promising candidates for next generation higher areal density magnetic recording technology. For MAMR writer, spin torque oscillator (STO) is required that should have a size of 30-40 nm and be able to generate large $\mu_0 H_{ac} > 0.1$ T with a frequency of 20-30 GHz at a small current density $J < 1.0 \times 10^8$ A/cm² [1]. In this study, we numerically demonstrate the potential of the all-in-plane STO, which composes in-plane magnetized spin-injection layer (SIL) and field-generating layer (FGL), that can possess small thickness and current density compared to the mag-flip STO [2].

Micromagnetic simulations showed that the magnetization direction of SIL can be switched to the opposite direction to that of the applied external magnetic field by use of spin-transfer-torque that results in oscillation of FGL with a large cone angle at a reduced J . An example is shown in Fig. 1 (a) in which when the current density increases from 1.3×10^8 A/cm² to 1.4×10^8 A/cm², magnetization of SIL switches opposite to the applied magnetic field direction, increases the resonance frequency to 20 GHz with oscillation cone angle of $\sim 45^\circ$. We designed SIL to reduce the critical current density, J_{cr} , required for the magnetization switching of SIL. The materials with a smaller $\mu_0 M_s$ and spin polarization (β) in SIL and larger β for FGL results in reduction of J_{cr} , as shown in Fig. 1(b), and enables STO to oscillate with frequency of above 20 GHz with a large out-of-plane oscillation cone angle of $45\text{-}50^\circ$ [2]. The validity of this finding was studied experimentally by developing all-in-plane STO with FeNi as SIL and FeCo as FGL. At the end of the talk, we will discuss the oscillation behavior of each layer in all-in-plane STO based on experimental results as well as micromagnetic simulations [3].

Acknowledgement: This work was in-part supported by JSPS KAKENHI Grant Nos. JP19K05257 and JP17K14802.

[1] A. Takeo et al. Proc. Of the digest of Intermag conference, AD-02, 13M, 2014.

[2] H. Sepehri-Amin *et al.* JMMM 476 (2019) 361-370.

[3] W. Zhou *et al.* Appl. Phys. Lett. **114** (2019) 172403.

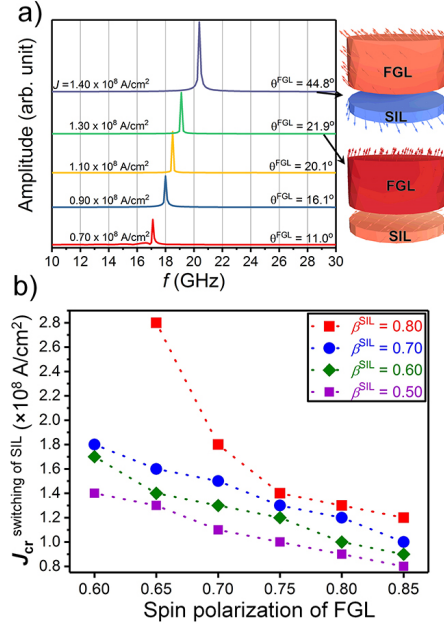


Figure 1: (a) RF spectra calculated from M_x oscillation of FGL for $\beta^{SIL} = 0.80$ and $\beta^{FGL} = 0.75$ for different J . The oscillation cone angle of FGL is also shown. (b) Critical current density required for the magnetization switching of SIL as a function of β^{FGL} and β^{SIL} in all-in-plane STO.

Effect of intermixing on HAMR dynamics in exchange spring media

Andrea Meo^a, Roy. W. Chantrell^b, Phanwadee Chureemart^a, Jessada Chureemart^a

^a Mahasarakham University, Mahasarakham, Thailand

^b University of York, York, UK

Heat assisted magnetic recording (HAMR) technology is now considered the future candidate for high density storage applications. HAMR exploits the effect of local heating on the magnetic layer during the writing process to reduce the coercive field of the high anisotropy grains, therefore making possible to reverse the magnetisation and write the information [1,2]. The subsequent fast cooling restores the grain high anisotropy and guarantees the long retention time that characterises storage devices. However, to achieve areal density as large as 4Tb/in² optimisation of both the medium properties and writing/reading mechanisms are required. A path to improve HAMR performances is to engineer the magnetic layer by coupling the hard FePt grains, characterised by large magnetic anisotropy, with grains that are soft and have higher Curie temperature. Such a coupled structure would allow to reverse the magnetisation under weaker external fields and lower temperature, if the coupling between the two layers is tuned properly. Sputtering is a very common fabrication technique employed in industrial applications. However, how the growth process might affect the smoothness and quality of interfaces has not been taken into account widely yet. For this reason, in this work we focus on the effect that intermixing between the two different phases could have on the system properties and magnetisation dynamics induced by fabrication process. We perform atomistic spin simulations of a single magnetic grain composed of FePt and a soft material, shown in Figure 1(a), by varying the degree of intermixing as function of the exchange coupling between hard and soft phase. We determine the temperature dependent equilibrium properties and investigate the magnetisation dynamics when the system is subjected to a temperature pulse and external field simultaneously. Our results (Figure 1(b)) suggest that the grain magnetisation can be reversed by temperature pulses reaching lower temperatures for a small intermixing between the two layers. However, intermixing seems to cause broader dispersion in the switching probability and this could affect the transition jitter noise negatively, degrading the device properties. Further investigation is required to understand the impact of fabrication defects on the properties and performances of HAMR media comprehensively.

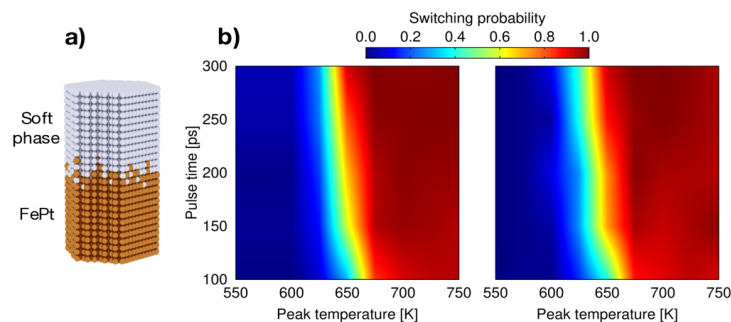


Figure 1: (a) Atomic structure of the investigated grain composed of FePt (gold) and Soft phase (silver) showing the intermixing. (b) Comparison of switching probability as function of pulse time and peak temperature for zero (left) and small intermixing (right).

[1] R.E. Rottmayer *et al*, IEEE Trans. Magn. **42**, 2417 (2006).

[2] D. Weller *et al*, J. Vac. Sci. Technol. B, **34**, 060801 (2016).

Phase stability and finite temperature magnetism of novel antiferromagnet CuMnAs

K. Carva^a, K. Uhlířová^a, P. Baláž^a, I. Turek^a, F. Máca^b, J. Kudrnovský^b, V. Drchal^b

^a DCMP, Charles University, Ke Karlovu 5, 121 16 Praha 2, Czech Republic

^b Institute of Physics of the Czech Academy of Sciences, Condensed Matter Theory,
Na Slovance 2, 182 21 Praha 8, Czech Republic

The antiferromagnetic semimetal CuMnAs has recently attracted attention of physicists due to its potential in spintronics. A controlled rotation of magnetic moments' orientation by means of an applied electrical field has been demonstrated in tetragonal CuMnAs, employing spin-orbit torques [1]. This effect allows for creation of a unique non-volatile memory device faster than flash memory and robust against magnetic field. Furthermore, it can be used to construct micron-size bit cells acting as a multi-level memory-counter [2] with potential applications in nanoelectronics. However, bulk CuMnAs natively crystallizes in the orthorhombic phase, which has different interesting properties. Tetragonal CuMnAs phase has been achieved in epitaxially deposited samples or by inserting lattice defects linked to non-stoichiometry in CuMnAs [3]. The tendency towards tetragonal phase with an increased Cu content has been confirmed by *ab initio* calculations [3].

Electronic, magnetic, and transport properties of the antiferromagnetic (AFM) CuMnAs alloy with both tetragonal and orthorhombic structure are studied here from first principles using the total energy calculations [4]. We have estimated the stability of different phases and calculate formation energies of possible defects in the alloy. Mn_{Cu} and Cu_{Mn} antisites and vacancies on Mn or Cu sublattices were identified as most probable defects in CuMnAs. We have found that the interactions of the growing thin film with the substrate and with vacuum are important for the phase stability of real samples prepared as a thin film on the appropriate substrate. We estimated also the in-plane resistivity of CuMnAs with defects of low formation energies. Our numerical simulations fitted experiment very well if we assumed concentrations 3.5-5% Mn_{Cu} antisites in the samples, much larger concentrations would be needed for Cu_{Mn} antisites or Mn-vacancies.

Finally, we have determined the exchange interactions and estimate the Néel temperature of the ideal and disordered AFM-CuMnAs alloy using the Monte Carlo approach. The decrease of the Néel temperature in the presence of antisites and vacancies has been evaluated as well [5]. A good agreement of the calculated resistivity and Néel temperature with experimental data makes it possible to estimate the structure and composition of real CuMnAs samples.

[1] P. Wadley et al., *Science* **351** (2016) 587

[2] K. Olejnik et al., *Nat. Commun.* **8** (2017), 1543

[3] K. Uhlířová et al., *Journal of Alloys and Compounds* **771** (2018) 680

[4] F. Maca, J. Kudrnovský, V. Drchal, K. Carva, P. Balaz, I. Turek, *Phys. Rev. B* **96** (2017) 094406

[5] F. Máca, J. Kudrnovský, P. Baláž, V. Drchal, K. Carva, I. Turek: *J. Magn. Magn. Mater.* **474** (2019), 467 .

All-optical switching in FeCoB/Ta/[Tb/Co]_N electrodes for the development of ultrafast magnetic tunnel junctions

L. Avilés-Félix^a, A. Olivier^a, G. Li^b, C. Davies^b, L. Álvaro-Gómez^a, M. Rubio-Roy^a, S. Auffret^a, A. Kirilyuk^{b,c}, Th. Rasing^b, L. Buda-Prejbeanu^a, R. Sousa^a, B. Dieny^a and I. L. Prejbeanu^a

^a Spintec, Université Grenoble Alpes, CNRS, CEA, Grenoble INP, IRIG-SPINTEC, 38000 Grenoble, France

^b Radboud University, Institute for Molecules and Materials, Heyendaalseweg 135, 6525 AJ Nijmegen, The Netherlands

^c FELIX Laboratory, Radboud University, 7c Toernooiveld, 6525 ED Nijmegen, The Netherlands

This work reports the development of all-optical switching electrodes consisting of a FeCoB/Ta/[Tb/Co]_N for its integration into a magnetic tunnel junction. We explore the magneto-optical properties of [Tb/Co]_N multilayers and its thermal stability upon different annealing temperatures. All-optical helicity independent - switching of the [Tb/Co] multilayers was observed in samples as-grown and even after annealing at 250 °C. In order to fabricate optically switchable electrodes, [Tb/Co] multilayers were coupled to a FeCoB layer through a Ta ultra-thin layer. Reversal of the magnetization using ultrafast single laser pulses was kept after the addition of the FeCoB layers using 60 fs- and 5 ps-long laser pulses with fluences down to 4.7 mJ/cm². Our all-optical switching electrodes FeCoB/Ta/[Tb/Co]_N were finally integrated into a perpendicularly magnetized tunnel junction. Electrical evaluation of nanopatterned AOS-MTJ showed TMR ratios up to 40 % depending on the diameter of the junctions and on the number of repetitions of the [Tb/Co] bilayers. Our results can contribute to important advances in ultrafast magnetic random access memories with new functionalities, particularly the ability to control the magnetization of the storage layer with ultrafast laser pulses.

The authors acknowledge the funding support from project SPICE (EU ITC 2020 grant agreement No. 713481)

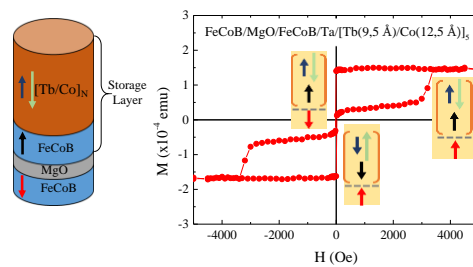


Figure 1: Left: Schematic of the AOS-MTJ. Right: $M(H)$ of the AOS-MTJ including the optically switchable electrodes and the FeCoB sensing layer.

Advances in Magnetism 2020-21, June 13-16, 2021

**Magnetic materials for
energy applications
&
Additive manufacturing of
magnetic materials**

[Abstracts can be easily browsed through the bookmarks](#)

Development of high coercivity SmFe₁₂-based permanent magnets

H. Sepehri-Amin, I. Dirba, Xin Tang, A. K. Srinithi, T. Ohkubo, K. Hono

National Institute for Materials Science, Tsukuba, Japan

Recent investigations on the intrinsic magnetic properties of SmFe₁₂-based compounds with ThMn₁₂ structure has shown that Sm(Fe_{0.8}Co_{0.2})₁₁Ti and Sm_{0.8}Zr_{0.2}(Fe_{0.8}Co_{0.2})_{11.5}Ti_{0.5} alloys reach comparable intrinsic hard magnetic properties with those of Nd₂Fe₁₄B and even superior high temperature performance [1]. However, considering their large room temperature anisotropy field, no significant coercivity has been yet reported [2-3]. This is due to the lack of understanding on the microstructure origin for their low coercivity [2-5]. In this work, in order to shed a light on how a large coercivity can be realized in these magnets, the contribution of grain size, grain boundaries, and interface defects to the coercivity of SmFe₁₂-based magnets is investigated.

We first focused on the reduction of the grain size in SmFe₁₂-based magnets by use of hydrogenation disproportionation desorption recombination (HDDR) process. We optimized HDDR process, such as hydrogen pressure during HD and temperature/time of HD and DR process to develop ultra-fine grain sized powders with ThMn₁₂ type structure [3]. However, no coercivity was realized in these powders that was due to the lack of the intergranular phase. Nevertheless, a large coercivity of 1.0 T was only realized in the rapidly solidified ribbons with composition of SmFe₁₁TiV. Detailed microstructure characterization on the ribbons showed a large coercivity cannot be realized unless only nano-sized grains with ThMn₁₂ structure are formed without SmFe₂ phase. In addition, 3DAP results showed segregation of Sm in the grain boundaries only for the sample with a larger coercivity. In order to decouple SmFe₁₂-based grains, desired grain boundary phase should be realized without formation of ferromagnetic secondary phases. We found trace addition of Ga into the Sm(Fe_{0.8}Co_{0.2})_{11-x}TiGa_x alloy lead to the formation of non-ferromagnetic Sm-Ga rich intergranular phase. Using this alloy, we will address our attempts to develop anisotropic bulk SmFe₁₂-based magnet with high coercivity.

[1] P. Tozman, H. Sepehri-Amin *et al.* Acta Mater. 153 (2018) 534.

[2] A. M. Gabay, G. C. Hadjipanayis, Scripta Mater. 154 (2018) 284.

[3] I. Dirba, H. Sepehri-Amin *et al.* Acta Mater. 165 (2019) 373.

[4] I. Dirba, H. Sepehri-Amin *et al.* J. All. Comp. 804 (2019) 155.

[5] I. Dirba, Y. Harashima, H. Sepehri-Amin *et al.* J. All. Comp. 813 (2020) 15224.

3D printing of isotropic and anisotropic hard magnets

C. Huber¹, K. Sonnleitner¹, Santiago Cano², S. Schuschnigg², M. Groenefeld³, I. Teliban³, S. Kobe⁴, B. Saje⁵, D. Suess¹

¹ CD - Laboratory for Advanced Magnetic Sensing and Materials, 1090 Vienna, Austria

² Institute of Polymer Processing, Montanuniversitaet Leoben, 8700 Leoben, Austria

³ Magnetfabrik Bonn GmbH, 53119 Bonn, Germany

⁴ Dep. of Nanostructured Materials, Jožef Stefan Institute, 1000 Ljubljana, Slovenia

⁵ Kolektor Magnet Technology GmbH, 45356 Essen, Germany

dieter.suess@univie.ac.at

Within this talk a compilation of different additive manufacturing methods for permanent magnets will be given including (i) fused deposition modeling (FDM) [1] (ii) selective laser melting (SLM) [2] and Stereolithography [3]. We will present that it is possible to produce NdFeB polymer bonded magnets with gradual change in magnetic properties, which is not possible to realize with any other method. Extending the 3D printing process allows the manufacturing of anisotropic magnetic structures by aligning the magnetic easy axis of ferromagnetic particles inside a paste-like compound material along an external magnetic field. This is achieved by two different approaches. First, the magnetic field for aligning the particles is provided by a permanent magnet. Second, the 3D printing process itself generates an anisotropic behavior of the structures. An inexpensive and customizable end-user fused filament fabrication 3D printer is used to print magnetic samples. The magnetic properties of different magnetic anisotropic Sr ferrite and SmFeN materials will be investigated and discussed (Figure 1) [4]. In the presence of an external alignment field, the Sr ferrite particles inside the PA12 matrix can be aligned along an external magnetic field. The remanence can be increased by 40% by printing anisotropic structures. For the 55 vol. % filled filament, a remanence of 212.8 mT and a coercivity of 307.4 mT are measured. The capabilities of printing magnetic anisotropic structures in a complex external field are presented with a Halbach-array arrangement.

References

[1] C. Huber et al., Appl. Phys. Lett., **109** 162401 (2016).

[2] C. Huber et al., Acta Materialia **172** 66-71 (2019).

[3] C. Huber et al., Materials **13.8** 1916 (2020)

[4] K. Sonnleitner et al., Applied Physics Letters, **116.9** 092403 (2020).

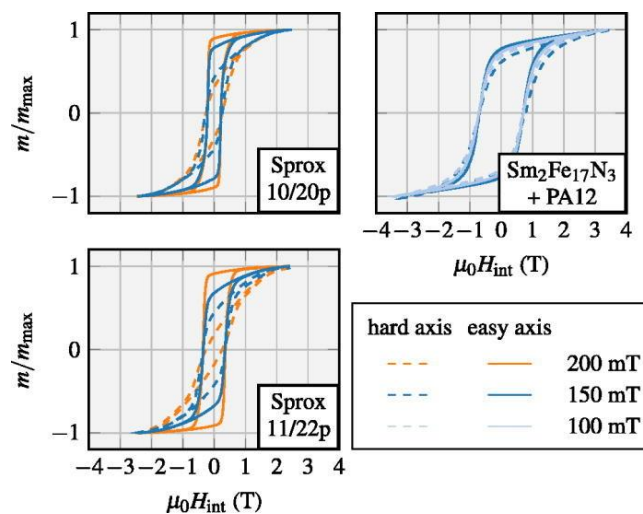


Figure 1. Hysteresis loops in hard and easy axes of three samples measured with the VSM, where H_{int} is the internal field, considering a demagnetization factor of $N = 1/3$. The samples are aligned with different magnitudes of the external field [4].

IS A CIRCULAR ECONOMY ECOSYSTEM FOR NdFeB-TYPE MAGNETS FEASIBLE

Benjamin Podmiljsak¹, Spomenka Kobe¹, Carlo Burkhardt², Antje Lehmann²,

¹ Institute Jozef Stefan, Jamova 39, 1000 Ljubljana, Slovenia;

² Pforzheim University, Tiefenbronner Strasse 65, 75175 Pforzheim, Germany;

ABSTRACT

Availability of magnetic materials is most crucial for modern Europe, as they are integral to energy conversion across the renewable energy and electric mobility sectors. Unfortunately, even though the alloying constituents of NdFeB magnets have been classified as EU Critical Raw Materials and 90% are produced outside of the EU, there is still no circular economy to reuse and capture value for these types of materials.

With the prediction that the need for RE magnets will double in the next 10 years, this problem becomes even more urgent. At present, the only way to recover end of life (EOL) magnets from waste streams of electric and electronic equipment is by shredding and recycling by chemicals and pyrometallurgical routes, which is expensive and energy intensive.

Another problem is that the quality of the recollected materials varies significantly, especially with respect to alloying constituents and state of corrosion and employed corrosion protection, with no classification system for recycle grades of EOL NdFeB magnets.

To enable a circular economy ecosystem for NdFeB magnets, a whole range of measures is necessary:

- a) the development of an eco-labelling system for newly produced RE permanent magnets to clearly identify different magnets types and qualities to categorise the EOL NdFeB magnets by technical pre-processing requirements,
- b) using the highly effective HPMS process (Hydrogen Processing of Magnetic Scrap) for re-processing extracted materials directly from NdFeB alloy,
- c) better treatments to eliminate pre-processing residue which contaminates the HPMS process,
- d) upgrading the magnetic properties of EOL NdFeB magnets by tailoring the microstructure, phase ratio and phase composition, and
- e) developing industrial up-scalability.

The feasibility of the above proposed measures will be discussed and related to actual results generated in the EU-funded projects MaXycle and SUSMAGPRO, which will have a great impact by overcoming existing low recycling rates due to poor collection, high leakages of collected materials into non-suitable channels, and inappropriate interface management between logistics, mechanical pre-processing and metallurgical metals recovery.

Predicting new rare earth lean permanent magnets by computational design -- the challenge of the 4f electrons

Heike C. Herper^a and Olle Eriksson^{a,b}

^a Department of Physics and Astronomy, Uppsala University, Sweden

^b School of Science and Technology, Örebro University, Örebro, Sweden

The rapid development of new technologies for green energy applications is related to the search for new materials for permanent magnets (PM). Today, nearly all high-performance magnets are based on Nd₂Fe₁₄B and the demand for such magnets is increasing, but the new materials should have a smaller environmental footprint. The class of Fe-based ThMn₁₂ phases contain less RE material than the commercially used compounds and is therefore interesting. An efficient and resource saving way to identify out of this class new phases suitable for PM is by computational materials design. However, an accurate prediction of magnetic properties for 4f systems can be tricky since the localization of the 4f electrons determines the level of theory needed for a reliable description.

We showed that in case of CeFe₁₁Ti the 4f states can still be viewed as valence states and for SmFe_{12-x}V_x the fully localized picture with 4f electrons in the core applies [1,2] while in NdFe₁₁Ti the 4f electrons are partially localized as can be seen from the hybridization function in Fig. 1a. The hybridization function can be viewed as a qualitative measure for the interaction with the valence electrons in a system [3].

As a consequence of the partial localization, the cone type magnetocrystalline anisotropy (MCA) of the latter system is only observed in a DFT+U description with an intermediate Hubbard U value. Assuming full localization (4f in core) results in a uniaxial MCA which contradicts the experimental findings at low temperatures. Plain DFT also fails.

We also discuss how the strong dependence of the MCA and related magnetic properties of NdFe₁₁Ti influences the prediction of new phases. Here, we focus on Nd_{1-x}Y_xFe_{12-y}Ti_y phases as an example.

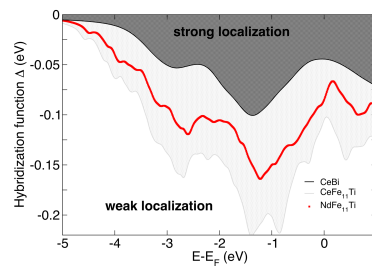


Figure 1: Hybridization function of NdFe₁₁Ti in comparison to weak localized CeFe₁₁Ti and the strongly localized CeBi system.

This work was supported by NOVAMAG (EU686056) and Swedish Foundation for Strategic Research (EM16-0039). Computational resources were provided via SNIC (Swedish National Infrastructure for Computing).

[1] A. Schönhöbel *et al.*, Journal of Alloys and compounds **786**, 969 (2019)

[2] R. Martinez-Casado *et al.*, Journal of Physics: Condensed Matter **31**, 505505 (2019)

[3] H. C. Herper *et al.*, Phys. Rev. Materials **1**, 033802 (2017)

Developing alternative permanent magnets: from the synthesis of tuned composites to additive manufacturing

Ester M. Palmero, Daniel Casaleiz, Javier de Vicente, Alberto Bollero

Division of Permanent Magnets and Applications, IMDEA Nanoscience, Madrid, Spain

Additive manufacturing (AM) is attracting much interest in many high-tech sectors as it allows for fabricating complex objects with tuned properties and high performance [1]. For developing permanent magnets (PMs) by AM, it is necessary an increased filling factor and no deterioration of their PM properties during fabrication. Many works on AM of PMs focus on NdFeB [2], however it is of large scientific and technological interest to broaden the studies by including rare earth-free alternatives. Improved ferrites and the promising MnAl-based alloys are expected to partially cover the gap between conventional ferrites and NdFeB, provided successful development of PM properties. Moreover, they show high availability, low costs and environmental impact of extraction and processing of raw materials [3].

Composites (PM particles/polymer) were synthesized and extruded into homogeneous and continuous filaments (Fig. 1(a)). Gas-atomized τ -MnAlC, Sr-ferrite and hybrid (Sr-ferrite/NdFeB) particles were used for studying different alternative PM materials. The influence of particle size, fine-to-coarse particle ratio, polymer and fabrication parameters on the properties of the final products was analysed [4], being key factors for obtaining flexible filaments with a high filling factor (>80%) and length over 10 m. Magnetic measurements (Fig. 1(b)) revealed non-deteriorated PMs properties of the particles after processing [4]. MnAlC-based filament was used for fabricating 3D objects under controlled printing temperature, proving that alternative PM materials can be efficiently synthesized and processed to develop novel PMs by AM [4].

Authors acknowledge fruitful collaboration and discussions with Höganäs AB (Sweden), and IMA S.L.U. (Spain).

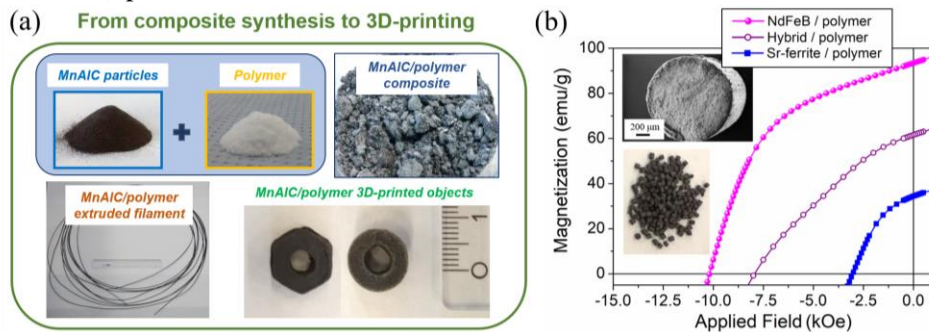


Figure 1: (a) Images of gas-atomized MnAlC particles, polymer, MnAlC/polymer composite, filament and 3D-printed objects; and (b) second quadrant of room temperature hysteresis loops for NdFeB-, hybrid (NdFeB/Sr-ferrite)- and Sr ferrite- based materials. Insets show a SEM image of the cross section of a filament and an image of Sr-ferrite/polymer pellets.

[1] L.E. Murr, *J. Mater. Sci. Technol.* **32** (2016) 987.

[2] C. Huber et al., *Appl. Phys. Lett.* **109** (2016) 162401; L. Li et al., *Sci. Rep.* **6** (2016) 36212; J. Jaćimović et al., *Adv. Eng. Mater.* **19** (2017) 1700098.

[3] A. Bollero et al., *ACS Sustainable Chem. Eng.* **5** (2017) 3243; J. Rial et al., *Acta Mater.* **157** (2018) 42.

[4] E.M. Palmero et al., *Sci. Technol. Adv. Mater.* **19** (2018) 465; Submitted (2019); *IEEE Trans. Magn.* **55** (2019) 2101004.

Magnetic Hysteresis in Electrical Steel under Arbitrary Induction Field: Preisach Model Vs Neural Network Approach

Simone Quondam Antonio^a, Francesco Riganti Fulginei^b, Antonino Laudani^b,
Antonio Faba^a, Ermanno Cardelli^a

^a University of Perugia, Italy

^b Roma Tre University, Italy

The supply conditions of recent electrical machines and magnetic devices, from automotive to industry applications, frequently involve highly distorted flux densities and non-symmetric magnetic induction waveforms. The accurate characterization of the hysteretic behaviour of the electrical steel by a computationally efficient simulation tool, accounting for the generic excitations expected, is still an open challenge. On one hand, Preisach-type hysteresis models turned out to be accurate and robust approaches, which can be directly identified from the measurements of symmetric quasi-static hysteresis cycles [1]. However, the computational time is quite high, as well as the RAM memory allocation. On the other hand, feedforward neural nets are much less time and memory consuming, but they do not intrinsically have memory and the training process is very complex [2]. Indeed the same set of symmetric quasi-static hysteresis cycles is not sufficient to effectively train the neural network and further experimental data must be provided. The authors propose here to identify a Preisach hysteresis model and use it to generate the data to be used as training set for the neural network. The aforementioned procedure has been developed for a sample of NGO electrical steel (material grade: 35H270), which was previously measured via an Epstein testing method in our laboratory. A set of 20 first-order reversal curves (FORCs), simulated via the Preisach model, turned out to be an optimum training set. The best network architecture, characterized by two hidden layers having 9 and 5 neurons respectively, has been found experimentally. Finally, the neural network-based hysteresis model is realized by including the net in a dedicated algorithm with the aim to improve the accuracy in case of highly distorted magnetic flux density waveforms. The obtained neural network-based hysteresis model, which can be easily inverted, has been compared with the Preisach model in the reconstruction of both sinusoidal and non-sinusoidal magnetization loops, that have not been used in the training data set. In the second case, that is shown in Fig. 1, the magnetic induction has been defined as the sum of a third order harmonic added to a fundamental tone at 1 Hz. In the final version of the paper, the comparison will be further extended to other magnetic flux densities, such as DC+AC, linear+AC and triangular waveforms.

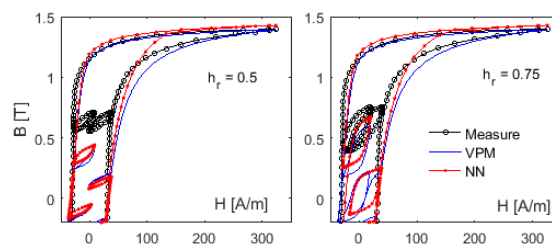


Figure 1: Hysteresis cycles obtained by a fundamental plus the 3rd order harmonic of B: measured curves are compared with those simulated by either the Preisach model (VPM) or the Neural Network (NN) for two different values of the harmonic ratio h_r .

[1] E. Della Torre et al., *Physica B*, Vol. 372, 111-114, 2006.

[2] F. Riganti Fulginei and A. Salvini, *IEEE Trans on Mag*, Vol. 48, N. 2, 307-310, 2012.

Exchange coupled magnetic nanoheterostructures with enhanced energy product

Beatrice Muzzi^{a,b}, Alberto López-Ortega^c, Martin Albino^d, Michele Petrecca^d,
Claudia Innocenti^{b,d}, Giovanni Bertoni^e, César de Julián Fernandez^e, Claudio Sangregorio^{b,d}

^a Dept. of Biotechnology, Chemistry and Pharmacy, Univ. of Siena, 53100 Siena, Italy

^b ICCOM – CNR and INSTM, Sesto F.no, 50019 Italy

^c Dept. de Física Aplicada, Universidad de Castilla-La Mancha, 45071 Toledo, Spain

^d INSTM and Dept. of Chemistry “U. Schiff”, Univ. of Florence, 50019 Sesto. F.no, 50109, Italy

^e IMEM - CNR, Parco Area delle Scienze, 37/A, Parma, 43124, Italy

Magnetic hybrid nanostructures have been largely investigated in the recent past. The combination at the nanoscale of components endowed with different magnetic properties, indeed, enable the emergence of novel intriguing phenomena, the most prominent being exchange bias and exchange spring magnet. These phenomena have been proposed in the recent past as efficient strategies to enhance the performance of magnetic materials employed in several applications, and particularly to increase the energy storage capability of permanent magnets. [1,2] The CoFe/Co_{1-x}Fe_xO/Cobalt ferrite system is particularly suited to investigate such exchange phenomena, as it comprises a soft material with the highest saturation magnetization, (245 Am²kg⁻¹ for CoFe₂), an antiferromagnet with tuneable ordering temperature in the 205 K - 295 K range, and a highly anisotropic hard magnet, which can convert one into each other by simple oxidation/reduction processes.

In this contribution we present the synthesis and investigation of the structural, morphological and magnetic properties of a series of nano-heterostructure of variable composition, belonging to the CoFe/Co_{1-x}Fe_xO/Cobalt ferrite family, aimed at investigating the possibility to exploit exchange coupling to enhance the energy product, BH_{max}, of magnetic nanoparticles. The magnetic nanostructures were prepared by thermal decomposition of metal-organic precursors (Co,Fe mixed oleate) in high-boiling solvent containing oleic acid and sodium oleate as stabilizing surfactants, and their size, shape and composition was tuned by fine control of the synthesis parameters, namely, the boiling temperature of the solvent and oleic acid to sodium oleate ratio.[3] The effect of the introduction of Ni²⁺ ion in the spinel lattice on the magnetic properties is also discussed.

This research was supported by EU- H2020 AMPHIBIAN Projects (n. 720853).

-
- [1] E. Lottini, A. Lopez-Ortega, G. Bertoni, et al. Chem. Mater. 28 (2016) 4214.
[2] A. López-Ortega, E. Lottini, G. Bertoni, et al. Chem. Mater. 29 (2017) 1279.
[3] B. Muzzi, M. Albino, C. Innocenti, et al. Nanoscale, 12, (2020) 14076.

Controlling magnetic coupling in hard-soft oxide nanocomposites

Pierfrancesco Maltoni^a, Tapati Sarkar^a, Gaspare Varvaro^b, Gianni Barucca^c, Davide Peddis^{b,d}, Roland Mathieu^a

^a Department of Materials Science and Engineering, Uppsala University, Uppsala, Sweden

^b Institute of Structure of Matter, Italian National Research Council (CNR), Rome, Italy

^c Università Politecnica delle Marche SIMAU, Ancona, Italy

^d Dipartimento di Chimica e Chimica Industriale, Università di Genova, Genova, Italy

Magnetic nanocomposites (NCs) have gained a lot of interest over the last years, due to the possibility to finely control and modify their features at the nanoscale, which allows to extend their applicability as permanent magnets in a multitude of energy-related technological areas [1,2]. In this regard, exchange coupled hard-soft NCs have received significant attention, as a promising strategy to achieve high magnetic performances. By combining materials with intrinsically different physical properties, the large coercivity (H_C) of the hard-magnetic phase and high saturation magnetization (M_S) of the soft one can be maximized simultaneously in the same material. Hereby our focus is on the role of synthesis strategy in obtaining efficiently magnetically coupled NCs, based on $SrFe_{12}O_{19}$ (SFO) and $CoFe_2O_4$ (CFO) ferrites. This work is aimed at extensively studying the evolution of the magnetic properties of various SFO/CFO NCs (SFO/CFO w/w % ranging from 50/50 to 90/10 with a step of 10%) as a function of the particle size and shape. Particularly, we address the sol-gel self-combustion chemical approach as a unique way to develop such NCs, compared to physically mixing [3,4]. By means of X-ray powder diffraction (XRPD), transmission electron microscopy (TEM) and SQUID magnetometry we demonstrate that the magnetic behaviour of the different samples is closely related to their morphology and composition. We achieve a significant control over the size (with SFO ranging between ~ 132 and 51 nm) and shape of the crystallites of the individual phases, also suggesting for the first time an oriented growth of the two phases. Our results reveal that the CFO and SFO phases are strongly coupled inside the NC as the switching field distributions clearly exhibit a single reversal process of magnetization. Furthermore, introducing larger amounts of the soft CFO phase decreases H_C from ~ 463 to 178 kA/m. In conclusion, our study clearly shows that the synthesis strategy plays a critical role in the extent of magnetic coupling that can be achieved between the hard-soft phases.

We thank the Swedish Energy Agency and Swedish Research Council (VR) for financially supporting this work.

[1] R. Skomski, P. Manchanda, P. K. Kumar, B. Balamurugan, A. Kashyap, D. J. Sellmyer, *IEEE Trans. Magn.* **49** (2013), 3215-3220

[2] K. P. Skokov, O. Gutfleisch, *Scr. Mater.* **154** (2018), 289-294

[3] F. Sayed, G. Kotnana, G. Muscas, F. Locardi, A. Comite, G. Varvaro, D. Peddis, G. Barucca, R. Mathieu, T. Sarkar, *Nanoscale Adv.* **2** (2020), 851-859

[4] P. Maltoni, T. Sarkar, G. Varvaro, G. Barucca, S. Ivanov, D. Peddis, R. Mathieu, J. *Phys. D: Appl. Phys.* **54** (2021), 124004

Structural and electronic properties of cobalt doped NdMnO₃

Farooq H. Bhat^a, Ghazala Anjum^b,

^aDepartment of Physics, Islamic University of Science and Technology, Awantipora, India

^bDepartment of Physics, SP College, Cluster University Kashmir, Srinagar, India

The perovskite manganites are fascinating compounds to study because of the myriad properties they exhibit like ferromagnetism, anti-ferromagnetism, metal-insulator transition, etc. It is known that Co induces ferromagnetism (FM) in LaMnO₃ on doping at Mn site, but finds no general agreement on exchange mechanism responsible for it [1,2]. In Co doped NdMnO₃ no such study has been done; therefore, this work was undertaken to study the effect of Co on structural and electronic properties of NdMnO₃, Nd being magnetic.

Single phase NdMn_{1-x}Co_xO₃ (x = 0.0, 0.3, 0.7) (NMCO) samples were prepared using conventional solid state reaction method. X-ray diffraction studies reveal their orthorhombic perovskite structure with *Pbnm* as a space group. It is observed that for NdMnO₃ (NMO) $c/\sqrt{2} < a < b$; hence take O' type orthorhombic structure due to Jahn-Teller (J-T) distortion and rest of the samples take O type orthorhombic structure with $a < c/\sqrt{2} < b$. It is a known fact that Mn³⁺ is a highly J-T ion and our XAS results confirm Mn is in +3 valence state in NMO; therefore, its O' type orthorhombic structure is explained. The XRD studies indicate the lattice contraction due to Co substitution at Mn site resulting in the decrease of unit cell volume. This decrease could be attributed to the presence of Co²⁺/Co³⁺ and Mn⁴⁺ valence states in addition to Mn³⁺ in NdMn_{0.7}Co_{0.3}O₃ (NMCO3) and NdMn_{0.3}Co_{0.7}O₃ (NMCO7) samples, confirmed from XAS studies; since the ionic radii of Mn³⁺ > Co²⁺/Co³⁺ and Mn⁴⁺ ions. The Electronic structure was studied using x-ray absorption spectroscopy (XAS) in total electron yield (TEY) mode at L_{3,2} -edges of Mn and Co and K-edge of O. In Mn XAS spectra the shift of spectra towards higher energy with a change in shape from NMO to NMCO7 suggest the increase in the valence state of Mn from Mn³⁺ to Mn⁴⁺. While as in the case of Co XAS spectra it is seen that NMCO3 has the major contribution of Co³⁺ LS along with a small percentage of HS Co²⁺/Co³⁺ and in NMCO7 the contribution of Co²⁺ HS and Co³⁺ HS increases as compared to NMCO3. O K-edge confirms these results.

Thus it is concluded that Co substitution at Mn site in NdMn_{1-x}Co_xO₃ induces mixed valence state of Mn and Co itself too is found in mixed valence/spin states. This will lead to superexchange ferromagnetic (FM) and antiferromagnetic (AFM) interaction among various valence/spin states of Mn and Co along with double exchange interaction among Mn³⁺ and Mn⁴⁺ ions. This hints at the possibility of FM glassy state in NdMn_{1-x}Co_xO₃ samples.

References:

- [1] J.B. Goodenough, et al. Phys. Rev. **124** (1961), 373-384.
- [2] J. H. Park et al., Phys. Rev. B **55** (1997), 11072-11075.

Hexaferrite nanoparticles for new magnets

César de Julián Fernández^a, Durgamadhab Mishra^{a,b}, Michele Petrecca^c, M. Albino^c, Anna Zink Eikeland^d, Marian Stingaciu^e, Riccardo Cabassi^a, J. Guzmán-Mínguez^f, Fulvio Bolzoni^a, Franca Albertini^a, Beatrice Muzzi^{g,h}, Blac Belec^a, Adrian Quesada^f, T. Schlieschⁱ, Mogens Christensen^d, Petra Jenus^j, Stefano Deledda^e, Claudio Sangregorio^h

^a Institute of Materials for Electronics and Magnetism - CNR, Parma, Italy

^b Department of Physics, Indian Institute of Technology Jodhpur, Jodhpur, India
^c INSTM and Dept. Of Chemistry "U. Schiff", Univ. of Florence, Sesto. Fno, Italy

^d Department of Chemistry, Aarhus University, Aarhus, Denmark

^e Institute for Energy Technology, Kjeller, Norway

^f Instituto de Cerámica y Vidrio -CSIC, Madrid, Spain

^g Dept. Biotechnology, Chemistry and Pharmacy, Univ. of Siena, Siena, Italy.

^h Institute of Chemistry of Organometallic Compounds - CNR, Sesto Fiorentino, Italy

ⁱ Max Baermann GmbH, Bergisch Gladbach, Germany.

^j Dept. Nanostructured Materials, Jožef Stefan Institute, Ljubljana, Slovenia.

The nanostructural and magnetic properties of M-type hexaferrite single-domain particles with different nanometric sizes and morphologies will be discussed considering their application for magnets. Most ceramic magnets are composed by Sr or Ba M-type hexaferrites. These ferrite magnets exhibit a maximum energy product $((BH)_{\max})$ smaller than most of the magnets composed by other hard materials, being a large energy gap between the $(BH)_{\max}$ of the hexaferrites magnets (20- 40 kJm^{-3}) and that of the high performing Rare-Earth magnets (maximum 400 kJm^{-3}). However ferrite magnets constitute the second market in the magnet production and for sales thanks to the low production costs, large thermal stability and electric insulating properties [1]. Being ferrites magnets constituted by multidomain grains, improvements in the properties are expected in the case that magnets are composed by nanometric grains. In first instance, the single-domain nature of grains should improve the coercivity. Moreover, other effects like morphology and surface effects can also add to improve the final properties. Hybrid hard-soft magnets require that hard moiety be nanometric sized in order to get an efficient exchange or dipolar coupling between the two phases [2,3].

In this contribution we present a wide structural, morphological and magnetic study of the properties of Sr -hexaferrite (SFO) particles with nanometric dimensions prepared by three different methods: solid state synthesis, sol-gel route and hydrothermal synthesis. We will compare the properties of SFO platelets with sizes from 20 nm to microns and shape ratios from 2 to 10. The single-to-multidomain regime crossover is identified by magnetic characterizations and it is correlated to the structure and morphology, in particular the platelet thickness. The effective magnetic anisotropy of these nanomaterials is determined by the Singular Point Detection technique. Different magnetic measurements show that, in opposite to what was expected, the larger anisotropy fields correspond with the smaller coercive fields. The magnetic anisotropy field of the different platelets is correlated to their morphology (shape anisotropy) but also for their size (single/multidomain regime). The employment of these nanomaterials for the magnet applications will be discussed.

This research was supported by EU-H2020 AMPHIBIAN project (n. 720853).

[1] O. Gutfleisch *et al.* Adv. Mater. **23** (2011) 821–842.

[2] A. Quesada *et al.* Adv. Electron. Mater. **2** (2016)1500365–1500372.

[3] S. Erokhin and D. Berkov Phys. Rev. Appl. **7** (2017) 014011–014025.

Investigation of high coercivity in Al and Cr substituted strontium hexaferrites (SrFe₁₂O₁₉) by x-ray, neutron diffraction and magnetic measurements

Durgamadhab Mishra ^{a,b}, Marian Stingaciu ^c, Riccardo Cabassi ^b, Fulvio Bolzoni ^b, Franca Albertini ^b, Claudio Sangregorio ^d, Michele Petrecca ^d, Mogens Christensen ^e, Anna Zink Eikeland ^e, Stefano Deledda ^c, César de Julián Fernández ^b

^a Department of Physics, Indian Institute of Technology Jodhpur, Jodhpur, India

^b Institute of Materials for Electronics and Magnetism - CNR, Parma, Italy

^c Institute for Energy Technology, Kjeller, Norway

^d Institute of chemistry of organometallic compounds - CNR, Sesto Fiorentino, Italy

^e Department of Chemistry, Aarhus University, Aarhus, Denmark

M-type hexaferrites are one of the promising materials for rare-earth free permanent magnets due to high magnetic anisotropy and attractive thermal and electrical properties [1, 2]. The current research is focused on development of M-type ferrites with increased coercivity and saturation magnetization without affecting the crystalline and magnetic structure. In this context, cation substitution is an attractive and simpler way to achieve high coercivity and magnetization in M-type hexaferrites. Most investigations have shown that substitution of Ca and Al in SrFe₁₂O₁₉ leads to increase in coercivity upto 2 T and reduction in saturation magnetization to 12.9 emu/g [3]. Therefore, there is a need to improve the magnetization without affecting the high coercivity.

We report here, effect of Cr and Al incorporation on structural and magnetic properties of Ca doped SrFe₁₂O₁₉. A series of powder samples of Sr_{0.67}Ca_{0.33}Fe₉Al_{3-x}Cr_xO₁₉ (x = 0, 0.5, 1.5, 2.5, 3) were prepared by sol-gel route. High resolution x-ray powder diffraction and neutron diffraction were performed to reveal the detail structural and magnetic unit cell. Rietveld refinement of the data revealed a single phase hexaferrite structure with some hematite impurities. The refinement shows that lattice parameter increases and c/a ratio decreases with increase in Cr content while preserving the magnetoplumbite structure, which plays a role in the macroscopic magnetic properties. Moreover, combined Rietveld refinement of x-ray and neutron diffraction data reveals that Al³⁺ has a larger affinity towards octahedral sites (2a and 12k) than the tetrahedral and bipyramidal site in the lattice, which reduces saturation magnetization by a factor of 3 compared to pure SrFe₁₂O₁₉. Cr also shows an affinity to go to 2a and 12k sites by replacing Al in the lattice and maintains spins collinearity to c-axis as well as ferrimagnetic nature of the sample. Magnetic hysteresis measurements show that Cr substitution leads to increase in saturation magnetization and a decrease in coercivity compared to Al substituted samples. The reversal process for all the samples exhibit similar trend in switching field distribution and remanence to saturation magnetization ratio. The anisotropy fields of all the samples and the reversal mechanisms were studied by Singular Point Detection technique in pulsed field (up to 11 T) at room temperature. Out of all the samples, the highest value of $\mu_0 H_c = 1.4$ T was obtained for Sr_{0.67}Ca_{0.33}Fe₉Al_{2.5}Cr_{0.5}O₁₉ with a saturation magnetization of 25 emu/g and remanence of 13.5 emu/g. The combined structural and magnetic characterization reveals that cation substitution could be a promising route to obtain rare-earth free materials with high coercivity with moderate magnetization. This research was supported by EU- H2020 AMPHIBIAN Projects (n. 720853).

[1] R. C. Pullar, Progress in Materials Science 57 (2012) 1191.

[2] X. F. Pan et al, Materials Science and Technology 23 (2007) 865.

[3] L. A. Trusov et al, Chem. Commun. 54 (2018) 479.

Magnetic ferrites: a tunable system for innovative applications

G. Barrera¹, M. Coisson¹, F. Celegato¹ and P. Tiberto¹

¹. INRIM, Metrology for Advanced Materials and Life Science, Torino, Italy;

Spinel ferrite particles exhibit different, peculiar physical properties such as high electrical resistivity, low-power loss at high frequency, high magnetic saturation and coercivity. These features make them a viable alternative for a variety of applications, spanning from replacing partially rare-earth elements in permanent magnets to suitable materials for devices operating at high frequency, magnetic actuation and biomedical application [1-2]. Their magnetic properties tunability can be ascribed to several factors such as chemical compositions, cation distribution, particle shape and size. Another variable is that they can be exploited either as-prepared powders or as particles dispersed in a non-magnetic medium, i.e. liquid or in polymeric matrix.

It is well known that the study of parameters directly connected to magnetic losses as Specific Loss power (SLP) is of utmost importance for biomedical application [3]. On the other hand, magnetic torque generated by self-assembly of magnetic nanoparticles during the polymerization process is the key property for magnetic actuation [4]. In both cases, a fine tuning of hysteresis properties is required to optimize material response for applications.

In this talk, the thermal stability of the non-equilibrium cation distribution and the filling of empty interstitial sites in the spinel ferrites structure with suitable cations (Zn-ferrite powders with Co and Li substitution) is shown to be an important tool to finely tune the ferromagnetic behavior of ferrites according to practical demands. Hysteresis losses have to be maximized according to the limit imposed by biological constraints in order to optimize heat-assisted biomedical applications (i.e. magnetic hyperthermia). On the other hand, to enhance actuation induced by magnetic torque high magnetization remanence values are desirable and can be obtained by increasing magnetic interaction among nanoparticles.

[1] M. Seehra, *Magnetic Spinel: Synthesis, Properties and Applications*, IntechOpen, 2017.

[2] G. Barrera, et al., *J. Magn. Magn. Mater.* **456** (2018) 372–380.

[3] G. Barrera, et al., *Sensors*, **20** (2020) 2151.

[4] S. Lantean, et Al., *Advanced Materials Technologies*, **4** (2019) 11.

EMI soft ferrite filters design for power conversion systems applications

G. Ala^a, G. Giglia^a, A. Imburgia^a, R. Miceli^a, P. Romano^a, F. Viola^a,
S. Quondam Antonio^b, H. P. Rimal^b

^a Università degli Studi di Palermo, Dipartimento di Ingegneria, Palermo, Italy

^b Università degli Studi di Perugia, Dipartimento di Ingegneria, Perugia, Italy

The switching power converters are used in a broad variety of applications, from renewable energy production systems to consumer electronics, from the transportation context to the industrial automation framework. In each of these applications, the conversion systems which present more compact size and reduced weight, at the same power, are strongly required in relation to stringent design constraints. The increase of the switching frequency of power electronics devices allows an improvement of the power density, thanks to the possibility of reducing the sizes of the energy storage passive components. On the other hand, high speed commutation makes such systems unintentional EMI sources. Therefore, EMI attenuation solutions are necessary; in particular, EMI filtering is required to ensure the compliance with the emission limits imposed by the stringent EMC technical standards. In this paper, after having discussed the main features of an automatic design procedure built-up by the authors and oriented at obtaining high performing EMI filters with the minimum volume/weight, the problem of power-loss evaluation in soft magnetic components which are part of the whole filter, is approached. In fact, low power losses are basic requirement to enable a compact realization, and low production costs are requirements in the actual development of power electronic converters. The study is oriented to evaluate how these aspects can influence the optimal design of an EMI filter.

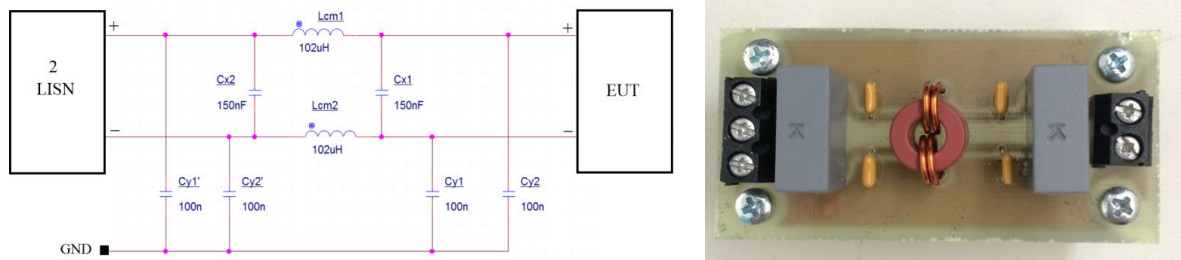


Fig. 1: General circuitual scheme of the single stage EMI filter and built up a prototype.

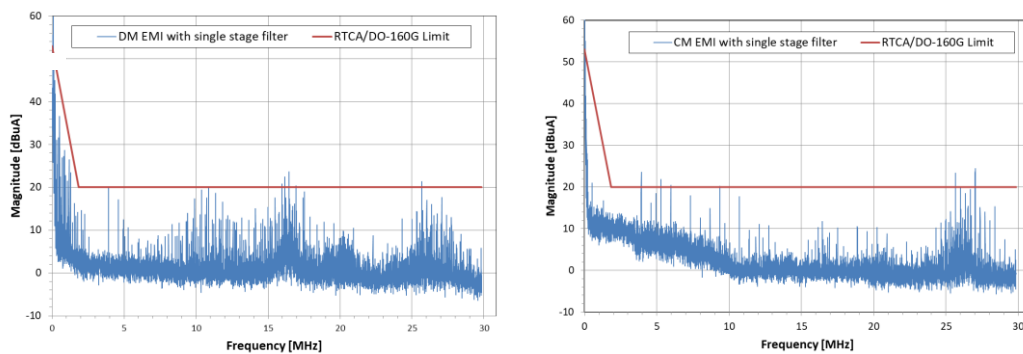


Fig. 2: CM and DM EMI with the single stage filter used for an actuator for avionic environment.

As an example, in Fig. 1, the general electrical scheme and the prototype built up for an actuator for avionic environment, are shown. In Fig. 2 the related CM and DM emission spectra compared with standard limits are reported.

- [1] G. Ala, G. Giglia, A. Imburgia, R. Miceli, G. Rizzo, P. Romano, F. Viola, S. Quondam Antonio, H.P. Rimal, "Design of Soft Ferrite Filters for EMI Reduction in Power Conversion Systems," Proceedings of IEEE 5th RTSI, 2019, Firenze, Italy, September 9-12, 2019, pp. 394-399.

Magnetic losses in amorphous and nanocrystalline alloys

up to 1 GHz: an analytical approach

S. Dobák^a, C. Ragusa^b, C. Beatrice^c, F. Fiorillo^c

^aInstitute of Physics, Faculty of Science, P.J. Safárik Univesity, Košice, Slovakia

^bPolitecnico di Torino, Energy Department, Torino, Italy

^cAdvanced Materials Metrology and Life Science Division, INRIM, Torino, Italy

Suitably heat-treated amorphous and nanocrystalline ribbons can display good magnetic response over a broad range of frequencies, from DC to a few hundred MHz, with higher permeability and lower energy losses than soft ferrites, the materials of choice for high-frequency applications. However, assessing the loss properties over such a wide useful frequency range in conducting magnetic plates is an unsolved problem. One would obviously expect a major role by the eddy current losses and a dominant effect of the classical loss component $W_{\text{eddy}}(f)$, the one associated with the macroscopic eddy current patterns, to arise under increasing frequencies. But a calculation of $W_{\text{eddy}}(f)$ based on the usual assumption of rate-independent magnetic constitutive equation $B(H)$ turns out to diverge strongly from the experiments at high frequencies. Actually, there are no direct ways, in general, to predict the evolution of the intrinsic $B(H)$ with f . A very interesting case, however, is the one provided by the amorphous and nanocrystalline ribbons endowed with homogeneous transverse anisotropy. Since their native anisotropy is close to zero, one can induce transverse easy axis with low anisotropy constant, of the order of 10-20 J/m³, with resulting sharp transverse domains and near-linear quasi-static magnetization curve. Since the ensuing domain structure is transverse to the applied field, the main contribution to the magnetization process is provided by spin rotation, without creation of internal poles, a feat leading to best high-frequency response. In addition, the restraining action of the exchange field hinders the skin effect. We show that in this case one can determine the rate-dependent constitutive equation as solution of the

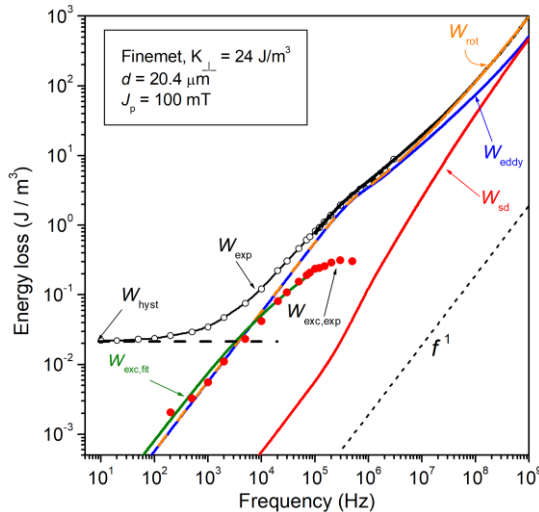


Figure 1: DC-1 GHz energy loss $W(f)$ in a nanocrystalline ribbon with transverse anisotropy $K_{\perp} = 24 \text{ J/m}^3$. Once the quasi-static loss $W_{\text{hyst}} = \lim_{f \rightarrow 0} W(f)$ is identified, the rotational contribution $W_{\text{rot}}(f)$, the sum of eddy current $W_{\text{eddy}}(f)$ and spin damping $W_{\text{sd}}(f)$ terms, and the domain wall related dynamic loss contribution $W_{\text{exc}}(f)$ are obtained.

linearized Landau-Lifshitz equation and correspondingly calculate the rotational energy loss $W_{\text{rot}}(f)$, the combination of eddy current $W_{\text{eddy}}(f)$ and spin damping $W_{\text{sd}}(f)$ dissipative contributions. A contribution from the dissipation mechanisms directly related to the motion of the domain walls is then identified and calculated as the sum of a quasi static loss term W_{hyst} and a dynamic one $W_{\text{exc}}(f)$ (Fig. 1). We further show that, in the general case where the magnetization process does not comply with the simple model embodied by the transverse domain structure, a rate-dependent constitutive equation $B(H)$ can be derived, at least within a quasi-linear approximation, starting from the measured complex permeability and iteratively searching for the intrinsic one satisfying the Maxwell's diffusion equation and complying with the Kramers-Kronig relations.

Magnetic and structural properties of Fe-Ni-Al and Co-Ni-Sn Heusler alloys

Vasiliy Buchelnikov^a, Olga Miroshkina^{a,b}, Vladimir Sokolovskiy^a, Arthur Sanosyan^a, Markus E. Gruner^b, Peter Entel^b

^a Chelyabinsk State University, Chelyabinsk, Russia

^b University of Duisburg-Essen, Duisburg, Germany

Ferromagnetic shape memory (FSM) alloys are promising candidates for application as actuators, sensors, magnetomechanical devices, harvesters, and magnetic cooling systems [1-3]. FSM compounds can be categorized to the high-performance smart materials with both large deformation and fast response. The wide range of their potential applications is directly associated with unique properties such as thermally- and magnetically- induced shape memory effects, giant magnetically-field-induced strains, superelasticity, the giant magnetoresistance and magnetocaloric effects, as well as exchange bias effect, etc. [1-3].

Fe-Ni-Al and Co-Ni-Sn alloys are an interesting subgroup, as these materials are ductile, cheap, and easily synthesized, while possessing a high Curie and martensitic transformation temperature. In this work, we report on systematic first-principle investigations of the structural and magnetic properties of $\text{Fe}_2\text{Ni}_{1+x}\text{Al}_{1-x}$ and $\text{Co}_2\text{Ni}_{1+x}\text{Sn}_{1-x}$ Heusler alloys. We calculated the ground state energy and magnetic properties of different structural motives and degree of order. For the most favorable structures, we evaluated magnetocrystalline anisotropy, magnetic exchange coupling and lattice free energy to assess the equilibrium properties for the compositions under study.

This work was supported by Russian Foundation for Basic Research No. 20-42-740003 and the German Research Foundation (DFG) – TRR 270, B06. Part of calculations were performed on MagnitUDE supercomputer (DFG INST 20876/209-1 and 20876/243-1 FUGG).

-
- [1] A. Planes, et al., J. Phys.: Condens. Matter **21** (2009), 233201.
 - [2] P. Entel, et al., Mater. Sci. Forum **583** (2008), 21.
 - [3] Y.-I. Matsushita, et al., J. Phys. D: Appl. Phys. **50**, 095002 (2017).

Magnetic-shape-memory Heusler thin films for thermo-magneto-mechanical systems: mastering martensitic configuration from continuous films to nanostructures

Milad Takhsha^{a*}, Francesca Casoli^a, Jon A. Arregi^b, Michal Stano^b, Michal Horky^b, Jan Hajducek^b, Alisa Chirkova^c, Fernando Maccari^c, Lucia Nasi^a, Simone Fabbri^a, Riccardo Cabassi^a, Federica Celegato^d, Paola Tiberto^d, Oliver Gutfleisch^c, Vojtech Uhler^b, Franca Albertini^a

^a IMEM-CNR, Parma, Italy

^b CEITEC-BUT, Brno, Czech Republic

^c Functional Materials, TU Darmstadt, Darmstadt, Germany

^d INRIM, Turin, Italy

Ferromagnetic shape memory materials such as Ni-Mn-Ga show a strong coupling between magnetic and structural degrees of freedom. In particular, epitaxial thin films are of special interest due to fine control of the microstructure and possible integration into micro and nanosystems. By varying the temperature, Ni-Mn-Ga encounters a reversible phase transformation between cubic austenitic phase and low symmetry martensitic phase. In order to maintain the compatibility of the two phases and to accommodate the stress caused by martensitic transformation, martensite cells form arrays of twin variants. In epitaxial Ni-Mn-Ga films, twin variants grow along two directions: at 90° or 45° with respect to the substrate plane. The 90° boundaries (so-called Y-type) show in-plane magnetic easy axis, whereas 45° (so-called X-type) show out of plane magnetic easy axis of the cells [1]. Controlling X- and Y-type configurations in epitaxial films and nanostructures would fully enable multifunctional applications such as magnetic stray field dependent actuation and energy harvesting at the micro- and nanoscale [2-4].

The films were epitaxially grown using radio frequency sputtering technique at 623 K on MgO(100). We have been able to observe directly the formation of X-type and Y-type twin variants by AFM/MFM imaging with varying temperature and magnetic field. We have been able to study the hysteretic behaviour of the two different type of variants and found that for Y-type microstructure the thermal hysteresis is reduced, a desirable feature for any kind of application with cyclic martensitic phase transformations, e.g., magnetorefrigeration and actuation.

We have demonstrated a number of during-growth and post-growth treatments to manipulate the formation of Y-type and X-type microstructures, i.e., applying bending stress to the substrate during and after the growth (growing directly on MgO or on Cr under-layer [1]), applying local stress perpendicular to the substrate after the growth, magnetic field cooling after growth, reducing growth temperature and subsequently post-annealing the film.

In terms of application, the material needs to keep its properties down to micron and nanometre size. To investigate this, we implemented ultra-high resolution ultra-violet and electron beam lithography on 40-200 nm Ni-Mn-Ga films, followed by combinations of chemical, reactive ion and Ar etching. Our achievements pave the way towards Heusler based micro- and nanostructures for micro-magneto-mechanical systems.

-
- [1] P. Ranzieri et al., *Advanced Mater.* **27** (2015) 4760.
 - [2] M. Kohl et al., *Appl. Phys. Lett.* **104** (2014) 043111.
 - [3] M. Campanini et al., *Small* **14** (2018) 1803027.
 - [4] G. Marcel, et al. *Adv. Energy Mater.* **4** (2014): 1400751.

Structural and magnetic properties of $\text{Fe}_{100-x}\text{Ga}_x$ bulk alloys

M. Coïsson^a, A. Fnidiki^b, N.K. Dakmak^b, L. Diallo^b, J. Juraszek^b, E.S. Olivetti^a, L. Martino^a, M. Pasquale^a, C.P. Sasso^a, F. Celegato^a, G. Barrera^a, P. Tiberto^a

^a INRIM, Torino, Italy

^b Normandie University, INSA Rouen, UNIROUEN, CNRS, GPM, 76800 Rouen, France

Galfenol is an alloy attracting a significant interest since it does not depend on rare earths. In addition to being cheaper, its properties (magnetic, mechanical) are very interesting, and they can be tailored to the application requirements by varying the Ga concentration. In order to study the behaviour of this material, $\text{Fe}_{100-x}\text{Ga}_x$ bulk alloys ($x = 18-23$ at.%) have been prepared by arc melting. As-prepared samples, cut from the bulk, have then been submitted to structural (X-ray diffraction, Mössbauer spectroscopy, differential scanning calorimetry), magnetic (hysteresis loops, Curie temperature, magnetic force microscopy) and magnetostriction measurements to correlate the magneto-mechanical properties to microstructure. On increasing the Ga content, multiple structural phases appear in the parent phase A2 (notably D0_3 and B2), characterised by different Curie temperatures and magnetic behaviour. This is reflected by the magnetic domain configuration, that is reported in Figure 1. In panel (a), the Ga18 sample is shown, with a typical disordered stripe domain configuration that is associated with the A2 crystalline phase. Upon increasing the Ga content to 21%, a second crystalline phase appears (according to structural and magnetic data), that is reflected in a magnetic domain configuration where the stripes are less parallel and tend to develop bifurcations (see Figure 1(b)). This specific domain configuration is associated with the beginning of the development of the ordered phase D0_3 or B2. The sample with the highest Ga content (23%) shows a much more significant presence of the D0_3 phase, which turns out to further let the domain structure evolve into large areas where the MFM magnetic contrast fades out or is almost lost (see Figure 1(c)).

Magnetostriction measurements performed on platelets using the strain gauges technique report a significant correlation of this property with the microstructure, that is discussed in details.

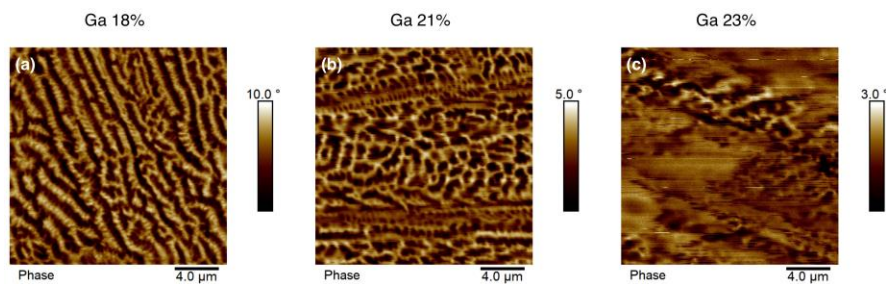


Figure 1: MFM images of Ga18%, Ga21% and Ga23% samples.

A High Throughput Study of FePt Thin Films

Yuan Hong^a, Stéphane Grenier^a, Edith Bellet-Amalric^b,
Thibaut Devillers^a and Nora M. Dempsey^a

^a*Université Grenoble-Alpes, CNRS, Institut NEEL, 38000 Grenoble, France*

²*Université Grenoble-Alpes, CEA, INAC, PHELIQS, 38000, Grenoble, France*

L1₀ FePt-based films have great potential for use in ultrahigh-density storage media, magnetic micro-systems, and as a coating for high coercivity magnetic force microscopy probes, due to their excellent magnetic properties and good chemical stability. In this work we deposited FePt films with a composition gradient, by magnetron sputtering of a Fe target partially covered by Pt foil. The films were deposited at room temperature, on thermally oxidised 100 mm Si substrates. 2D composition maps of as-deposited films were made using EDX (Energy Dispersive X-Ray) analysis in an SEM. Post-deposition annealing of full substrates was carried out using a rapid thermal annealing furnace. We investigated the influence of the size of the Pt foil and the annealing temperature and time on the magnetic and structural properties of the films. High throughput magnetic characterisation was carried out using an in-house developed scanning MOKE (Magneto-Optic Kerr effect) system with a high intensity μ s pulsed magnetic field source [1]. More detailed magnetic characterisation of certain sample parts was carried out using SQUID-VSM. High throughput XRD measurements were made to investigate changes in crystal structure and lattice parameters with film composition. We will demonstrate the great potential of high throughput film preparation and characterisation in the optimisation of L1₀ FePt-based hard films.

Keywords: Permanent magnets; FePt films; Compositionally graded films, high throughput characterization

[1] A. Dias, G. Gomez, D. Givord, M. Bonfim and N. M. Dempsey AIP ADVANCES 7 (2017) 056227

The future of magnetic refrigeration and heat pumping

Andrej Kitanovski^a

^a University of Ljubljana, Faculty of Mechanical Engineering, Ljubljana, Slovenia

The magnetocaloric refrigeration and heat pumping represents one of the most important future alternatives to mature vapor compression. In the last two decades, we have seen a significant increase in basic and applied research. This presentation will address the evaluation of existing barriers and associated solutions required to bring the technology to several niche markets. Particular emphasis will be placed on novel static magnetic field sources that, when combined with thermal control elements such as thermal diodes or thermal switches, can result in fully static magnetocaloric devices with very high power density and excellent energy efficiency. The future aspects of the technology and the related research efforts are addressed by given guidelines to solve the future challenges towards the first market applications.

Compositionally graded LaFeSi films

Erika Fontana^a, Thibaut Devillers^a, Nora M. Dempsey^a

^a Université Grenoble Alpes, CNRS, Grenoble INP, Institut Néel, 38000 Grenoble, France

La(Fe, Si)₁₃ has been widely studied for use in magnetic refrigeration and more recently in energy harvesting. This alloy family exhibits a large magnetocaloric effect (MCE) due to a magneto-volume effect that occurs during the transition from the paramagnetic to the ferromagnetic state, in the temperature between 200 and 254 K. Adjusting the Si-content, it is possible to modify the crystal structure (cubic \leftrightarrow tetragonal), magnetisation, Curie temperature and the magnetocaloric effect [1]. Furthermore, the Curie temperature can be increased to above room temperature by doping and hydrogenation [2]. All the studies reported in literature focus on bulk material, but recent work from our group reported for the first time the possibility to fabricate thick films of La(Fe, Si)₁₃ [3]. Synthesize of the material in film form opens new possibilities for material studies and micro-system applications.

Here we report on the fabrication of compositionally graded films of La(Fe, Si)₁₃. The films are deposited onto stationary, thermally oxidised Si substrates of diameter 100 mm, by concurrent triode sputtering of three targets (Fe-La, Fe, Fe-Si). All films are deposited onto

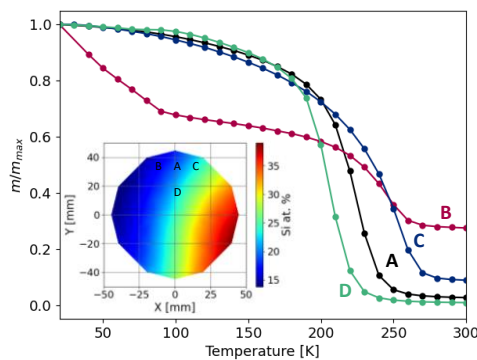


Figure 1: $M(T)$ measured in-plane under an applied field of 50 mT, as a function of position of a La-Fe-Si film of nominal thickness 5 μm , annealed at 900°C for 5 minutes. Inset: Si composition map of the same film in the as-deposited state.

non-heated substrates and then annealed ex-situ in a Rapid Thermal Annealing furnace. The nominal film thickness was varied in the range 1-5 μm . Automated EDX analysis is used to measure the composition of as-deposited films (e.g., see inset of Figure 1). Following annealing, samples selected from specific regions on the film with distinct compositions are characterised by optical and scanning electron microscopy, x-ray diffraction and VSM-SQUID magnetometry. Examples of $M(T)$ measurements made on a La-Fe-Si film of nominal thickness 5 μm are shown in Figure 1. The presentation will give details about how the structural and magnetic properties vary as a function of film composition, thickness and annealing conditions. Prospects for further developments and possible applications will also be discussed.

-
- [1] Mi-Kyung Han and Gordon J. Miller, *Inorg. Chem.* **47** (2008), 515-528
 - [2] B. G. Shen, et al., *Adv. Mater.* **21** (2009), 4545-4564
 - [3] N. H. Dung, et al, *J. Appl. Phys.* **127** (2020), 215103

Degradation of the magnetocaloric effect in promising materials in cyclic magnetic fields

Akhmed M. Aliev^a, Abdulkarim A. Amirov^a, Adler G. Gamzatov^a,
Akhmed B. Batdalov^a, Lazer N. Khanov^a, Gennady A. Govor^b, Konstantin P.
Skokov^c, Victor V. Koledov^d, Vladimir G. Shavrov^d

^a Amirkhanov Institute of Physics of DFRC RAS, Makhachkala, Russia

^b Scientific-Practical Materials Research Centre of the National Academy of Sciences of
Belarus

^c Technische Universität Darmstadt, Germany

^d Kotelnikov Institute of Radio Engineering and Electronics of RAS, Moscow, Russia

Refrigerating machines are devices with periodic sweeps of cycles, so there is a substantial need to study the magnetocaloric properties of materials under repeated cyclic exposures to magnetic fields. Magnetocaloric properties of the materials under single and repeated application of the cyclic magnetic fields can exhibit significantly different behavior for a variety of reasons. Furthermore, the magnetocaloric properties of materials with a magnetostructural phase transition in cyclic fields can degrade over time. Obviously, practical applications require materials with time-stable magnetocaloric properties.

In this work, we present results of studying the magnetocaloric properties in various families of promising magnetic materials as $(\text{La}(\text{FeSi})_{13})$, $\text{MnFe}(\text{AsP})$, FeRh , $\text{Gd}_5(\text{GeSi})_4$ and Ni-Mn-X Heusler alloys in cyclic magnetic fields. It was found that in the most materials the effect of degradation of the magnetocaloric properties is observed, namely, a decrease in the magnitude of the MCE, and in some cases a change in the temperature of the maximum of the effect under the action of cyclic magnetic fields. The effect of degradation varies in the different studied materials. Namely, in some materials, the effect is irreversible at room temperatures and, in order to restore the initial properties of the alloy, a thermal procedure of heating the sample above its Curie point is required (FeRh). Otherwise, the original properties can be recover by approaching the austenitic phase at room temperatures (Ni-Mn-X), or by removing the external cyclic magnetic field. An explanation of the observed behavior of the MCE in cyclic magnetic fields is given in the report. It is shown that the degradation effect results in some limitations for using the magnetocaloric materials in magnetic cooling technology. The La-Fe-Si based compounds, as well as gadolinium, can be considered as the most optimal materials for the magnetic cooling application, because to the absence of the MCE degradation in cyclic magnetic fields of moderate intensity.

The research was supported by a grant of the Russian Science Foundation (Project No. 18-12-00415).

Probing the magnetic structure of austenitic $\text{Ni}_{48}\text{Mn}_{34}(\text{In},\text{Sn})_{16}$ Heusler compounds

Francesco Cugini^{a,b}, Simone Chicco^a, Greta Cavazzini^{a,b}, Fabio Orlandi^c, Giuseppe Allodi^a, Vincenzo Vezzoni^a, Markus Gruner^d, Lara Righi^e, Simone Fabbrici^b, Franca Albertini^b, Massimo Solzi^{a,b}

^a SMFI Department, University of Parma, Parma, Italy

^b IMEM-CNR Institute, Parma, Italy

^c ISIS Facility STFC, Rutherford Appleton Laboratory, Didcot, UK

^dDepartment of Physics, CENIDE, University of Duisburg-Essen, Duisburg, Germany

^eSCVSA Department, University of Parma, Parma, Italy

The lattice of Ni_2MnX Heusler compounds ($X = \text{Ga}, \text{In}, \text{Sn}, \text{Sb}, \dots$) allows, by changing composition, the development of different crystallographic and magnetic structures. The possibility to fine tailoring the critical temperatures and the magnetic states makes this class of compounds very promising as active elements in thermomagnetic devices, like magnetic refrigerators and wasted heat harvesters.

In this work, we study the $\text{Ni}_{48}\text{Mn}_{36}\text{In}_{16-x}\text{Sn}_x$ ($x = 0-16$) series with the purpose of investigating the physical mechanisms that control the magnetic properties of the austenitic phase in (Ni,Mn)-based Heusler alloys. All the compositions show a cubic austenitic phase down to 5 K with a Curie transition slightly above room temperature. The replacement of In with Sn brings to a progressive decrease of the saturation magnetization whereas the related Curie temperature is featured by a non-monotonic variation (Figure 1). This unexpected behaviour cannot be easily explained solely by the minute contraction of the crystallographic lattice but conversely, it is related to a complex interplay of the different magnetic interactions between Mn and Ni atoms. Magnetometry, neutron diffraction and ^{55}Mn nuclear magnetic resonance experiments combined with first-principles calculations were used to fix the different physical mechanisms determining the saturation magnetization and the critical temperature in these compounds.

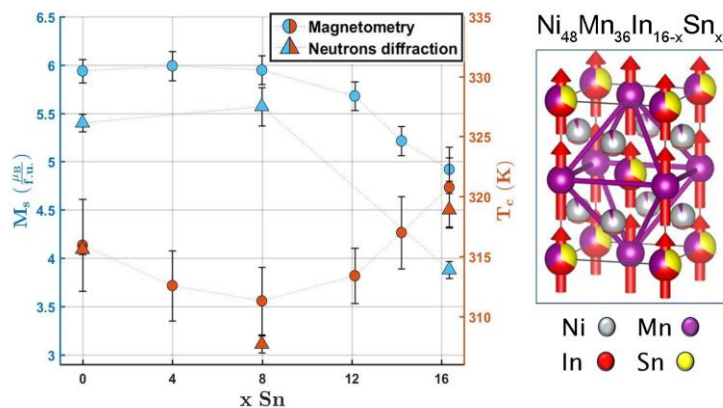


Figure 1: On the left: dependence of the saturation magnetization and Curie temperature versus the Sn at.% content. On the right: sketch of the magnetic and nuclear structures of $\text{Ni}_{48}\text{Mn}_{36}\text{In}_{16-x}\text{Sn}_x$.

Design, enhanced thermal and flow efficiency of an active magnetic regenerator

Stefano Dall'Olio^a, Urban Tomc^a, Katja Klinar^a, Andrej Kitanovski^a

^a University of Ljubljana, Faculty of Mechanical Engineering, Ljubljana, Slovenia

To increase the cooling power and the coefficient of performance (COP) of a magnetic refrigeration prototype, we optimized the core component of the technology, i.e. the active magnetic regenerator (AMR). In our prototype the fluid passes through a porous media consisting of a packed bed of 45 g of gadolinium spheres having an average diameter between 100 and 300 μm . The regenerator has a cross section of 167 mm^2 , length of 55mm, and is 3D printed with the technique of stereolithography (SLA). The optimization of the regenerator has been achieved by focusing on three main areas: structural characteristics of the housing, flow distribution and heat losses of the regenerator to the environment.

For each of the previous points, there was an iterative process based on numerical simulations carried out in ANSYS in order to decrease the amount of dissipations.

For the mechanical design of the regenerator, we considered 8 bar as the highest working pressure of the flow, and we consequently optimized the geometry in order to have a maximum deformation of the housing lower than 150 μm , threshold which corresponds to the average sphere diameter. This process has been quite delicate because another source of performance loss is the total mass of the regenerator itself. This happens because the regenerator walls may act as passive regenerator surrounding the active material, decreasing the temperature gradient and consequently the cooling power.

Another important source of performance reduction is the flow maldistribution inside the regenerator, together with the size of the dead volume. Therefore, a flow distribution chamber has been added at the regenerator inlet and outlet, and the geometry of this space has been adjusted to have the most uniform flow along the regenerator. The effect of the different chamber shapes on the flow distribution has been verified in FLUENT (see fig. 1). Because the distribution chamber acts as dead volume for the regenerator, we tried to keep it as small as possible. Moreover, we also focused on how to decrease the parasitic losses to the environment. This process has been done by insulating the regenerator outer walls and by installing some passive heat sink on the iron core.

In our system the magnetic flux is provided by an electromagnet and the applied flux can reach a magnitude of 2 T in the high field mode, while being close to zero when the coil is not activated. The magnet can work at a frequency up to 25 Hz.

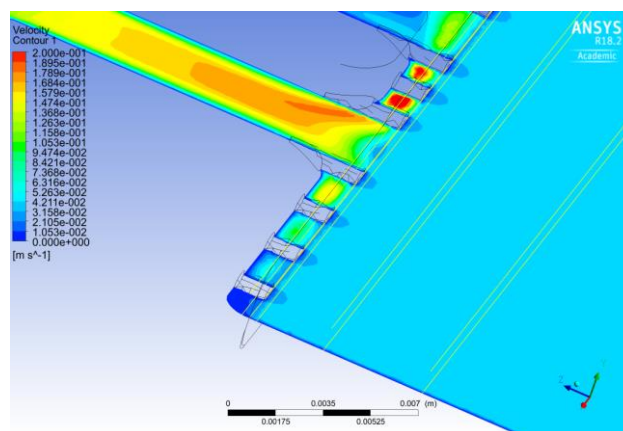


Figure 1: FLUENT simulation of the flow distribution at the inlet of the regenerator.

Advances in Magnetism 2020-21, June 13-16, 2021

Spin waves and magnonics

Abstracts can be easily browsed through the bookmarks

Localised modes and spin wave focusing in synthetic antiferromagnets

Aurore Finco^a, Vincent Jacques^a, Jean-Paul Adam^b, Joo-Von Kim^b

^a Laboratoire Charles Coulomb, CNRS, Université de Montpellier,
34095 Montpellier, France

^b Centre de Nanosciences et de Nanotechnologies, CNRS, Université Paris-Saclay,
91120 Palaiseau, France

Synthetic antiferromagnets (SAFs) comprise coupled thin ferromagnetic films with a variety of ground states that can be stabilized at room temperature by tuning the magnetic parameters such as the effective anisotropy, interlayer exchange, and Dzyaloshinskii-Moriya interactions. As a result, nonuniform spin textures such as domain walls, spin spirals, and skyrmions can be stabilised under zero applied fields [1], which can be detected using quantum spin sensing [2]. Here, we present results of micromagnetics simulations in which we examined the spin wave dispersion associated with localised modes of domain walls, spin spirals, and skyrmions in such SAF structures. For domain walls and spin spirals, the combination of dipole-dipole and Dzyaloshinskii-Moriya interaction results in spectra with frequency-wave vector nonreciprocity which results from asymmetries in the micromagnetic ground state. Skyrmion breathing modes are found to be in the low GHz range, which differs from their counterparts in confined ferromagnetic systems. We also discuss spin wave focusing effects for canted states under applied magnetic fields, where it is shown that caustic patterns depend strongly on the acoustic or optic nature of the mode.

[1] W. Legrand *et al.*, Nat. Mater. **19**, 34 (2020).

[2] A. Finco *et al.*, Nat. Commun. **12**, 767 (2021).

Excitation and amplification of spin waves by spin-orbit torque

S.O. Demokritov^a, B. Divinskiy^a, V.E. Demidov^a, S. Urazhdin^b, R. Freeman^b

^aInstitute for Applied Physics, University of Muenster, Muenster, Germany.

^bDepartment of Physics, Emory University, Atlanta GA 30322, USA

The emerging field of nano-magnonics utilizes high-frequency waves of magnetization – the spin waves – for the transmission and processing of information on the nanoscale. The advent of spin-transfer torque has spurred significant advances in nano-magnonics, by enabling highly efficient local spin-wave generation in magnonic nanodevices. Furthermore, the recent emergence of spin-orbitronics, which utilizes spin-orbit interaction as the source of spin torque, has provided a unique ability to exert spin torque over spatially extended areas of magnonic structures, enabling enhanced spin-wave transmission. Here, it is experimentally demonstrated that these advances can be efficiently combined. The same spin-orbit torque mechanism is utilized for the generation of propagating spin waves, and for the long-range enhancement of their propagation, in a single integrated nano-magnonic device. The demonstrated system exhibits a controllable directional asymmetry of spin wave emission, which is highly beneficial for applications in non-reciprocal magnonic logic and neuromorphic computing [1].

Figure 1 (top) shows the schematic of the experiment. The test devices are 180 nm wide Py(15 nm)/Pt(4 nm) nano-waveguides with a 200 nm wide and 10 nm deep rectangular nano-notch in the center. The injected spin current I_s , excites magnetization auto-oscillations in the

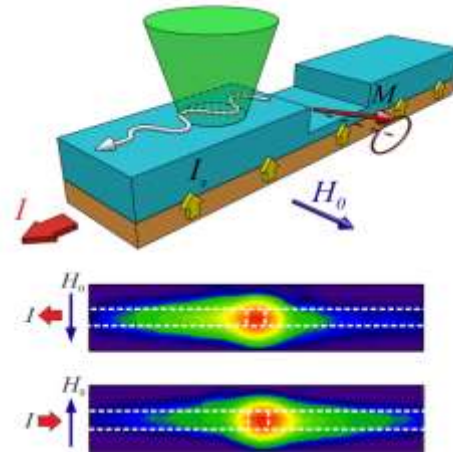


Figure 1: Top: Schematic of the experiment. Bottom: spatial maps of the spin-wave intensity recorded with reversed directions of the magnetic field and of the driving current.

nano-notch, resulting in the spin wave emission into the waveguide. Figure 1 (bottom) illustrates spin-wave emission by the nano-notch oscillator by showing color-coded recorded spatial maps of the spin-wave intensity. Dashed lines on the maps show the outlines of the waveguide and of the nano-notch. Two maps were measured with reversed directions of the static magnetic field and of the driving current.

We expect our results to spur significant advances in spin-orbit magnonics, enabling the implementation of efficient spin wave-based computing systems.

[1] B. Divinskiy et al. Adv. Mater., 1802837 (2018).

Electric-field control of propagating spin waves in multiferroic heterostructures

Huajun Qin^a, Rouven Dreyer^b, Georg Woltersdorf^b, Tomoyasu Taniyama^c, Sebastian van Dijken^a

^a Department of Applied Physics, Aalto University School of Science, 00076 Aalto, Finland

^b Institute of Physics, Martin Luther University Halle-Wittenberg, 06120 Halle, Germany

^c Department of Physics, Nagoya University, Nagoya, 464-8602, Japan

Active manipulation of spin wave transport using an electric field is attractive for low-power magnonics. Here, we experimentally demonstrate reversible electric-field control of propagating spin waves in a multiferroic heterostructure comprising a 26-nm-thick Fe film grown on top of a ferroelectric BaTiO₃ substrate [1]. The effect, which arises when the ferroelectric polarization underneath the Fe film is switched from an in-plane orientation to a perpendicular direction (or vice versa) through lateral domain wall motion, originates from a strain-induced change of magnetic anisotropy. The anisotropy modulation gradually tunes the spin wave dispersion relation (Fig. 1). As a result, the transmission of spin waves is turned on or off by the application of voltages across the BaTiO₃ substrate in certain frequency bands. Moreover, the multiferroic heterostructure allows for continuous tuning of the spin wave phase and amplitude, offering prospects for voltage-controlled magnonic logic.

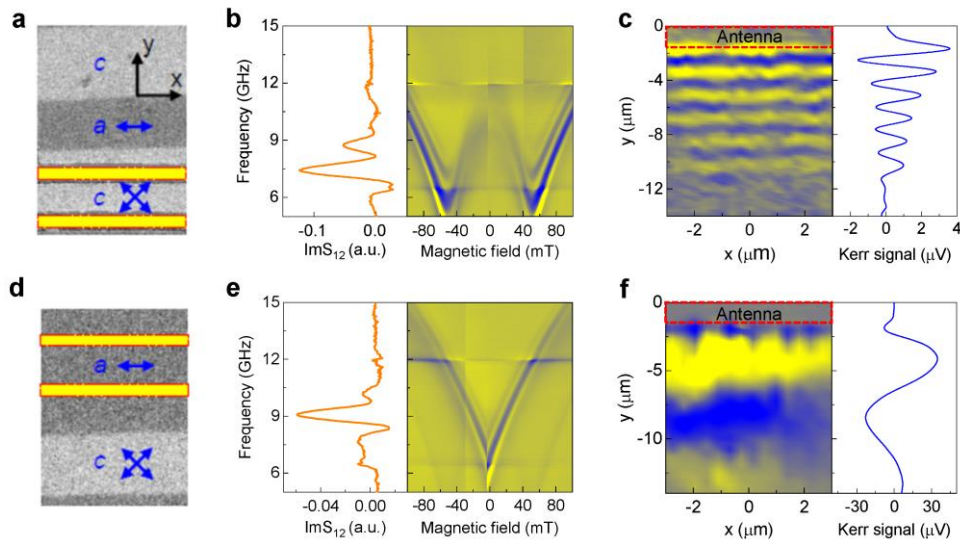


Figure 1: Spin wave transmission signals through the Fe film measured between two microwave antennas on top of a ferroelectric domain with perpendicular polarization (*c* domain, top row) and a ferroelectric domain with in-plane polarization (*a* domain, bottom row). The panels (b,e) compare spin wave signals as a function of an in-plane bias field (parallel to antennas) and panels (c,f) show time-resolved Kerr microscopy measurements of propagating spin waves in both domains at 14 GHz. A bias voltage across the BaTiO₃ substrate switches the polarization state.

[1] K.J.A. Franke, B. Van de Wiele, Y. Shirahata, S.J. Hämäläinen, T. Taniyama, S. van Dijken. Reversible electric-field-driven magnetic domain-wall motion. *Phys. Rev. X* **5**, (2015), 011010

Nonreciprocal nano-optics with spin-waves in synthetic antiferromagnets

Edoardo Albisetti^{a,b}, Silvia Tacchi^c, Raffaele Silvani^{c,d}, Giuseppe Scaramuzzi^a,
Simone Finizio^e, Sebastian Wintz^e, Jörg Raabe^e, Giovanni Carlotti^d,
Riccardo Bertacco^a, Elisa Riedo^f and Daniela Petti^a

^a Dipartimento di Fisica, Politecnico di Milano, Milano, Italy.

^b Advanced Science Research Center, CUNY Graduate Center, New York, USA.

^c Istituto Officina dei Materiali del CNR (CNR-IOM), Unità di Perugia, Perugia, Italy.

^d Dipartimento di Fisica e Geologia, Università di Perugia, Perugia, Italy

^e Paul Scherrer Institute, Villigen PSI, Switzerland

^f Tandon School of Engineering, New York University, New York, USA

Optically-inspired wave-based analog computing is envisioned to outperform conventional digital processing in a set of specific tasks, such as image processing, recognition and filtering. Nanoscale integration, however, represents a major challenge, due to the centimeter-long wavelength of electromagnetic radiation in the GHz frequency range used for processing. In this view, spin-waves represent a promising route due to their nanoscale wavelength, tunability and rich phenomenology.

Here, we realize a versatile optically-inspired platform using spin-waves, demonstrating the wavefront engineering, focusing, and robust interference of spin-waves with nanoscale wavelength¹. By coupling radiofrequency magnetic fields with engineered magnonic nanoantennas consisting of nanoscale spin-textures, we generate and shape spin-waves propagating in a synthetic antiferromagnet.

First, we demonstrate the use of thermally assisted magnetic scanning probe lithography (tam-SPL)^{2,3} for nanopatterning spin-textures in synthetic antiferromagnets. Then, we show the generation of spin-waves with planar, radial, convex and concave wavefronts, the directional emission of spin-wave beams, and their diffraction-limited focusing into dimensions comparable to their nanoscale wavelength. By combining the emission of multiple nanoantennas, we generate robust interference patterns, which span for more than 15 times the spin-wave wavelength. Furthermore, we show that intriguing features, such as resilience to back-reflection, naturally arise from the spin-wave nonreciprocity in synthetic antiferromagnets, preserving the high quality of the interference patterns from spurious counterpropagating modes.

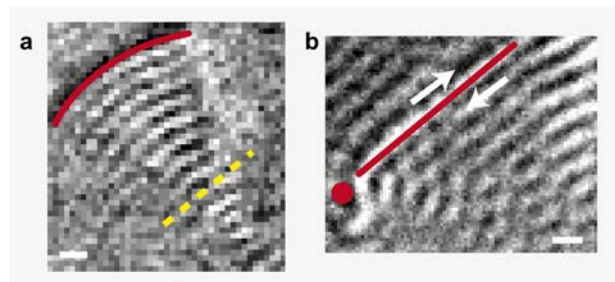


Figure 1: STXM image of (a) spin-wave focusing and (b) interference from radial and planar wavefronts. Scale bars: 500 nm

[1] E. Albisetti et al., arXiv:1902.09420 (2019).

[2] E. Albisetti et al., Nat. Nanotechnol. **11** (2016), 545–551;

[3] E. Albisetti, et al., Commun. Phys. **1** (2018), 56.

Spin waves in YIG based magnonic networks: design and technological aspects

Yuri Khivintsev^{a,b}, Galina Dudko^a, Alexander Kozhevnikov^a, Valentin Sakharov^a,
Yuri Filimonov^{a,b}, Alex Khitun^c

^a Kotel'nikov IRE RAS, Saratov Branch, Saratov, Russia

^b Chernyshevskii Saratov State University, Saratov, Russia

^c University of California -Riverside, Riverside, USA

Spin waves propagation in YIG thin film based magnonic networks in the form of $N \times N$ square lattices of orthogonal microwaveguides was studied both experimentally and theoretically. The studied structures for $N=2$ and 5 are shown in Figure 1a and b, respectively. The external bias field was applied in plane of the structures. The nondissipative signal attenuation caused by energy splitting at the cross-junctions was analyzed. It is shown that signal attenuation of the order of -5 dB takes place at the cross-junctions. Possibility to control the energy distribution at the cross-junctions by means of waveguides width appodization was examined. The role of the periodicity in $N \times N$ magnonic network on the spin waves propagation was studied. It is shown that for sufficiently big N , the network exhibits features typical to magnonic crystal: the magnonic band gaps appear. An influence of waveguides cross-section shape on spin waves propagation was studied. Such problem was essential for the structure 5×5 fabricated by chemical etching technique when cross-section shape takes trapezoidal form instead of rectangular one. It is shown that the surface spin waves is much more sensitive to trapezoidal shape than the backward volume spin waves.

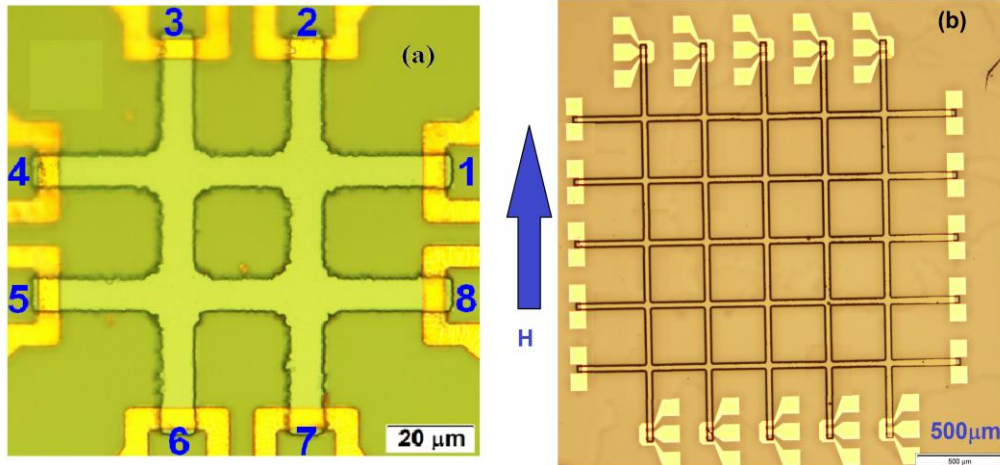


Figure 1: Studied 2×2 (a) and 5×5 (b) structures. YIG films with the thickness of 1 and $3.5 \mu\text{m}$ were used for the structures (a) and (b), respectively. At the ends of the waveguides, π -shaped and coplanar waveguide antennas are shown. Arrow in the central part of the figure shows the bias field direction. The structures were fabricated by photolithography and etching techniques. For the 2×2 structure the ion-etching technique was used. Structure 5×5 was formed by the liquid chemical etching.

Support by Russian Science Foundation grant 17-19-01673 is acknowledged.

Spin dynamics in free standing 3D YIG nanoresonators

Georg Schmidt^a

^a Institut für Physik, Martin-Luther-Universität Halle-Wittenberg,
Von-Danckelmann-Platz 3,
D-06120 Halle, Germany

Nano electromechanical systems are interesting candidates for quantum information processing technology. Typical examples are the transfer of energy between mechanical and electromagnetic oscillators [1,2], but also spin wave excitations, so called magnons, can be used. An ideal material in this respect is Yttrium Iron Garnet. It combines long lifetimes as well for spin waves (magnons) as for mechanical waves (phonons) and a coupling mechanism for both (magnetoelastic coupling or magnetostriction).

We have developed a process to fabricate high quality monocrystalline freestanding 3D YIG nanostructures which can be designed for example as suspended bridges or cantilevers [3] or even more complex structures. For the fabrication we use an electron beam lithography based process which was originally designed to realize metallic air bridges by evaporation and lift-off [4]. A newly developed deposition process for YIG using pulsed laser deposition at room temperature [5] allows for the fabrication and lift-off of amorphous structures. Surprisingly subsequent annealing leads to monocrystalline bridges even if the length of the span is as large as several micrometers.

The structures were investigated using transmission electron microscopy indicating high crystalline quality. Detailed investigation of spin dynamics was done using time and spatially resolved Kerr microscopy. Here we see various standing spin waves including Damon Eshbach Modes and Backward Volume Modes. The minimum linewidth in ferromagnetic resonance at 8 GHz is as small as 140 μT while the intrinsic linewidth at zero field is 75 μT . Based on measurements at various frequencies the damping for a single resonator could be determined to $\alpha \approx 2.5 \times 10^{-4}$. The modes observed can be nicely reproduced in 3D micromagnetic simulations.

Furthermore the process facilitates the growth of YIG structures on other substrates or to use YIG nanostructures which are separated from the original substrate by simple means.

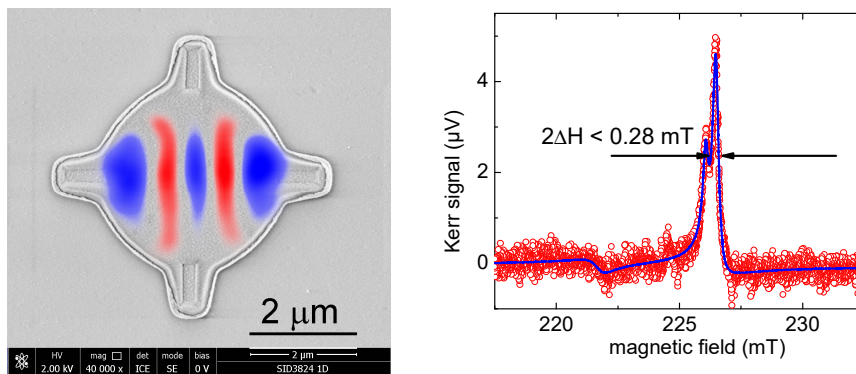


Fig. 1: Free standing YIG disk with magnon pattern measured by TR-MOKE (left). FMR resonance line as measured by TR-MOKE for a single free standing bridge.

-
- [1] Y. Chu et al. Science 358, 199 (2017)
 - [2] A. D. O'Connell et al. Nature 464, 697 (2010)
 - [3] F. Heyroth et al. cond-mat.1802.03176
 - [4] T. Borzenko et al. Microelectronic Engineering 75, 210 (2004)
 - [5] C. Hauser et al. Scientific Reports 6, 20827 (2016)

Excitation and control of spin waves at the micro and nano scales

Marco Madami^a, Gianluca Gubbiotti^b

^a Dipartimento di Fisica e Geologia, Università degli Studi di Perugia, Italy

^b Istituto Officina dei Materiali del CNR (CNR-IOM), Unità di Perugia, Italy

The idea to employ spin waves as a potential data carrier in future wave-based computing devices is now widespread. This is due to the peculiar properties of spin waves which make them particularly attractive: their wavelengths which span from the micro- to the nano-meter range, their frequencies which reach the THz range, their ultralow losses, do to the absence of Joule heating, resulting in very long propagation distances. For all the above reasons the excitation and manipulation of spin wave propagation, at these scales, is of crucial importance. In this presentation we will review recent experimental results from our own group and others leading groups around the world which show both the potentiality and possible limits in the use of spin waves in future wave-based logic devices.

We will show how it is possible to exploit reflection and refraction of spin waves at a thickness step [1] and transmission of spin waves at a domain wall [2] to steer spin wave propagation and reduce its wavelength at the same time. Non reciprocal spin wave propagation will be addressed as well by showing how curved spin wave transducer [3] can be used to excite non reciprocal spin wave beams in a quasi-backward geometry. Furthermore we will show how the chirality of the dipolar interaction between the uniform mode of Co nanowires and the exchange spin waves of an yttrium iron garnet film [4] can be exploited to produce unidirectional excitation of spin waves. Finally the effect of the antisymmetric exchange (Dzyaloshinskii–Moriya interaction) will be addressed.

Financial support from the EMPIR programme 17FUN08-TOPS, co-financed by the Participating States and from the European Union's Horizon 2020 research and innovation programme, is kindly acknowledged

[1] J. Stigloher, et al. Phys. Rev. Lett. **117**, 037204 (2016).

[2] S.J. Hämäläinen, et al. Nature Comm. **9**, 4853 (2018).

[3] M. Madami, et al. Appl. Phys. Lett. **113**, 152403 (2018).

[4] J. Chen, et al. Phys. Rev. B, **100**, 104427 (2019).

Spin Superfluidity versus magnonic BEC

Yury M. Bunkov

Russian Quantum Center, Skolkovo, 143025 Moscow, Russia

The spin superfluid state is a quasi-equilibrium state of coherent magnons which emerges on the background of the ordered magnetic state, and which can be described in terms of the condensation of magnetic excitations to a coherent quantum state. This state was observed in 1984 in antiferromagnetic superfluid $^3\text{He-B}$ [1]. The spin superfluid state is a magnetic analog of mass superfluid and electron superconducting states. There was found the magnetic analogous of the all superfluid phenomena, including spin supercurrent and phase-slippage at critical spin supercurrent in the channel, Josephson spin-current effect, spin-current, vortices and Goldstone collective excitations (the analog of the second sound in ^4He) [2]. Recently the spin superfluid state was observed in a normally magnetized single-crystal yttrium iron garnet (YIG) film. This is the first superfluid state, which exist at a room temperature. The properties of this state will be highlighted at the presentation.

The magnonic Bose-Einstein Condensate (BEC) forms in a weakly interacting gas of non-equilibrium magnons. Contrary the superfluid liquid of magnon forms at a high density of excited magnons at the conditions of a strong repulsive interaction. This interaction leads to the frequency shift from the Larmore frequency $\omega_S - \omega_L$, which stabilize the spin supercurrent. The critical phase gradient of supercurrent reads:

$$\nabla\alpha_c = 1/\xi_{GL} = \sqrt{\omega_L(\omega_S - \omega_L)}/c_{SW},$$

where c_{SW} is spin waves velocity and ξ_{GL} is a Ginzburg Landau coherence length.

In the case of pulse magnons excitation the spatial inhomogeneity of magnetic field excites the spin supercurrent, which redistributes magnons until all the magnon became precessing homogeneously [3]. The domain with coherent homogeneous precession (HPD) forms and radiates a long living induction decay signal, which may be in a few orders of magnitude longer than one from a noninteracting magnons. The inhomogeneity of magnetic field is compensated by a spatial distribution of frequency shift $\omega_S(x) - \omega_L(x)$.

The magnon superfluid state may exist continuously at the conditions, when the losses (evaporation) of magnons are replenished by excitation of new ones.

By excited magnon system we are able to investigate the transition from magnon gas to a magnonic BEC at relatively small density of magnons and to a superfluid state at a higher density of non-equilibrium magnons. The report is aimed at introducing the principles of magnon superfluidity.

Financial support by the Russian Science Foundation within the Grant 19-12-00397 “Spin Superfluids” is gratefully acknowledged.

[1] A. S. Borovik-Romanov et al., JETP Lett. **40** (1984), 1033; I. A. Fomin, JETP Lett. **40** (1984), 1037.

[2] Yu. M. Bunkov and G. E. Volovik, “Spin Superuidity and Magnon BEC” in “*Novel Superuids*”, (eds. Bennemann, K. H. & Ketterson, J. B. Oxford Univ. Press, Oxford, (2013); [arXiv:1003.4889v3](https://arxiv.org/abs/1003.4889v3).

[3] Yu. M. Bunkov, Appl. Mag. Res. 51, 1711-1721 (2020)

Spectrum evolution of optically-excited magnetostatic waves in metallic ferromagnetic films with in-plane anisotropy

Nikolai E. Khokhlov^a, Iaroslav A. Filatov^a, Petr I. Gerevenkov^a, Mu Wang^b,
Andrew W. Rushforth^b, and Alexandra M Kalashnikova^a

^a Ioffe Institute, St. Petersburg, Russia

^b School of Physics and Astronomy, The University of Nottingham, Nottingham, UK

Femtosecond laser pulses became a powerful tool for driving ultrafast magnetization dynamics at nanoscale with a number of significant advantages over conventional techniques [1]. Consistent evolution of modern magnetism brought femtomagnetism [1] in touch with magnonics [2], as the optical excitation of spin waves (SWs) was demonstrated in transparent dielectrics and metals recently [3, 4]. On the other hand, active optical control of SWs propagation is up-to-date task in magnonics [5], but it is yet to be extended to ultrafast timescales. Therefore, exploiting femtosecond laser pulses in reconfigurable magnonics is modern challenge for fundamental magnetism with potential impact on future data processing applications.

In the present work we use two-color optical pump-probe technique with spatial scanning to study the influence of femtosecond laser pulses on propagation of magnetostatic surface waves (MSSW) in ferromagnetic metallic films of iron and galfenol ($\text{Fe}_{0.81}\text{Ga}_{0.19}$). The feature of the films is pronounced in-plane magnetic anisotropy unlike model magnonic metal permalloy (NiFe). We show that this feature provides the opportunity to excite MSSW via ultrafast thermal magnetocrystalline anisotropy changes [6]. Next, we examine feasibility of MSSW control with fs-laser pulses not only during excitation but upon propagation as well. Particularly, we demonstrate experimentally the narrowing of the spectrum of the laser-excited MSSW wave packet as it propagates away from the excitation area [7]. Moreover, we control whether the low- or high-frequency part of the spin waves spectrum is suppressed upon propagation by changing the orientation of external magnetic field with respect to anisotropy axes. The theoretical description of the effect is given in terms of the spatial gradient of magnetization and anisotropy parameters of the film induced by the laser pulse. The concept of controlling MSSW by fs laser pulses is extended further by analysing properties of the MSSW optically excited near a Néel domain wall in the thin film. Micromagnetic modelling reveals the appearance of controllable resonance peaks in the MSSW spectrum, and shows that the combination of femtosecond optical excitation with magnetic non-uniformity of the film, e.g. a domain wall, serves as a tuneable source of magnetostatic wavepackets [8].

The work is supported by RFBR (project 20-32-70149) and BASIS foundation (project 19-1-3-42-1).

-
- [1] A.V. Kimel, et al., Phys. Reports **852** (2020) 1-46.
 - [2] S.A. Nikitov, et al. Phys.-Usp. **63** (2020) 945.
 - [3] T. Satoh, et al. Nat. Photonics **6** (2012) 662-666.
 - [4] Y. Au, et al. Phys. Rev. Lett. **110** (2013) 097201.
 - [5] M. Vogel, et al. Nat. Physics **11** (2015) 487–491.
 - [6] N.E. Khokhlov, et al. Phys. Rev. Applied **12** (2019) 044044.
 - [7] Ia.A. Filatov, et al., J. Phys. Conf. Ser. **1697** (2020) 012193.
 - [8] N.E. Khokhlov, et al. (2021) arXiv:2101.11931.

Propagating spin-waves generated in a spin Hall nano-oscillator

Himanshu Fulara^a, Mohammad Zahedinejad^a, Roman Khymyn^a, Shreyas Muralidhar^a, Ahmad. A. Awad^{a,b}, Mykola Dvornik^a, and Johan Åkerman^{a,b,c}

^aDepartment of Physics, University of Gothenburg, 412 96 Gothenburg, Sweden

^bNanOsc AB, Kista 164 40, Sweden

^cDepartment of Applied Physics, School of Engineering Sciences, KTH Royal Institute of Technology, Electrum 229, SE-16440 Kista, Sweden

Spin Hall nano-oscillators (SHNOs) are one of the most promising spintronics devices as they are CMOS compatible tunable microwave nanoscale sources and exhibit robust long-range mutual synchronization both in chains and two-dimensional arrays at frequencies amenable to high-speed neuromorphic computing [1,2]. However, all demonstrations have relied on localized spin-wave (SW) modes interacting through dipolar coupling and/or direct exchange [1]. As nanomagnonics requires propagating SWs for energy-efficient data transfer and non-conventional wave-based computing, it would be highly advantageous if the localization could be mitigated in these SHNOs to excite truly propagating SWs.

Here, we demonstrate how interface induced perpendicular magnetic anisotropy (PMA) can efficiently overcome the localization of SWs in nano-constriction based W(5nm)/CoFeB(1.4nm)/MgO(2nm) SHNOs, resulting in the controllable excitation of field-

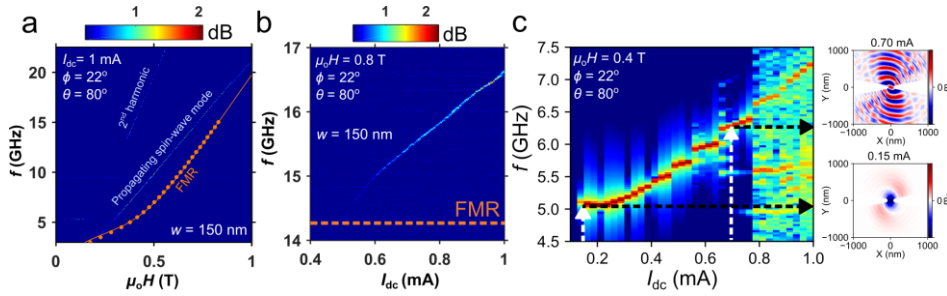


Figure 1: (a) Field sweep (b) Current sweep, and (c) Micromagnetic simulated, SW auto-oscillations excited on a 150 nm nano-constriction SHNO

and current-tunable propagating SWs over a wide range of about 3 to 22 GHz [3]. High frequency microwave measurements combined with micromagnetic simulations establish that the large positive non-linearity brought about by the strong PMA of thinner CoFeB layer raises the frequency of SW auto-oscillations well above the FMR spectrum, indicating the propagating nature of SW auto-oscillations (see Figure 1a-c). The capability of such low-operational current generation of propagating SWs not only makes these SHNOs directly adaptable to nanomagnonic circuits but also ensures long-range mutual synchronization for scaling neuromorphic computing to large dynamical neural networks.

-
- [1] A. A. Awad, P. Dürrenfeld, A. Houshang, M. Dvornik, E. Iacocca, R. K. Dumas, J. Åkerman, Nat. Phys. 13, 292-299 (2017).
 [2] M. Zahedinejad, A. A. Awad, S. Muralidhar, R. Khymyn, H. Fulara, H. Mazraati, M. Dvornik, J. Åkerman, arXiv preprint arXiv:1812.09630 (2018).
 [3] H. Fulara, M. Zahedinejad, R. Khymyn, A. A. Awad, S. Muralidhar, M. Dvornik, J. Åkerman, Sci. Adv. 5, eaax8467 (2019).

Advances in Magnetism 2020-21, June 13-16, 2021

Spintronics, multiferroics and voltage control of magnetism

[Abstracts can be easily browsed through the bookmarks](#)

***In-operando* adjustable orbital polarization in LaNiO₃ thin films**

H. B. Vasili^a, D. Pesquera^{b,c}, M. Valvidares^a, P. Gargiani^a, E. Pellegrin^a, F. Bondino^d,
E. Magnano^d, A. Barla^e, and J. Fontcuberta^b

^a ALBA Synchrotron Light Source, E-08290 Cerdanyola del Vallès, Barcelona, Catalonia,
Spain

^b Institut de Ciència de Materials de Barcelona (ICMAB-CSIC), Campus UAB, 08193,
Bellaterra, Catalonia, Spain

^c Department of Materials Science, University of Cambridge, Cambridge CB3 0FS,
United Kingdom

^d Istituto Officina dei Materiali (IOM), Consiglio Nazionale delle Ricerche (CNR),
I-34149 Trieste, Italy

^e Istituto di Struttura della Materia (ISM), Consiglio Nazionale delle Ricerche (CNR),
I-34149 Trieste, Italy

Electronic occupation of atomic orbitals is a key parameter that governs the properties of atoms and solids. More precisely, the electronic occupation of the 3dⁿ, 4dⁿ and 4fⁿ orbitals in the metal oxides have major consequences on their electric and magnetic properties and thus its understanding and control provide a knob to tune their properties. Superconducting cuprates, for instance, have Cu²⁺:3d⁹ ions. The layered structure creates a crystal field that splits the 3d-e_g (x²-y², z²) manifold and the single hole, residing in the upper lying x²-y² orbital, is thought to be key for HTSC. Therefore, it is said the 3d-e_g orbitals are 100% orbitally polarized. In nickelate perovskites, such as LaNiO₃, the Ni³⁺:3d⁷ ions in a cubic structure have the single e_g¹ electron occupying a degenerate (x²-y², z²) manifold; therefore, the system is metallic and the orbital polarization is zero. Breaking the cubic symmetry may allow to induce orbital polarization, that could mimic that of the HTSC cuprates. Here we report on the achievement and demonstration of *in-operando* voltage-controlled tuning of the orbital occupation in LaNiO₃ epitaxial thin films grown on piezoelectric substrates. The different static contributions to the orbital occupation are disentangled, namely the epitaxial strain and the surface symmetry breaking, and the superimposed piezo-electric related orbital polarization is determined by exploiting x-ray linear dichroism at the Ni-L_{2,3} edges. Remarkably, it is found that the voltage-controlled orbital polarization largely amplifies the effects of epitaxial strain. Perspectives for further developments shall be discussed.

[1] H.B. Vasili et al. Submitted. September 2019

High resistive unipolar switching in thin film antiferromagnet CuMnAs

Zdeněk Kašpar^{a,b}, Miloslav Surýnek^b, Jan Zubáč^{a,b}, Filip Křížek^a, Vít Novák^a,
Tomáš Jungwirth^{a,c} and Kamil Olejník^a

^a Institute of Physics, Czech Academy of Sciences, Prague, Czech Republic

^b Faculty of Mathematics and Physics, Charles University, Prague, Czech Republic

^c School of Physics and Astronomy, University of Nottingham, Nottingham, United Kingdom

Antiferromagnetic materials have potential to start a new revolution in information storage. The precession dynamics exceeds GHz range due to large exchange interaction and storage density can be extremely high due to zero stray field. On the other hand, manipulation of the antiferromagnetic moments is extremely challenging. The Neel-order spin-orbit torque was proposed to be present in antiferromagnets with special crystal symmetry, like Mn₂Au and CuMnAs [1]. In the latter one the first experimental observation of electrical switching of the antiferromagnet was achieved [2]. The switching can be observed using subnanosecond electrical pulses [3] and even with THz radiation excitation [4]. Current induced domain wall motion was recently observed in the same material [5].

In this work we present a new mechanism of reversible resistive switching in antiferromagnetic CuMnAs memory cell [6]. The amplitude of this switching signal can reach up to 20% of sheet resistance at room temperature by sequence of two perpendicular 100μs electric pulses. The relaxation follows stretched exponential rule indicating complex magnet nano-texture origin. This new mechanism allows the use of simple two-terminal device with set and reset pulsing sequence as shown in Fig.1.

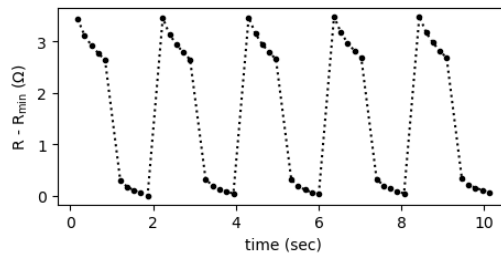


Figure 1: Example of set ($1.03 \times 10^7 \text{Acm}^{-2}$) and reset ($0.96 \times 10^7 \text{Acm}^{-2}$) sequence on unipolar two-terminal device.

-
- [1] J. Železný, Physical Review Letters **113**, 157201 (2014).
 - [2] P. Wadley, Science **351**, 587 (2016).
 - [3] K. Olejník, Nature Communications **8**, 15434 (2017).
 - [4] K. Olejník, Science Advances **4** (3), eaar3566 (2018).
 - [5] P. Wadley, Nature Nanotechnology **13**, 362–365 (2018)
 - [6] Z. Kašpar, arXiv:1909.09071

A journey into the antiferromagnetic spin textures of BiFeO₃

Angela Haykal^a, Johanna Fischer^b, Waseem Akhtar^a, Aurore Finco^a, Jean-Yves
Chauleau^c, Daniel Sando^d, Cécile Carrétéro^b, Nicolas Jaouen^e, Manuel Bibes^b, Michel
Viret^c, Stephane Fusil^{b,f}, Vincent Garcia^b, Vincent Jacques^a

^a Laboratoire Charles Coulomb, CNRS-UM2, Montpellier, France

^b Unité Mixte de Physique, CNRS, Thales, Palaiseau, France

^c SPEC, CEA, CNRS, Gif-sur-Yvette, France

^d School of Materials Science and Engineering, University of New South Wales, Sydney,
Australia

^e Synchrotron SOLEIL, Gif-sur-Yvette, France

^f Université d'Evry, Université Paris-Saclay, Evry, France

Antiferromagnetic (AF) thin films are currently attracting considerable excitement for low dissipative spintronic devices [1,2]. However, most of conventional real-space magnetic microscopy techniques cannot probe the AF order at the nanoscale because magnetic moments are mostly compensated, resulting in very low magnetic signals. This is a major obstacle to the fundamental understanding of nanoscale AF order and its response to external stimuli, such as spin polarized currents or electric fields. To release the full potential of AFs for next-generation spintronics, the nanoscale control and imaging capabilities that are now routine for ferromagnets must be extended to AF materials.

Here we show that scanning magnetometry based on a single nitrogen–vacancy (NV) defect in diamond is ideally suited for imaging complex AF orders at the nanoscale, even under ambient conditions. As a proof of principle, we report on the first real-space visualization of a non-collinear AF order in a thin film of bismuth ferrite BiFeO₃ (BFO), a room-temperature multiferroic material in which the AF order is intimately linked to the ferroelectric one via magnetoelectric coupling. We first image the cycloidal AF order in a BFO thin film and demonstrate that magnetoelectric coupling can be exploited to manipulate the cycloid propagation direction by an electric field [3]. We then investigate the effect of epitaxial constraint on the behaviour of the AF order in strained BFO thin-films [4]. Different substrates were used for the growth in order to tune the strain. Using scanning NV-magnetometry, we proved that tuning strain can stabilize different propagation directions of the cycloid, can change the plane in which the cycloid rotates or can collapse the cycloid into G-type antiferromagnetic domains in highly strained films. These results demonstrate how BFO can be used to design reconfigurable AF spin textures on demand.

-
- [1] V. Baltz et al., *Rev. Mod. Phys.* **90** (2018), 015005.
 - [2] T. Jungwirth et al., *Nat. Nanotechnol.* **11** (2016), 231-241.
 - [3] I. Gross et al., *Nat.* **549** (2017), 252-256.
 - [4] D. Sando et al., *Nat. Mater.* **12** (2013), 641-646.

Magnetic properties of self-assembled Co and Ni porphyrins in Fe-based spinterfaces

A. Brambilla^a, A. Lodesani^a, A. Picone^a, A. Calloni^a, M. S. Jagadeesh^a, G. Bussetti^a, G. Vinai^b, G. Panaccione^b, L. Duò^a, M. Finazzi^a, F. Ciccacci^a

^a Physics Department, Politecnico di Milano, Milano, Italy

^b Istituto Officina dei Materiali (IOM)-CNR, Laboratorio TASC, Trieste, Italy

A so-called spinterface is an interface between an organic semiconductor (OS) and a ferromagnetic (FM) substrate. This kind of system raised an ever increasing interest in the last few years, first through the realization of organic spintronics prototypical devices (e.g. organic spin valves, where an organic layer is sandwiched between two FM electrodes) then by showing new intriguing phenomena (such as inducing a magnetic moment at the surface of a Cu substrate) related to the formation of hybridized interface states (HIS), created by the overlapping between the electronic orbitals of the adjacent species at the interface (for a comprehending review, see Ref. 1).

Metallo-Tetra Phenyl Porphyrins (M-TPP) are ideal candidates for building spinterfaces because of their flat morphology and of the fact that their ion core can have its own magnetic moment, on account of the presence of unpaired spins on the metal ion [2]. One can in fact expect, in principle, that different magnetic configurations may occur at a M-TPP/FM spinterface, driven by the formation of HIS where the hybridization also involves the metal ion core and, thus, its magnetic moment.

Typically, an OS layer can strongly interact with the surface of a FM substrate, making it difficult to obtain well-ordered structures. The present work focuses on the growth and the characterization of self-assembled monolayers of Zn-, Co- and Ni-TPP on bare and O-passivated Fe(001). The samples were extensively investigated in terms of electronic properties, crystal structure and morphology by means of electron spectroscopies, electron diffraction and Scanning Tunneling Microscopy (STM). Furthermore, the spin-dependent behavior of Co- and Ni-TPP based spinterfaces were studied by Spin-Resolved Photoemission Spectroscopy (SR-PES) and by X-ray Magnetic Circular Dichroism (XMCD). The obtained results show that the passivation of the metal surface is able to stabilize the growth of the molecules and to promote their self-assembly [3]. See an example in Fig. 1. STM measurements also reveal that the arrangement of the molecules on the passivated substrate varies with the ion core species.

From the point of view of the magnetic properties, spin-dependent effects were observed for relevant spinterfaces, in particular for Co-TPP/Fe(001)-*p*(1x1)O [4]. They will be discussed in details.

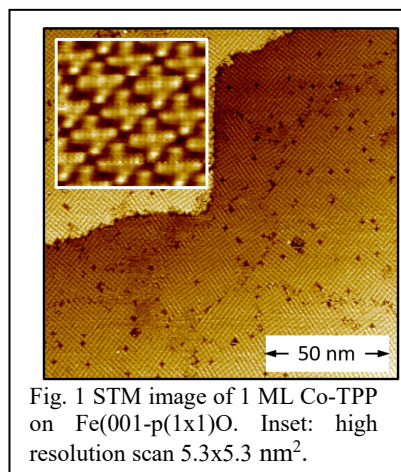


Fig. 1 STM image of 1 ML Co-TPP on Fe(001)-*p*(1x1)O. Inset: high resolution scan 5.3x5.3 nm².

[1] M. Cinchetti, V. A. Dediu, L. E. Hueso, *Nature Mater.* **16** (2017) 507-515.

[2] J. M. Gottfried, *Surf. Sci. Rep.* **70** (2015) 259.

[3] A. Picone, D. Giannotti, A. Brambilla, et al., *Appl. Surf. Sci.* **435**, (2018) 841-847

[4] M.S. Jagadeesh, A. Calloni, A. Brambilla, et al., *Appl. Phys. Lett.* **115**, 082404 (2019).

Measurement of the spin relaxation anisotropy in 3d ferromagnets

M. Cosset-Cheneau^{1,2}, L. Vila¹, G. Zahnd¹, D. Gusakova¹, A. Marty¹, and J.-P. Attané¹

¹ SPINTEC, CEA-INAC/CNRS/Univ. Grenoble Alpes, F-38000 Grenoble, France

² Département de Physique, Ecole Normale Supérieure de Lyon, F-69342, France

The relaxation of a spin current into a ferromagnetic material occurs through different processes depending on the spin currents' polarization orientation. For a polarization collinear with the material magnetization, the relaxation occurs through diffusive processes controlled by the spin diffusion length [1]. When the polarization is transverse with the magnetization, the relaxation is driven by ballistic processes due to band structure mismatch and non-coherent spin precession [2]. Despite being a key ingredient for the understanding of phenomena like Spin Transfer Torque, this anisotropy has never been directly observed so far.

In this presentation, we report the observation of the spin relaxation anisotropy on a single device by using a spin absorption method in Lateral Spin Valves (LSVs) [3]. Using a magnetic field, we control the relative orientation between the spin current polarization and the magnetization of a nanodisk-shaped ferromagnetic absorber (fig. 1). We observed that the efficiency of the spin current absorption increases when this polarization and the absorber magnetization have transverse directions.

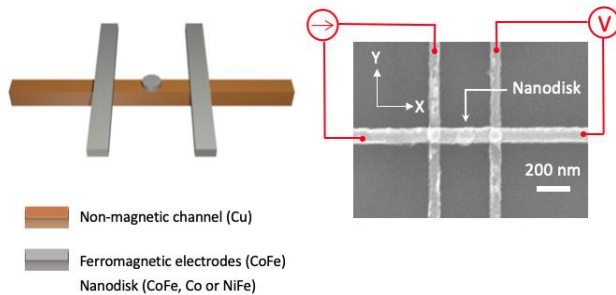


Figure 1: Drawing and SEM picture of the device used for the absorption anisotropy measurement. The nanodisk absorbs the spin current that flows between the ferromagnetic electrodes. Its isotropic shape allows to change its magnetization orientation by using a weak external magnetic field

We will present a device that allows the study of spin transport in a LSV with non-collinear ferromagnetic component. By demonstrating a good control over its magnetic states, we will show that we indeed observed the spin current relaxation anisotropy in a single device. We carried an analysis by introducing bulk characteristic lengths of the transverse spin relaxation, and the spin mixing conductance describing transverse interfacial spin relaxation processes. This data analysis points out the role of both interfacial and bulk contribution in the non-collinear spin current relaxation.

[1] T. Valet and A. Fert, Phys. Rev. B 48, 7099 (1993)

[2] C. Petitjean et al., Phys. Rev. Lett. 109, 117204 (2012)

[3] G. Zahnd et al., Phys. Rev. B 98, 175514 (2018)

All-optical imaging of magnetic skyrmions with a scanning-NV magnetometer

S. Chouaieb^a, A. Finco^a, F. Fabre^a, W. Akhtar^a, A. Haykal^a, A. Hrabec^b, A. Thiaville^b, S. Rohart^b, M. Belmeguenai^c, M. S. Gabor^d, G. Rana^e, L. Prejbeanu^e, O. Boulle^e and V. Jacques^a.

^a Laboratoire Charles Coulomb, Université de Montpellier and CNRS, 34095 Montpellier, France

^b Laboratoire de Physique des Solides, CNRS UMR 8502, Université Paris-Sud and Université Paris Saclay, 91405 Orsay Cedex, France

^c Laboratoire de Science des Procédés et des Matériaux, CNRS-Université Paris 13, Sorbonne Paris Cité, 93430 Villetaneuse, France

^d Center for Superconductivity, Spintronics and Surface Science, Technical University of Cluj Napoca, 400114 Cluj-Napoca, Romania

^e Spintec Université Grenoble Alpes, CNRS, CEA, Grenoble INP, INAC-Spintec, 38000 Grenoble, France

In this work, nitrogen-vacancy (NV) magnetic microscopy [1] is employed in the quenching mode as a non-invasive, high resolution tool to investigate the physics of skyrmions in ultrathin magnetic films [2].

We first investigate current-induced dynamics of skyrmions stabilized in thin ferromagnetic wires of a Huesler Alloy (Co₂FeAl) grown on top of Platinum. Combining scanning-NV magnetometry with current pulse injection, we demonstrate current-induced nucleation and motion of skyrmion through spin-orbit torques. Our findings illustrate the dramatic impact of disorder on skyrmion dynamics, even in a material known for its intrinsically low magnetic damping [3].

We then report on the stabilization of sub-100 nm skyrmions at zero external magnetic field in an exchange-biased multilayer stack. Here exchange bias at the interface between a ferromagnet and an antiferromagnet is used as an internal field to nucleate skyrmions, without the need of an external magnetic field. Compared to magnetic force microscopy, the main advantage of scanning-NV magnetometry is here the absence of magnetic back-action on the sample which provides unambiguous magnetic field images. This is particularly important for the study of spin textures in ultrathin films, which are often highly sensitive to magnetic perturbations.

Besides providing new insights into the properties of skyrmions in thin ferromagnets, this work also highlights the unique potential of NV magnetometry in quenching mode to study ferromagnetic textures with high spatial resolution under ambient conditions.

This research is supported by the DARPA TEE programm through (grant MIPR no. HR0011831554) and the European Research Council (ERC-StG-2014, Imagine).

[1] L.Rondin et al., *Reo. Prog. Phys.* 77, 056503 (2014)

[2] I. Gross et al., *Physical Review Materials*, 2, 024406 (2018)

[3] W. Akhtar et al., *Physical Review Applied*, 11, 034066 (2019)

Two-dimensional mutually synchronized spin Hall nano-oscillator arrays for highly coherent microwave signal generation and neuromorphic computing

Johan Åkerman^{a,b,c}, Mohammad Zahedinejad^{a,c}, Ahmad A. Awad^{a,c}, Shreyas Muralidhar^a, Roman Khymyn^{a,c}, Himanshu Fulara^{a,c}, Hamid Mazraati^{b,c}, and Mykola Dvornik^{a,c}

^a Physics Department, University of Gothenburg, 412 96 Gothenburg, Sweden

^b Material and Nanophysics, School of Engineering Sciences, KTH Royal Institute of Technology, Electrum 229, 164 40 Kista, Sweden

^c NanOsc AB, Electrum 229, 164 40 Kista, Sweden

Mutually synchronized spin torque nano-oscillators (STNOs) are one of the promising platforms for bioinspired computing and microwave signal generation [1, 2]. Using STNOs one can achieve 90% recognition rate in spoken vowels [3]. However, in order to do more complex tasks, larger scale synchronized oscillators are needed, something that is not easily done with the STNOs demonstrated so far.

In my talk, I will describe a different type of spin current driven device called spin Hall nano-oscillators (SHNOs), which can generate microwave frequencies over a very wide frequency range [4]. The SHNOs are based on 50 – 120 nm wide nano-constrictions in Pt(5)/Hf(0.5)/NiFe(3) trilayers (all numbers in nm). When multiple nano-constrictions are fabricated close to each other (300 – 1200 nm separation) they can mutually synchronize and chains of up to nine nano-constrictions have been demonstrated to exhibit complete synchronization [5]. For the first time, we can now also synchronize two-dimensional SHNO arrays with as many as $8 \times 8 = 64$ SHNOs [6]. The mutual synchronization is observed both electrically and using scanning micro-BLS microscopy. Both the output power and linewidth of the microwave signal improves substantially with increasing number of mutually synchronized SHNOs, such that quality factors of about 170,000 can be reached. Following the approach of Romera et al [3], we also demonstrate neuromorphic computing using a 4×4 SHNO array with two injected microwave signals as inputs.

Given their high operating frequency (~10 GHz), easy fabrication, and highly robust synchronization properties, nano-constriction SHNO arrays are likely the most promising candidates for neuromorphic computing based on oscillator networks.

-
- [1] J. Grollier, D. Querlioz, and M. D. Stiles, Proc. IEEE **104**, 2024 (2016).
 - [2] J. Torrejon et al, Nature **547**, 428 (2017)
 - [3] M. Romera et al, Nature **563**, 230–234 (2018)
 - [4] T. Chen, R. K. Dumas, A. Eklund, P. K. Muduli, A. Houshang, A. A. Awad, P. Dürrenfeld, B. G. Malm, A. Rusu, and J. Åkerman, Proc. IEEE **104**, 1919 (2016)
 - [5] A. A. Awad, P. Dürrenfeld, A. Houshang, M. Dvornik, E. Iacocca, R. K. Dumas, and J. Åkerman, Nature Physics **13**, 292–299 (2017)
 - [6] M. Zahedinejad, et al. arXiv:1812.09630 (2018)

Anomalous electroactive magnetic excitations in frustrated magnets

Shin Miyahara^a

^a Fukuoka University, Fukuoka, Japan

In magnetoelectric multiferroics, there is a strong coupling between magnetization and electric polarization. Such a coupling induces static magnetoelectric effects, i.e., the magnetic structure can be controlled by the external electric fields and vice versa. Moreover, the electromagnon, i.e., the electro active magnon, process arise due to the coupling, where electric component of light can excite a spin wave excitation through the magnetoelectric couplings.

The typical example of an electromagnon is a magnon excitation in helical magnets [1]. The spin wave can be simultaneously excited by oscillating magnetic and electric fields and the cross correlation effects induces anomalous behaviors. Such a cross correlation can be observed as nonreciprocal direction dichroism in absorption under external magnetic fields [2]. Moreover, the spin wave spin current under the external magnetic fields shows the non-reciprocal property, i.e., the way of the propagation of the spin wave depends on the direction of the propagation. Such nonreciprocal properties can be tuned not only by the external magnetic fields but also the external electric fields due to the magnetoelectric coupling.

The electromagnetic coupling induce anomalous excitation processes even in spin gapped systems. In the Heisenberg system, the spin gap excitation from the singlet ground state cannot be excited by oscillating magnetic fields. However, such a spin gap excitation can be excited as an electro active process and, thus, the absorption of light can show the resonance due the spin gap excitation. As a typical example, we show that the spin gap excitation in Shastry-Sutherland material $\text{SrCu}_2(\text{BO}_3)_2$ [3] can be excited by the electric components of light.

[1] H. Katsura, A.V. Balatsky, and N. Nagaosa, Phys. Rev. Lett. **98**, 027203 (2007).

[2] S. Miyahara and N. Furukawa, Phys. Rev. B **89**, 195145 (2014).

[3] S. Miyahara and K. Ueda, J. Phys.:Condens. Matter **15**, R327 (2003).

Synthesis, magnetic properties and inhomogeneities in Pd_{1-x}Fe_x alloy ultrathin epitaxial films

Roman Yusupov^a, Igor Yanilkin^a, Amir Gumarov^a, Andrey Petrov^a, Airat Kiiamov^a, Alexander Rodionov^a, Sergey Nikitin^a, Lenar Tagirov^{a,b}

^a Kazan Federal University, Kazan, Russia

^b Zavoisky Physical-Technical Institute, FRC Kazan Scientific Center of RAS, Kazan, Russia

Palladium-iron alloys Pd_{1-x}Fe_x with low ($x < 0.10$) iron content are promising materials for the F-layer in S/F/S (superconductor/ferromagnet/superconductor) thin film heterostructures that serve as a basis for superconducting spintronic devices [1,2]. These “supertronics” elements are capable to operate at extreme high frequencies (up to THz) with an ultralow power consumption (about 10^{-19} J/switch). Requirements to the F-layer include low saturated magnetization, in-plane anisotropy, low coercive field and high magnetic homogeneity. All these have to be satisfied for the same material.

In the talk, we present the procedure for high-quality Pd_{1-x}Fe_x epitaxial film synthesis on MgO (001) substrate ($x = 0 \dots 0.08$), results on its structure and morphology characterization as well as magnetization studies. Magnetic anisotropy has been explored with ferromagnetic resonance; dependences of the anisotropy constants on the iron content x will be presented and described. Also, the relevancy of the existing models of diluted Pd_{1-x}Fe_x alloys ferromagnetism applied to the $M_s(T)$ data will be addressed.

Ferromagnetic layer inhomogeneity has been assigned as a source for improper characteristics of S/F/S structures based on Pd_{1-x}Fe_x alloy with x values of 0.01, 0.013 and 0.03 [3]. This is not surprising for diluted alloys with inevitable local Fe-content variation. We have found that femtosecond optical and magneto-optical laser spectroscopy is a powerful tool for this kind of magnetic inhomogeneity studies. In particular, we will show that a number and a character of relaxation components in the reflectivity and magneto-optical Kerr rotation transients studied in a wide temperature range of 4 – 300 K provide with information on occurrence and even amount of the residual paramagnetic phase at low temperatures. Also, the minimum iron content ensuring the magnetic homogeneity of Pd_{1-x}Fe_x thin epitaxial films will be proposed and discussed.

-
- [1] V.V. Ryazanov, V.V. Bol'ginov, D.S. Sobanin, I.V. Vernik, S.K. Tolpygo, A.M. Kadin, O.A. Mukhanov, *Physics Procedia* **36** (2012), 35-41.
 - [2] D.S. Holmes, A.L. Ripple, and M.A. Manheimer. *IEEE Trans. Appl. Supercond.* **23** (2013), 1701610.
 - [3] J.A. Glick, R. Loloee, W.P. Pratt, Jr., N.O. Birge, *IEEE Trans. Appl. Supercond.* **27** (2017), 1800205.

Spin to charge conversion in the topological insulator HgTe and in STO-based two-dimensional electron gas

P. Noel^a, C. Thomasⁱ, F. Trier^b, D. C. Vaz^b, Y. Fu^a, A. Johansson^d, B. Haasⁱ, P-H. Jouneau^a, S. Gambarelli^a, B. Göbel^j, F. Bruno^e, G. Singh^f, S. McKeown-Walker^e, L. M. Vicente-Arche^b, J. Bréhin^b, S. Fusil^b, V. Garcia^b, A. Sander^l, S. Valencia^g, P. Bruneel^h, M. Vivek^h, M. Gabay^h, N. Bergeal^h, F. Baumberger^e, H. Okuno^a, A. Fert^b, A. Barthélémy^b, I. Mertig^d, T. Meunier^c, P. Balletⁱ, L. Vila^a, M. Bibes^b, and J. P. Attané^a

^a Univ. Grenoble Alpes, CEA, IRIG, 38000 Grenoble (France)

^b Unité Mixte de Physique CNRS, Thales, Univ. Paris-Sud & Paris-Saclay, France

^c CNRS, Institut NEEL, 38042 Grenoble, France

^d Institute of Physics, Martin Luther University Halle-Wittenberg, 06099 Halle Germany

^e Department of Quantum Matter Physics, University of Geneva, Geneva (Switzerland)

^f Lab. de Physique et d'Etude des Matériaux, ESPCI Paris, PSL University, Paris France

^g Helmholtz-Zentrum Berlin für Materialien und Energie, Berlin, Germany

^h Laboratoire de Physique des Solides, CNRS, Univ. Paris-Sud & Paris-Saclay, Orsay France

ⁱ Univ. Grenoble Alpes, CEA, LETI, MINATEC Campus, F38054 Grenoble, France 3

^j Max Planck Institute of Microstructure Physics, 06120 Halle (Germany)

While classical spintronics has traditionally relied on ferromagnetic metals as spin generators and spin detectors, a new approach called spin-orbitronics exploits the interplay between charge and spin currents enabled by the spin-orbit coupling in non-magnetic systems. In this contribution, we report the observation of spin-to-charge current conversion in strained mercury telluride, using spin pumping experiments at room temperature. We show that a HgCdTe barrier can be used to protect the HgTe topological surface states, leading to high conversion rates, with inverse Edelstein lengths up to 2.0 ± 0.5 nm. These measurements, associated with the temperature dependence of the resistivity, suggest that these high conversion rates are due to the spin momentum locking property of HgTe surface states [1].

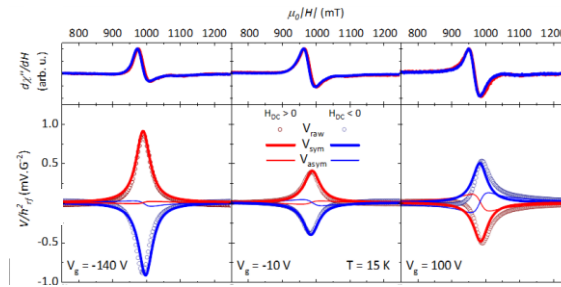


Figure 1: *FMR curves (top) and spin signals (bottom) for different values of the gate voltage in a STO-based 2DEG, for a positive (red) and negative (blue) applied DC magnetic field.*

We then focus on the SrTiO₃ (STO)-based 2D electron system, presenting experiments performed on NiFe/Al/STO heterostructures. We investigate the nature of the spin-to-charge conversion through a combination of spin pumping, magnetotransport, spectroscopy and gating experiments, finding a very highly efficient spin-to-charge conversion, with inverse Edelstein lengths beyond 20 nm. More importantly, we demonstrate that the conversion rate can be tuned in amplitude and rate by a gate voltage (cf. fig.1).

[1] P. Noel *et al.*, Phys. Rev. Lett. 120, 167201 (2018)

[2] D. C. Vaz *et al.*, Nature Materials 1-7 (2019)

A comparative study of GMI effect calculation for magnetic thin film via theoretical deduction and machine learning

Guangcun Shan^{a, b}, Xin Li^{a, b},

^a School of Instrumentation Science and Opto-electronics Engineering, Beihang University, Beijing, China

^b Department of Materials Science, City University of Hong Kong, Hong Kong

Attributed to the Giant Magnetoimpedance (GMI) effect, the AC impedance of soft magnetic alloys will change with the change of the applied DC magnetic field under the drive of AC current, which makes GMI based magnetic sensor have excellent sensitivity [1],[2]. Since the discovery of the magnetoimpedance (MI) effect just over a decade ago, international research interest into the GMI effect has been growing. This work aims to provide a comprehensive summary of the GMI topic, encompassing fundamental understanding of the GMI phenomena, the processing and properties of GMI materials and the design and application of GMI-based magnetic sensors. It starts with the definition of GMI and an assessment of the current theoretical understanding of the frequency dependence of GMI. Based on the theory of classical electrodynamics and ferromagnetism [3], including Maxwell equations and Landau-Lifshitz equation, the GMI effect of amorphous thin film with the architecture of closed sandwich structure was calculated. Properties of existing GMI materials including magnetic, mechanical, electrical and chemical properties are described, and a correlation between domain structures and magnetic properties is established, which enables the selection of optimal conditions to design high-performance GMI-based sensors.. An Artificial Neural Networks model was well trained, which could also describe the relationship among GMI ratio, H and f without complicated background knowledge of physics, as shown in Fig. 1(b). Our study has shown that the data-driven machine learning method proposed here works for experimental data, and can be easily expanded to predict other properties of GMI devices without complicated formula derivation.

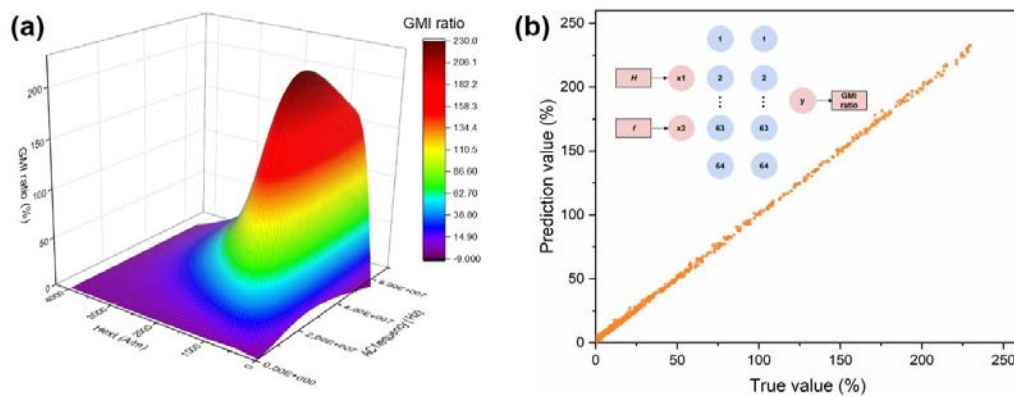


Figure 1: GMI effect of amorphous thin film with closed sandwich structure calculated based on (a) classical electrodynamics and ferromagnetism and (b) machine learning model.

- [1] M.-H. Phan and H.-X. Peng, Prog. Mater. Sci. **53** (2008), 323–420.
- [2] T. Wang, Biosens. Bioelectron. **90** (2017), 418–435.
- [3] C. Dong, S. Chen, and T. Y. Hsu (Xu Zuyao), Journal of Magnetism and Magnetic Materials **250** (2002), 288–294

Memristors make unruly spin Hall nano-oscillators synchronize and remember.

Mohammad Zahedinejad^a, H. Fulara^a, S. Fukami^b, S. Kanai^b, H. Ohno^b, J. Åkerman^a

^a Physics Department, University of Gothenburg, Gothenburg, Sweden

^b Laboratory for Nanoelectronics and Spintronics, Tohoku University, Sendai, Japan

Mutual synchronized spin Hall nano-oscillators (SHNOs) are one of the promising platforms for microwave signal generation and bioinspired computing [1,2]. However, in order to do complex tasks, larger scale synchronized oscillators with individual control are needed. In addition, the platform should have actual internal memory hardware in order to tune the coupling and frequency of individual oscillators for training purpose.

In this work, we present W/CoFeB/MgO based spin Hall nano-oscillators (SHNOs) with an embedded memristor (CoFeB/MgO/AlO_x/SiN_x/Ti/Cu) having both a high-resistance state (HRS) and a tunable low-resistance state (LRS), which we successfully use to tune the SHNO frequency. Fig.1A shows the SHNO frequency versus drive current (I_{SHNO}) of four free running oscillators in a chain without any applied voltage to the memristor. After reaching the auto-oscillation threshold current, the chains start at synchronized state. The synchronization, however, breaks apart for $I_{SHNO} > 600 \mu\text{A}$. We set $I_{SHNO} = 712 \mu\text{A}$ at which the synchronization is broken and study the output signal of the chain vs. memristor voltage. When the memristor operates in its HRS (Fig.1B) it acts as an insulating gate applying a strong electric field to the MgO/CoFeB interface. The electric field modifies the perpendicular magnetic anisotropy (PMA), which directly translates into a change auto-oscillation (AO) frequency of the two SHNOs affected. At a memristor voltage of about 2.5 V, the SHNO chain mutually synchronizes. As the voltage is further increased, the memristor switches to its LRS ($V_G = V_{set}$), and a certain amount of additional current I_m is then injected into the SHNO underneath. As a consequence, the AO frequency experiences a drastic change, now based on current dependent tuning. The oscillators remain synchronized when the voltage is swept back until the memristor switches to LRS (Fig.1C).

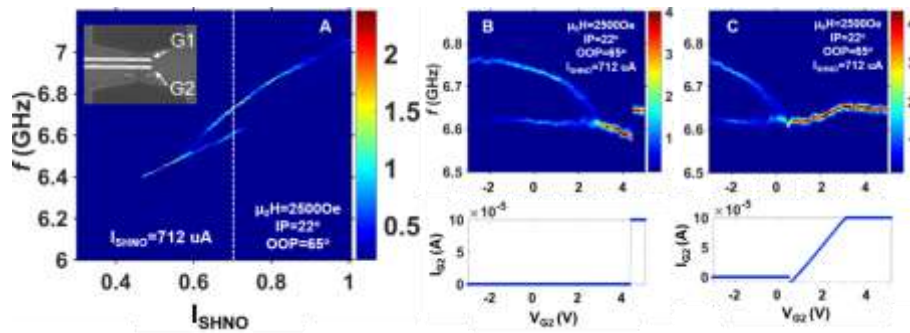


Figure 1. (A) Frequency vs. SHNO current profile. The inset shows were to top electrodes are located. Effect of memristor voltage (V_G) sweep on power spectral density for forward (-3 to +4.5 V) and (C) backward (+4.5 to -3 V) sweeps.

We have hence demonstrated both instantaneous and non-volatile tuning of SHNO synchronization, which can be used for on-chip learning at the oscillator level. Our demonstration can be extended to larger 1D and 2D SHNO arrays where the individual oscillators frequencies can be tuned to push the entire ensemble to synchronization at a frequency corresponding to a memorized template to be recognized by the network. Embedding the memristors helps to recall the previous coupling value (weight) between oscillators.

Ferroelectric control of spin-to-charge conversion in GeTe

S. Varotto^{a,b}, L. Nessi^a, F. Fagiani^a, S. Cecchi^c, P. Noël^d, S. Petrò^a, A. Novati^a,
R. Calarco^c, M. Cantoni^a, J.-P. Attané^d, L. Vila^d, M. Bibes^b, J. Slawinska^e,
M. B. Nardelli^e, S. Picozzi^f, R. Bertacco^a, C. Rinaldi^a

^aDipartimento di Fisica, Politecnico di Milano, 20133 Milano, Italy

^bUnité Mixte de Physique, CNRS, Thales, Université Paris-Saclay, Palaiseau, France

^cPaul-Drude-Institut für Festkörperelektronik, 10117 Berlin, Germany

^dUniv. Grenoble Alpes, CNRS, CEA, Grenoble INP, IRIG-SPINTEC, Grenoble, France

^eDepartment of Physics, University of North Texas, Denton, United States of America

^fConsiglio Nazionale delle Ricerche, CNR-SPIN c/o Università G. D'Annunzio, Chieti, Italy

Scalable and energy efficient spin-orbit logic has been very recently pointed out by Intel as technologically suitable computing alternative to CMOS devices [1]. It comprises an electrically driven memory element, with a spin-orbit-based detection of the state performed by spin-to-charge conversion. In this talk, we show that the ferroelectric Rashba semiconductor Germanium Telluride [2] offers memory as well as spin-orbit readout in a silicon-compatible semiconductor.

GeTe possesses a giant bulk Rashba-like spin texture, which can be reversed by its non-volatile ferroelectricity, thus paving the way to the electric control of spin-to-charge conversion. We have already proved the existence of two opposite spin textures in GeTe thin films, corresponding to opposite ferroelectric states [3].

Here, we first demonstrate the switchability of the ferroelectric polarization in films of GeTe through gate electrodes. The switching is obtained through voltage pulses and measured as resistance variation of metal/GeTe heterojunctions. The modulation of resistance is due to the different local band bending induced at the metal/semiconductor interface by the screening of the polarization charge. Piezoresponse Force Microscopy was used to correlate the microscopic distribution of ferroelectric domains with the electrical resistivity of the junction. The low-voltage control is provided by the coercive voltage (3-7 V), with modulation of resistivity up to 300%, and the switching is robust, with endurance up to 10^5 cycles. Moreover, by changing the number of subsequent voltage pulses, their amplitude and duration, we can explore ferroelectric minor loops, enabling a continuous distribution of intermediate resistive/ferroelectric states.

The control of ferroelectricity in GeTe enables the electric control of spin-to-charge interconversion. The latter is studied by spin pumping experiments [4] in Fe/GeTe heterostructures [5]. A spin current generated by the resonant precession of the magnetization of the iron layer is injected into the adjacent GeTe layer. In an open circuit configuration, the charge current I_C produced in GeTe by spin-to-charge conversion is estimated by detecting the transverse voltage difference at the edges of a slab. The current production is significant after ferroelectric poling, and the sign of I_C switches with the ferroelectric polarization.

The results open the way to the non-volatile, electric control of spin transport and spin-to-charge conversion in a CMOS-compatible semiconductor.

-
- [1] S. Manipatruni *et al.*, Nature **565**, 35 (2019)
 - [2] D. Di Sante *et al.*, Adv. Mater. **25**, 509 (2013)
 - [3] C. Rinaldi *et al.*, Nano Letters **18**, 2751 (2018)
 - [4] C. Rinaldi *et al.*, APL Mater. **4**, 032501 (2016)
 - [5] J. Slawinska *et al.*, Phys. Rev. B **99**, 075306 (2019)

Beating the ordering temperature limit of FeO with antiferromagnetic proximity in FeO/CoO

A. Koziol-Rachwał^a, J. Korecki^b, M. Szpytma^a, M. Ślęzak^a, P. Drózdź^a, W. Janus^a,
H. Nayyef^a, M. Zając^c and T. Ślęzak^a

^a Faculty of Physics and Applied Computer Science, AGH University of Science and Technology, Krakow, Poland

^b Jerzy Haber Institute of Catalysis and Surface Chemistry, Polish Academy of Sciences, Krakow, Poland

^c National Synchrotron Radiation Centre SOLARIS, Jagiellonian University, Kraków, Poland

Antiferromagnets (AFMs), due to their unique set of properties, are promising candidates for future spintronics. However, low ordering temperature (Néel temperature, T_N) makes a wide group of AFM materials not applicable. Hence, tuning ordering temperature and spin configuration due to magnetic proximity effect in AFM/AFM systems has been recently identified as an important field of research [1].

In our studies we investigated how the proximity of antiferromagnetic layer with a higher ordering temperature influences the T_N of FeO in FeO/CoO bilayer. The FeO(1.7nm)/CoO(2nm) bilayers were grown by molecular beam epitaxy on MgO(001) substrate and coated with a 5nm-thick MgO buffer. The magnetic properties of FeO were studied with Conversion Electron Mössbauer Spectroscopy (CEMS). Figure 1 shows CEMS spectra collected at 240K for MgO/⁵⁷FeO/MgO (Fig. 1(a)) and ⁵⁷FeO/CoO/MgO (Fig. 1(b)). As the temperature of 240K is above the T_N of FeO (198K) for MgO/FeO/MgO we collected the CEMS spectrum characteristic for wüstite in paramagnetic state (Fig. 1(a)) [2]. Interestingly, proximity of CoO causes a serious modification of the spectrum, it becomes magnetically split (Fig. 1(b)). Systematic CEMS measurements recorded as a function of temperature for FeO/CoO revealed that the magnetic character of spectrum is preserved up to 260K. To determine T_N of CoO in FeO/CoO bilayer we performed X-ray Magnetic Linear Dichroism (XMLD) measurements, which revealed that the ordering temperature of CoO layer in FeO/CoO/MgO stack is comparable to the T_N of bulk CoO (293K). Enhancement of ordering temperature of FeO should result in increase in exchange interaction between ferromagnetic (FM) layer and FeO in FM/FeO/CoO multilayer. During my presentation I will show how the proximity of CoO layers with different thicknesses affects the exchange bias field in the Fe/FeO/CoO stack.

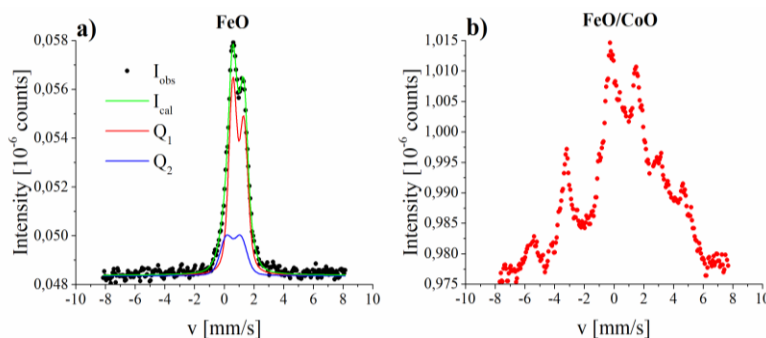


Figure 1: CEMS measurements of FeO (black points) in MgO/FeO/MgO (a) and MgO/FeO/CoO (b).

[1] S. Fukami et al., Journal of Applied Physics 128 070401 (2020).

[2] A. Koziol-Rachwał et al., Applied Physics Letters 108 041606 (2016).

The anomalous Nernst effect in Co₂MnSi thin film

J. Harknett^a, C.D.W. Cox^a, M.T. Greenaway^a, K. Morrison^a

^a Loughborough University, Leicestershire, UK

The Anomalous Nernst Effect (ANE) in a magnetic material gives rise to an electric field (\mathbf{E}) perpendicular to an applied temperature difference (ΔT), or heat flux (\mathbf{J}_Q), and magnetisation vector (\mathbf{M}), (Figure 1). Recently a wide range of materials, from thin films to bulk single crystals, dilute magnetic semiconductors and topological insulators, have been shown to exhibit an enhanced ANE due to the topological properties of their band structures [1],[2]. In particular these materials exhibit Weyl-like transport phenomena and have large values of the Berry curvature around the Fermi level [3].

The Berry curvature enhances the transverse velocity of the electrons [4] in addition to the statistical force produced by the ΔT , thereby generating a large anomalous thermoelectric response. The family of Heusler alloys contain proposed (and confirmed) magnetic Weyl semimetals most notably Co₂MnGa. However, another Heusler alloy which is of interest, particularly in the magnetic recording field is Co₂MnSi, identified for its 100% spin polarisation [5] and high magnetisation and Curie temperature.

Here, we study the ANE and the anomalous Hall effect (AHE) in a series of polycrystalline Co₂MnSi thin films where there is dependence of the lattice ordering upon annealing temperature (T_{Ann}) (Figure 1)[6]. We find that the fully ordered L2₁ phase exhibits an ANE with a Seebeck coefficient of $S = 0.114 \mu\text{VK}^{-1}$ but remarkably, for the disordered A2 phase we observe a ~ 6 times enhancement with $S = 0.662 \mu\text{VK}^{-1}$. A similar trend with the disorder is seen in the anomalous Hall resistivity (which is expected to scale with the ANE).

Whilst Co₂MnSi in the L2₁ phase does not exhibit any form of non-trivial band structure, the increase in the ANE and AHE (in contrast to the decrease in magnetisation with increasing disorder) seen here suggests a topological origin arising from a subtle difference in the band structures. We compare our measurements with Density Functional Theory (DFT) calculations to reveal the role of band topology on the observed enhancement of the ANE.

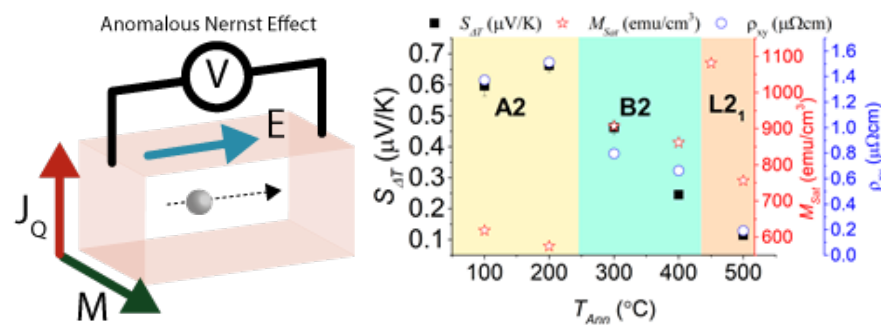


Figure 1: Figure 1: Left: Schematic of the ANE. Right: Dependence of ANE, magnetisation and anomalous Hall resistivity on the ordering of Co₂MnSi thin films.

- [1] H. Reichlova, R. Schlitz, S. Beckert *et al.*, *Appl. Phys. Lett.* **113**, 212405 (2018).
- [2] S.N. Guin, P. Vir, Y. Zhang *et al.*, *Adv. Mater.* **31**, 1806622 (2019).
- [3] S.N. Guin *et al.*, *NPG Asia Mater* **11**, 16 (2019).
- [4] D. Xiao *et al.*, *Rev. Mod. Phys.* **82**, 1959 (2010).
- [5] M. Jourdan, J. Minár, J. Braun *et al.*, *Nat. Commun.* **5**, 3974 (2014).
- [6] C.D.W. Cox, A.J. Caruana, *et al.*, *J. Phys. D: Appl. Phys.* **53**, 035005 (2020).

Coexistence of topological and Rashba states in ferroelectric SnTe

L. Nessi^a, F. Fagiani^a, A. Novati^a, Matteo Cantoni^a, Stefano Cecchi^b,
Giovanni Vinai^c, Debashis Mondal^{c,d}, Raffaella Calarco^c, Silvia Picozzi^e,
Riccardo Bertacco^a, Christian Rinaldi^a

^aDipartimento di Fisica, Politecnico di Milano, 20133 Milano, Italy

^bPaul-Drude-Institut für Festkörperelektronik, 10117 Berlin, Germany

^dIstituto Officina dei Materiali (IOM)-CNR, Laboratorio TASC, Trieste, Italy

^eInternational Centre for Theoretical Physics (ICTP), Trieste, Italy

^fConsiglio Nazionale delle Ricerche, CNR-SPIN c/o Università G. D'Annunzio, Chieti, Italy

The chalcogenides GeTe [1] and SnTe [2] are the prototypes of ferroelectric Rashba semiconductors (FERSC), a class of materials in which ferroelectricity is coupled to the Rashba spin texture, enabling the non-volatile ferroelectric control of spin-to-charge conversion [3]. While the properties of GeTe as FERSC have been widely investigated [4, 5], SnTe is mostly known as topological material, probably due to the low Curie temperature (100 K) as bulk ferroelectric. However, attempts to bring the critical temperature of ferroelectric SnTe to room temperature [6] are motivated by the prediction of giant intrinsic spin Hall conductivity in its Rashba phase [7], with the possibility of controlling the spin-to-charge conversion ferroelectrically.

Here we propose to identify some conditions leading to stable ferroelectric SnTe at room temperature by exploiting the dipolar interaction with ferroelectric GeTe. First, we study the growth of epitaxial thin SnTe(111) films on GeTe(111)/Si(111) by molecular beam epitaxy. Then, by spin and angular photoemission spectroscopy experiments, we access the band dispersion of the SnTe in such heterostructure as a function of temperature.

The work shows the coexistence of topological and Rashba states in SnTe(111), suggesting that the ferroelectric distortion of SnTe on GeTe survives up at room temperature, possibly thanks to the dipolar interaction with the ferroelectric GeTe underneath. We find a nice agreement with density functional theory calculations [2] which also predict the tunability of topological and Rashba bands with the orientation of the ferroelectric polarization.

These preliminary results open the way to the investigation of SnTe/GeTe for reconfigurable spin-based transistors based on the ferroelectric control of the spin transport.

C.R. and S.P. acknowledges the project TWEET, grant no. 2017YCTB59 by MIUR.

-
- [1] D. Di Sante *et al.*, *Adv. Mater.* **25**, 509 (2013).
 - [2] E. Plekhanov, S. Picozzi *et al.*, *Phys. Rev. B* **90**, 161108(R) (2014)
 - [3] P. Noël *et al.*, *Nature* **580**, 483-486 (2020)
 - [4] C. Rinaldi *et al.*, *Nano Letters* **18**, 2751 (2018)
 - [5] C. Rinaldi *et al.*, *APL Mater.* **4**, 032501 (2016)
 - [6] K. Chang *et al.*, *Science* **353**, 274 (2016)
 - [7] H. Wang *et al.*, *npj Comput. Mater.* **6**, 7 (2020)

Field-free switching between orthogonal spin states in antiferromagnetic NiO(111) on Fe(110)

M. Ślęzak^a, H. Nayyef^a, P. Drózdź^a, W. Janus^a, A. Koziół-Rachwał^a, M. Szpytma^a, M. Zając^b, T. O. Menteş^c, F. Genuzio^c, A. Locatelli^c, T. Ślęzak^a

^a AGH University of Science and Technology, Faculty of Physics and Applied Computer Science, Kraków, Poland

^b National Synchrotron Radiation Centre SOLARIS, Jagiellonian University, Kraków, Poland

^c Elettra - Sincrotrone Trieste, Basovizza, Trieste, Italy

Recently we showed that in a uniform thickness NiO(111)/Fe(110) epitaxial bilayer system, at given temperature near 300 K, two magnetic states with orthogonal spin orientations can be stabilized in antiferromagnetic NiO [1]. Field-free, reversible switching between these two AFM states was demonstrated. Our approach relies on temperature induced in-plane Spin Reorientation Transition (SRT) in ferromagnetic Fe sublayer combined with the interfacial FM-AFM exchange coupling that triggers the SRT in antiferromagnetic NiO overlayer. In this contribution we present more systematic investigations of such field-free, temperature induced switching of AFM NiO spins. A sample prepared for that purpose contained several 300 μm wide Fe stripes with different thickness in the range of (92Å – 113Å). Fig. 1 shows temperature dependence of XMLD for various thicknesses of Fe. Only heating branch is shown for clarity. It is clear that depending on the Fe thickness a critical temperature of SRT in AFM NiO can be tuned. With increasing Fe thickness the critical temperature, at which NiO spins rotate in-plane by 90° from NiO[01-1] \parallel Fe[001] towards NiO[-211] \parallel Fe[1-10] direction, continuously increases. This provides possibility to cover wide temperature window (250 – 380 K) for field-free, reversible switching of AFM spins.

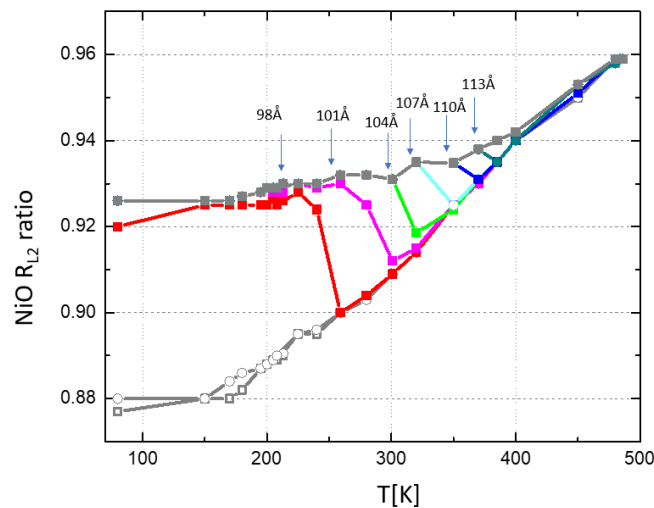


Figure 1: Temperature dependence of XMLD, defined here as R_{L2} ratio of two absorption peaks of NiO at the L2 edge. Possibility to tune the critical temperature of AFM spins switching is demonstrated.

[1] M. Ślęzak, P. Drózdź, W. Janus, H. Nayyef, A. Koziół-Rachwał, M. Szpytma, M. Zając, T.O. Menteş, F. Genuzio, A. Locatelli and T. Ślęzak, *Nanoscale* 12 (2020) 18091.

Advances in Magnetism 2020-21, June 13-16, 2021

Spin-orbit torque

[Abstracts can be easily browsed through the bookmarks](#)

Determination of Spin-Orbit Torques in Pt / Co / Al / (Pt | Ta) Skyrmion Magnetic Multilayers

S. Krishnia, F. Ajejas, Y. Sassi, S. Collin, A. Fert, J. M. George, N. Reyren, V. Cros, H. Jaffrès
Unité Mixte de Physique, CNRS, Thales, Université Paris-Saclay, 91767, Palaiseau, France.

Current-induced spin-orbit torques (SOTs) provide a unique mechanism to manipulate the magnetization of diverse class of magnetic and spin-orbit based multilayers and related devices¹. The core of the phenomenon is the so-called charge to spin-current conversion in ferromagnetic/heavy-metal heterostructures which is governed by spin-orbit interactions mainly through spin Hall effect in heavy metals and/or Rashba effect at interface with broken inversion symmetry². The non-equilibrium spin-current (of spin $\vec{\sigma}$) interacts with local magnetic moments (\vec{m}) via exchange interaction and creates two different components of spin-transfer torques: damping-like ($\vec{\tau}_{DL} = \vec{m} \times (\vec{m} \times \vec{\sigma}) = \vec{m} \times \vec{H}_{DL}$) and field-like ($\vec{\tau}_{FL} = \vec{m} \times \vec{\sigma} = \vec{m} \times \vec{H}_{FL}$), where H_{DL} and H_{FL} are damping-like and field-like effective fields³.

In this talk, we will present the mechanism of spin-transport in ultrathin magnetic multilayer whose thicknesses range from less to above the characteristic spin-dephasing length and how it results in the two components of the effective fields nearby the crossing point of this specific length. To this aim, we have quantified SOTs in a series of samples Pt 8|Co x|Al 1.4|Pt 3 with x = 0.55, 0.7, 0.9, 1.2, 1.4 (numbers are thickness in nm) using AC harmonic Hall voltage measurement. The measured H_{DL} and H_{FL} show linear dependency with current. Our experiments demonstrate the presence of very large field-like torque in Pt 8|Co x|Al 1.4|Pt 3 metallic systems arising from Co/Al interface⁴. In particular, for Co thickness smaller than spin-dephasing length, this field-like torque largely dominates over the damping-like torque owing to the existence of a strong Rashba-like Co/Al interface. On the other hand, the Rashba interaction was negligible for Co/Cu interface taken as a reference sample. The results suggest for the contribution of additional mechanisms of spin-current generation which will be discussed in details during the talk.

Acknowledgement

French ANR grant TOPSKY (ANR-17-CE24-0025), DARPA TEE program grant (MIPR#HR0011831554) and EU grant SKYTOP (H2020 FET Proactive 824123) are acknowledged for their financial support.

References

1. Soumyanarayanan, A., Reyren, N., Fert, A. & Panagopoulos, C. *Nature* **539**, 509–517 (2016).
2. Garello, K. *et al. Nat. Nanotechnol.* **8**, 587–593 (2013).
3. Hayashi, M., Kim, J., Yamanouchi, M. & Ohno, H. *Phys. Rev. B - Condens. Matter Mater. Phys.* **89**, 1–15 (2014).
4. S. Krishnia et al., To be submitted (2021)

Scanning magneto-thermoelectric imaging of spin-orbit torque switching in antiferromagnetic films

T. Janda^a, J. Godinho^{a,b}, E. Pfiltzner^c, G. Ulrich^d, S. Reimers^e, Z. Šobán^b, H. Reichlová^{b,f}, V. Novák^b, R. P. Campion^e, P. Wadley^e, K. W. Edmonds^e, S. S. Dhesi^g, F. Maccherozzi^g, R. M. Otxoa^h, P. E. Roy^h, K. Olejník^b, P. Němec^a, T. Jungwirth^{b,e}, B. Kaestner^d, J. Wunderlich^{b,h}

^a Faculty of Mathematics and Physics, Charles University in Prague, Ke Karlovu 3, 121 16 Prague 2, Czech Republic

^b Institute of Physics ASCR, v.v.i., Cukrovarnická 10, 162 53 Praha 6, Czech Republic

^c Department of Physics, Freie Universitaet Berlin, 14195 Berlin, Germany

^d Physikalisch-Technische Bundesanstalt, 38116 Braunschweig and 10587 Berlin, Germany

^e School of Physics and Astronomy, University of Nottingham, Nottingham NG7 2RD, United Kingdom

^f Institut fuer Festkoerper- und Materialphysik, Technische Universitaet Dresden, 01062 Dresden, Germany

^g Diamond Light Source, Chilton, Didcot, United Kingdom

^h Hitachi Cambridge Laboratory, Cambridge CB3 0HE, United Kingdom

Spin-orbit coupling effects such as the electrical anisotropic magnetoresistance (AMR) and the X-ray magnetic linear dichroism in combination with photoemission electron microscopy (XMLD-PEEM) have been used so far to reveal some of the most important properties of antiferromagnets, namely the ultrafast and the neuron-like switching of antiferromagnetic domains.

By exploiting the equivalent thermal effect, the anisotropic magneto thermal power (AMTP), in patterned antiferromagnetic CuMnAs films, we resolve magnetic domains in response to locally generated thermal gradients. We image the effects of reversible spin-orbit torque switching and find a direct correlation between spin-orbit torque induced changes in the locally generated AMTP signal and in the anisotropic magnetoresistance response. We confirm the magnetic domain structure by comparing our thermo-electric measurements with XMLD-PEEM.

Effect of the oxide termination on both the Dzyaloshinskii-Moriya interaction and the perpendicular magnetic anisotropy in BTO/CoFeB/Pt

Silvia Tacchi,^a Weinan Lin^b, Baishun Yang^c, Andy Paul Chen^d, Xiaohan Wu^b, Rui Guo^b, Shaohai Chen^b, Qidong Xie^b, Xinyu Shu^b, Liang Liu^b, Yajuan Hui^b, Gan Moog Chow^b, Yuanping Feng^{d,e}, Giovanni Carlotti^f, Hongxin Yang^c, Jingsheng Chen^{b,d}

^a Istituto Officina dei Materiali del CNR (CNR-IOM), Sede Secondaria di Perugia, c/o Dipartimento di Fisica e Geologia, Università di Perugia, Perugia, Italy

^b Department of Materials Science and Engineering,

National University of Singapore, Singapore

^c Ningbo Institute of Materials Technology and Engineering, Chinese Academy of Sciences, Ningbo, China; Center of Materials Science and Optoelectronics Engineering, University of Chinese Academy of Sciences, Beijing, China

^d NUS Graduate School of Integrative Sciences and Engineering,

National University of Singapore, Singapore

^e Department of Physics, National University of Singapore, Singapore

^f Dipartimento di Fisica e Geologia, Università di Perugia, Perugia, Italy

The Dzyaloshinskii-Moriya interaction (DMI) and the perpendicular magnetic anisotropy (PMA) at the oxide/FM interface, BTO/CoFeB, have been investigated both experimentally and theoretically, on changing both the oxide termination and the ferroelectric polarization. The precise control of the termination and the polarization of the BTO film helps us to distinguish the role of the termination and polarization in influencing the strength of the PMA and DMI at the oxide/FM interface. In particular, a larger PMA has been observed for the CoFeB films grown on a BaO-BTO substrate, while a higher value of the DMI constant has been found for a TiO₂-BTO substrate. First principle calculations show that this behaviour can be ascribed to the different electronic states around the Fermi level at the oxide/FM interfaces. These results provide a further degree of freedom to manipulate the PMA and DMI in a FM layer and we are confident that they will stimulate further analysis of the interface characteristics in various oxide/FM systems, paving the way to the design of layered structures with tailored DMI to be exploited in forthcoming energy-efficient devices.

Financial support by the European Metrology Programme for Innovation and Research (EMPIR), under the Grant Agreement 17FUN08 TOPS is kindly acknowledged.

Very large domain wall velocities in Mn₄N ferrimagnetic thin films

S. Ghosh^{1,2}, T. Gushi^{1,2}, M. Klug³, A. Hallal², J. Peña Garcia³, T. Komori¹, M. Chshiev², J. Vogel³, J.P. Attané², T. Suemasu¹, L. Vila² and S. Pizzini³

¹ Institute of Applied Physics, University of Tsukuba, Japan

² Université Grenoble Alpes, CNRS, SPINTEC, Grenoble, France

³ Université Grenoble Alpes, CNRS, Institut Néel, Grenoble, France

Ferrimagnetic Mn₄N thin films grown epitaxially on SrTiO₃ (001) substrates possess remarkable properties such as a perpendicular magnetic anisotropy (PMA), a very large extraordinary Hall angle and smooth domain walls (DWs) indicating weak pinning.

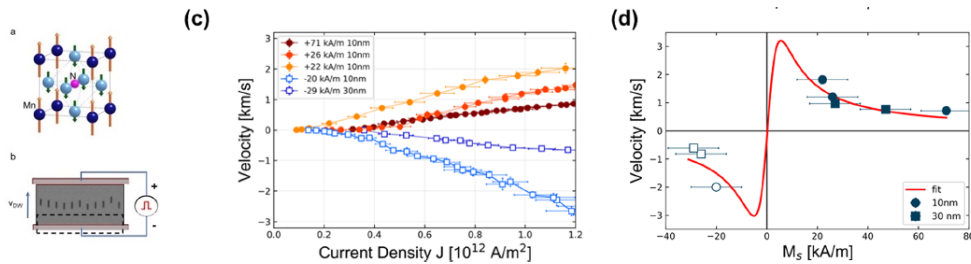


Figure 1: (a) anti-perovskite structure of Mn₄N; (b) differential Kerr images showing the DW displacement in 1 μ m-wide strips under the application of current pulses; (c) DW speed vs. current density for Mn_{4-x}Ni_xN films with different Ni content, below and above the magnetisation compensation point; (d) fit to the q - ϕ model.

In 2019 we showed that DWs in Mn₄N can be moved at record speeds - around 1000 m/s for 1.4×10^{12} A/m² - by spin polarised current, as shown in Fig. 1(brown curve) [1]. In this system DWs move in the direction of the electron flow, and there is no evidence of the presence of Dzyaloshinskii-Moriya interaction (DMI) so that DWs have Bloch structure. This implies that the driving mechanism for DW movement is the “classical” spin transfer torque (STT).

The net magnetisation of Mn_{4-x}Ni_xN can be finely tuned by doping with Ni. For a critical Ni content ($x=0.18$, corresponding to 3.6 at.% Ni) the net magnetisation M_s cancels out (magnetisation compensation point, MCP) and, for larger Ni content, M_s changes direction. The current driven DW velocities increase as the magnetisation decreases, reach up to 3000 m/s close to the MCP, and change direction of motion when the MCP is crossed (Figure 1(c)) [2]. These STT-driven domain wall velocities are of the same order of magnitude of the largest ones found in systems with DMI where the SHE-SOT is the driving mechanism, showing that STT, whose study was abandoned 10 years ago, can be extremely efficient. The large DW velocities and the reversal of the direction of motion can be explained by the analytical q - ϕ model for a ferrimagnetic system (Figure 1(d)) [3]. The large STT-driven DW velocities are related to the increase of the DW mobility close to the angular momentum compensation point and to the large spin net spin polarisation ($P \approx 0.65$) of the conduction electrons. The change of DW direction of motion is related to the change of the relative alignment between the net spin polarisation and the net angular momentum, as confirmed by band structure calculations.

[1] T. Gushi et al. Nano Lett. 2019, 19, 8716.

[2] S. Ghosh et al. Nano Letters 2012; doi: 10.1021/acs.nanolett.1c00125

[3] Haltz et al. PRB 2021, 103, 014444; T. Okuno et al. Nat. Electron. 2019, 2, 389.

Staggered spintronics

Paul Haney^a, Fei Xue^{a,b}, Vivek Amin^{a,b}, Christoph Rohmann^{a,b}

^aNational Institute of Standards and Technology, Gaithersburg MD, USA

^bMaryland NanoCenter, University of Maryland, College Park MD, USA

Spintronics studies the coupling between the electric and magnetic response of systems, often with the aim of furthering information technology applications. Spin-orbit torques are a prominent recent realization of this coupling that enable electric field-induced magnetic switching in bilayer systems composed of a heavy metal and a thin film ferromagnet. These systems demonstrate the key ingredients for spintronic phenomena: spin-orbit coupling and some degree of symmetry breaking.

Quite generally, a system's response is dictated by its symmetry properties. Lower symmetry enables additional types of responses, potentially enabling new functionality. The distinction between local and global symmetry has been recently recognized in a variety of contexts, including in the site-dependent spin splitting in diamond lattices like Silicon [1], and the staggered spin-orbit torque components in bilayers with substrates of non-symmorphic symmetry [2]. In general, the local symmetry may be lower than the global symmetry. In this case, some components of the system response can be "staggered": the unit cell-averaged response vanishes while the site-resolved response is nonzero (being equal and opposite on the two equivalent sites).

In this talk, we discuss two examples of staggered spintronic responses. First, we consider the staggered spin Hall effect in transition metal dichalcogenides and the associated spin-orbit torques in bilayers with transition metal dichalcogenides substrates. We present a general methodology for computing the staggered spin Hall conductivity and provide its formal symmetry requirements [3]. We show that the unconventional spin-orbit torque in recent experiments [2] can be quantitatively ascribed to the staggered spin Hall effect in WTe_2 [4]. We next consider the staggered spin-orbit torques in antiferromagnetic bilayer CrI_3 . We discuss the differences between CrI_3 and other well-studied antiferromagnets such as $CuMnAs$, and show that a staggered dampinglike torque enables electric field-induced switching of the Neel order parameter for bilayer CrI_3 [5].

[1] X. Zhang et al, Nature Physics 10, 387 (2014).

[2] D. MacNeill et al, Nature Physics 13, 300 (2017).

[3] F. Xue et al, Physical Review B 102, 195146 (2020).

[4] F. Xue et al, Physical Review B 102, 014401 (2020).

[5] F. Xue et al, arXiv:2104.05155 (2021).

Role of current driven torques on skyrmion motion in Antiferromagnets

Riccardo Tomasello^a, Akshaykumar Salimath^b, Fengjun Zhuo^b, Giovanni Finocchio^c and Aurelien Manchon^b

^a Institute of Applied and Computational Mathematics, FORTH, Heraklion, Greece

^b King Abdullah University of Science and Technology (KAUST), Thuwal, Saudi Arabia

^c Department of Mathematical and Computer Sciences, Physical Sciences and Earth Sciences, University of Messina, Messina, Italy

Absence of gyroscopic forces for skyrmionic textures combined with higher velocity and zero stray field make antiferromagnets attractive materials for next generation integrated circuits [1-5]. In addition, it has recently been shown that spin currents arising from the non-trivial topology of antiferromagnetic skyrmions can significantly enhance their mobility compared to their ferromagnetic counterpart [6]. In this work, we study the skyrmion motion in bulk and synthetic antiferromagnets in the high velocity regime through both micromagnetic simulations and analytical approach based on the Lagrangian formalism. We investigate the anisotropic deformation of the skyrmion under the action of spin Hall torque, spin transfer torque and topological torque, and analyze its impact on the skyrmion mobility. In bulk antiferromagnets, when the skyrmion is driven by the spin Hall torque, the velocity increases linearly at low applied current density followed by a parabolic increase owing to the lateral skyrmion expansion at high current densities. In contrast, in synthetic antiferromagnets, we observed that the velocity increases linearly at low applied current density followed by a sublinear increase owing to the internal magnetization tilting at high current densities. When driven by spin transfer torque, the topological torque arising from the topological spin Hall effect, reduces the skyrmion expansion and results in sublinear increase of skyrmion velocity at high current density in both synthetic antiferromagnets and bulk antiferromagnets. This study suggests that, while spin Hall torque induces an asymmetric expansion of the antiferromagnetic skyrmion, spin transfer torque supplemented by the intrinsic topological torque can lead to a rigid motion of an antiferromagnetic skyrmion.

This work was supported by the project “ThunderSKY” funded from the Hellenic Foundation for Research and Innovation and the General Secretariat for Research and Technology, under Grant No. 871.



-
- [1] X. Marti et al., Nat. Mater. 13, 367 (2014).
 - [2] K.M.D. Hals et al., Phys. Rev. Lett. 106, 107206 (2011).
 - [3] A.N. Bogdanov et al., Phys. Rev. B 66, 214410 (2002).
 - [4] J. Barker et al., Phys. Rev. Lett. 116, 147203 (2016).
 - [5] T. Shiino et al., Phys. Rev. Lett. 117, 087203 (2016).
 - [6] Akosa et al. Phys. Rev. Lett. 121, 097204 (2018).

Advances in Magnetism 2020-21, June 13-16, 2021

Skymions

Abstracts can be easily browsed through the bookmarks

Theory of Néel-Bloch transition for compact magnetic skyrmions

Anne Bernand-Mantel^a, Cyrill B. Muratov^b, Thilo M. Simon^c

^a Université de Toulouse, Laboratoire de Physique et Chimie des Nano-Objets,
UMR 5215 INSA, CNRS, UPS, 135 Avenue de Rangueil,
F-31077 Toulouse Cedex 4, France

^b Department of Mathematical Sciences, New Jersey
Institute of Technology, Newark, NJ 07102, USA

^c Institute for Applied Mathematics, University of Bonn, Endenicher Allee 60, 53115 Bonn,
Germany

Magnetic skyrmions are a prime example of topologically non-trivial spin textures observed in a variety of magnetic materials. They emerge when the exchange and anisotropy energies promoting parallel alignment of spins in a ferromagnet enter in competition with energies favoring non-collinear alignment of spins such as the Dzyaloshinskii-Moriya interaction (DMI), the long-range dipolar interaction or higher-order exchange interactions. The orthodox theory of skyrmions in ultrathin ferromagnetic layers with interfacial DMI relies on a model that accounts for the dipolar interaction through an effective anisotropy term, neglecting long-range effects. At the same time, in single ferromagnetic layers with interfacial DMI, large chiral skyrmions, also called skyrmionic bubbles have been observed, suggesting a non-trivial interplay between DMI and long-range dipolar effects [1]. The competition between these two energies also leads to the formation of skyrmions exhibiting spin rotations with intermediate angles between Néel and Bloch, a phenomenon also present in domain walls. In addition, there is a growing body of theoretical evidence that points to a need to take into account the long-range dipolar energy in the models describing magnetic skyrmions. The above considerations put into question the validity of the commonly used assumption that the long-range contribution of the dipolar interaction is negligible.

Here we use rigorous mathematical analysis to develop a skyrmion theory that takes into account the full dipolar energy in the thin film regime and provides analytical formulas for compact skyrmion radius, rotation angle and energy [2,3]. We demonstrate that the DMI threshold at which a compact skyrmion loses its Néel character is a factor of 3 higher than that for a single domain wall. A reorientation of the skyrmion rotation angle from Néel to intermediate Néel-Bloch angles is predicted as the layer thickness is increased in the low DMI regime, which is confirmed by micromagnetic simulations. The estimation of this reorientation thickness is important for applications as the skyrmion angle affects its current-induced dynamics.

[1] A. Bernand-Mantel et al. *Scipost* 4, 27 (2018)

[2] A. Bernand-Mantel, Cyrill Muratov, Thilo Simon, *Physical Rev. B* 101, 045416 (2020)

[3] A. Bernand-Mantel, Cyrill Muratov, Theresa Simon, *Archive for Rational Mechanics and Analysis* **239** 219 (2021)

Lifetime of skyrmions in the systems with infinitesimal lattice constant

M.N. Potkina^{a,b,c}, I.S. Lobanov^{a,c}, H. Jónsson^b, V.M. Uzdin^{a,c}

^a St. Petersburg State University, St. Petersburg, Russia

^b University of Iceland, Reykjavik, Iceland

^c ITMO University, St. Petersburg, Russia

A theoretical study of the mechanisms responsible for the ordering and stability of chiral magnetic states in nano and microsystems is presented. It is believed that the stability of such structures with respect to thermal fluctuations and external perturbations is topological in nature. However, in real magnetic systems, where magnetic moments are defined on the atomic lattice, there is no strict topological protection. Instead, the topological states are separated from each other and from the trivial (i.e., homogeneous) state by energy barriers of finite size, which determine their stability. How the topological protection is formed when the lattice constant d decreases in comparison with the characteristic size of the structure and the system approaches the continuous limit will be reported on example of skyrmion states.

The theoretical approach is based on transition state theory (TST) for magnetic degrees of freedom [1]. It presupposes the analysis of multidimensional energy surfaces of magnetic systems, the construction of minimum energy paths between locally stable states and the calculation of energy barriers between them. Barrier between metastable skyrmion and homogenous ferromagnetic (FM) states determines the activation energy for skyrmion annihilation [2]. Calculations were performed for gradually decreasing lattice constant, which determines the distance between nearest neighbor spins. All the parameters of the system, such as exchange (J) and anisotropy (K) constants as well as Dzyaloshinskii-Moriya interaction (D) were chosen in such a way to keep absolute size of skyrmion and its energy unchanged at each lattice constant. These parameters correspond to the values, which can be used for the description of skyrmions of the same size in a continuous micromagnetic model. The number of magnetic moments in the system has been reaching more than million and therefore the dimensionality of the energy surface was several millions.

Then we estimated the pre-exponential factor in the Arrhenius law within the harmonic approximation to the transition state theory (HTST) for set of decreasing lattice constants which allowed to estimate a value corresponding to the limit of the continuous model. New method for calculation of preexponential factor without calculation of eigen values of Hessian of energy was developed. It gave the possibility to find lifetime of the system with millions magnetic moments that was not possible by standard methods so far [2]. We demonstrate that for infinitesimal lattice constant the difference between energies of transition state and the FM state approaches to Belavin-Polyakov limit $4\pi J$ [3]. Entropy term in pre-exponential factor decreases with decrease of lattice constant but also approach to the constant for very small d . Strong decrease of pre-exponential factor with increase of the skyrmion size let us explain possible stability of micrometer skyrmion at room temperature. The possibility of taking into account the long-range magnetic dipole-dipole interaction is discussed.

This work was supported by Russian Science Foundation under Grant 19-42-06302

[1] P. F. Bessarab, V. M. Uzdin, and H. Jónsson, Phys. Rev. B **85**, (2012) 184409

[2] I. S. Lobanov and V. M. Uzdin, arXiv:2008.06754 (2020).

[3] A.A. Belavin and A.M. Polyakov, Sov. Phys. JETP Lett, 22 (1975) 245

Current induced motion of magnetic skyrmion in double injection (Pt/Co/Al/Ta)_N system

Yanis Sassi, Sachin Krishnia, William Legrand, Fernando Ajejas, Sophie Collin, Karim Bouzehouane, Aymeric Vechiola, Nicolas Reyren, Vincent Cros, Albert Fert

Unité Mixte de Physique, CNRS, Thales, Université Paris-Saclay, 91767 Palaiseau, France

Magnetic skyrmions are localized magnetic textures in thin magnetic materials, behaving as single particles being topologically different from the uniform state. They have been identified as extremely promising for future applications, as well as of fundamental interest [1]. The magnetism community has provided a great effort in the last years to succeed to stabilize them at room temperature, most often by designing magnetic and heavy-metal multilayers combining perpendicular magnetic anisotropy (PMA) and Dzyaloshinskii-Moriya interaction (DMI) [2]. These skyrmionics spin textures, combined with spin-orbit torques (SOT) generated in the different heavy-metal layers, allows efficient current-induced motion of skyrmions [3] which make them a promising system for further applications (racetrack memory, neuromorphic computing, etc).

In this study we present a current induced motion of isolated skyrmions measured by MFM in (Pt/Co/Al/Ta)_N multilayers (with *N* the number of repetitions) with a variety of track designs realized by laser lithography at room temperature. Pt and Ta present opposite spin Hall angles and therefore they contribute additively to the total SOT leading to a more efficient motion [4]. We will discuss the design of the multi-repeats stacking and then the impact of the geometry regarding the nucleation. The skyrmion density being controlled by tuning the external field, allow us reaching a state with isolated skyrmions. We will also show the evolution of the skyrmion velocity as a function of the current density (Figure 1). Finally, we will describe how those results depend on the number of repetitions *N*.

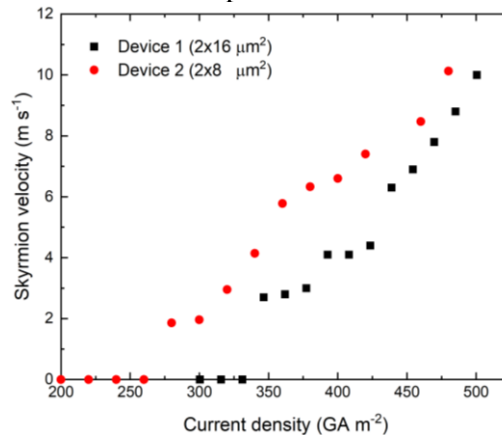


Figure 1: Average skyrmion velocity as a function of current density

French ANR grant TOPSKY (ANR-17-CE24-0025), DARPA TEE program grant (MIPR#HR0011831554) and EU grant SKYTOP (H2020 FET Proactive 824123) are acknowledged for their financial support.

-
- [1] A. Fert, N. Reyren, V. Cros, *Nat. Rev. Mat.* **2** (2017), 17031.
 - [2] C. Moreau-Luchaire *et al*, *Nat. Nanotech.* **11** (2016), 444 ; S. Woo *et al*, *Nat. Mater.* **15** (2016), 501 ; A. Soumyanarayanan *et al*, *Nat. Mater.* **16** (2017), 898 ; A. Hrabec *et al*, *Nat. Comm.* **8** (2017), 15765.
 - [3] K. Litzius *et al*, *Nat. Phys.* **13** (2017), 170 ; S. Woo *et al*, *Nat. Comm.* **8** (2017), 15573.
 - [4] S.Woo, M.Mann, A. J. Tan, L. Caretta, G. S. D. Beach, *Appl. Phys. Lett.* **105**, 212404 (2014)

Voltage-Controlled Skyrmion Chirality Switch

Charles-Elie Fillion^a, Raj Kumar^a, Aymen Fassatoui^b, Stefania Pizzini^b, Laurent Ranno^b, Stéphane Auffret^a, Isabelle Joumard^a, Olivier Boulle^a, Gilles Gaudin^a, Liliana Buda-Prejbeanu^a, Claire Baraduc^a and H el ene B ea^a

^a Univ. Grenoble Alpes, CEA, CNRS, Grenoble INP, IRIG-Spintec, Grenoble, France

^b Univ. Grenoble Alpes, CNRS, N el Institute, Grenoble, France

Magnetic skyrmions are spin-swirling, topologically stable spin textures with homochiral domain walls (DW) that hold promise for next-generation spintronic devices [1]. The interfacial Dzyaloshinskii-Moriya interaction (iDMI) [2,3] contributes to the stabilization of these non-trivial spin textures, by imposing their DW structure and chirality. Skyrmions currently attract wide interest thanks to an efficient manipulation by spin-orbit torques (SOT). They can be moved at high speed in a direction that depends on the chirality of their DW [4]. Here, we show a local voltage-induced inversion of the current-driven motion direction (CDMD) of magnetic skyrmions in Ta/FeCoB/TaOx trilayers. We experimentally observed this effect with polar magneto-optical Kerr effect (p-MOKE) microscope. Besides, we report a reversible and non-volatile CDMD inversion on chiral domain walls. We interpret this CDMD inversion by a gate-control of the DW chirality and thus of iDMI sign, which we attribute to ionic migration of oxygen [5]. Micromagnetic simulations show that such a chirality reversal is feasible on sub-micronic skyrmions without annihilation, paving the way towards local manipulation of individual skyrmions.

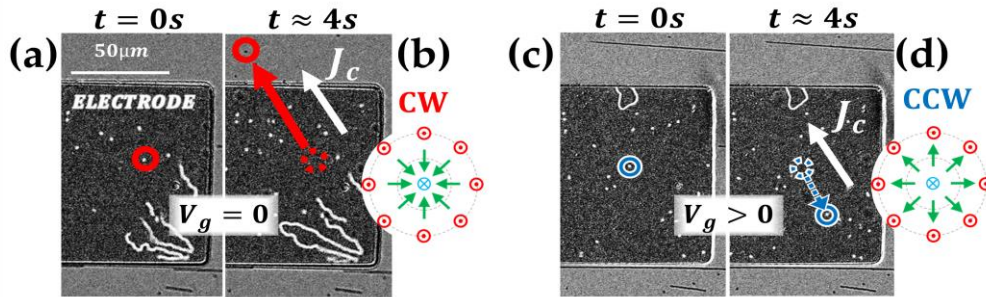


Figure 1: Voltage-induced current motion inversion of micronic skyrmions measured under p-MOKE microscope. The white arrow represents the in-plane current density. (a)-(b) Initially, skyrmions move along the current density (solid red arrow), indicating a clockwise (CW) chirality, as represented in the inset of (b). (c)-(d) Instead, when applying a positive gate voltage on the electrode, an inversion of the skyrmion motion occurs, indicating a counterclockwise (CCW) chirality, as represented in the inset of (d).

-
- [1] A. Fert et al., Nature Review Materials **46** (2017), 6
 - [2] I. E. Dzyaloshinskii, J. Exptl. Theoret. Phys., (U.S.S.R.) **46** (1964), 960
 - [3] T. Moriya, Physical Review **120** (1960), 91-98
 - [4] A. Thiaville et al., EPL (Europhysics Letters) **100**, (2012), 57002
 - [5] U. Bauer et al., Nature Materials **14** (2015), 174-181

Current limits of high-resolution and quantitative magnetic force microscopy

Hans J. Hug^{a,b}, A.-O. Mandru^a, O. Yildirim^a, M. A. Marioni^a

^a Empa, Ueberlandstrasse 129, CH-8600 Duebendorf, Switzerland

^b Department of Physics, University of Basel, Klingelbergstrasse 82, CH-4056 Basel, Switzerland

Magnetic Force Microscopy (MFM) is a versatile technique to map the dependence of the micromagnetic state of a sample in the applied field and temperature with high spatial resolution. Highest sensitivity is obtained by operation in vacuum using cantilevers with quality factors up to 1 million (Fig 1a). These and the operation under vacuum conditions require suitable operation modes to control the tip-sample distance with highest precision even when the temperature is changed or strong magnetic fields are applied. Using frequency-modulate tip-sample distance control [1] MFM data acquisition becomes reproducible such that differential imaging to separate the different contributions to the measured signal can be dis-entangled. Among the latter is the topography, local variations of the Kelvin contrast, magnetic fields arising from spatial variations of the sample thickness and roughness, and stray fields arising from the micromagnetic state of the sample [2] (Fig. 1b). The latter usually is of most interest, but MFM measures the deconvolution of the sample stray field with the a-priori unknown tip equivalent magnetic charge distribution. We have developed calibration procedures for the latter almost two decades ago [3], and used the calibrated response of the tip to measure the density of uncompensated spins in exchange coupled systems [4], closure domain states in CuNiCu trilayers [5], and more recently the local Dzyaloshinskii-Moriya interaction [6], chirality of skyrmions [6] (Fig. 1c) and Néel walls [7].

Particularly the recent work on systems with Dzyaloshinskii-Moriya interaction [2,6,7] demonstrates the detailed information on the topological structure of the micromagnetic state can be obtained by quantitative MFM techniques.

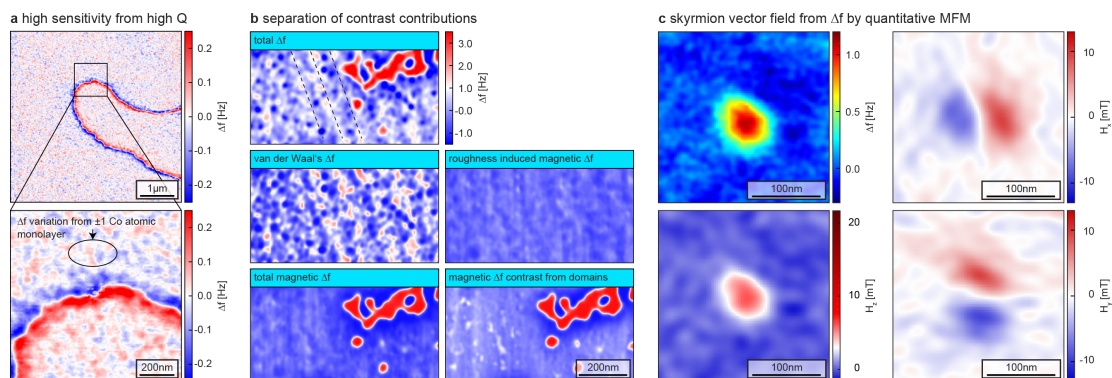


Figure 1: a) MFM data of a Pt(10nm)/Co(0.6nm)/Pt(3nm) trilayer recorded with a cantilever with $Q = 1'000'000$. b) Separation of MFM contrast contributions required to make sub-10nm skyrmions visible. c) MFM data of an isolated skyrmion in a $[\text{Ir}(1\text{nm})/\text{Co}(0.6\text{nm})/\text{Pt}(1\text{nm})]_{\times 5}$ -multilayer with all vector components of the field obtained by quantitative MFM techniques.

- [1] Zhao et al., New J. Phys. 20 (2018) 0113018
- [2] Meng et al., Nano Lett. 19 (2019) 3169
- [3] van Schendel et. al. J. Appl. Phys. 88 (2000) 435
- [4] Schmid et al., Phys. Rev. Lett. 105 (2010) 197201
- [5] Marioni et al., Phys. Rev. Lett. 96 (2006) 027201
- [6] Bacani et al., Sci. Rep. 9 (2019) 3114
- [7] Marioni et al., Nano Lett. 18 (2018) 2263

Toward room-temperature nanoscale skyrmions in ultrathin films

Anastasiia S. Varentcova^{a,b}, Stephan von Malottki^c, Maria N. Potkina^{a,b}, Grzegorz Kwiatkowski^b, Stefan Heinze^c, Pavel F. Bessarab^{a,b}

^a ITMO University, St. Petersburg, Russia

^b University of Iceland, Reykjavík, Iceland

^c University of Kiel, Kiel, Germany

Breaking the dilemma between small size and room temperature stability is a necessary prerequisite for skyrmion-based information technology. In this study [1], it is explored to what extent the lifetime of nanoscale, isolated skyrmions in ultrathin ferromagnetic films can be enhanced under ambient conditions. Fixing the skyrmion size still leaves a space for the optimization of the skyrmion stability by tuning the skyrmion shape, and this possibility is systematically analyzed using the atomistic spin Hamiltonian and harmonic transition state theory.

In contrast to previous studies, the analysis of the skyrmion stability diagram goes beyond the evaluation of the collapse energy barrier and involves definite calculations of the Arrhenius pre-exponential factor, also referred to as the attempt frequency, instead of treating it as a phenomenological parameter. An extreme sensitivity of the prefactor to magnetic interactions is discovered and explained, thus providing a deep insight into the skyrmion stabilization. Thanks to the pronounced material dependence of the prefactor, it is actually possible to realize long-lived sub-10 nm skyrmions in ferromagnetic films at room temperature and zero applied magnetic field. This finding contrasts sharply with conclusions of previous studies where the skyrmion stability is assessed exclusively based on estimation of the energy barrier. Although it is indeed unfeasible to reach energy barriers exceeding thermal energy by a factor of 40–50 at room temperature—a commonly used criterion for reliable information storage—while keeping the skyrmion size at nanoscale, the long lifetime of ultrasmall skyrmions can still be achieved due to the remarkably low attempt frequency, which is a unique phenomenon in magnetism. A dramatic decrease in the attempt frequency is achieved due to softening of magnon modes of the skyrmion, thereby lowering the entropy of the skyrmion with respect to the transition state for collapse. Increasing the number of skyrmion deformation modes should be a guiding principle for the realization of nanoscale, room-temperature stable skyrmions. This stabilization scenario is particularly realized for skyrmions with a bubble-like profile.

[1] A.S. Varentcova et al., *npj Comput. Mater* **6** (2020), 193.

Magnetic skyrmions on cylindrical nanotubes: Formation, stability and electrical detection

Dimitris Kechrakos^{a*} and Leda Tzannetou^b

^a Physics Laboratory, Department of Education, School of Pedagogical and Technological Education (ASPETE), 15122 Athens, Greece

^b Core Department, National and Kapodistrian University of Athens, 34400 Chalkida, Greece

Magnetic skyrmions with diameter of a few nanometres can be stabilized by the competition between symmetric exchange (Heisenberg) and antisymmetric exchange (Dzyaloshinskii-Moriya) interactions arising at the interface between a ferromagnet (FM) and a heavy metal (HM). They have potentials as next generation magnetic information carriers owing to the possibility of being driven by spin polarized currents in planar nanostrips, which constitute the basic element of skyrmion-based racetrack memory (Sk-RTM) devices. A considerable obstacle in optimizing a Sk-RTM is the occurrence of the Skyrmionic Hall effect, namely the transverse motion of the current-driven skyrmions and their eventual annihilation at the side edges of the nanostrip. In the search for routes to tackle the problem of skyrmionic edge-annihilation, we study here the skyrmion formation and electrical detection on cylindrical composite nanowires with HM core and FM shell, which naturally do not contain free side boundaries. Our model system is a thin FM cylindrical nanoshell with chiral (DM) magnetic interactions. The total energy contains contributions from nearest neighbor Heisenberg and DM interactions, radial anisotropy and Zeeman. We obtain the zero temperature equilibrium state of the system by a field-cooling protocol using the Metropolis Monte Carlo algorithm. Our numerical results demonstrate that the evolution of the skyrmion phase with the radius of the cylindrical nanoshell is controlled by the competition between two characteristic lengths, namely the curvature radius, R (geometrical length) and the skyrmion radius, R_{Sk} (physical length). In narrow nanotubes ($R < R_{\text{Sk}}$) the skyrmion phase evolves to a stripe phase, while in wide nanotubes ($R > R_{\text{Sk}}$) a mixed skyrmion-stripe phase emerges, which however, contains spatially separated skyrmions from stripes owing to the direction of the applied field relative to the surface normal. The evolution of the topological charge and topological susceptibility with the curvature angle signify a gradual transition from the purely skyrmionic phase of planar stripes to a mixed skyrmion-stripe phase of curved nanostrips. The spatial boundary on the nanotube surface between the skyrmion and stripe phases is determined by the condition that the radial component of the applied uniform field equals the critical normal field in the planar nanostrip. Finally, the “skyrmion pocket” of the field-anisotropy phase diagram is shown to shrink with decreasing cylinder radius. Shape analysis of skyrmions on cylindrical nanotubes demonstrates a weak perturbation of the circular shape that is preserved up to the annihilation point at the critical nanotube radius. The evolution of phases with surface curvature is associated with characteristic features in the field-dependent magnetoresistance, which is modelled for an isolated nanowire in the ballistic regime within the effective mass approximation and the s - d scattering model, implementing the Landauer formalism with realistic micromagnetic configurations. Our results demonstrate the possibility of electrically detecting the evolution of the skyrmion phase in nanotubes.

Work supported by the Special Account for Research of ASPETE through programs *NanoSky* (Project No 80146). DK acknowledges dissemination of the work through program *Strengthening of Research in ASPETE*.

* dkehrakos@aspete.gr

[1] D. Kechrakos, L. Tzannetou and A. Patsopoulos, Phys. Rev. B **102** (2020), 054439.

Advances in Magnetism 2020-21, June 13-16, 2021

Mathematical modeling and micromagnetics

Abstracts can be easily browsed through the bookmarks

Deep learning magnetization dynamics

Thomas Schrefl^a, Alexander Kovacs^a, Harald Oezelt^a, Markus Gusenbauer^a,
Thomas G. Woodcock^b, Panpan Zhao^b

^a Department for Integrated Sensor Systems, Danube University Krems, Austria

^b Leibniz IFW Dresden, Institute for Metallic Materials, Germany

Deep learning has been successfully applied in computational physics. Examples are the time evolution of fluid flow [1] and the estimation magnetic fields [2]. Here we give two examples that show how deep convolutional neural networks can be used to support computational micromagnetics.

(1) We train a neural network to predict the time evolution of the magnetization in thin film magnetic elements. The basic idea is to learn the magnetic state at time $t+\Delta t$ from the magnetic state at time t . We first compress the magnetization and then learn time stepping in a low-dimensional latent space. Compression reduces the total number of unknowns required to describe a magnetic state. It makes learning time stepping less expensive and less data intensive. We find that the predictions of the neural network model agree well with the solution of the Landau-Lifshitz-Gilbert equation obtained with the micromagnetic solver. Fig. 1 shows the ground truth and the predicted magnetic states at different times.

(2) We apply a physics inspired machine learning model to predict the local coercivity in permanent magnets. A large number of micromagnetic simulations is performed directly from Electron Backscatter Diffraction (EBSD) data using an automated meshing, modeling and simulation procedure. The computed local coercive fields are used to train a machine learning model that relates microstructure and coercivity. The coercivity of permanent magnets is often described by $H_c = \alpha H_{N,\min} - N_{\text{eff}} M_s$, where $H_{N,\min}$ is the minimum switching field of misoriented grains [3]. Taking into account this relation in the convolutional neural network for coercivity reduces the prediction error.

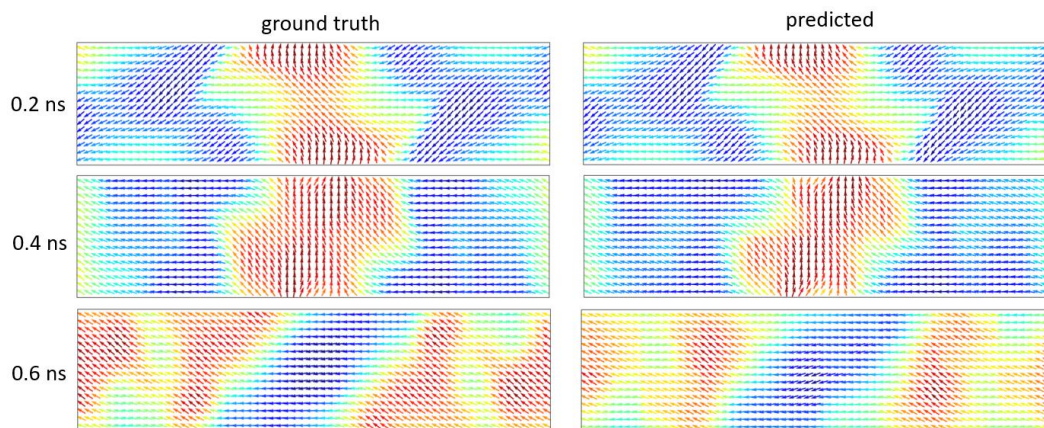


Figure 1: Magnetization patterns at different times for the micromagnetic standard problem #4. Left: Micromagnetic simulation. Right: Neural network prediction.

Work supported by the Austrian Science Fund (FWF), Project: I 3288-N36 and the German Research Foundation (DFG), Project: 326646134.

-
- [1] S. Wiewel, M. Becher, N. Thuerey, N., Computer Graphics Forum **38** (2019), 71-82.
 - [2] A. Khan, V. Ghorbanian, D. Lowther, IEEE Trans. Magn. **55** (2019), 7202304.
 - [3] G. Martinek, H. Kronmüller, J. Magn. Mater. **86** (1990), 177-183.

Comparison of various simulation methods for determination of the switching rate of magnetic nanoelements

Elena Semenova, Dmitry Berkov, Natalia Gorn

General Numerics Research Lab, Jena, Germany

Prediction of the long-time stability of magnetic memory cells (MRAM) is a highly important task for the development of the next-generation MRAM. The straightforward simulation of the information life time τ_{sw} (or, equivalently, switching rates) in these devices using Langevin dynamics (LD) is impossible due to the exponentially growth of the simulation time with energy barrier height ΔE . To overcome this difficulty, we have optimized several numerical methods especially developed for this purpose. In this contribution, we provide the corresponding analysis for the macrospin model of a *biaxial* nanoelement.

In our study we have employed (i) the ‘energy bounce’ method (EnB) [1], (ii) time-temperature extrapolation (TTE) [2], and (iii) Forward Flux sampling (FFS) [3]. We have compared our numerical results with analytical approximations τ_{an} given by the general formalism outlined in [4], which we have adopted for our biaxial macrospin. These methods use various ways to overcome a high energy barrier in a reasonable simulation time, namely: (i) EnB does not allow the system energy to drop below some "bounce energy", which is increased after each stage, until the region near the saddle point is reached; (ii) TTE extrapolates switching times obtained for higher temperatures to the room temperature; (iii) FFS computes the transition probabilities between energy interfaces inserted between the two minima and multiplies these probabilities to compute the final switching rate. For systems with relatively small barriers ΔE we have also performed LD simulations to have a reference value.

We have applied all these methods for the determination of the switching time τ_{sw} for macrospins with parameters equivalent to thin elliptical nanoelements (thickness $h = 3$ nm) with short axis $b = 40$ nm and varying long axis $a = 50 - 100$ nm, made of Permalloy (covering the range $\Delta E = 10 - 60$ kT). The relation of obtained τ_{sw} to the analytical time τ_{an} is shown on Fig.1. In our presentation, we compare the advantages and drawbacks of all methods to establish the one most suitable for the computation of the switching rate.

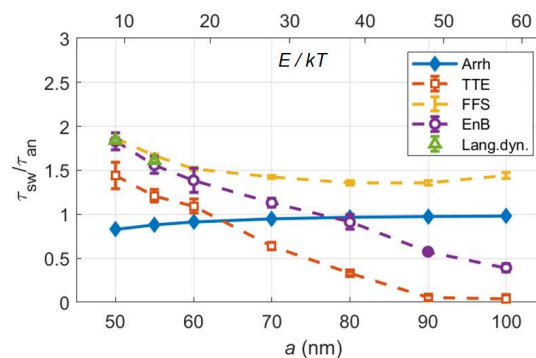


Figure 1: Relation of switching times to the analytical approximation for all simulation methods, as the function of a long axis a .

- [1] S. Wang and P.B. Visscher, IEEE Trans. Magn. **43**, 2893 (2007)
- [2] J. Xue and R.H. Victora, Appl.Phys.Lett. **77**, 3432 (2000)
- [3] R.J. Allen, D. Frenkel and P.R ten Wolde, J. Chem. Phys. **124**, 194111 (2006)
- [4] P. M. Déjardin, D. S. F. Crothers, W. T. Coffey, and D. J., McCarthy, Phys. Rev. E **63**, 021102 (2001)

Coarse-graining in micromagnetic simulations of dynamic hysteresis loops

Razyeh Behbahani^{a,b}, Martin L. Plumer^a, Ivan Saika-Voivod^a

^a Department of Physics and Physical Oceanography, Memorial University of Newfoundland, St. John's, Canada

^b Department of Applied Mathematics, Western University, London, Canada

Micromagnetic simulations based on the stochastic Landau-Lifshitz-Gilbert equation are used to calculate dynamic magnetic hysteresis loops relevant to magnetic hyperthermia. With the goal to effectively simulate room-temperature loops for large iron-oxide based systems at relatively slow sweep rates on the order of 1 Oe/ns or less, a coarse-graining scheme is proposed and tested. The scheme follows from a previously developed renormalization group (RG) approach [1]. Loops associated with nanorods, used as building blocks for larger nanoparticles that were employed in preclinical studies [2], serve as the model test system (Fig. 1, top row). The scaling algorithm is extended to include magnetostatic interactions and shown to produce nearly identical loops over several decades in the model grain sizes (Fig. 1, bottom row, b panel) [3,4]. Sweep-rate scaling involving the damping constant α is also demonstrated, allowing for at least another order of magnitude speedup (Fig. 1, bottom row c panel) [3].

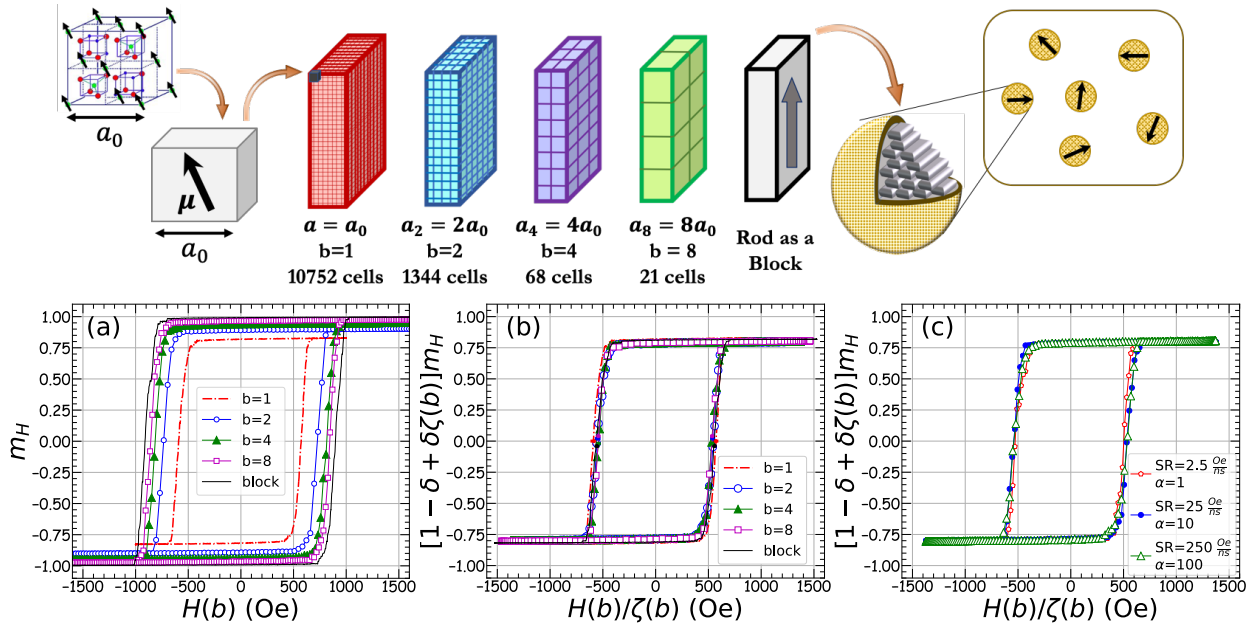


Figure 1: Top row: Micromagnetic models of nanorods ($a_0 = 0.839$ nm) as building blocks for spherical nanoparticles. Bottom row: hysteresis loops of nanorods modelled with different cell sizes. (a) None of the magnetic parameters are scaled with the cell size. (b) The exchange, anisotropy constants and field are rescaled based on the RG approach suggested in Ref. [1] and a phenomenological modification for magnetization scaling is applied ($t = T/T_c, b = a/a_0, \zeta = t/b + 1 - t, \delta = 0.511$) [3]. Magnetostatic interactions are also rescaled [4]. (c) Loops are invariant when SR/α is held fixed (results shown for $b=4$).

- [1] G. Grinstein and R. H. Koch, Phys. Rev. Lett. **20** (2003), 207201.
- [2] C. L. Dennis, A. J. Jackson, J. A. Borchers, et al. Nanotechnology **20** (2009), 395103.
- [3] R. Behbahani, M. L. Plumer, I. Saika-Voivod, J. Phys.: Condens. Matter. **32**, 35LT01 (2020)
- [4] R. Behbahani, M. L. Plumer, I. Saika-Voivod, arXiv:2010.08848 (2020)

Cayley transform based time integration applied to a 3D micromagnetic solver

Riccardo Ferrero^a, Alessandra Manzin^a

^a Istituto Nazionale di Ricerca Metrologica (INRIM), Torino, Italy

The spatial integration of the Landau-Lifshitz-Gilbert (LLG) equation can be computationally very demanding due to the need of simulating phenomena at the exchange length scale and long-range interactions as the magnetostatic field. Particular care has also to be devoted to the time integration, which should guarantee the preservation of the magnetization amplitude with sufficiently large time-steps [1]. To face these problems, we have implemented a 3D micromagnetic solver that uses an FFT-based approach for the magnetostatic field evaluation and exploits GPU-parallelization [2]. The time update is performed by means of a geometric integration method based on the Cayley transform [3, 4], to preserve the magnetization constraint independently of the scheme order and time-step size. In particular, we solve a generalized form of the LLG equation:

$$\dot{\mathbf{M}}(\mathbf{r}, t) = [\mathbf{A}(\mathbf{M}(\mathbf{r}, t)) + \sigma \mathbf{M}(\mathbf{r}, t)] \times \mathbf{M}(\mathbf{r}, t), \quad (1)$$

where \mathbf{A} is the generator that depends on the magnetization vector \mathbf{M} and on the effective field [3]. Equation (1) is equivalent to the LLG equation for $\sigma = 0$; this form is particularly advantageous for the computation of static hysteresis loops, since the addition of term $\sigma \mathbf{M}$ can speed up the reaching of equilibrium, allowing the use of larger time-steps [5].

Here, we test the efficiency of the solver, focusing on the calculation of the equilibrium states of 3D nanostructures. The figure below shows the damping effect of parameter σ in the determination of the remanent state of a permalloy nanosphere, demonstrating that for values of σ in the order of the gyromagnetic ratio γ it is possible to reach equilibrium in less time with a reduced number N of time-steps ($\sigma = 0$: $N \approx 3 \times 10^6$; $\sigma = 9\gamma$: $N \approx 1 \times 10^5$). However, very high values of σ can lead to an overdamping. When $\sigma = 22.5\gamma$, the magnetization may remain stuck in a local energy minimum, if a not sufficiently strong equilibrium convergence condition is imposed, or may evolve very slowly towards the global minimum, reducing the computational advantage obtained with the numerical dampening ($N \approx 2 \times 10^5$).

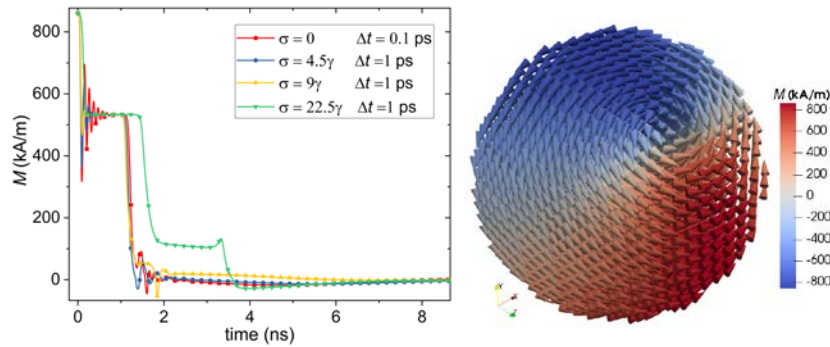


Figure 1: Left: Time evolution from saturation to remanence state of the radial component of the magnetization of a 100 nm permalloy nanosphere, showing the effect of σ . Right: Remanent state of the sphere; the cones represent the magnetization vector direction.

-
- [1] M. D'Aquino et al., J. Comput. Phys. **209** (2005), 730-753.
 - [2] R. Ferrero and A. Manzin, J. Magn. Magn. Mat. **518** (2021), 167409.
 - [3] D. Lewis and N. Nigam, J. Comput. Appl. Math. **51** (2003), 141-170.
 - [4] O. Bottauscio and A. Manzin, IEEE Trans. Magn. **47** (2011), 1154-1157.
 - [5] A. Manzin and O. Bottauscio, J. Appl. Phys. **108** (2010), 093917.

Micromagnetic approach to analysis of temperature-dependent exchange bias properties of polycrystalline films

Nikita A. Kulesh^a, Mikhail E. Moskalev^a, Alexander N. Gorkovenko^a, Ilya A. Pushkarev^a, Vladimir V. Vas'kovskiy^{a,b}, Vladimir V. Lepalovskij^a

^a Ural Federal University, Ekaterinburg, Russia

^b Institute for Metal Physics, Ural Division of Russian Academy of Sciences, Ekaterinburg, Russia

Exchange bias (EB) is an interfacial phenomenon that appears between two magnetically ordered systems, which are often represented by relatively thin ferromagnetic (FM) and antiferromagnetic (AFM) or ferrimagnetic layers. Although EB was studied extensively since its discovery and many models explaining hysteresis properties of FM layer were proposed, a universal model allowing to predict all the accompanying effects, including asymmetry of the hysteresis loops, training effect, enhanced coercivity, temperature effects etc. is still lacking. In this work we analyzed temperature dependencies of EB field and coercivity of the FM layer in nanocrystalline FeMn/FeNi and NiMn/FeNi films using experimental data and micromagnetic simulation.

Ta(5nm)/FeNi(5nm)/AFM(20nm)/FeNi(40nm)/Ta(5nm) films with AFM = FeMn or NiMn were deposited onto the glass substrates by magnetron sputtering. The direction of exchange bias was set by applying the magnetic field of 25 mT parallel to the samples plane during the deposition. Seed Ta and FeNi layers were used to promote fcc crystal structure in the AFM layer.

For the films containing FeMn and NiMn AFM layers we obtained temperature dependencies of coercivity and EB field following simplified protocols: cooling down in large positive or negative field to the minimal temperature of 5 K, performing one full hysteresis cycle to minimize training effect, measuring a hysteresis loop, ramping temperature to the next value, and repeating the hysteresis loop measurement. For the NiMn-based system additional data was collected according to the York protocol [1]. As the AFM state cannot be set in the framework of the continuous micromagnetic approach, we followed the model proposed in [2] by substituting the AFM layer for FM with magnetostatic and Zeeman energy contribution turned off. Polycrystalline FM and AFM layers were modeled using Voronoi tessellation. For the AFM layer, several types of magnetic anisotropy constant distributions in crystallites were considered: lognormal, normal, and mixed double-phase.

As a result, typical monotonic (cooled in a positive field) and non-monotonic (cooled in a negative field) experimental dependencies of EB field and coercivity for FeMn-based system were successfully reproduced within the described micromagnetic approach. For NiMn-based films cooled in a positive field, the EB field demonstrated a strong increase at 5 K and a local maximum around 350 K, which could not be explained using the chosen model. An in-depth analysis suggested the presence of several crystalline AFM phases magnetic state of which could be set differently during the deposition. In conclusion, this case study demonstrated the applicability of the micromagnetic approach to analysis of temperature effects in complex polycrystalline bilayer systems with exchange bias. This approach could be useful for hypothesis checking and estimating material parameters including the distribution of AFM grain magnetic anisotropy constants.

This work was supported by the Russian Science Foundation (project No 19-72-00141).

[1] K. O'Grady et al. *JMMM* **322** (2010), 883-899

[2] J. De Clercq et al. *J Phys. D: Appl. Phys.* **49** (2016), 435001.

Various *ab initio* contributions to electrical transport at nonzero temperatures

Dominik Legut^a, David Wagenknecht^{a,b,c}, Karel Carva^b, Ilja Turek^{b,c}

^aVSB - TU Ostrava, 17. listopadu 2172/15, 708 00 Ostrava-Poruba, Czech Republic

^bDepartment of Condensed Matter Physics, Charles University, Ke Karlovu 3 121 16
Praha 2, Czech Republic

^cInstitute of Physics of Materials, AS CR, Žitkova 513/22, 616 62 Brno, Czech Republic

To describe physical phenomena for nonzero temperatures, including effects of spin fluctuations, has been problematic for a long time. In recent years, the alloy analogy model (AAM) became popular for a treatment of finite-temperature effect from the first principles [1]. Phonons, described as uncorrelated displacements of atoms, can be combined with spin fluctuations (magnons) and chemical disorder. The realistic inclusion of spin fluctuations is crucial especially for spintronic properties such as the spin polarization of the electrical current [2].

The AAM within the tight-binding linear-muffin-tin orbital method and the coherent potential approximation (CPA) successfully describes electrical transport at nonzero temperatures even in multisublattice half-Heusler alloys [3]. In the previous studies [1-3] (i) the Debye theory was employed for a conversion between displacements and temperature, (ii) the total magnetization as a function of temperature was obtained from experiments, and (iii) a change of a volume with temperature was neglected. These simplification will be addressed in details. A route to overcome it by proper *ab initio* approaches is envisaged. Obtained corrections are a few percents (compared to the previous techniques) for some materials. However, this more precise approach is essential for systems where the Debye theory fails. Moreover, the description of finite temperatures is finally obtained completely from the first principles. It is done by synergizing precise supercell methods with the numerically efficient CPA. We will present the usage of novel techniques for pure transition metals, both nonmagnetic and magnetic, but it can be easily generalized for more complex systems, such as previously studied random [1,2] and ordered [3] alloys.

Acknowledgement: This work was supported by the European Regional Development Fund in the IT4Innovations national supercomputing center - path to exascale project, project number CZ.02.1.01/0.0/0.0/16_013/0001791 within the Operational Programme Research, Development and Education.

[1] DW et al. IEEE Trans. on Mag. **5311** (2017), 1700205

[2] DW et al. Proc. SPIE 10357, Spintronics X (2017), 103572W

[3] DW et al. JMMM **474** (2019), 517–521

An interplay between dimensionality and topology in thin ferromagnetic films

Cyrill B. Muratov^a

^a Department of Mathematical Sciences, New Jersey Institute of Technology, Newark, NJ, USA

This talk presents an overview of modelling and analytical challenges associated with the studies of topological solitons in thin film ferromagnetic materials. These materials have been recently demonstrated to support a variety of topologically non-trivial spin textures, including *magnetic skyrmions* – local swirls of spins that exhibit particle-like behavior, nanometer size and room temperature stability. The above properties of magnetic skyrmions, as well as a possibility of their control by electric fields and currents make them attractive as possible information carriers in a new generation of magnetic memory and spintronic logic.

The basic starting point for theoretical studies of magnetic skyrmions is a 2D model which treats skyrmions as critical points of the micromagnetic energy that includes exchange, perpendicular magnetic anisotropy, Dzyaloshinskii-Moriya interaction, Zeeman energy, and stray field energy in the local approximation [1-3]. The first mathematically satisfactory treatment of existence of skyrmion profiles was presented in [4], where magnetic skyrmions were treated as global energy minimizers of this energy under sufficiently strong out-of-plane applied magnetic fields among all topologically nontrivial magnetization configurations. Without the applied field and with full nonlocal stray field energy the above definition of magnetic skyrmions needs to be further refined to distinguish between compact magnetic skyrmions and magnetic bubbles, leading to a notion of *local* minimizers satisfying a quantitative upper bound on the exchange energy [5].

It is reasonable to expect that this picture readily carries over to the full 3D micromagnetic energy describing ferromagnetic films of small but finite thickness. Yet this innocent modification of the model presents significant challenges to theory. The first one is purely mathematical and is due to the fact that 3D magnetization configurations have qualitatively different topological properties than 2D ones. For example, in 3D films of finite thickness it is possible to define the 2D topological charge of the magnetization on each horizontal material plane. However, due to the possibility of appearance of Bloch points the jumps in the topological charge between different planes cannot be ruled out. In particular, as a consequence the Belavin-Polyakov topological lower bound on exchange, which plays the key role for existence of skyrmion profiles in 2D, is no longer available for 3D films of finite thickness, no matter how small, and a new definition of a skyrmion profile is necessary.

The second challenge has to do with modeling, since in thin film ferromagnetic materials both the out-of-plane anisotropy and the Dzyaloshinskii-Moriya interaction are often of interfacial origin and, therefore, need to be modeled as boundary contributions to the energy. This presents further complications to the basic well-posedness of the resulting variational problem, as the energy may favor formation of singularities close to the film interfaces. Therefore, a proper theoretical description of skyrmion profiles in 3D films requires an integrated modeling and analytical treatment to resolve the above challenges.

-
- [1] A. N. Bogdanov and D. A. Yablosnkii, Sov. Phys. JETP **68** (1989), 101–103.
 - [2] A. N. Bogdanov et al., Soviet Physics - Solid State **31** (1989), 1707–1710.
 - [3] B. A. Ivanov et al., J. Magn. Magn. Mater. **88** (1990), 116–120.
 - [4] C. Melcher, Proc. R. Soc. A **470** (2014), 20140394.
 - [5] A. Bernand-Mantel et al., arXiv:1906.05389 (2019).

Optimization of core-shell nanocomposite materials for permanent magnets: micromagnetic approach

Sergey Erokhin, Dmitry Berkov

General Numerics Research Lab, Jena, Germany

Combination of two magnetic phases (one with a high coercivity and another – with a large magnetization) is one of the most promising trends in the development of permanent magnet materials, especially for rare-earth-free magnets, e.g. ferrites. The most important task in this technology is the optimization of a nanocomposite material in terms of volume fraction of phases, structural parameters and exchange coupling in order to achieve the maximal energy product. Recent achievements [1] in micromagnetic simulations allow to *a priori* obtain statistically accurate estimation of the performance of permanent magnets based on such materials.

In this talk, the influence of the size of crystallites and the exchange coupling between them on coercivity, remanence and energy products is demonstrated on the examples of $\text{SrFe}_{12}\text{O}_{19}/\text{Fe}$ and $\text{CoFe}_2\text{O}_4/\text{Co}$ nanocomposites with the core-shell structure of a crystallite. The magnetization distribution in both phases and the absolute value of the average magnetization of every crystallite during the remagnetization process are used for the analysis of hysteresis curves obtained by simulations. Such an analysis opens up the way for the recommendations concerning the manufacturing of these materials in terms of the corresponding geometric and magnetic microstructure. Comparison of a core-shell composite with its analogon made of individual hard and soft crystallites demonstrates the advantage of the core-shell approach, with up the energy product being up to 2 times higher due to the enlarged area of the interface between phases. This our result supports the statement that the spatial microstructure of a nanocomposite is a decisive factor determining the magnetic material performance.

Financial support of the EU Horizon-2020 Program under the project No. 720853 (“AMPHIBIAN”) is gratefully acknowledged.

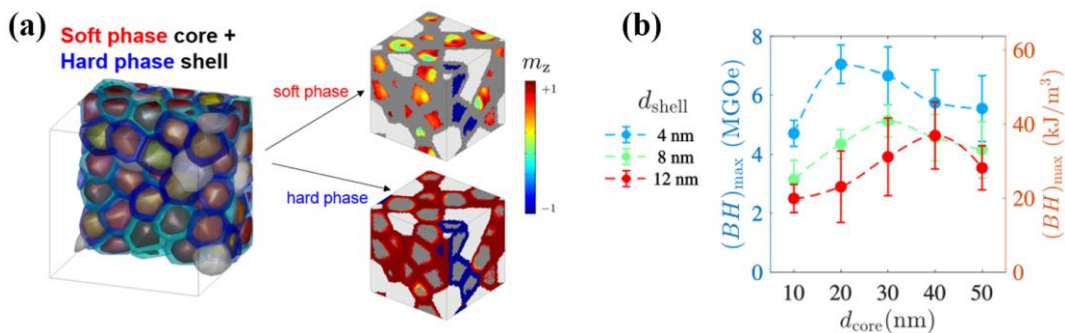


Figure 1: (a) An example of a ferrite nanocomposite material with a core-shell grain structure including 20% of pores (left) and magnetization distribution in this material at the external field $H = -1.75$ kOe. (b) Numerically obtained energy products of the $\text{CoFe}_2\text{O}_4/\text{Co}$ nanocomposite with a hard phase core and soft phase shell plotted as functions of the core diameter for various shell thicknesses.

Designing reconfigurable magnetic gratings

Christina Vantaraki^a, Sam D. Slöetjes^a, Paula Mellado^b, Vassilios Kapaklis^a

^a Department of Physics and Astronomy, Uppsala University, Uppsala, Sweden

^b School of Engineering and Sciences, Adolfo Ibáñez University, Santiago, Chile

Diffraction gratings are basic optical components which consist of periodic patterns, resulting in incident light being diffracted. These are commonly made by patterning surfaces of materials. A periodic magnetic domain structure can also act as a grating for light, considering magneto-optical effects. Previously, we have experimentally explored the use of the 1D periodic magnetic domain structure of an Yttrium-Iron Garnet (YIG) film [1]. The sample exhibits a field-tunable periodic stripe-like magnetic domain structure, which due to the Faraday effect, results in diffraction patterns for transmitted light (Figure 1) [1,2]. Here we focus on the realization of an artificial analogue. We exploit a metamaterial approach and the related micromagnetic structure. We propose a design for the magnetic order and relevant length-scales. This is achieved by introducing periodic modulations of the relative placement of the patterned elements (Figure 2) and we study the hysteretic behavior, using micromagnetic simulations and the analytical models.

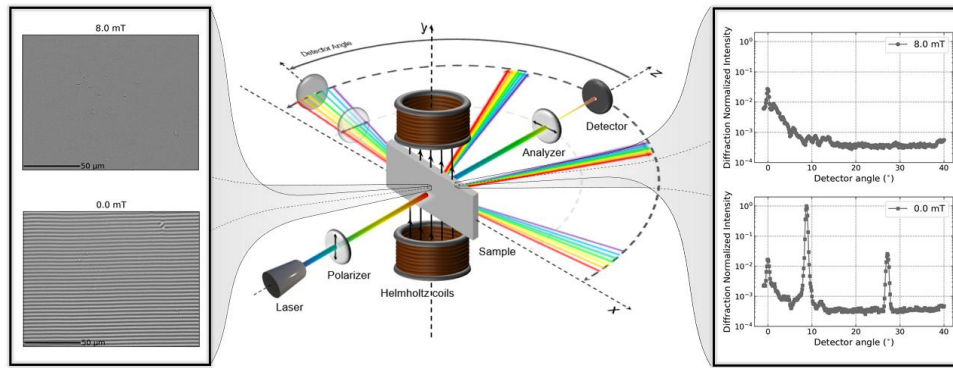


Figure 1. Magneto-optical diffraction from a YIG sample. Left panel: Kerr microscope images at saturation (8.0 mT) and remanence (0.0 mT). Right panel: Resulting scattering from the YIG magnetic grating at saturation (8.0 mT) and remanence (0.0 mT).

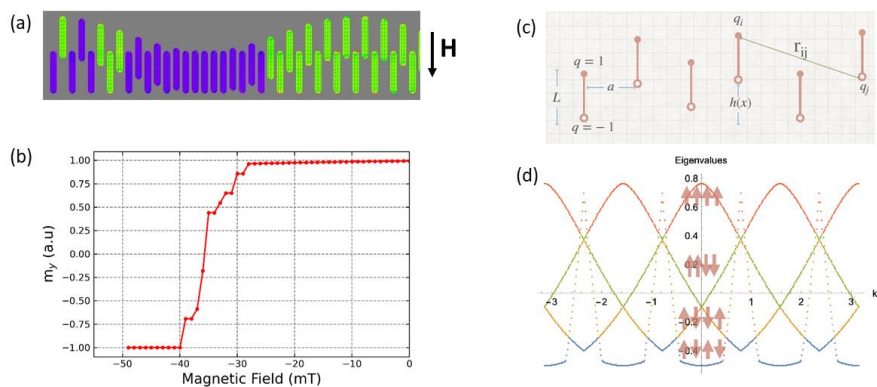


Figure 2. (a) Schematic of a structure with a periodic modulation and (b) its hysteretic behavior calculated using (b) micromagnetic simulations. (c) Schem featuring the dumbbell model used to characterize the energetics of the system and (d) the resulting energy bands of the possible magnetic states of a modulated chain of dumbbells.

- [1] I.-A. Chioar, C. Vantaraki *et al.*, *Spatiotemporal steering of light using magnetic textures*, in preparation (2021).
- [2] A. K. Zvezdin and V. A. Kotov, *Modern Magneto-optics and Magneto-optical Materials*, IOP Publishing Ltd (1997).

General analytical description of ferro-, ferri-, and antiferromagnetic materials.

Luis Sanchez-Tejerina¹, Vito Puliafito², Mario Carpentieri¹, Giovanni Finocchio³

^a Dipartimento di Ingegneria Elettrica e dell'Informazione, Politecnico di Bari, Via Orabona 4, 70125 Bari, Italy

^b Dipartimento di Ingegneria, Università di Messina, C.da Di Dio s/n, 98166 Messina, Italy

^c Department of Mathematical and Computer Sciences, Physical Sciences and Earth Sciences, University of Messina, Viale F. Stagno d'Alcontres 31, 98166 Messina, Italy

The manipulation of magnetic textures in ferromagnetic (FM) material has been the focus of intense research in recent years [1,2]. More recently, this focus has been displaced towards the use of antiferromagnetic (AFM) [3,4], and ferrimagnetic (FiM) materials [5], being more robust against external perturbation and being able to sustain faster magnetization dynamics.

In this context, simplified models have been proved very useful to predict and clarify the phenomenology of both, FM [6] and AFM [7,8] materials. Nevertheless, these models, in their present form, remain detached in the sense it is not possible to recover the FM model from the AFM one. Here we present a general model describing magnetically ordered materials from the AFM state to the FM one by introducing a saturation magnetization dependence on the magnetic parameters. Besides, we have benchmarked the one dimensional simplification of this model with the corresponding full micromagnetic simulations, as depicted in Fig. 1 for the domain wall width parameter, Δ .

In brief, we have generalized the previous micromagnetic models to achieve a framework valid for FM, FiM, and AFM materials.

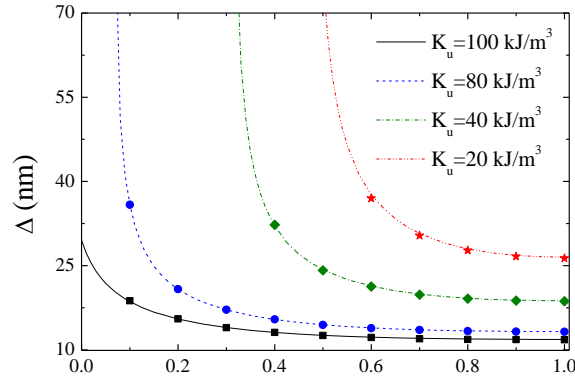


Figure 1: Domain wall size as a function of the two sublattice saturation magnetization ratio. Dots are micromagnetic simulations and lines one dimensional approximation.

-
- [1] S. S. P. Parkin, M. Hayashi, and L. Thomas, *Science*, **320**, 190 (2008).
 - [2] S. Lequeux, *et. al*, *Sci. Rep.* **6**, 31510 (2016).
 - [3] T. Jungwirth, *et. al.*, *Nat. Nanotechnol.* **11**, 231 (2016).
 - [4] O. Gomonay, M. Kläui, and J. Sinova, *Appl. Phys. Lett.* **109**, 142404 (2016).
 - [5] S. A. Siddiqui, *et. al.*, *Phys. Rev. Lett.*, **121**, 057701 (2018).
 - [6] A.Thiaville, *et. al.*, *J. Magn. Magn. Mater.*, **242–245**, **2**, 1061-1063. (2002).
 - [7] L. Sánchez-Tejerina, *et. al.*, arXiv:1904.02491.
 - [8] E. Martinez, V. Raposo, O. Alejos, *J. Magn. Magn. Mater.*, **491**, 165545 (2019).

Advances in Magnetism 2020-21, June 13-16, 2021

Macroscale modeling of magnetic and multifunctional materials and devices

Abstracts can be easily browsed through the bookmarks

Magnetocaloric materials for magnetic refrigeration

V. Basso, M. Kuepferling, E. Olivetti

Istituto Nazionale di Ricerca Metrologica, Strada delle Cacce 91, 10135, Torino Italy.

Magnetic refrigeration is an environmentally friendly technique that employs the magnetocaloric effect of magnetic materials [1]. Although the magnetic field induced temperature change of magnetocaloric materials is rather limited (around a few K/T), cooling devices have been optimized to temperature spans of several tens of degrees by using the principle of active magnetic regeneration or by cascading several materials [2]. Therefore also the thermo-magnetic energy generation, corresponding to the same thermodynamic cycle run in the inverse fashion, becomes feasible [3]. The choice of the appropriate magnetocaloric material still remains one of the most critical issues [4] along with the possibility to obtain specific parts in the form of spheroids or platelets. In this paper we will investigate on the magnetocaloric properties the hydrogenated La(Fe,Si)₁₃-type materials, in which it is possible to have a fine tuning of the transition temperatures, as a function of the shapes [5]. We will further investigate the possibility to achieve the desired magnetocaloric properties by proper treatments of materials already in the final shape, as for example by chemically enhanced hydrogenation [6].

-
- [1] A. Kitanovski et al, Magnetocaloric Energy Conversion: From Theory to Applications, Springer (2015)
 - [2] A. Greco et al, A review of the state of the art of solid-state caloric cooling processes at room-temperature before 2019, International Journal of Refrigeration, 106, 66 (2019)
 - [3] S. Ahmim et al., Thermal energy harvesting system based on magnetocaloric materials, Eur. Phys. J. Appl. Phys. 85, 10902 (2019)
 - [4] T. Gottschall et al., Making a Cool Choice: The Materials Library of Magnetic Refrigeration, Adv. Energy Mater. 9, 1901322 (2019)
 - [5] V. Basso et al. Specific heat and entropy change at the first order phase transition of La(Fe-Mn-Si)₁₃-H compounds, J. Appl. Phys. 118 053907 (2015).
 - [6] A. Troia et al. Sonochemical hydrogenation of metallic microparticles, Ultrasonics - Sonochemistry 55, 1 (2019)

Optimization of continuous three-axis magnetic motion tracking by magnet topology design

Perla Malagò^a, Stefano Lumetti^a, Michael Ortner^a

^a Silicon Austria Labs GmbH, Sensor Systems, Europastraße 12, 9524 Villach, Austria

Magnetic position and orientation (MPO) sensor systems, consisting of permanent magnets that move relative to magnetic field sensors, are widely used in the industry to track movements in mechanical systems with typical motion in the range of a few millimetres. For the design of such systems, state-of-the-art implementations rely mostly on experience and educated guesses combined with point-wise finite element simulations for layout testing and optimization. A computationally efficient method based on analytical magnetic field evaluation, using the Magpylib package [1], and optimization by differential evolution algorithms is outlined in [2]. The method is then applied to a specific problem of tracking the continuous motion of a three-axis joystick with only one 3D magnetic field sensor and a single cubic permanent magnet, as outlined in fig. 1(a).

For practical reasons, only cubical magnets, available off-the-shelf, are used in [2]. However, topology optimization [3] and shape variation [4] of permanent magnets have been applied in the literature as powerful tools to improve magnetic sensor systems by optimally designing the magnetic field. Here, the shape variation technique is exploited to demonstrate that state separation in such a sensor system can be improved by almost a factor of 2 for a magnet of similar volume (and thus similar cost) but optimized topology. The result (see fig. 1(b)) shows that state separations of more than 1.4 mT/deg can be achieved for a large magnet with a volume of 125 mm³, a remanence field of 1000 mT and an airgap of 2 mm.

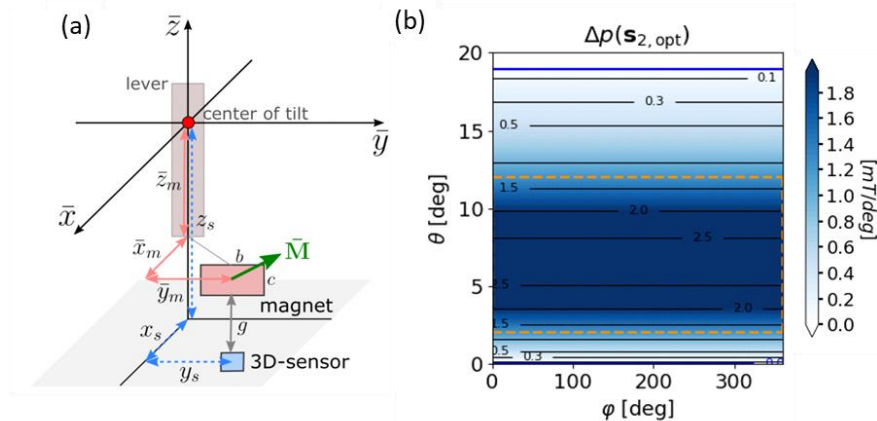


Figure 1: (a) Sketch of the MPO design parameters. (b) Minimal (all tilt directions) state separation of the optimized system with lever tilt angle θ and rotation angle ϕ .

-
- [1] P. Malagò et al., "Magnetic Position System Design Method Applied to Three-Axis Joystick Motion Tracking.", *Sensors* **20.23** (2020), 6873.
 - [2] M. Ortner & L. G. C. Bandeira, "Magpylib: A free Python package for magnetic field computation.", *SoftwareX*, **11** (2020), 100466.
 - [3] C. Huber, et al., "Topology optimized and 3D printed polymer-bonded permanent magnets for a predefined external field.", *J. Appl. Phys.* **122**, (2017), 053904.
 - [4] M. Ortner, "Improving magnetic linear position measurement by field shaping.", in *Proceedings of the 2015 9th International Conference on Sensing Technology (ICST)*, Auckland, New Zealand, 8–10 December 2015; pp. 359–364.

Gold-coated core-shell magnetic nanoparticles as a powerful tool for immunosensing devices

Bartolomeo Della Ventura^{a,b}, Valerio Cosimo Elia^b, Raffaele Campanile^b, Antonio Morone^c, Vincenzo Iannotti^b, Raffaele Velotta^b

^a Politecnico di Milano, Milan, Italy

^b Università di Napoli *Federico II*, Naples, Italy

^c CNR-ISM Unità di Tito Scalo, Potenza, Italy

The importance of gold coated magnetic nanoparticles (Au@MNPs) relies on their capability to show both the properties of Au nanoparticles and those offered by magnetic nanoparticles. While the former have unique surface chemical features joined to the plasmonic response when interrogated by an electromagnetic wave, the latter can also be “steered” thereby offering a powerful tool in realizing devices at the microscale. The gold surface of Au@MNPs lends themselves to be easily functionalized by antibodies thereby becoming “analyte catcher” at nanoscale with inherent application to biosensing devices [1]. To test the occurrence of both optical and magnetic properties, we used Au@MNPs ($\phi \approx 50$ nm) to reduce the limit of detection of a colorimetric immunosensor previously developed, which is based on the change of the plasmonic resonance taking place when the nanoparticles aggregate as a result of the presence of the analyte, which in such a scheme acts as a linker [2]. The rationale of our approach relies on the higher nanoparticle mobility induced by a microstirrer realized in a pipette placed off-axis with respect to a rotating magnet (see figure 1(a)). The rotating magnetic field acts as an external force, which pushes the otherwise slow nanoparticles so to increase the collision rate among Au@MNPs and analytes. This, in turn, is directly related to the efficiency with which the aggregates are formed and, hence, to the limit of detection. In figure 1(b) such an improvement is demonstrated by the colour change that takes place when IgG 250 ng/mL is mixed to a colloidal solution of Au@MNPs, whereas no effect could be observed when simple gold nanoparticles ($\phi \approx 50$ nm) were used (left). It is worth noticing that the stirring realized by our approach takes place in a volume as small as 50 μ L.

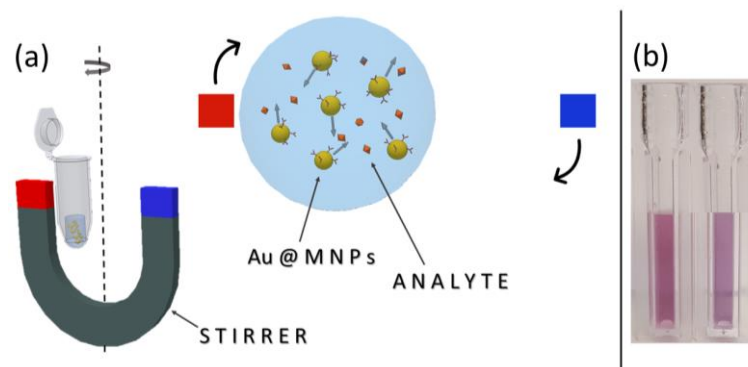


Figure 1. (a) A rotating magnet improves the mobility of magnetic nanoparticles thereby making more effective the aggregate production. (b) A colloidal solution of Au@MNPs (left) changes its colour when 2 μ L of IgG solution (250 ng/mL) is added (right).

- [1] S. Moraes Silva, R. Tavallaie, L. Sandiford, R. D. Tilley and J. J. Gooding, *Chem. Commun.*, 2016, **52**, 7528–7540.
- [2] M. Iarossi, C. Schiattarella, I. Rea, L. De Stefano, R. Fittipaldi, A. Vecchione, R. Velotta and B. Della Ventura, *ACS Omega*, 2018, **3**, 3805–3812.

Overview of structural magnetostrictive alloys

Alison Flatau, Souk Min Na, Jung Jin Park, Ganesh Raghunath, Brooks Muller

University of Maryland, College Park, Maryland, USA

Novel sensors and energy harvesting transducers take advantage of the significantly expanded design space made possible by recent advances in structural magnetostrictive alloys. These alloys can be machined and welded, have high fracture toughness, and can actuate, sense, and carry load while subjected to tension, compression, and bending. This talk will include an introduction to magnetostrictive materials and transduction, and to the subset of magnetostrictive alloys called structural magnetostrictive alloys because of their unique combination of mechanical and magnetostrictive properties. A particularly attractive benefit of structural magnetostrictives is that they can be produced using low-cost deformation processing (rolling) methods with high-temperature annealing for development of a preferred texture in lieu of more costly crystal growth methods for making highly oriented, single-crystal-like iron-gallium (Galfenol) and iron-aluminum (Alfenol) alloys. The process of using structural magnetostrictive materials to convert mechanical energy into magnetic energy and then into electrical energy is explained and demonstrated using sensors and energy harvesting devices as examples.

Examples of magnetostrictive devices include prototypes ranging in size from nanowire-based pressure sensors [1] to non-contact torque sensors [2] like that shown in Figure 1, and to huge, commercially available structures floating in the ocean that convert wave energy into electrical power for “community-scale” energy needs. Another benefit of structural magnetostrictives is they are well suited for stress annealing and/or magnetic field annealing strategies [3,4]. These methods for simplifying device design and enhancing device performance will also be discussed.

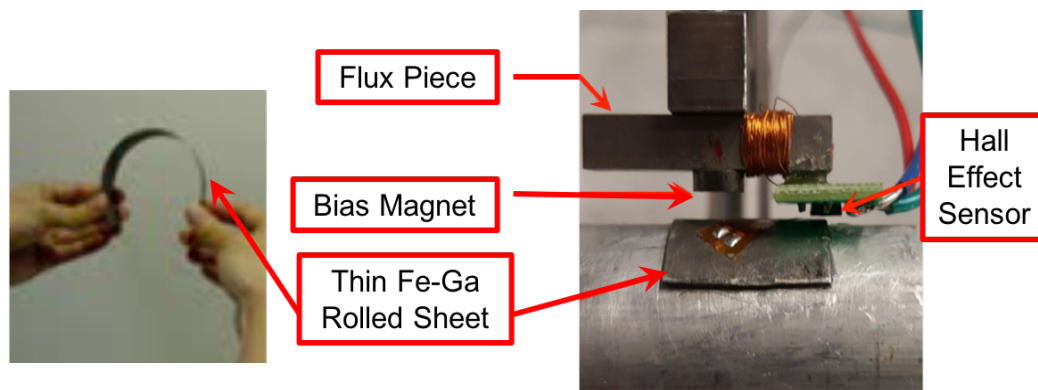


Figure 1: Left: Thin Fe-Ga rolled sheet undergoing large curvature. Right: Application of Fe-Ga for measuring torque in a rotating shaft.

-
- [1] Park et al., IEEE Sensors Journal, Vol. 17, No. 7, Apr. 2017, 2015-2020.
 - [2] Muller et al. AIP Advances **9**, 045113 _1-5 (2019).
 - [3] Park et al. AIP Advances **6**, 056221 _1-8 (2016). doi: 10.1063/1.4944772
 - [4] Park et al. AIP Advances **7**, 056431 _1-7 (2017). doi: 10.1063/1.4978006

Analysis of instantaneous magnetising power of ferromagnetic core in time domain

Branko Koprivica^a, Srđan Divac^b

^a University of Kragujevac, Faculty of Technical Sciences Čačak, Serbia

^b PhD Scholarship of the Ministry of Education, Science and Technological Development of Serbia

The aim of this paper is to present an analysis of the time variation of the magnetising power of a toroidal sample made of electrical steel. The analysis of power loss of ferromagnetic materials is a topic of interest in many recent publications [1-3]. However, only a few publications are related to the power loss and instantaneous magnetising power [4], which are closely related.

The paper will present the time waveforms of magnetic field, magnetic flux density and magnetising power. The waveforms of magnetic field $H(t)$ and magnetic flux density $B(t)$ will be represented using finite number N of harmonic components. These harmonic components will be used for calculation of the instantaneous magnetising power $p(t)$ using (1):

$$p(t) = H(t) \frac{dB(t)}{dt} = \sum_{i=1}^N (H_{si} \sin(i\omega t) + H_{ci} \cos(i\omega t)) \frac{d}{dt} \left(\sum_{i=1}^N (B_{si} \sin(i\omega t) + B_{ci} \cos(i\omega t)) \right), \quad (1)$$

where H_{si} , H_{ci} , B_{si} and B_{ci} are the harmonic components of the magnetic field and magnetic flux density, ω is the angular frequency of fundamental harmonic, t is the time and i is the index of harmonic order. Power $p(t)$ can be represented by two components, $p_1(t)$ and $p_2(t)$, as shown in Fig. 1 for the case of sinusoidal and triangular shape of $B(t)$ at 50 Hz. The analysis will be done also for the frequency of 1 Hz. A relation of the results obtained to the Bertotti's method of power loss separation will be examined.

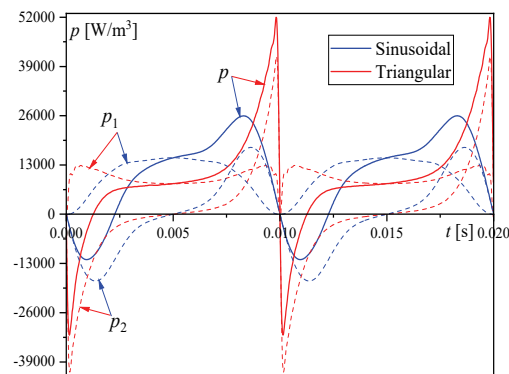


Figure 1: Instantaneous magnetising power and its components.

-
- [1] W.A. Pluta, Przegląd Elektrotechniczny (Electrical Review), **87** (2011), 37-42.
 [2] H. Zhao, C. Ragusa, O. de la Barrière, M. Khan, C. Appino, F. Fiorillo, IEEE Trans. Magn., **53** (2017), 2003804.
 [3] M.S. Lancarotte, A.A. Pentado, Jr., IEEE Trans. Energy Convers., **16** (2001), 174-179.

Hybrid spinel iron oxide nanoarchitecture combining crystalline and amorphous parent material

Sawssen Slimani^{a,c}, Giorgio Concas^b, Francesco Congiu^b, Gianni Barucca^d, Nader Yaacoub^e, Alessandro Talone^{c,f}, Davide Peddis^{a,c}, Giuseppe Muscas^b

^aUniversità degli Studi di Genova, Dipartimento di Chimica e Chimica Industriale, Via Dodecaneso 31, I-16146 Genova, Italy.

^bDepartment of Physics, University of Cagliari, Cittadella Universitaria di Monserrato, S.P. 8 Km 0.700, I-09042 Monserrato (CA), Italy.

^cIstituto di Struttura della Materia-CNR, 00015 Monterotondo Scalo (RM), Italy.

^dUniversità Politecnica delle Marche, Dipartimento di Scienze e Ingegneria della Materia, dell'Ambiente ed Urbanistica, Via Brecce Bianche 12, 60131 Ancona, Italy.

^eIMMM, Université du Main, CNRS UMR-6283, Avenue Olivier Messiaen, Le Mans 72085, France.

^fUniversità degli Studi 'Roma Tre', Dipartimento di Scienze, Roma, Italy.

When preparing nanostructured magnetic materials, the presence of an amorphous component is often considered a weakness of the synthesis method. This stems from the fact that the amorphous fraction is often pictured as a “dead” magnetic component, showing little to no contribution to the magnetic properties. e.g., saturation magnetization. Here we propose a hybrid-structured nanoarchitecture that combines crystalline cobalt ferrite and the amorphous parent material. This nanocomposite was prepared by coprecipitation method [1] without further steps employed after the main synthesis process. Transmission electron microscopy (TEM) analysis evidenced small crystalline particles ($\langle D_{\text{TEM}} \rangle \sim 3\text{nm}$) embedded in amorphous matrix. By Applying the Debye-Scherrer formula to the most intense reflection of the XRD pattern peak confirm an average size of the crystalline structure of about 3 nm. The investigation of the magnetic properties by SQUID magnetometer and the magnetic structure by means of Mössbauer on the crystalline/amorphous sample pointed out that the amorphous phase contributes partially to the total magnetic moment accompanied by a strong variation in the anisotropy (i.e., $H_c = 1.3(1)\text{ T}$, at 5K). Cross-checking the obtained information from structural and magnetic characterization, we have proposed a micromagnetic model using the software Mumax3, which sheds light on the contribution of each component elucidating the active role of the amorphous phase as a “non dead magnetic phase”, but a magnetically canted structure [2], with low effective magnetization and very large magnetic anisotropy coupled with the regular core structure .

[1] R. Safi, A. Ghasemi, R. Shoja-Razavi, M. Tavousi, J. Magn. Mater. **396**, 288 (2015).

[2] D. Zákutná, D. Nižňanský, L.C. Barnsley, E. Babcock, Z. Salhi, A. Feoktystov, et al., Phys. Rev. X. **10**, 031019 (2020).

Biased alternating current method for Fe-Si laminated inductors characterization

Hari Rimal^{a,b}, AbdelRahman M. Ghanim^{a,b}, S. Quondam Antonio^{a,b}, A. Laudani^c, A. Faba^{a,b}, F. Chilosi^{b,d}, E. Cardelli^{a,b}

^a Department of Engineering, University of Perugia, Perugia 06100, Italy

^b Center of Magnetics Innovative Technologies (CMIT), Perugia 06100, Italy

^c Department of Engineering, Roma Tre University, Rome 00146, Italy

^d TAMURA Magnetics Engineering, Corciano 06073, Italy

The use of magnetic reactors in power electronics is common, especially for low pass filtering applications. The power amount is usually beyond tens of kW, and in some application of HVDC, traction power trains, or wind generation system, reaches and overpass the MW limit. It turns out that an appropriate working level of current and magnetic induction is necessary. Up to few tens of kHz, the solution of magnetic cores made of laminated electrical steels is, again, the best choice. Special low magnetic losses, low thickness electric steels are at disposal for that. A typical example is the grain oriented GO electrical steel M3T23 grade, and the not grain oriented NGO electrical steel 35H270 grade. The reference standard [1] underlines, correctly, that the linked flux vs current is the more appropriate relationship to describe the magnetic behaviour of the reactor. It is assumed in the cited standards that the hysteresis phenomenon can be neglected, since the magnetic characteristic is mainly influenced by the air gaps. Another assumption of the standards cited is that when a sinusoidal voltage is applied to the reactor a sinusoidal current will flow, at least far from saturation. Again in the cited standards the inductance, the differential inductance and the ac inductance are suitably defined. Finally a measurement technique of the magnetic characteristic of the reactor with the so called DC current charging-discharging method is suggested. Due to the criticality of the measurement method proposed in terms of feasibility, accuracy and repeatability we propose here an alternative procedure that we called Biased Alternating Current Method (BACM). This paper aims to discuss the validity of the proposed method in comparison with the standard one, in particular several experimental measurements and numerical computations taking into account different models of a benchmark inductor is presented and discussed. A preliminary result is shown in Fig. 1

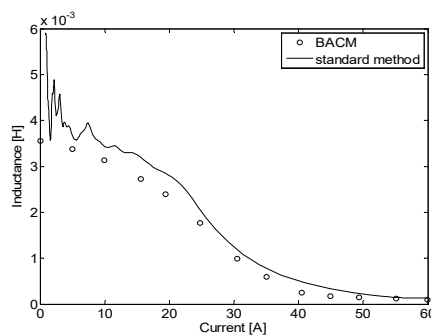


Figure 1: Preliminary results about the comparison between the proposed method and the standard procedure.

[1] IEC 60076-6 Ed. 1.0 b: 2007, Power Transformers - Part 6: Reactors

Advances in Magnetism 2020-21, June 13-16, 2021

FORC-based identification techniques

[Abstracts can be easily browsed through the bookmarks](#)

First order reversal curves and characterisation of intrinsic parameters in correlated systems

Sergiu Ruta¹, Ondrej Hovorka², Kangkang Wang³, Pin-Wei Huang³, Ganping Ju³, Roy Chantrell¹

¹Physics Department, University of York, York, UK

²Faculty of Engineering and the Environment, U. of Southampton, Southampton, UK

³Seagate Technology, Fremont, CA, USA

First Order Reversal Curve (FORC) method is extensively applied as a tool to qualitatively capture the general aspects of a magnetic system: mixed magnetic phases, cluster/long-range ferromagnetic state, magnetic characterization of geological mixtures minerals and different magnetization reversal mechanisms [1]. There is an increased interest in using the FORC method for quantitative investigation of intrinsic switching field distribution (SFD) and interaction field distribution (IFD) [2]. The SFD is a fundamental characteristic of granular magnetic materials. Being able to evaluate the thermal SFD of a system of coupled grains dominated by thermally activated hysteresis behaviour remains a challenge and is an essential for practical applications such as magnetic recording technology. We have shown that the FORC method has limitations in quantifying the SFD, which need to be taken into account[3]. The limitation is due to correlated switching in strongly interacting systems, where individual switching behaviour is masked by the collective switching. We quantify the parameter range of the FORC methods and we demonstrate that FORC methods can be applied only when interaction induced correlations are negligible (Fig. 1). FORC data certainly contains information on the interactions and SFD, but the Preisach-based analysis cannot, in general, reliably carry out the required deconvolution of the relative contributions. The Preisach-based analysis maps the FORC data directly onto a (H_u , H_c) plane whilst neglecting the degree of correlation in the magnetization structure.

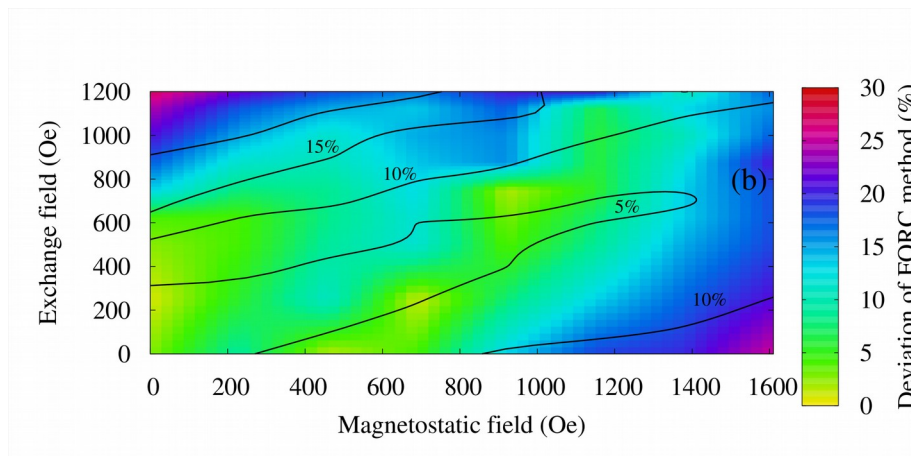


Fig1. Validity diagram: Diagram showing the deviation of σ_{SFD} from the FORC method in comparison with the expected value. The contour line are indicate the correlations for the same interactions.

1. A. Stancu, et. al, Journal of Applied Physics, 2003.
2. Dustin A Gilbert, et. al. Scientific reports, 2014.
3. Ruta, Sergiu, et al. Scientific reports, 2017.

Modern FORC data analysis and interpretation approaches

Joachim Gräfe^a, Felix Groß^a, José Carlos Martínez-García^b, Sven Ilse^a,
Eberhard Goering^a, Gisela Schütz^a, Montserrat Rivas^b

^a Max Planck Institute for Intelligent Systems, Stuttgart, Germany

^b University of Oviedo, Gijón, Spain

First-order reversal-curves (FORCs) are a powerful tool, which is increasingly used in material science and nano-magnetism as well as ferroelectricity, geology, archeology, and for spin-transition materials [1-4]. Ideally, it can access microscopic distributions of interaction and coercive fields without the need for lateral resolution [5]. Unfortunately, the reliable data analysis and interpretation poses a major challenge. This is why FORC is often seen as a magnetic fingerprint instead of a measurement method yielding quantitative information. To push past these limitations, we present a fast and user-independent analysis algorithm and possibilities to interpret the resulting FORC diagrams beyond the Preisach model.

We present a new evaluation approach which exploits the diversity of Fourier space to not only speed up the calculation by a factor of 1000 but also move away from the conventional smoothing factor towards real field resolution. By comparing the baseline resolution of the new and the old algorithm we are able to deduce an analytical equation which converts the smoothing factor into field resolution making the old and new algorithm comparable. We find excellent agreement not only for various systems of increasing complexity but also over a large range of smoothing factors. The achieved speed up enables us to calculate a large number of first-order reversal-curve diagrams with increasing smoothing factor allowing for an autocorrelation approach to find a hard criterion for the optimum smoothing factor. This previously computational prohibitive evaluation of first-order reversal-curves solves the problem of over- and undersmoothing by increasing general readability and preventing information destruction.

However, these measured FORC densities are not always straightforward to interpret, especially if the system is interaction dominated and the Preisach-like interpretation of the FORC density breaks down. To understand additional features arising from the interactions in the system, we purposely designed permalloy microstructures which violate the Mayergoyz criteria [7]. These artificial systems allow us to isolate the origin of an additional interaction peak in the FORC density. Modeling the system as a superposition of dipoles allows us to extract interaction strength parameters from this static simulation. Additionally, we suggest a linear relation between integrated interaction peak volume and interaction strength within the system. The presented correlation could be used to investigate the interaction behavior of samples as a function of structural parameters within a series of FORC measurements. This is an important step towards a more quantitative understanding of FORCs which violate the Mayergoyz criteria and away from a fingerprint interpretation.

-
- [1] J. Gräfe, Phys. Rev. B, 93 (2016) 014406
 - [2] F. Groß, Phys. Rev. B, 99 (2019) 064401
 - [3] C.-I. Dobrota, J. Appl. Phys., 113 (2013) 043928
 - [4] C. R. Pike, Phys. Rev. B, 71 (2005) 134407
 - [5] J. Gräfe, Rev. Sci. Instr., 85 (2014) 023901
 - [6] D. Cimpoesu, J. Appl. Phys., 125 (2019) 023906
 - [7] I. D. Mayergoyz, Phys. Rev. Lett., 56 (1986) 1518

FORC investigations of large-scale nano-ellipses arrays

Hubert Brückl^a, Astrit Shoshi^a, Thomas Schrefl^a, Michael J. Haslinger^b, Tina Mitterramskogler^b, Stefan Schrittwieser^c, Jörg Schotter^c

^a Dept. for Integrated Sensor Systems, Danube University Krems, Wiener Neustadt, Austria

^b PROFACTOR GmbH, Steyr-Gleink, Austria

^c AIT Austrian Institute of Technology, Vienna, Austria

Magnetic nanoparticles operating in the magnetic vortex configuration are of interest in magnetic field sensors [1] and as magnetic nanoprobes for immunoassay diagnostics [2]. In both applications, vortex states are found to be more advantageous compared to single-/multi-domain magnetization states.

We use nanoimprint and thin film technologies to reliably produce and controllably stabilize magnetic spin-textures in large-area nanoparticle arrays [3]. The periodically arranged nanoparticles are quasi-monodisperse elliptically shaped cylinders with highly uniform geometric and magnetic properties (fig. 1). The size distribution is very narrow within 3% standard deviation.

The ideal and well-defined model system is used to study magnetic vortex behavior, magnetic phase transition prior to the vortex nucleation and interaction between the array elements. For this, two master stamps for elliptical elements are available: 400 nm x 200 nm with a periodicity of 600 nm x 400 nm and 250 nm x 150 nm with a periodicity of 600 nm x 500 nm. By increasing the thickness of NiFe and CoFeB cylinders from 5 to 50 nm, the magnetization switches from quasi-single domain to the vortex state. The system is anisotropic.

First order reversal curves (FORC) provide insight into the relative proportions of reversible and irreversible magnetization processes. We like to analyse the interaction fields and critical field distributions (nucleation and annihilation) from FORC diagrams. The experiments are supported by (micro)magnetic simulations in order to better interpret the FORC results based on the well-known structure and geometry.

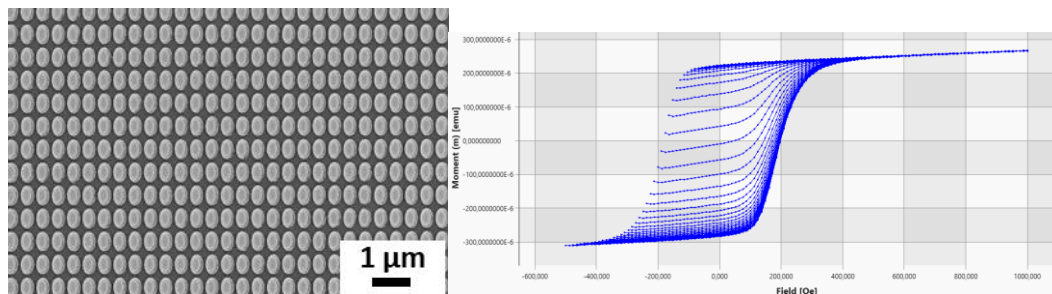


Figure 1: Left: Scanning electron microscopy image of a nano-imprinted array of elliptical cylinders of size 400nm x 200nm. The total number of ellipses is more than 10^8 on 1 cm^2 . Right: Example of FORC measurement of this array with 40 nm thick CoFeB.

-
- [1] D. Suess, A. Bachleitner-Hofmann, A. Satz, H. Weitenfelder, C. Vogler, F. Bruckner, C. Abert, K. Prügl, J. Zimmer, C. Huber, S. Luber, W. Raberg, T. Schrefl, H. Brückl, *Nature Electronics* 1, 362–370 (2018)
 - [2] S. Schrittwieser, F. Ludwig, J. Dieckhoff, K. Soulantica, G. Viau, L.-M. Lacroix, S.M. Lentijo, R. Boubekri, J. Maynadié, A. Huetten, H. Brueckl, J. Schotter, *ACS Nano* 6, 791 (2012)
 - [3] T. Mitterramskogler, M.J. Haslinger, A. Shoshi, S. Schrittwieser, J. Schotter, H. Brueckl, M. Muehlberger, *Proc. of SPIE*, Vol. 10775, 107750Y 4 (2018)

Analyzing time-dependent magnetization in multiphase systems using a dynamic Stoner-Wohlfart model and FORC diagrams

Laurentiu Stoleriu, Gheorghe Amanoloaei, Alexandru Stancu

Faculty of Physics and CARPATH Centre, "Al. I. Cuza" University, Iasi, Romania

The simulation of dynamical processes that occur in magnetic materials at the mesoscopic scale can be done using Landau-Lifschitz (LL) [1] type differential equations that describe the behaviour of the magnetization when an external applied field acts on the system. Despite its efficiency, the LL model exerts a strain on the computational performance when it's used to describe a system with lots of particles. To combat this problem, we propose a new dynamic model derived from the rotational coherent model, also known as the Stoner-Wohlfarth model [2, 3].

This new model is based on calculating the time it takes the magnetization vector to reach equilibrium given certain initial conditions. Using this approach, we were able to approximate the moment's trajectories and the major hysteresis loops of a single domain particle for different applied field frequencies (Fig.1-left).

This approach, although approximative, gives very good results for times significantly longer than the Larmor period while decreasing the computation time with at least an order of magnitude compared to the differential equation solving. This opens, the opportunity of studying complex systems with several components having a wide range of relaxation time values (Fig. 2) [4].

In this paper we use FORC method to explore how interactions mediate time-dependent magnetization processes in multicomponent systems.

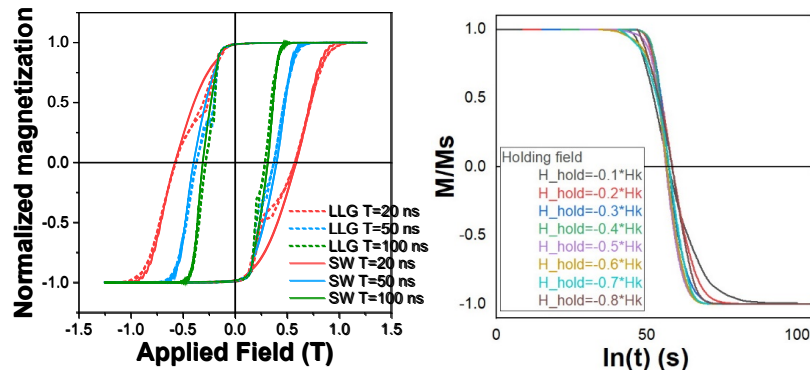


Figure 1: Dynamic MHLs using the dynamic SW model compared to LLG (right). Thermal decay curves obtained with the time-dependent SW model superposed onto a universal relaxation decay curve (left)

-
- [1] L.D. Landau, E.M. Lifschitz, Phys. Z. Sowjetunion, **8** (1953), 153.
 - [2] E.C. Stoner, E.P. Wohlfarth, Phil. Trans. Roy. Soc. **A240** (1948), 599.
 - [3] D. Cimpoesu, L. Stoleriu, A. Stancu, J. Appl. Phys. **114** (2013), 223901.
 - [4] M. Strungaru, S. Ruta, et. al., J. Magn. Magn. Mater., **486** (2019), 165281.

FORC diagrams of hcp-Co particle ensembles from micromagnetic simulations

Leoni Breth^a, Thomas Schrefl^a, Johann Fischbacher^a, Alexander Kovacs^a, Harald Oezelt^a, Hubert Brückl^a,
Christoph Czettl^b, Julia Pachlhofer^b, Maria Schwarz^b, Christian Storf^b

^a Department for Integrated Sensor Systems, Danube University Krems, Austria
^b Ceratizit Austria GmbH, R&D Cutting Tools, Reutte, Austria

First Order Reversal Curve (FORC) diagrams have over 30 years of history as a tool to characterize ensembles of magnetic particles reaching from applications in geophysics to detect the prevalence of carriers of paleomagnetic signals [1] to the measurement of magnetic recording media properties [2]. Based on this present understanding we introduce the idea of using FORC diagrams to detect the crystalline structure of the cobalt binder phase in tungsten carbide (WC-Co), a hard metal used in a wide range of high-tech applications (e.g. drills or cutting inserts) [3]. The goal is to interpret FORC diagrams from experimental measurements by micromagnetic simulations as information source for a fast characterization of tungsten carbide binders. Here, we present FORC diagrams generated from our own framework of micromagnetic simulation and FORC evaluation code. The simulations provide a means to assemble mixtures of particles with a known distribution of various properties. We have used energy minimization [4] to compute FORCs of hcp-Co cubes with uniaxial magnetocrystalline anisotropy and sizes of 50, 80 and 100 nm (see Figure 1). Our first results for ensembles of non-interacting particles with varying anisotropy axis orientation show a transition from single domain behaviour to a more feature rich FORC diagram for increasing particle size. By analyzing the micromagnetic magnetization reversal the features can be explained by domain nucleation and annihilation processes. Such FORC diagrams together with information on particle size and other properties serve as input to machine learning algorithms, which are available as part of modern open source frameworks such as scikit-learn.

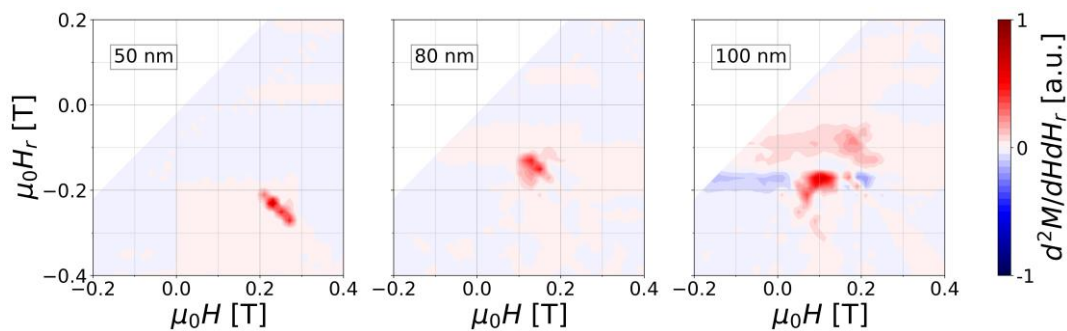


Figure 1: FORC distributions for randomly oriented Co particles with increasing size

The financial support by the Austrian Federal Ministry of Climate Action, Environment, Energy, Mobility, Innovation and Technology (BMK) in the KI-Carbide project (#877141) is gratefully acknowledged.

[1] A. R. Muxworthy and D. J. Dunlop, *Earth Planet. Sci. Lett.* 203, 369-382 (2002)

[2] M. Winklhofer and G. T. Zimanyi, *J. Appl. Phys.* 99, 08E710 (2006)

[3] J. García et al., *Int. J. Refr. Met.* 80, 40-68 (2019)

[4] L. Exl, J. Fischbacher, A. Kovacs et al., *Comp. Phys. Comm.* 235, 179-186 (2019)

Visualization of fine structure in FORC distributions

Pieter Visscher^a, Joseph B. Abugri^b, Bill Clark^c, and Subhadra Gupta^d

^a Physics Department, University of Alabama, Tuscaloosa, AL, USA

^b Department of Electrical and Computer Engineering, U. of Alabama, Tuscaloosa, AL, USA

^c Intel Corporation, Hillsboro, OR, USA

^d Department of Metallurgy and Materials Science, U. Of Alabama, Tuscaloosa, AL, USA

The FORC (First Order Reversal Curve) method has become widely used for the characterization of magnetic materials. In systems of non-interacting uniaxial ferromagnetic particles (Preisach hysterons) the FORC distribution gives the density of hysterons in the H - H_R (applied field-reversal field) plane. However, it has also proved to be a useful probe of interparticle interactions in systems that do interact. In particle systems, the distribution is slowly varying in the field plane and it is possible (and often necessary) to smooth the data to suppress noise, to get a useful contour plot of the density. However, in systems such as sheet films which switch by domain-wall motion, the distribution can be dominated by very fine-scale features, which will be wiped out by smoothing. Software for displaying color maps of densities is designed to assume that fine-scale features are noise, and eliminate them.

We have developed a visualization program (“FORC+”) that deals with noise in a different way. A FORC experiment gives a function $M(H, H_R)$ [M = magnetic moment, H = applied field, H_R = reversal field, the beginning of each FORC curve (Fig. 1(a))] which has a natural discretization -- the moment is measured on a nearly regular grid in the H - H_R plane. The simplest discrete representation of the FORC density [the crossed partial derivative of $M(H, H_R)$] is defined for each grid square, and is simply the sum of the M 's on the corners of the square, with alternating signs. If this grid data is input to a commercial contouring program, noise will make the contours very jagged and hard to interpret. FORC+ (Fig. 1(c)) represents positive and negative density with complementary colors (orange and blue) so that noise (a mixture of positive and negative squares very close together) appears white (or grey) from a distance. Thus a region where the local average is positive will appear orange, and a predominantly negative region will appear bluish. In our case of a 20 nm CoPd alloy film [2], there are a positive and a negative ridge close together, a “dipole tail” [2], which stands out clearly even if it is only one pixel wide. The original magnetometer data $M(H, H_R)$ can be exactly recovered from the FORC+ display colors (with the reversible switching field distribution [1]) – no information is lost to averaging.

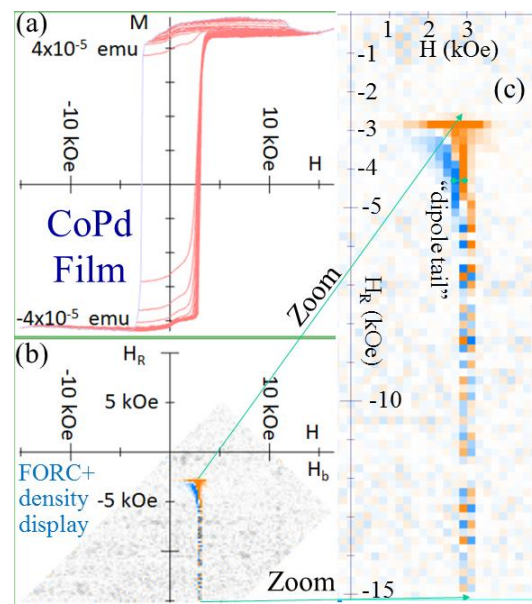


Figure 1: (a) FORC curves (M vs. H); (b) FORC distribution; (c) enlarged view of dipole tail.

[1] <http://MagVis.org>

[2] J.B. Abugri, P. B. Visscher, B.D. Clark, Jie Gong, and Subhadra Gupta, “MFM and FORC+ study of switching mechanism in $\text{Co}_{25}\text{Pd}_{75}$ films”, J. Appl. Phys. **126**, 013901 (2019).

Advances in Magnetism 2020-21, June 13-16, 2021

**Advanced
measurement
techniques
&
Artificial intelligence,
optimization and
inverse problems**

Abstracts can be easily browsed through the bookmarks

Imaging non-collinear antiferromagnetic textures via single spin relaxometry

Aurore Finco^a, Angela Haykal^a, Rana Tanos^a, Florentin Fabre^a, Saddem Chouaieb^a, Waseem Akhtar^{a,b}, Isabelle Robert-Philip^a, William Legrand^c, Fernando Ajejas^c, Karim Bouzehouane^c, Nicolas Reyren^c, Thibaut Devolder^d, Jean-Paul Adam^d, Joo-Von Kim^d, Vincent Cros^c and Vincent Jacques^a

^a Laboratoire Charles Coulomb, Université de Montpellier, CNRS, Montpellier, France

^b Department of Physics, JMI, Central University, New Delhi, India

^c Unité Mixte de Physique, CNRS, Thales, Université Paris-Saclay, Palaiseau, France

^d Centre de Nanosciences et de Nanotechnologies (C2N), CNRS, Université Paris-Saclay, Palaiseau, France

Antiferromagnets attract a great interest for spintronics owing to the robustness of magnetic textures and their fast dynamics. However, since they exhibit no net magnetization, antiferromagnets are challenging to work with. NV-center magnetometry, which provides a μT sensitivity combined with a nanoscale spatial resolution, has emerged in the last years as a powerful technique to investigate them [1].

Here we introduce a new imaging mode of the NV-center magnetometer which does not rely on the measurement of the static magnetic stray field but on the detection of magnetic noise originating from spin waves inside the non-collinear antiferromagnetic textures of interest. The presence of magnetic noise accelerates the NV spin relaxation. As a consequence, the emitted photoluminescence is reduced, allowing a simple detection of the noise sources [2,3].

We demonstrate this new technique on synthetic antiferromagnets (SAF) [3,4] consisting of two ferromagnetic Co layers antiferromagnetically coupled through a Ru/Pt spacer. We first image domain walls and prove that we perform noise-based imaging by measuring a shorter NV spin relaxation time above an antiferromagnetic domain than above a domain wall. Calculations of the spin waves dispersion both in the antiferromagnetic domains and in the domain walls as well as maps of simulated magnetic noise intensity enable us to conclude that the noise which we probe arises from spin waves channelled in the domain walls.

Going further, we tune the composition of the SAF stacks in order to stabilize spin spirals or antiferromagnetic skyrmions. In both cases, our relaxometry-based technique is able to image the non-collinear structures, demonstrating its efficiency and opening new avenues of exploration in the characterization of complex structures in magnetically-compensated materials.

This project has received funding from the European Union's Horizon 2020 research and innovation programme under the Marie Skłodowska-Curie grant agreement No 846597 and from the DARPA TEE Program.

[1] I. Gross et al, Nature, 549, 252 (2017)

[2] A. Finco et al, arXiv:2006.13130 (2020)

[3] M. Rollo et al, arXiv:2101.00860 (2021)

[4] W. Legrand et al, Nature Materials, 19, 34 (2020)

Kubo spins in nanoscale aluminum grains:

A muon spin relaxation study

Nimrod Bachar^a, Aviad Levy^b, Thomas Prokscha^c, Andreas Suter^c, Elvezio Morenzoni^c, Zaher Salman^c, and Guy Deutscher^b

^a Department of Quantum Matter Physics, University of Geneva, CH-1211 Geneva 4, Switzerland

^b Raymond and Beverly Sackler School of Physics and Astronomy, Tel Aviv University, Tel Aviv 69978, Israel

^c Laboratory for Muon Spin Spectroscopy, Paul Scherrer Institute, 5232 Villigen PSI, Switzerland

We report muon spin relaxation rate measurements on films composed of aluminum grains having a size of a few nm, with a large energy level splitting of the order of 100 K. The films range from weakly metallic to insulating. In the insulating case, the low-temperature relaxation rate is consistent with the presence of single electron spins in grains having an odd number of electrons, known as Kubo spins. The relaxation rate temperature dependence follows an activation law having an energy scale in agreement with the average level splitting. In weakly metallic films, inter-grain junction spins may contribute substantially to the smaller relaxation rate.

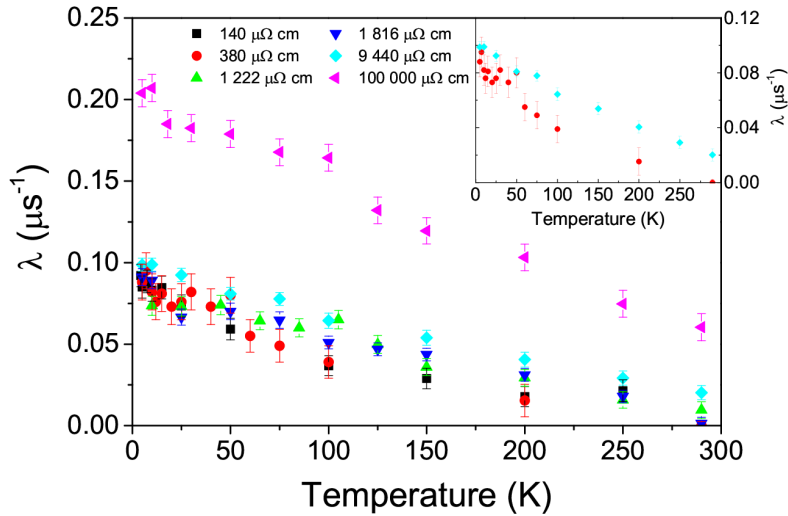


Figure 1: Temperature dependence of the muon spin relaxation rate of electronic origin for all samples in this work.

[1] N. Bachar *et al.*, Phys. Rev. B **101**, 024424 (2020)

Quantitative issues in magnetic force microscopy

Daniele Passeri^a

^a Department of Basic and Applied Sciences for Engineering, Sapienza University of Rome, Italy

Magnetic force microscopy (MFM) is an atomic force microscopy (AFM) based technique which enables the acquisition of images reflecting the distribution of magnetic domains of the sample at the nanometer scale simultaneously to the topography. MFM has a broad range of applications, e.g., from magnetic recording media to magnetic nanomaterials, nanocomposites, and biological materials [1,2]. Extraction of quantitative information from the acquired MFM images, however, is not straightforward and requires the use of suitable experimental approaches and accurate analytical methods.

The purpose of this work is to give an overview of some applications of MFM, with particular emphasis on the biological and biomedical ones, to highlight some experimental issues which are fundamental in the quantitative analysis of MFM data, and to discuss some possible approaches and solutions.

-
- [1] D. Passeri et al., *Biomatter* **4** (2014), e29507.
 - [2] D. Passeri et al., *Magnetic force microscopy*, in *Magnetic characterization techniques for nanomaterials*, C.S.S.R. Kumar (Ed.), Springer-Verlag Berlin Heidelberg (2017), Chapter 7, pp 209-259.

Magnetic particle spectroscopy to determine the reproducibility of magnetic nanoparticle syntheses

Frank Wiekhorst^a, Patricia Radon^a, Norbert Löwa^a, Abdulkader Baki^b, Regina Bleul^b

^a Physikalisch-Technische Bundesanstalt, Berlin, Germany

^b Fraunhofer Institute for Microengineering and Microsystems IMM, Mainz, Germany

Magnetic nanoparticles (MNP) comprise one of the largest families of nanomaterials and are widely employed for biomedical purposes: for in-vitro diagnostics, specifically for the separation and extraction of cells, viruses, proteins, and DNA from blood. In addition, new cancer therapies like magnetic drug targeting or hyperthermia and technical applications like magnetic bearings, magnetic separation, or loudspeakers make intensive use of MNP. Despite of these vast biomedical and technical MNP applications, there are no standardised measurement procedures to determine structural and magnetic properties, and in addition, measures of the reproducibility of these properties.

We demonstrate the capability of magnetic particle spectroscopy (MPS) [1] to analyse the reproducibility of two different state-of-the-art synthesis approaches (individual batch and continuous micromixer [2] precipitation of MNP from aqueous, alkaline solutions of iron salts). MPS is a fast and specific technique detecting the nonlinear dynamic magnetic susceptibility of MNP, sensitive to their size, shape, and crystal structure. We synthesized five individual MNP samples with each approach and analysed the reproducibility of the magnetic properties using two characteristic MPS-parameters: the amplitude of the 3rd harmonic normalized to iron amount (A_3^*) and the concentration independent spectral shape factor obtained from the ratio of 3rd and 5th harmonic (A_5/A_3).

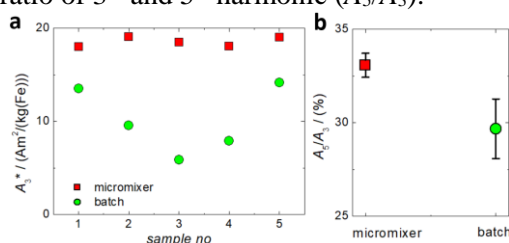


Figure: Dynamic magnetic susceptibility of MNP samples from two different synthesis approaches: **a:** Variation of 3rd harmonic amplitude of five MNP samples synthesized by micromixer (red squares) and conventional batch (green) procedure. **b:** Mean and standard deviation of the corresponding MPS spectra for micromixer and batch synthesized samples.

MNP produced by micromixer synthesis show a lower variation of MPS parameters (see figure) than batch synthesis. MPS is a valuable, fast tool to analyse the reproducibility of MNP synthesis products. Moreover, MPS has a great potential for online monitoring of MNP synthesis due to its outstanding sensitivity (detectable moments down to 10^{-12} Am²), and wide dynamic range (six orders of magnitude) combined with a high measurement speed (temporal resolution of seconds).

[1] N. Löwa, M. Seidel, P. Radon, F. Wiekhorst. Magnetic nanoparticles in different biological environments analyzed by magnetic particle spectroscopy. *JMMM* 427:133-38, 2017.

[2] R. Bleul, R. Thiermann, G. U. Marten, M. J. House, T. G. St. Pierre, U. O. Häfeli, and M. Maskos. Continuously manufactured magnetic polymersomes – a versatile tool (not only) for targeted cancer therapy. *Nanoscale*, 5(23):11385–11393, 2013.

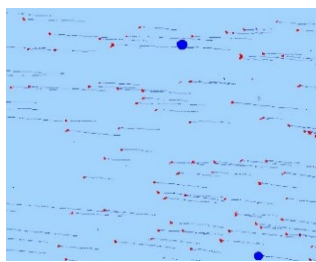
Measuring magnetophoretic mobility of single magnetic nanoparticles

Abhinav Sannidhi^a, Paul W. Todd^b, Thomas R. Hanley^a

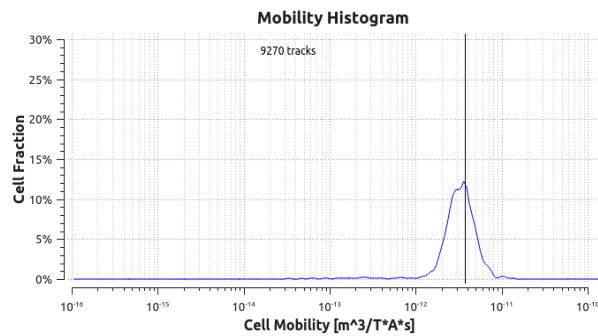
^aDepartment of Chemical Engineering, Auburn University, AL 36849

^bMagnaquant, 11760 Commonwealth Drive, Louisville, KY 40299

Paramagnetic beads used in diagnostic, biochemical, molecular and cell-biological applications have typically been in the microparticle size range, 700 to 10,000 nm in diameter. It has been amply demonstrated that paramagnetic particles in this size range can be characterized magnetically, measuring saturation magnetization and apparent volume susceptibility on the basis of magnetophoretic mobility [1]. Magnetophoretic mobility, velocity per magnetic energy gradient, is typically determined by particle tracking velocimetry using a dark-field video microscope and an isodynamic magnetic field [2]. However, current trends, especially in proposed therapeutic applications of paramagnetic beads, are toward the use of smaller particles in the nanoparticle size range, 10 to 200 nm. Optical signals from particles in this size range are within the “noise” range of microscope velocimetry and inaccessible for analysis. Previously such particles were attached to non-magnetic microbeads to observe their motion, but the number of nanoparticles per microbead is an unknown. We tested two methods of estimating nanobead (105 nm) magnetophoretic mobility, one based on the optical clearing rate of a bead suspension and one based on the mobility of chains of nanobeads using the optics and magnetic field of a commercial velocimeter. In the former case it was found that the high concentration of particles required to produce detectable optical absorbance resulted in excessive bead aggregation in the applied magnetic field and therefore a gross overestimation of magnetophoretic mobility. At greater dilutions (about 0.5×10^6 beads per cm^3) the chains that formed could be detected and their images analysed for length-to-width ratio, L/W . A two-parameter display of mobility vs. L/W was fitted using a drag-force relationship for particle chains, and this function was evaluated at $L/W = 1$ to obtain the mobility of a single bead. In the case of the 105-nm beads studied the average magnetophoretic mobility was found to be about $0.034 \times 10^{-12} \text{ m}^3 \text{ T}^{-1} \text{ A}^{-1} \text{ s}^{-1}$, in reasonable agreement with an expected value.



Particles trajectories in the applied magnetic field



Magnetophoretic mobility distribution

-
- [1] Sannidhi, A., Todd, P. W., & Hanley, T. R. (2019). Estimation of Intrinsic Magnetic Properties of Single Particles by Particle Tracking Velocimetry. *IEEE Magnetics Letters*, 10, 1-5.
- [2] Zhou, C., Boland, E. D., Todd, P. W., & Hanley, T. R. (2016). Magnetic particle characterization—Magnetophoretic mobility and particle size. *Cytometry Part A*, 89(6), 585-593.

Magnetic Permeability vs Barkhausen Noise Measurements for Magnetic NDT Applications

Aphrodite Ktena^{a,b}, Mehrija Hasicic^c, Eleni Maggiorou^b, Spyridon Aggelopoulos^b, Evangelos Hristoforou^b

^a Energy Systems Laboratory, National and Kapodistrian University of Athens, Greece

^b Electronic Sensors Laboratory, National Technical University of Athens, Greece

^c Dept of Electrical and Electronics Engr, Int'l Burch University, Bosnia & Herzegovina

Magnetic permeability μ is a macroscopic property which reflects the microstructure of a magnetic material at the time of measurement and its interaction with external stimuli such as applied fields, mechanical stresses, or temperature. Magnetic Barkhausen Noise (mBN), on the other hand, results from the discrete magnetization jumps during the magnetization process of a material and reflects the energy required to nucleate or annihilate magnetic domains and overcome obstacles, such as impurities and dislocations, or misoriented grains and grain boundaries during magnetic domain rotation and wall propagation. Both μ and mBN vary with microstructural characteristics, such as type II stresses or grain size (Figure 1). However, there are several challenges that need to be met before either or both of these parameters can be used as metrics in standardized non-destructive testing methods for industrial applications. Their applicability in surface or bulk measurements, the wide range of arrangements, sensor technologies and techniques which have been proposed or tested, the variety of models which interpret μ or mBN measurements and correlate them with microstructural parameters, such as residual or applied stress and grain size, the specific parameters to be used as metrics, are some of them. For example, in practical applications, the differential magnetic permeability μ_{diff} is used instead of $\mu=B/H$. μ_{diff} , and its first derivative, is a more reliable metric for the determination of stresses in the elastic or plastic region, while mBN parameters such the RMS voltage of the Barkhausen noise envelope seems to correlate better with grain size. Finally, the effect of stress-induced inhomogeneities on the phenomenology of the magnetic hysteresis loop is studied through vector Preisach modeling and micromagnetic calculations using OOMMF software.

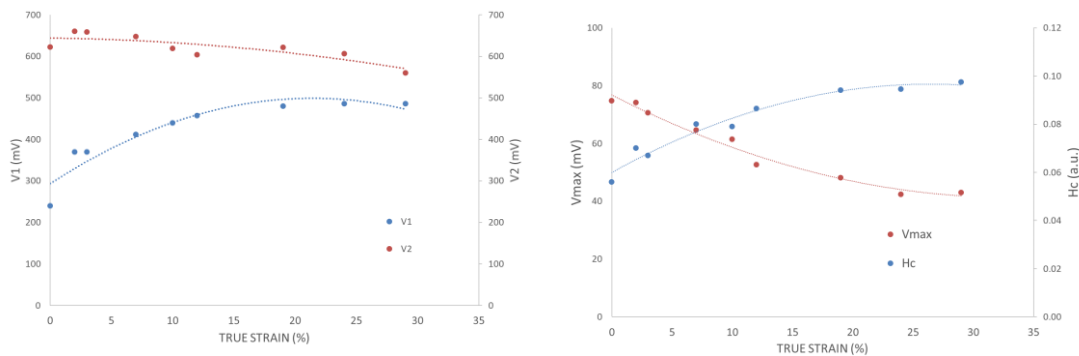


Figure 1: Magnetic parameters as a function of true strain in electrical steel laminates. Left: V2 is proportional to the differential permeability and V1 is the RMS value of the magnetic Barkhausen Noise envelope. Right: Coercivity Hc and the parameter Vmax, which is proportional to the maximum differential permeability, as obtained from a major loop measurement.

Developing bespoke magnetic measurement solutions: an NMI perspective

Stuart Harmon^a, Roberta Guilizzoni^a, Greame Finch^a

^a National Physical Laboratory, Teddington, United Kingdom

Traditionally National Measurement Institutes (NMI's) have maintained and disseminated a range of measurement standards through inter-comparison and artefact calibration with traceability back to base SI units. The most common magnetic parameters are generally measured in accordance with the IEC 60404 series of written standards. These standards outline methodologies and good practice to repeatably determine magnetic properties but are limited in the sample geometries that can be accommodated and generally don't include operational conditions encountered in industrial settings. Increasingly, NMIs such as NPL are being asked to develop bespoke measurement solutions that cannot be accomplished using commercial measuring equipment, but most crucially, are still underpinned by a robust methodology and uncertainty evaluation to improve the quality of the results. The work presented will outline research and development case studies where existing magnetic measurement standards have been utilised to expand NPLs capability in areas such as; 1) the non-destructive evaluation (NDE) of steel vessels in harsh environments and 2) evaluation of magnetic field exposure due to inductive power transfer (IPT) for electric vehicles. In both cases modelling was used to predict changes in material properties (related to mechanical condition) or field profiles (human exposure to magnetic fields) and then experimental work conducted to validate these models.

Case study 1) The development of a sensor to operate in harsh environments, including radiation, where the thickness of the un-seen lower steel sheet was determined. The sensor head was modelled to predict changes in magnetic properties related to different steel thicknesses. As a result, a proof-of-concept sensor was designed and evaluated [1].

Case study 2) Development of traceable calibration systems for magnetic field sensors used to evaluate IPT systems for electric vehicles [2]. Sensors were calibrated using the new calibration system and on-site trials conducted to evaluate the models, relating the measured magnetic fields to INCIRP guidelines for human exposure limits.

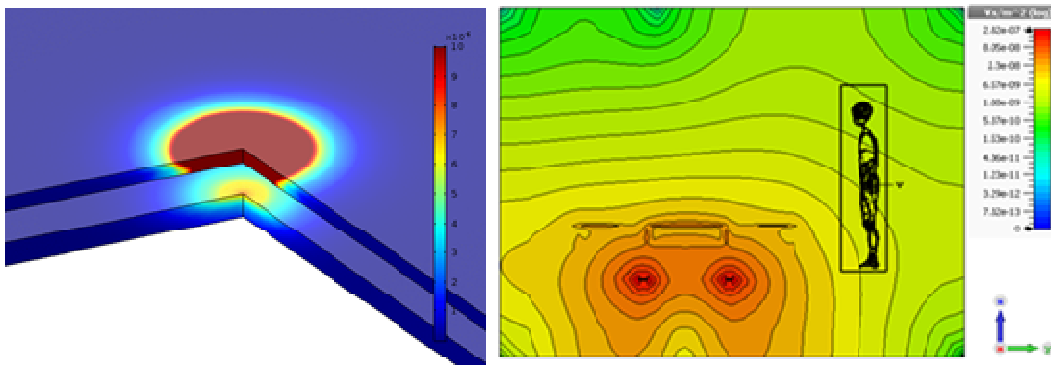


Figure 1: Left: modelling the magnetic field changes in two different steel plates to assess lower plate thickness using an Eddy current based sensor. Right: Human model relating the magnetic field produced by an IPT system to magnetic field exposure limits.

[1] R. Guilizzoni, G. Finch, S. Harmon, Sub-surface corrosion detection of industrial steel structures. Magnetic Frontiers 2019: Magnetic Sensors

[2] Metrology for Inductive Charging of Electric Vehicles (MICEV). AEIT 2019

The application of unsupervised learning to the AC susceptibility measurements of High-Temperature Superconductors

Marcin Kowalik^a, R. Zalecki^b, M. Giebułtowski^b, J. Niewolski^b, W. Tokarz^b

^a Rzeszów University of Technology, Rzeszów, Poland

^b AGH University of Science and Technology, Kraków, Poland

Machine learning (ML) is the study of computer algorithms that improve automatically through experience. ML algorithms are built on a mathematical model based on data, in order to make predictions or decisions without being explicitly programmed to do so. Unsupervised learning (UL) is a subfield of ML. UL algorithms look for previously undetected patterns in a dataset with no pre-existing labels and with a minimum of human supervision. Great progress has been made in a quest to discover, develop or refine various machine learning algorithms in recent years and new ways of data analysis have been shown. The ML application to the analysis of datasets is a state of the art technique which allows to make breakthroughs in various areas of science and engineering.

Our work aims to provide a first insight into application of clustering techniques to the large dataset of AC susceptibility measurements of High-Temperature Superconductors (HTS). It should allow recovering known relationships between different types of HTS and their superconducting properties.

We show that it is possible to represent the most significant features of a single AC measurement of a HTS sample as 5 numerical values by using a Convolutional 1D Autoencoder and the Bag Of Words model. The most distant 5D representations of $\chi(T)$ are for samples, which have the most different superconducting properties i.e. thin layer HTS and grinded and pressed polycrystalline HTS so the 5D representation of the $\chi(T)$ dataset preserves the most important features of the measurement of the HTS sample. However the cluster analysis of the 5D $\chi(T)$ dataset by two clustering algorithms did not reveal the existence of clearly distinct classes of $\chi(T)$ measurements. Though a t-SNE visualisation (fig. 1) in 3D space shows that some clustering exists and part of the measurements are mainly arranged on some sort of cluster boundary. Therefore, more advanced analysis could be performed.

Acknowledgements: This work was supported by The National Science Center Poland under Project No. DEC-2018/02/X/ST3/01741.

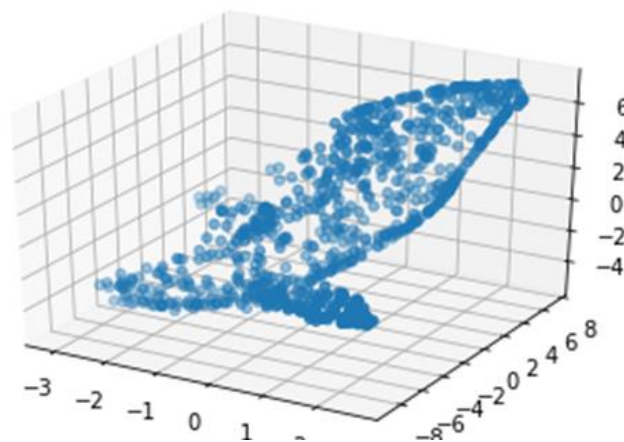


Figure 1: Visualisation of about 1000 $\chi(T)$ measurements of HTS samples in 3D space by t-SNE algorithm. A single measurement is a 5D vector and it is represented as a single circle. The x, y and z axes represents the t-SNE features.

Advances in Magnetism 2020-21, June 13-16, 2021

Electromagnetic non-destructive testing

[Abstracts can be easily browsed through the bookmarks](#)

Coupled electromagnetic models for nondestructive evaluation of materials

Christophe Reboud, Roberto Miorelli, Anastassios Skarlatos, Edouard Demaldent

CEA, LIST, Département Imagerie Simulation pour le Contrôle, Gif-sur-Yvette, France

This communication presents fast simulation tools dedicated to nondestructive testing applications. In order to take advantage of semi-analytical formalisms exploiting symmetries, the complete electromagnetic problem is solved as a set of interacting subproblems. Hence, in a configuration involving a complex eddy current testing (ECT) probe with 3D ferrite core, see Figure 1, a numerical formalism [1] is used to calculate the field emitted by the probe and a fast modal approach [2] is used to compute fields in the inspected piece with canonical geometry. Then the ECT signal is computed using an integral formalism based on the use of Green tensors of the planar stratified medium under test [3].

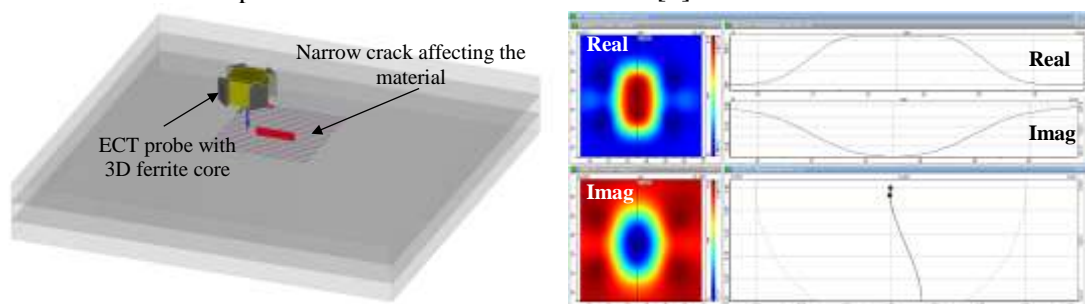


Figure 1: Simulation of an ECT inspection by means of a coupled approach. A 2D map of the complex impedance change of the probe due to the flaw is computed at a single frequency.

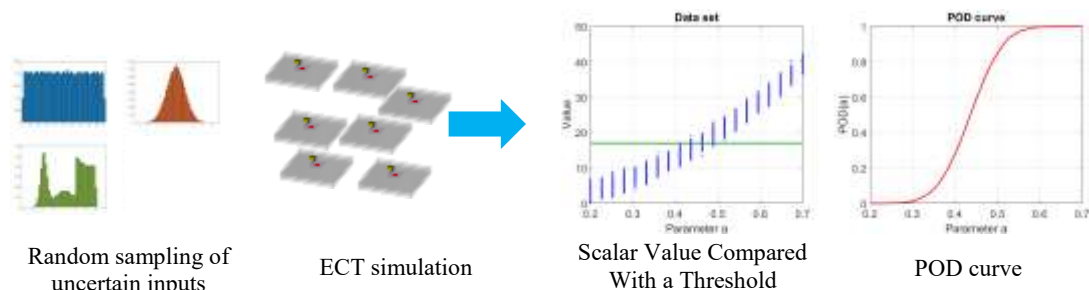


Figure 2: Typical model based approach for performance demonstration of a NDT method using Probability of Detection (POD) curves.

Once the reference problem is solved in an efficient way, it can be simulated in many different situations in order to evaluate the sensitivity of the ECT measured quantity to influential parameters and quantify the performance of the inspection method. This can be done by means of uncertainty propagation. After an introduction of the coupled formalisms constituting the forward model, accelerating techniques and model based statistical studies will be presented. Validation aspects of both forward model and statistical studies will also be discussed.

-
- [1] A. Skarlatos, E. Demaldent, A. Vigneron, C. Reboud, *Stud. Appl. Electr. Mech.* **39** (2014), 128-135.
 - [2] C. Reboud and T. Theodoulidis, *Electromagnetic Nondestructive Evaluation (XV)*, IOS Press (2012), 36.
 - [3] R. Miorelli, C. Reboud, D. Lesselier, T. Theodoulidis, *IEEE Trans. Mag.* **48** (2012), 2551-2559.

Non-destructive testing applications of the microwave Holographic RADAR

Lorenzo Capineri^b, Margarita Chizh^a, Andrey Zhuravlev^a, Vladimir Razevig^a, Sergey Ivashov^a, Tim Bechtel^c, Pierluigi Falorni^b, Andrea Bulletti^b, Luca Bossi^b

^a Remote Sensing Laboratory, Bauman Moscow State Technical University, Moscow, Russia

^b I Department of Information Engineering, University of Florence, Firenze, Italy

^c Franklin and Marshall College, Lancaster (PA), USA

Since 2004, the authors have been investigating holographic radar for several non-destructive testing applications. The main fields explored are civil engineering, cultural heritage and detection of unexploded ordnance (UXO) and humanitarian demining.

The paper briefly describes the operating principles and the electronic system of the holographic radar operating at different frequencies (2 GHz, 4 GHz, 7 GHz, and 22 GHz) in order to cover different penetration and resolution requirements for different dielectric materials. The RASCAN type of holographic radar can be designed to efficiently operate in contact or proximity (several cm) of the surface for producing high plan-view resolution imaging ($\lambda/4$). The evolution of the electronics for processing holographic signals has allowed the implementation of a reconstruction of the microwave holograms using a back-propagation technique with In-phase and Quadrature (I/Q) signals.

The second part of the paper reports the main successful NDT investigations for: civil and historical building structures, structural wood deterioration due to attacks of xylophagous insects, artworks under restoration, shallow hidden tracks of dinosaurs, moisture detection in dielectric foams and finally sub millimeter defects in foams bonded to metallic structure (as is common in the aerospace industry). More recently, the application to detection of plastic-cased minimum metal landmines has been developed and innovative imaging algorithms are proposed. A quantitative comparison of the advantages and disadvantages of this method relative to other NDT methods such as X-Ray and Infrared imaging is proposed.

Eddy current testing of ferromagnetic steel tubes under magnetization

Athanasios Kyrgiazoglou^a, Theodoros Theodoulidis^a, Nikolaos Poulakis^b

^a University of Western Macedonia, Department of Mechanical Engineering, Kozani, Greece

^b University of Western Macedonia, Department of Electrical and Computer Engineering, Kozani, Greece

Eddy current testing (ECT) is routinely applied to the aerospace, petrochemical industry and metal processing industry as well as to nuclear and conventional power generation. The vast majority of inspections, however, involve non-ferromagnetic structures since it is quite challenging to implement classical ECT on ferromagnetic media. The difficulty is related to the inhomogeneous and non-linear nature of the magnetic permeability which not only results to non relevant and noise signals but also decreases considerably the eddy current penetration depth up to the point of limiting the inspection to the surface of the test-piece.

In the case of ferromagnetic tubes testing, an external large coil is used to magnetize the ferromagnetic tubular specimens. Using different high-level DC current, the magnetic field can become very strong and drive the sample to the saturation point [1-2]. As a result, the tube material behaves almost as non-ferromagnetic. In this paper, we study the effect of the magnetization current on the detection of wall losses (either ID or OD), which is the most common flaw together with pitting.

First, the characteristic B-H curve of the tube material is measured in order to set the same curve in the simulation software (Comsol Multiphysics). Then, we observe the effect of the DC magnetic field on the coil impedance changes using a large number of magnetization current values range from 0 to 3A. As the tube is magnetized, a phase change is introduced between the various wall loss percentages and hence the classical technique of phase analysis can be utilized. Figure 1 presents the comparison results between experiments and simulation

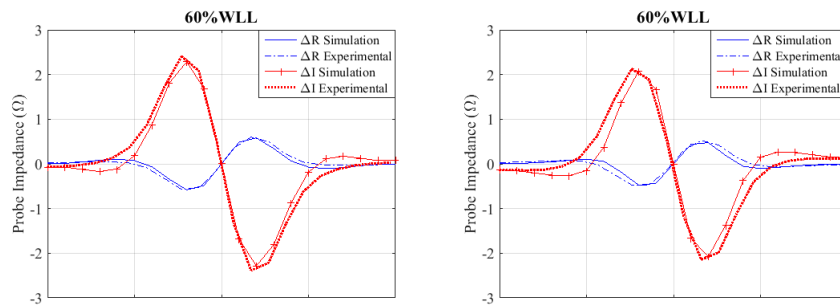


Figure 1: Comparison of experiment and simulation for the 60% wall loss for 1A (left) and 1.5A (right).

for two levels of magnetization current. The very good agreement between theoretical results and experimental measurements adds confidence on the use of the simulation software. This is then utilized for performing various parametric studies on the effect of the magnetization current on the acquired eddy current signals from various wall loss depths.

-
- [1] J.Y. Kim, J. Yi, S. Lee, Eddy current test of steel tubes employing electromagnet technique for dc magnetization, *Journal of Applied Physics* 60 (1986), 3327–3334.
[2] H. Fujiwara, T. Sakamoto, T. Takagi, Numerical simulation of eddy current testing in ferromagnetic tubes, *Non-Destructive Testing* (1992), 273-277.

Eddy Current Magnetic Signature (EC-MS): Experimental tests and Simulations

S. Zhang^a, A. Kita^a, B. Ducharne^b, T. Uchimoto^{c,d}

^a Graduate School of Engineering, Tohoku University, Japan

^b Laboratoire de Génie Electrique et Ferroélectricité, INSA Lyon, France

^c Institute of fluid science, IFS, Tohoku University, Japan

^d ELyTMaX UMI 3757, CNRS, Université de Lyon, Tohoku University, International Joint Unit, Tohoku University, Sendai, Japan.

Plastic deformations and residual stresses inevitably occur in metallic components due to industrial machining or heat treatment processes. These local changes of the microstructure affect the real-life performance of industrial parts. Measurements and analysis of residual stresses are necessary for quality assurance and maintenance anticipations.

The use of micro-magnetic techniques such as the Magnetic Barkhausen Noise (MBN) [1][2] or the Magnetic Incremental Permeability (MIP) [3][4] has increased exponentially in the industrial field. Recently, an even more sensitive method has been proposed by Matsumoto and al. [5]-[6]. This method named Eddy Current Magnetic Signature (EC-MS) relies on an incremental permeability experimental setup and consists of plotting the imaginary versus the real part of the sensor coil impedance or of the permeability during the magnetization process. The resulting trajectory in the impedance plan is studied. The size, length and direction of this trajectory are highly dependent on the distribution of the residual stress through the tested sample. EC-MS is a relatively new method and up to now the only published articles which focus on this method just comment and discuss experimental results obtained on carbon steel or chromium steel. The development of numerical tools for the simulation of the EC-MS have almost never been proposed [7]. However such simulation results could be particularly useful for the understanding and the interpretation of the EC-MS results.

In this study, EC-MS is tested on pure iron and iron silicon samples, experimental results are proposed such as a numerical method relying on the physical properties for the simulation of the ECMS technique. A link is established between the frequency dependent material hysteretic behavior and the dynamic contribution required for the EC-MS simulation.

[1] B. Ducharne & al., J. of Mag. And Mag. Mat., vol. 432, pp. 231-238, 2017.

[2] B. Ducharne & al., IEEE Trans. on Mag., vol. 99, pp. 1-6, 2018.

[3] B. Gupta & al., J. of Mag. and Mag. Mat., vol. 486, pp. 2019.

[4] B. Gupta & al., NDT & E Int., vol. 104, pp. 42-50, 2019.

[5] T. Matsumoto & al., J. of Mag. And Mag. Mat., vol. 479, pp. 212-221, 2019.

[6] T. Matsumoto & al., Proc of 14 Int. conf. on Flow Dyn., Sendai, Miyagi, Japan, 2017.

[7] T. Matsumoto & al., AIP Advance, vol. 9, iss. 3, 2019.

Optimized design of a "magnetic rope detector" according to UNI EN 12927-2019 standard

Francesco Comuzzi, Cesare Ciriani, Andrea Cernigoi, Boris Sosic

University of Trieste, Engineering Dept.

Magneto-inductive equipment is conveniently used for wire ropes non-destructive testing. This solution is used in various industrial sectors: public cableway transport, lifts, freight transport and so on. The MRT method represents a simple and reliable system to evaluate the maintenance in service of the rope itself.

The operating principle corresponds to the measurement and interpretation of dispersed electromagnetic fields emitted in correspondence with imperfections or defects of a magnetically saturated metallic element. The standard EN 12927 for cableway transport, in the recently updated version (June 2019), specifies the minimum requirements of a generic magneto-inductive device and defines the criteria for the performance test. These requirements are transferred to the magnetic project.

The purpose of the simulations is therefore to verify which parameters can be changed to reach an "optimal" realization of the instrument in terms of weight, dimensions, cost and / or intrinsic noise.

With this work we present the results obtained with three dimension-finite elements simulation compared with real models tested in "Domenico Di Santolo" Non-destructive Tests laboratory of the University of Trieste.

Advances in Magnetism 2020-21, June 13-16, 2021

Magnetic levitation and bearings, electrical machines and other electromagnetic devices

[Abstracts can be easily browsed through the bookmarks](#)

Multi-degree-of-freedom spherical actuator and magnetic gravity compensator – integrated solution for robotics applications

Elena Lomonova^a, Bob van Ninhuijs, Helm Jansen, Bart Gysen

^aTU Eindhoven, 5600MB Eindhoven, The Netherlands

In robotics applications such as arm-support systems, there is always a trade-off between the actuated degrees-of-freedom and the mobility of the robotic arm. When multiple joints are actuated, a separate actuator is usually used for every degree of freedom. In addition, arm-support systems need to compensate for a static load due to the weight of the human arm. Consequently, the multi-degrees-of-freedom joints result in large, cumbersome, and sometimes complex constructions that have a predefined sequence of rotation axes [1, 2].

To reduce the power consumption and provide free robotic arm movement [3], a new integrated design of a gravity compensator and an electromagnetic actuator with multi-degrees-of-freedom is proposed. An electromagnetic solution is considered which is capable of providing these requirements in a configuration such that the active and passive device does not influence each other's electromagnetic behavior.

To proceed with the electromagnetic design of a multi-degree-of-freedom actuation system with integrated gravity compensator for the application in a smart arm-support system the thorough electromechanical specifications are identified including the range of motion. Specifically, a three-degrees-of-freedom motor can be realized with one spherical actuator decreasing the mass and inertia. Additionally, the use of passive (magnetic) gravity compensation can significantly reduce the power consumption in an arm-support system too. Besides, the spherical gravity compensator should demonstrate a spring type behavior in one rotational direction while have a zero stiffness in the other rotational directions. To proceed with research of topologies and designs of passive spherical magnetic springs the fast semi-analytical magnetostatic field modeling techniques in the spherical coordinate system are developed.

These techniques allow for fast and comprehensive evaluations of multiple actuator and compensator topologies, in contrast to existing numerical techniques such as finite element analysis. Based on the extensive analysis of different configurations of spherical actuator design with integrated gravity compensator the optimal topology with a minimum power dissipation is defined based on the commutation algorithm that decouples the torques and currents. Three permanent magnet arrays with different pole pitches have been investigated. The unconventional hemispherical actuator design has been proposed and verified. An average torque requirement of 12 Nm has been found. By mapping the torque of the compensator for different inner and outer radii, an optimal torque density with respect to its volume has been reached.

- [1] A. Alutei, A. Vaida, D. Mandru, and M. Tatar, "Development of an active upper-limb orthosis", In Proceedings of the International Conference on Advancements of Medicine and Health Care through Technology, ser. IFMBE proceedings, vol. 26, pp. 405-408, 2009.
- [2] S. Ball, I. Brown, and S.Scott, "Medarm: a rehabilitation robotwith 5dof at the shoulder complex," In Proceedings of the IEEE/ASME International conference on Advanced intelligent mechatronics, Sept. 2007, pp.1-6.
- [3] J. Ditriche, "Innovations in dismantling robotics," Nuclear Engineering and Design, vol. 182, no. 3, pp. 267-276, 1998.

Free-form topology optimization for magnetic arrays of planar levitation systems

Karlo Radman^a, Wolfgang Gruber^b, Hubert Mitterhofer^a

^a Linz Center of Mechatronics GmbH, Linz Austria

^b Institute for electrical drives and power; Johannes Kepler University, Linz, Austria

Two dimensional arrays of permanent magnets are used in planar levitating systems to enable actuator movement in all six degrees of freedom. In combination with coil arrays, a wide range of solutions is possible to achieve system controllability. A simulation and optimization process were designed to evaluate variations of the magnetic arrays regarding performance and control.

As the levitating system consists only of permanent magnets and conductors without any ferromagnetic material, a 3D dipole analytical model was implemented to compute magnetostatic forces and torque acting on the actuator. In contrast to other analytic models, the dipole model does not restrict the shape of the magnets to cuboids. The solver calculates the interaction between the finite elements of the conductors and magnets, without the need to solve the magnetic fields in the whole problem space. Comparison with a commercial 3D FEM solver shows a calculation time reduction of two orders of magnitude and the results turn out to be less mesh size dependent than virtual displacement methods. This solver is coupled with a genetic optimisation algorithm to evaluate a high number of magnet array variations. The performance factors for topology comparisons are derived from the pseudoinverse control matrix which is based on the solver results.

The evaluation covers existing topologies (one is depicted in Fig. 1) and a new proposed geometry with a reduced number of magnets per poles. All topology optimizations start with a fully filled square magnetic array, and an array of underlying coils. The optimizer generates variations by removing some magnets, leading to a sparsely filled array.

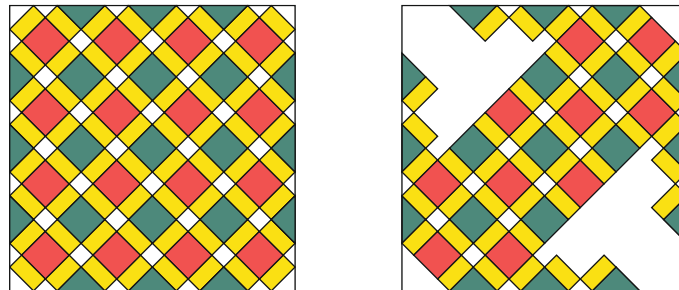


Figure 1: A 2D magnetic array, where the colors red and green represent the north and south poles while yellow represents magnets magnetized parallel to the array plane altogether forming a Halbach arrangement. Right: fully filled array. Left: a reduced array variation

In the case of elongated coils, which are longer than the magnetic array, reduction of some magnets is necessary to achieve rotational torque around the axis perpendicular to the magnet array. Reduction of magnets decreases the weight of the suspended actuator and improves the torque controllability, while deteriorating the overall force and torque generation. A compromise solution to fit all system requirements can be found in the pareto distributions of the optimization.

Contactless magnetic bearing based on second generation high temperature superconducting tape

Igor A. Rudnev, Maxim A. Osipov, Aleksander S. Starikovskii, Dmitriy A. Abin,
Sergey V. Pokrovskii, Irina V. Anishenko, Alexey I. Podlivaev

National Research Nuclear University MEPhI, (Moscow Engineering Physics Institute),
Moscow, Russia

The using a superconductor/permanent magnet in contactless bearings is promising not only because of the absence of friction forces in such bearings. The absence of direct mechanical contact between moving parts allows the effective use of magnetic bearings in high-speed technology: kinetic energy storages, gyroscopes and similar devices. The fabrication of a superconducting rotor (stator) from a bulk high-temperature superconductor (HTSC) is a rather complicated technological problem. Firstly, the bulk HTSC material is quite fragile. Secondly, a complex annealing regime is required to ensure uniformity of the superconducting properties of the material and manufacturing HTSC bulk of various shapes is too difficult. An alternative to a bulk superconductor can be a composite superconductor consisting stacks of second generation HTSC tapes. Analogous stacks of tapes can also be considered as short-circuited coils made from HTSC tapes. The use of HTSC tapes instead of bulk materials has several advantages. The technology for creating a superconducting composite of arbitrary shape made from tapes is simpler. Superconducting characteristics of a stack of tapes are not inferior to a bulk HTSC material. In addition, HTSC tapes have higher mechanical properties than bulk materials. Manufacturing a magnetic rotor also presents a technological problem. A permanent magnet of the desired shape and size should provide an axial symmetry magnetic field. An alternative to a solid magnet can be a set of magnets. The typesetting magnet means a mosaic consisting of a large number of small magnets. Each element of the mosaic is a uniformly magnetized magnet in form of parallelepiped. The disadvantage of this mosaic is heterogeneity of the magnetic field, especially at the junctions of neighboring elements. The inhomogeneity of the magnetic field can cause hysteretic remagnetization of superconductor. The remagnetization of superconductor is accompanied by the dissipation of energy and, therefore, the occurrence of a friction force in a bearing.

The aim of this work is to calculate and measure the energy losses and magnetic braking in a model magnetic levitation bearing with a rotor from a set of permanent magnets and a stator of single-layer and multi-layer rings formed from HTSC tapes of the 2nd generation. Theoretical calculations are used of the interaction of an inhomogeneous magnetic field created by permanent magnets on a rotor with electric currents induced in superconducting rotor rings. The characteristics of real HTSC tapes of the second generation are used in calculations. NdFeB magnets were considered as permanent magnets. The tangential component of the force of interaction of the rotor field with stator currents (friction force) for one stator ring was determined from Ampere's law.

The calculations showed that the force of magnetic friction and the resulting energy losses are not an obstacle to the creation of a combined bearing, the rotor of which consists of more than 8 magnets, and the stator - of several layers of HTSC tape. Experimental verification of the output, as well as analysis of the influence of other bearing parameters (eccentric position and misalignment of the rotor axis relative to the stator axis, defects in the HTSC stator tapes, etc.) that can critically degrade its characteristics will be carried out separately. It should be noted that the considered configuration of the magnetic rotor and the superconducting stator of HTS tapes has a fundamental advantage over the bearings on bulk HTSCs, since it allows for almost unlimited scaling of the device. Based on the calculations, a prototype magnetic levitation bearing was implemented.

Design Issues of a Rotating to Linear Motion Magnetic Converter for Short Distance Transport Applications

Mauro Andriollo, Simone Bernasconi, Andrea Tortella

Department of Industrial Engineering, University of Padova, Padova, Italy

New concepts of propulsion systems based on electromagnetic transmission can make transport infrastructures on heterogeneous routes with steep slopes in downtown areas or in hilly areas more environmentally friendly. The paper investigates a novel arrangement for the rotating to linear motion conversion (RLMC) using a magnetic gear (MG). The MG technology enables a variety of topologies with very good torque density [1]. The on-board proposed propulsion module (Fig.1a) consists of rotating PM cylinders (RPMCs) creating a translating p_c -pole pairs magnetic field facing a p_L -pole pairs array of planar PMs (PPMs); a purely passive ferromagnetic rack (MR) made by steel pieces is placed on the track side. A conventional high-speed motor drives the RPMCs at the speed Ω_c to enable a high force low speed transmission, leading to a quieter, more efficient and more reliable operation than conventional rack-pinion devices, with remarkably slighter requirements for the transmission interface coupling at the same time.

While the operating principle and the main design issues are described in [2] for a general feasibility study, more detailed analyses for a practical application are presented here. Fixed the speed v_s and p_c , Ω_c values, the influence of p_L is analysed, taking into account the following relations apply (n_s : per-module rack piece number, G_R : gear ratio, τ_c : RPMC pitch):

$$n_s = p_c + p_L, \quad G_R = v_s/v_c = p_c/n_s, \quad \tau_c = \pi v_s n_s / \Omega_c. \quad (1)$$

The thrust and torque performances, defined by a set of design indices will be evaluated by parametric 2D magnetostatic FE analyses, as well as the MR losses, estimated by elaborating the time-varying distribution of the flux density and of the magnetic potential vector on a suitable set of samples. The study will address the choice of the steel piece shape and material and the proper arrangement of the RPMC magnetization pattern.

As an example, Fig.1b shows the p.u. length thrust and the resultant RPMC torque with $\{n_s, p_L, p_c\} = \{6, 5, 1\}$. The spatial and angular positions x_s and θ_c are synchronized to obtain the maximum thrust. The dataset (A) is related to $n_A=5$ propulsion modules as in Fig.1a; in (B) configuration the torque ripple is compensated by adopting $n_B=10$ single RPMC spaced by $\Delta L_S = 50$ mm, the required propulsion performance being maintained (0.25 m/s² acceleration for a 1400 kg vehicle on a 20% slope, assuming an active length $l_m = 0.15$ m).

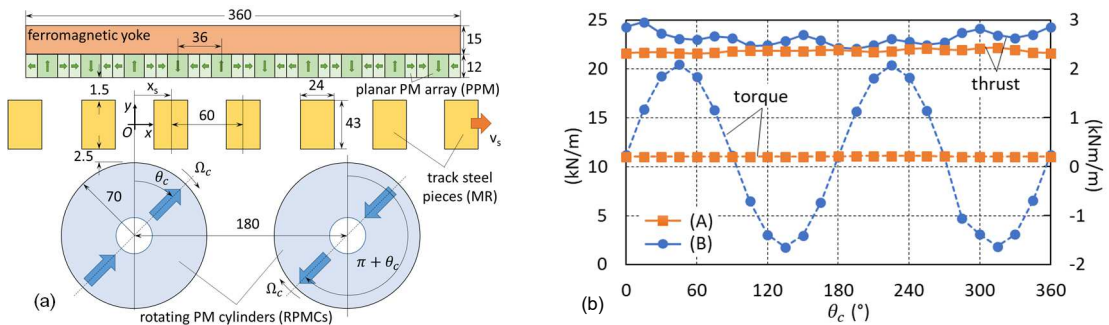


Figure 1: (a) RLMC module (sizes in mm); (b): Thrust and RPMC torque.

- [1] Y. Chen, W. N. Fu, S. L. Ho, and H. Liu, "A Quantitative Comparison Analysis of Radial-Flux, Transverse-Flux, and Axial-Flux Magnetic Gears," IEEE Trans. on Magnetics, vol. 50, no. 11, Nov. 2014.
- [2] M. Andriollo, F. Saracino, and A. Tortella, "Rotating to Linear Motion Magnetic Converter for Low Capacity Transport Applications", XXII Intl. Conf. on Electrical Machines (ICEM 2016), Lausanne, Sept. 4-7, 2016.

Semi-bearingless magnetic geared motor

Wolfgang Gruber^a, Edmund Marth^a, Gerald Jungmayr^b

^a Johannes Kepler University Linz, Linz, Austria

^b Linz Center of Mechatronics GmbH, Linz, Austria

High-speed drives offer the possibility to increase the power density significantly. Limitations of this concept lie in the applications with high rotational shaft speed and the increased bearing losses. A magnetic geared motor (representing a combination of a high-speed motor and a speed-reducing magnetic gear) [1] overcomes the first issue as the output speed gets into a more convenient range. However, the increased losses of the mechanical high-speed rotor bearing remain.

In this paper, we propose a magnetic geared motor with magnetically levitated high-speed rotor shaft to overcome the second drawback too. Figure 1 shows such a system, consisting of the inner high-speed permanent magnet excited rotor, a modulator featuring lower speed (representing the output shaft with high torque) and a permanent magnet excited and coil equipped stator. In common magnetic geared motors - sometimes also called pseudo direct drives (PDDs) [2] - the outer stator coils only provide driving torque for the inner high-speed rotor. In our system, these coils also provide suspension forces to enable bearingless motor operation. As the high-speed rotor is disk-shaped, the axial and tilting deflections are stabilized passively due to reluctance forces and need no further bearings. However, the low-speed modulator remains mechanically supported, hence, we call the system semi-bearingless.

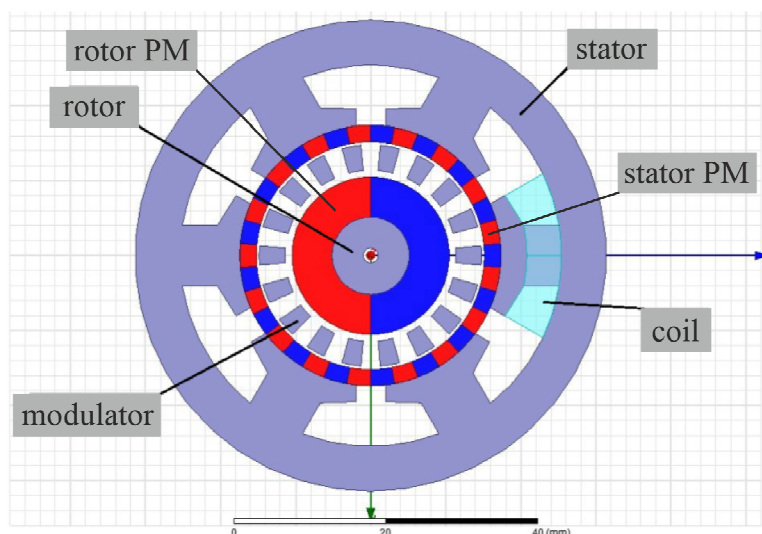


Figure 1: FEM simulation model of the proposed semi-bearingless magnetic geared motor.

The final paper will explain the concept in more detail. The results of a finite element method (FEM) based multi-objective optimization process are presented in form of Pareto fronts and discussed to find the best solution for prototype manufacture. Optimization goals are the reduction of cogging torque, the reduction of losses (especially the modulator teeth turned out to be critical) as well as the optimization of suspension forces and drive torque.

-
- [1] G. Jungmayr, E. Marth and G. Segon, "Magnetic-Geared Motor in Side-by-Side Arrangement - Concept and Design," *2019 IEEE International Electric Machines & Drives Conference (IEMDC)*, San Diego, CA, USA, 2019, pp. 847-853.
 - [2] K. Atallah, J. Rens, S. Mezani and D. Howe, "A Novel "Pseudo" Direct-Drive Brushless Permanent Magnet Machine," in *IEEE Transactions on Magnetics*, vol. 44, no. 11, pp. 4349-4352, Nov. 2008.

Active levitation in multiple degrees of freedom using null-flux coils

Hector Gutierrez^a, Hanri Luijten^b

^a Department of Mechanical and Aerospace Engineering, Florida Institute of Technology,
Melbourne, FL, USA.

^b Heidenhain Numeric BV, Eindhoven, The Netherlands

This paper presents the 5-DOF control of a Maglev suspension based on the active control of null-flux coils. A sled with built-in permanent magnets moves past an array of fixed null-flux coils to generate Lorentz forces that provide lift and guidance. When active control of the levitation coil currents is implemented, multi-DOF trajectory control can be achieved, leading to stable levitation that can actively reject disturbances independently of sled speed. This paper shows successful control of the multi-DOF trajectory of a passive sled by active control of the coil currents in a null-flux system, based on a sliding mode controller with nonlinear input mapping from coil currents to levitation forces, and a multi-DOF nonlinear observer. The use of look up tables vs. analytical models of the magnetic field density used to estimate the magnetic forces and torques acting on the sled is also discussed. The performance of the proposed approach was demonstrated experimentally.

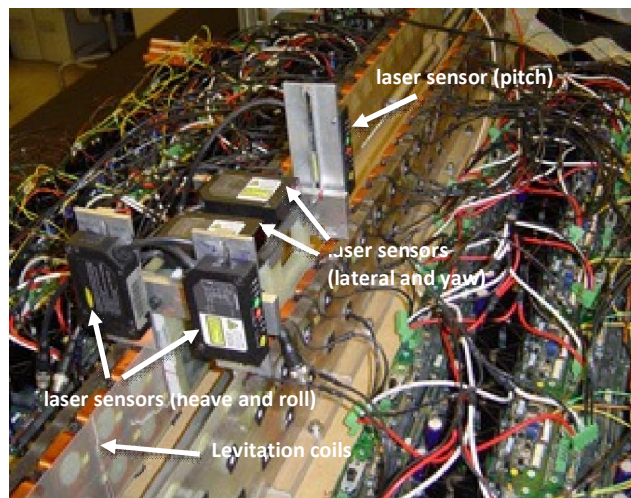


Figure 1. Experimental Setup – 5-DOF active levitation using null-flux coils. The five degrees of freedom are measured with laser gap sensors.

A magnetic lattice-based representation of power systems dedicated to transient stability analysis

Vincent Mazauric^a, Nadia Maïzi^b

^aSchneider Digital, 38TEC Building, 38050, Grenoble Cedex 9, France

^bMINES ParisTech, CMA, CS 10207, 06904, Sophia Antipolis, France

Free current density occurring within a power grid exhibits well-split scales allowing mean-field procedures, *i.e.* the global trend toward reversibility expressed on the second principle of thermodynamics [1] is replaced by embedded minimizations on the relevant scales involved by the power transmission. Various scales were already successfully explored from deep within the material to the device scale.

At the power management level, the Gibbs free-energy and the kinetic energy embedded in the whole system appear as the two constants of motion on which space aggregation and time reconciliation of all the scales involved in the power system may be respectively analysed. An X-Y lattice model is adopted to describe the interaction between the magnetic momentum carried by the rotor of a given generator and the mean-field resulting from all the others.

The question of ordering stability of two-dimensional systems was extensively studied in the context of phase transitions and critical phenomena. Whereas no long-range order exists in two-dimensional lattices with short range interaction between Heisenberg magnets, Onsager provided an exact resolution of the Ising model with first neighbor interactions. Hence, the X-Y model appears as a marginal case where the long-range ordering may vanish through a weak singularity under an external perturbation [2]. In the context of power system, the synchronism between rotors may therefore be jeopardized by long-range modes and it is convenient to study this problem within a second order Kuramoto's model [3] where the electrodynamic torque acting on the machines is derived from the magnetic Gibbs free-energy embedded in the power grid. A condition for keeping a stable solution – *i.e.* backing locally and exponentially to a synchronous steady-state after any small disturbance – expresses that the algebraic connectivity of the graph of admittances underlying the power flow of the grid is higher than the maximal rate of congestion expected on the grid [4].

In other words, the stability of the power grid is kept thanks to a strong enough correlated lattice – or actually a suitable voltage plan on the grid showing the critical role of the reactive power to maintain the synchronism – which provides large enough resistant electrodynamic torques to the generators therefore able to face to any admissible fluctuation. Then, the kinetic energy embedded in the whole power system may be aggregated to act as a global and huge inertia to prevent abrupt frequency deviations which therefore may only occur on several periods under a linear regime, typically around 50 or 60Hz.

Operation issues were endogenized in the technical optimal TIMES model to design a 40 to 100% renewable power system for France.

-
- [1] V. Mazauric, "From thermostatics to Maxwell's equations: A variational approach of electromagnetism," IEEE Transactions on Magnetics, vol. 40, pp. 945-948, 2004.
 - [2] J. M. Kosterlitz, "The critical properties of the two-dimensional xy model," Journal of Physics C: Solid State Physics, vol. 7, pp. 1046-1060, 1974.
 - [3] Y. Kuramoto, "Self-entrainment of a population of coupled non-linear oscillators," in International Symposium on Mathematical Problems in Theoretical Physics, ser. Lecture Notes in Physics, H. Araki, Ed. Springer Berlin Heidelberg, 1975, vol. 39, pp. 420-422.
 - [4] F. Dörfler, "Dynamics and control in power grids and complex oscillator networks," Ph.D. dissertation, Mechanical Engineering Department, University of California at Santa Barbara, Sept. 2013.

Stability investigation of UAQ4 high temperature superconducting MagLev system suspension

Giovanni Lanzara^a, Gino D'Ovidio^a

^a L'Aquila University, L'Aquila, Italy

The UAQ4 is an under development superconducting magnetically levitating train project whose suspension and propulsion devices feasibility has been successfully laboratory tested at the University of L'Aquila (Italy).

The UAQ4 Italian maglev train project is focused on the study and development of a transportation system with zero motion resistance (except aerodynamic drag) and greatly reduced energy consumption, approaching zero at a low constant speed.

An innovative architecture and suspension / propulsion devices have been realized [1,2]. The magnetic suspension, superconducting magnetic levitation (SML) technology based, uses the interaction between high temperature superconductors (HTS) set into proper "skates" of the vehicle and permanent magnets distributed on the track.

The levitation force due to the interaction between new sintered magnetic materials, such as Nd₂Fe₁₄B (NdFeB) permanent magnets (PMs) and YBa₂Cu₃O_x (YBCO) bulk high temperature superconductors make this system extremely useful in frictionless bearing transportation because of the inherent self-stability deriving from flux pinning phenomenon.

This paper deals with the dynamics stability of the UAQ4 experimental superconducting magnetically levitated vehicle that floats in a stable condition above the track in all phases of motion, zero speed included.

A scaled UAQ4 system demonstrator was built and laboratory tested. It is composed of a bogie floating and running above a track section (Fig.1).



Figure 1: Experimental UAQ4 MagLev system.

The track section (3,72m long and 0,81m wide) is constituted by three parallel permanent magnet guideways each of which consist of iron beam with NdFeB permanent magnets arranged in the inner beams surfaces according to a proper polarity configuration. The two lateral "V" shaped guides are used for levitation and guidance while the central one "U" shaped is used as the propulsion engine primary.

The dynamic behavior of the suspended vehicle is analyzed at standstill by two degrees of freedom model refined by experimental data.

-
- [1] G. Lanzara, G. D'Ovidio G., F. Crisi, (2014) "UAQ4 Levitating Train: Italian Maglev Transportation System" IEEE Vehicular Technology Magazine Vol. 9, N. 4, pp.71 -77,
[2] G. D'Ovidio, F. Crisi, G. Lanzara (2011), "Design and optimization of UAQ4 experimental maglev module", Material Science Forum in Applied Electromagnetic Engineering 1058, pp. 42-47

Design and analysis of 6/4, 8/6 and 10/8 switched reluctance motors using Ansys/Maxwell and MATLAB/ Simulink

Bekir Gecer^a, N.Fusun Oyman Serteller^b

^a Electric-Electronic Engineering, Institute of Science, Marmara University, Istanbul, Turkey

^b Electric-Electronic Engineering, Faculty of Technology, Marmara University, Istanbul, Turkey

Industrial applications of Switched reluctance motors (SRM) have gained attentions from researchers everywhere related in this area, due to their simple structure, high efficiency, high torque production, lower cost and robustness. In the present study, the 6/8, 8/6, 10/8 (stator pole/rotor pole) SRMs have been designed and analysed by the Ansys/Maxwell 2D and controlled by the MATLAB Simulink program. The SRM has a variable air gap and reluctance with respect to the rotor position [1]. The motor has a stator with a coil and a rotor without a coil, which is seen geometrical structure in Figure 1(a) on 8/6. Although 6/4, 8/6 and 10/8 models are identical (except the pole numbers) and have the same power converter systems; they exhibit different magnetic characteristics due to their different magnetic structures. The change in the values of motor speed, induced torque, current, magnetic induction ($B-T(wb/m^2)$) and flux ($\phi(Wb)$) are examined, (fig. 1(b) and (c)). The magnetic equation of SRM was solved by using the equation 1.

$$-\frac{1}{\mu} \nabla^2 A = J \quad (1)$$

Where, A is the vector potential in wb/m , μ (H/m) is the magnetic permeability and J is the current density in A/m^2 . The Figure 2 illustrates the MATLAB/Simulink model and magnetic flux behaviour of 8/6 SRM.

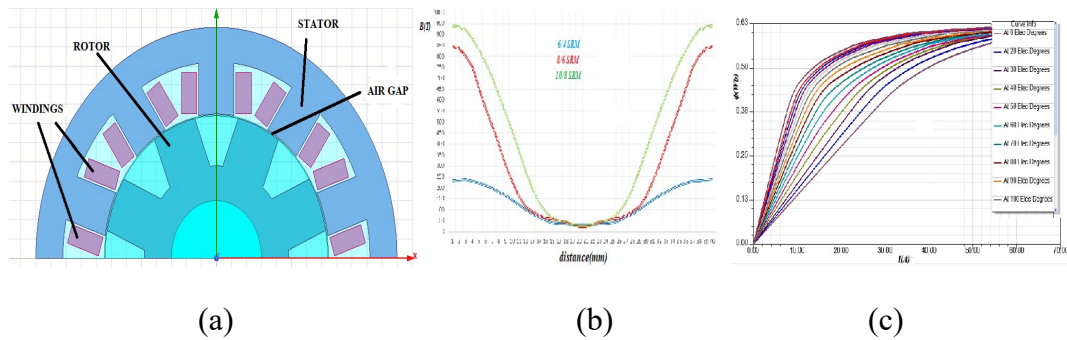


Figure 1: (a) Ansys/Maxwell 2D SRM structure (b) Analysis result of B versus to distance (c) ϕ versus I (Amper)

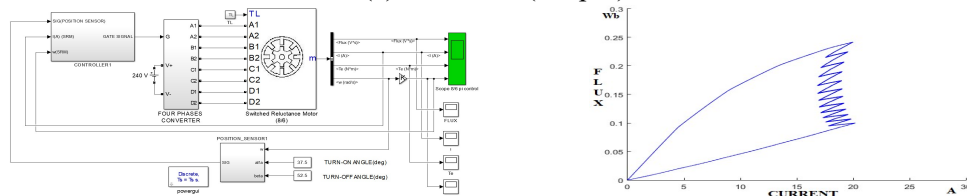


Figure 2:(a) The SRM Matlab Simulink model (b) ϕ versus I in Matlab.

[1] T.J.E. Miller, Switched reluctance motors and their control,(1993),Oxford, Magna.

Overview of the actuator of roll stabilization and steady posture

Qiang Liu, Qirui Wang, Zhuang Li, Heng Li, Kang Xu

Institute of Precision Electromagnetic Equipment and Advanced Measurement Technology,
Beijing Institute of Petrochemical Technology, Beijing, China

In the course of bumping in moving, the attitude of warships, tanks, etc. is often instable. The precision of loads, such as radar and sight, is reduced resulting in poor communication and inaccurate attack in motion. The key point for high-precision and high-stability of the equipment is reducing the load attitude wobble and stabilizing the load attitude. The way to achieve the roll stabilization and steady posture is roughly divided into two types. The first is reducing the attitude sway of the carrier such as the ship and the second is installation of platform on motion carrier. In this paper, two types of roll stabilization and steady posture actuators are introduced and analyzed.

The ship's anti-rolling is mostly by the roll stabilization of carriers. The actuator of anti-rolling and steady posture widely used in the world is the anti-rolling tank, the bilge keel, the fin stabilizer and the gyro [1]. These actuators with low bandwidth stabilize ship attitude by changing the hull structure to output moments. For the onboard measurement equipment, the tracking stability and measurement accuracy is limited by the shortcoming of the above-described actuators. Therefore, the actuator by installing the platform on motion carrier is widely required.

The platforms are rotary table and platform [2] of roll stabilization and steady posture, which uses inertial measurement unit to detect the posture information of moving object in real time, and stabilize the load by automatically moving in the opposite direction of interference through the actuator. Rotary table are mostly used in shipborne, airborne, missile-borne, such as gyro stabilized platform and three-axis platform.

In view of existing platform of roll stabilization and steady posture is applied with low bandwidth and precision, a Lorentz platform of roll stabilization and steady posture is proposed shown in Fig.1 in this paper. The high-precision control torque is produced by the linear Lorentz magnetic force to achieve the high frequency linear control and realized the goal of stabilize the platform posture with high precision. The high-precision torque is expressed as:

$$T = NBILD . \quad (1)$$

With large deflection angle, high attitude stabilization precision, large bandwidth and small volume, the Lorentz platform has broad application in the field of weaponry and civil applications.

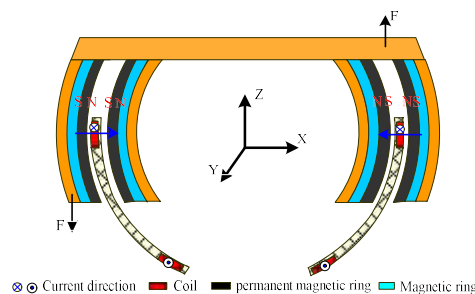


Figure 1: Principle of the Lorentz platform of roll stabilization and steady posture

[1] R. Moaleji, A. R. Greig. Ocean Eng. **34**(1) (2007), 103-121.

[2] F. Dong, X. Lei, W. Chou. IEEE T. Ind. Electron. **99** (2016), 1-1.

Transport system with «hooks & curtain» kind suspension

Evgeny Yu. Sundukov^a, Nadezhda A. Tarabukina^a, Veronika E. Sundukova^b

^a Institute for Socio-economic and energy problems of the North
of Komi Science Centre of Ural Division of the Russian Academy of Sciences,

^b Syktyvkar forest institute
(Syktyvkar, Russia)

Earlier we considered the possibilities of bilateral levitation to move transport modules relative to arch-type trestle [1]. Levitation relative to the internal working surface (under an arch) can be comparable to suspension of the «hooks & curtain».

Heavy curtains are suspended on many hooks by means of the eaves. At that loss by one hook (several hooks) of its function is not critical for system operability. Similarly, transport modules can be suspended relative to a guideway placed on the arch trestle.

We can add a picture (see fig. 1) that shows magnetolevitation system based on arch-type trestle with lower cockpit location.

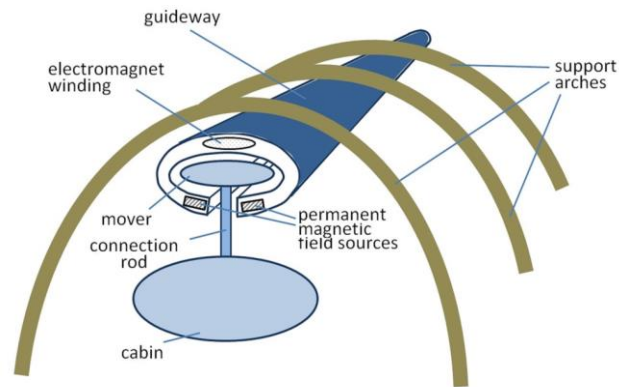


Figure 1: Magnetolevitation system based on arch-type trestle with lower cockpit location.

The transport module comprises the mover, the cabin and the connecting rod. The mover is a device comprising a magnetic constant field source (superconductor) for interacting with the magnetic field sources of the guideway. The levitating transport module receives acceleration at interaction of mover with the electromagnet winding powered by current. The cabin can be connected to several movers by means of connecting rods similarly as curtains to hooks.

The next step in the development of such transport systems may be the contactless connection of the mover and the cabin, which is provided by the use of the «magnetic potential hole» effect [2].

[1] Sundukov EYu, Tarabukina NA. The use of the bilateral levitation of transport modules relatively arch trestle. *Transportation Systems and Technology*. 2019;5(2):83-91. doi:10.17816/transsyst20195283-91.

[2] Kozoriz VV. *Dynamic systems of the magnetic interacting free bodies*. Kiev: Sciences thought, 1981. (In Russ).



Advances in Magnetics 2020-21, June 13-16, 2021

BOOK of ABSTRACTS

Poster Sessions

Abstracts can be easily browsed through the bookmarks

Advances in Magnetics 2020-21, June 13-16, 2021

Biomagnetism and biomedical applications

Abstracts can be easily browsed through the bookmarks

Design of a TEM applicator for *in vitro* testing of RF hyperthermia

Riccardo Ferrero^a, Ioannis Androulakis^b, Alessandra Manzin^a, Gerard Van Rhoon^b

^a Istituto Nazionale di Ricerca Metrologica (INRIM), Torino, Italy

^b Department of Radiotherapy, Erasmus MC Cancer Institute, Rotterdam, Netherlands

The efficacy of hyperthermia in increasing the potency of radiotherapy and chemotherapy for the treatment of tumours has been demonstrated in clinical applications [1]. Moreover, its general lack of side effects pushes forward the development of novel treatments in combination with standard therapies [2]. Radiofrequency (RF) electromagnetic fields are widely investigated as a mean to induce therapeutic hyperthermia [3]. The need for reliable and reproducible studies on this technique requires affordable, easy to setup and robust RF applicators for laboratory testing on cell cultures and small animal models [4]. The applicators should provide uniform heating in the target region, minimizing the sample misplacement, to guarantee control and reproducibility of the results.

In this work, we present the design and validation process of an RF hyperthermia applicator for *in vitro* experiments on cancer cell cultures or deep seated tumours in small animals. The applicator, based on a coaxial TEM design [5], consisting of an open-ended coaxial line with a hollow inner conductor, operates at 434 MHz. The strength of this particular design is that, independently of the shape or material properties of the sample, the peak of the power deposition is always focused towards the same point, on the central cylinder axis, simplifying the heating experiment. The chosen frequency guarantees both the required focus and the uniform heating of the sample.

The design of the applicator was optimised by means of high-frequency electromagnetic and thermal simulations, with the aim of depositing a sufficient power to heat the sample to 45°C in 1 cm³ region. Figure 1 show one of the modelling stages performed to optimize the power deposition pattern and to obtain the desired temperature increment. The position of the reflector is changed to improve the focus of the power deposition in the target region. The cavity is filled with a material having muscle properties.

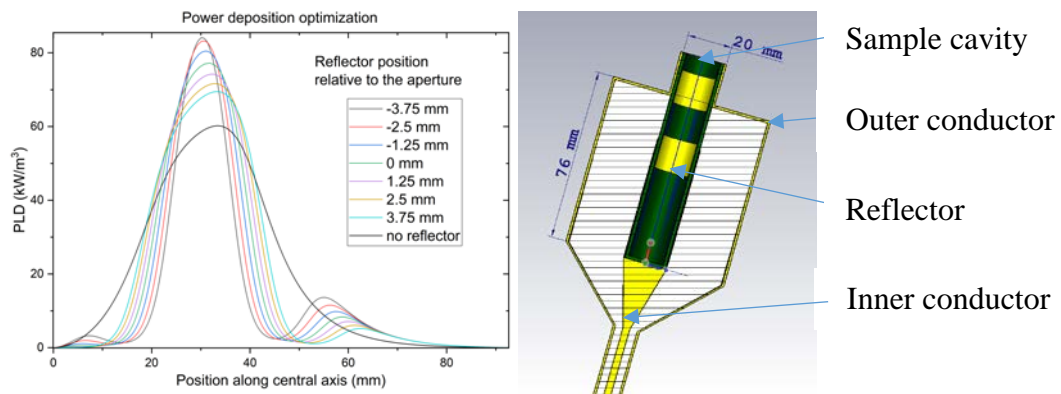


Figure 1: Left: Plot of the power loss density (PLD) along the central axis of the TEM applicator, from top to the bottom, for different positions of the copper reflector (cavity filled with muscle electrical properties). Right: Schematics of the TEM coaxial applicator.

-
- [1] J. van der Zee, *Annals of Oncology* **13** (2002), 1173–1184.
 - [2] M. Dunne, M. Regenold, C. Allen, *Adv. Drug Deliv. Rev.* **163–164** (2020), 98-124.
 - [3] M.M. Paulides et al., *Adv. Drug Deliv. Rev.* **163–164** (2020), 3-18.
 - [4] E. A. L. Raaijmakers et al., *Int. J. Hyperth* **34:6** (2018) 697-703.
 - [5] A. A. C. De Leeuw et al., *Int. J. Hyperth*, **6:2** (1990), 445-451.

Registration of Biological Molecules Using Magnetic Field Sensors

Levan P. Ichkitidze^{a,b}, Mikhail V. Belodedov^c, Aleksandr Yu. Gerasimenko^{a,b},
Dmitry V. Telyshev^{a,b}, Sergey V. Selishchev^a, Yanina V. Rezvantseva^b

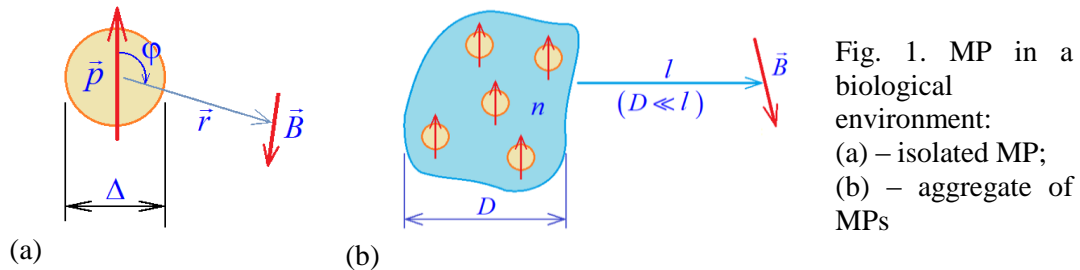
^a National Research University of Electronic Technology, MIET, Zelenograd, Moscow, Russian Federation

^b I.M. Sechenov First Moscow State Medical University, Moscow, Russian Federation

^c National Research University of Technology (BMSTU), Moscow, Russian Federation

Undoubtedly, DNA extraction is an important platform in various fields of research, such as biotechnology, diagnostics and therapy, forensic medicine, determination of paternity, etc. One of the modern techniques is based on the use of spherical magnetic particles (MPs) coated with active substances for the extraction of DNA and RNA. In our work, we investigate the methods of using magnetic particles in a biological environment and the possibility of their registration with modern magnetic field sensors (MFS).

Figure 1 shows the interaction of an external magnetic field B with a spherical MP in a biological environment, as well as with a set of such MPs, that is, with an aggregate of magnetic particles. It also lists the main parameters of the MP and the aggregate created from many MPs.



The maximum possible distance l that ensures reliable detection of the unit:

$$l \approx 0.01 \cdot D \cdot \Delta \cdot \sqrt[3]{\frac{J^* \rho n}{\delta B}}, \quad (1)$$

where δB is the threshold magnetic sensitivity of the MFS, J^* is the magnetic moment per mass of the magnetic material, and ρ is the density of the magnetic material. It has been established that magnetite particles (Fe_3O_4) with a specific magnetization of $J^* \sim 50 \text{ A}\cdot\text{m}^2/\text{kg}$ with a size of $\Delta \sim 50 \text{ nm}$ and a concentration of $n \sim 10^{18} \text{ m}^{-3}$ can be detected by a commercial superconducting magnetometer (SQUID MSgreen) at distances of $l \leq 0.1 \text{ m}$ [1]. This estimate follows from (1), where the following are taken into account: $\delta B \sim 10^{-14} \text{ T}$, $n \sim 10^{18} \text{ m}^{-3}$, $\rho \sim 5 \cdot 10^3 \text{ kg/m}^3$. Note that the existing research combined MFS (CMFS) [2], and CMFS with nanosizes elements [3,4] can have better magnetically sensitive parameters than commercial SQUID magnetometers [1].

Thus, single molecules of DNA, RNA, etc., (or their combination) attached to MPs in small ($\sim 10 \mu\text{m}$) aggregates can be non-invasively recorded by modern magnetometers and further isolated. Let us emphasize the fact that carbon nanotubes (CNTs), which are present at their ends, of catalytic ferromagnetic particles or encapsulated inside nanotubes, can serve as magnetic particles. In this case, after binding surface active substances to CNTs, they can also be used to fix and isolate DNA, RNA, and other biological molecules, along with MPs.

This work is supported by the Ministry of Science and Higher Education of the Russian Federation (project No. 075-03-2020-216 of December 27, 2019).

[1] <http://www.supracon.com/en/msgreen.html>

[2] M. Pannetier, C. Fermon, G. Le Goff, et al., *Science*. **304** (2004), 1648-1650.

[3] L.P. Ichkitidze, A.N. Mironyuk, *Physica C*. **472**(1) (2012), 57-59.

[4] L.P. Ichkitidze, *AIP Advances*. **3**(6) (2013), 062125 (8p).

FePd nanoparticles by solid-state dewetting for magnetic hyperthermia

Federica Celegato^a, Gabriele Barrera^a, Marco Coisson^a, Matteo Cialone^a, Riccardo Ferrero^a, Alessandra Manzin^a, Paola Rizzi^b, Franca Albertini^c, Paola Tiberto^a

^a INRIM, Istituto Nazionale di Ricerca Metrologica (INRIM), Torino, Italy

^b Department of Chemistry, Università di Torino, Italy

^c IMEM-CNR, Parma, Italy

Magnetic particles of controlled size have raised a broad technological interest in different areas such as catalysis, photonics, biomagnetism and, in general, for fabricating multifunctional magnetic systems. Solid-state dewetting is a promising thermally activated bottom-up method to pattern magnetic thin films into nanoparticles on a large scale. In dewetting method, the spontaneous agglomeration of a metallic thin solid film on a substrate into an assembly of particles is a controllable process by means of different factors (i.e. annealing parameters, substrate and film composition and thickness). Here, magnetic FePd particles from a continuous film are obtained. The starting Fe₇₀Pd₃₀ thin films are deposited on selected substrates (SiO₂ and Si/MgO) by rf-sputtering (film thickness about ranging from 7 to 100 nm). To promote dewetting, the as-deposited thin films are subsequently submitted to a furnace annealing in vacuum atmosphere at selected temperatures (ranging from 700 °C to 875 °C) and for different time (up to 100 minutes). The dewetting process of annealed films has been followed by scanning electron microscopy (SEM) images to investigate the progressive steps of dewetting. By finely tuning the annealing parameters and depending on film thickness, FePd nanoparticles with diameter varying in a wide interval (30 – 300 nm) have been obtained. After the dewetting process, the nanoparticles have been detached from the substrate by a sonication process and dispersed in deionized water. Isothermal magnetic hysteresis loops have been measured in the two different configurations (nanoparticles attached to the substrate and after their removal by sonication) by means of highly-sensitive magnetometry (AGFM and VSM).

A major issue preventing clinical applications of hyperthermia mediated by magnetic nanoparticles is determined by obtaining reproducible measurements of the amount of heat that is released by the nanoparticles submitted to an alternating electromagnetic field (Specific absorption rate, SAR). Here, SAR has been accurately evaluated by optical thermometric measurements both in adiabatic and isothermal conditions, under a r.f. (up to 400 kHz) magnetic field. 3D micromagnetic modelling of magnetization reversal process and hysteresis behavior is also performed to provide an interpretation of the experimental results

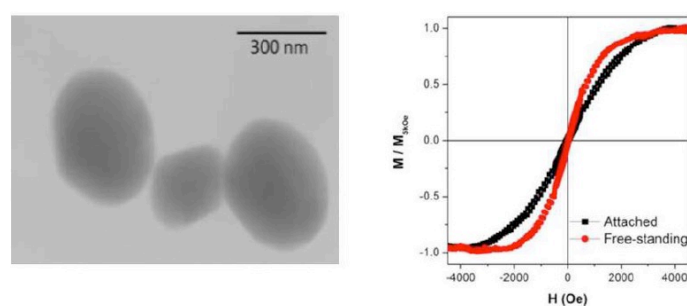


Figure1: Left: STEM images of free-standing FePd nanoparticles. Right: Normalized room-temperature hysteresis loops of FePd islands on the substrate (black curve) and after detaching and dispersion in acetone (red curve).

Numerical dosimetry of low-frequency electromagnetic fields by using reduced models of the source of the field

François Tavernier^a, Noël Burais^a, Riccardo Scorretti^a

^a Univ Lyon, Université Claude Bernard Lyon 1, INSA Lyon, EC Lyon, CNRS, Ampère, 69100, Villeurbanne, France

In order to evaluate the exposure of general population to low-frequency electromagnetic field, the source of the magnetic field has to be characterized experimentally, or basing on available information. When the source magnetic field exceeds some thresholds defined by national or international laws [1] and no field-reduction strategy can be applied, numerical dosimetry is generally required. Unfortunately in this case the measurement procedure required to characterize the exposure is generally time-consuming.

In this work we propose to develop a reduced model of the source magnetic field based on Proper Orthogonal Decomposition (POD). The idea is to compute a set of basis functions $\{\mathbf{f}_n(\mathbf{x})\}$ to represent the source magnetic field \mathbf{h} and, equivalently, the magnetic vector potential \mathbf{a} :

$$\mathbf{a}(\mathbf{x}) = \sum_{n=1}^N a_n \mathbf{f}_n(\mathbf{x}) \quad ; \quad \mathbf{h}(\mathbf{x}) = \sum_{n=1}^N \frac{a_n}{\mu_0} \text{curl} \mathbf{f}_n(\mathbf{x}) \quad (1)$$

The coefficients of the expansion (1) could be fitted with a lower number of measurements with respect of a completed 3D cartography of the magnetic field of the space of interest (occupied by the human body). Then the electric field induced in the human body, and all other relevant dosimetric indicators, can be computed by Finite Element [2] or other numerical methods by solving:

$$\text{div}[\sigma(j\omega\mathbf{a} + \text{grad}v)] = 0 \quad (2)$$

In the full article the application of this method to a wireless charging system will be presented.

[1] European Directive 2013/35/UE.

[2] R. Scorretti *et al.*, (2005). IEEE Trans. Mag. **41**(5), 1992-1995.

Quantitative 2D magnetorelaxometry imaging of magnetic nanoparticles using optically pumped magnetometers

Aaron Jaufenthaler^a, Peter Schier^a, Thomas Middelmann^b, Maik Liebl^b,
Dietmar Eberbeck^b, Daniel Baumgarten^a

^a Institute of Electrical and Biomedical Engineering, UMIT – Private University for Health Sciences, Medical Informatics and Technology, Hall in Tirol, Austria

^b Physikalisch-Technische Bundesanstalt, Berlin, Germany

Magnetic nanoparticles (MNPs) offer a large variety of promising biomedical applications thanks to their exciting physical properties, e.g. magnetic hyperthermia and magnetic drug targeting. For most applications, it is crucial to spatially quantify the amount of MNPs. In magnetorelaxometry (MRX), the magnetic moments of the MNPs are aligned by an external magnetic field, forming a net magnetic moment. After switching-off the field, the relaxation of this net moment is commonly detected by superconducting quantum interference devices (SQUIDs). The amplitude of this relaxation signal is directly proportional to the MNP quantity and thus, MRX with multiple sensors and/or varying excitation fields allows for quantitative reconstruction of the spatial MNP distribution [1]. Since the latest developments in OPM technology allow sensitivities comparable to those of SQUIDs, OPMs may be used in MRX [2], offering flexible positioning, reduced sensor-target-distances and the omission of cryogenic cooling.

We present quantitative 2D-imaging of MNP distributions with MRX and OPMs. Our setup consists of six printed circuit board excitation coils and six QuSpin zero field OPMs positioned on four sides of a 3D-printed 12 cm by 8 cm phantom holder (see fig. 1), allowing for a tomography-styled (and thus slice selective) MNP scanner. The whole setup is placed inside a magnetically shielded room (BMSR-2, PTB Berlin). The phantoms contain MNPs (BerlinHeart GmbH, Berlin, Germany), immobilized in gypsum cubes with an iron concentration of about 5 mg/cm³, which is of clinical relevance [3]. During the measurements, single activation coils are consecutively switched on. The field pulses have a duration of one second and a maximum magnetic flux density of 1 mT, during which the OPMs saturate. After switching off the field, the relaxation of the MNPs is measured by all OPMs after a dead time of 15 ms. By fitting a relaxation model to the measurement data and solving the inverse problem of the physical MRX forward model, accurate quantitative reconstructions of the phantoms have been achieved.

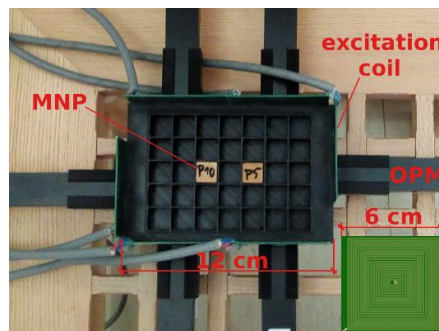


Figure 1: Setup for 2D OPM MRX imaging. Bottom right inlet: excitation coil geometry.

-
- [1] M. Liebl, *Phys. Med. Biol.* **59** (2014), 6607-6620.
 - [2] V. Dolgovskiy, *J. Magn. Magn. Mater.* **379** (2015), 137-150.
 - [3] F. Wiekhorst, *Magn. Particle Imag.* **140** (2012), 301-305.

Hazards related to switching gradient field heating for patients carrying orthopaedic implants during MRI sessions

Alessandro Arduino^a, Oriano Bottauscio^a, Rüdiger Brühl^b, Mario Chiampi^a and Luca Zilberti^a

^a Istituto Nazionale di Ricerca Metrologica, Torino, Italy

^b Physikalisch-Technische Bundesanstalt (PTB), Braunschweig and Berlin, Germany

Concerns about the hazards related to the interaction between electromagnetic fields of Magnetic Resonance Imaging (MRI) scanners and metallic implants is growing due to their large diffusion among population. While this problem has been largely studied in literature for what regards the interaction with the MRI radiofrequency fields (see for example [1]), few studies are available regarding the effects of switching gradient fields [2].

The *in-silico* study of the heating of metallic implants and surrounding tissues is made complex by the difficulties to account for the realistic MRI sequences and field spatial distribution in the electromagnetic and thermal solvers. In this work, we have developed a novel strategy that is based on the decomposition of the supply waveforms into sub-signals, leading to the solution of a set of time-harmonic electromagnetic field problems to compute the energy deposition in the implant. The thermal response is successively estimated through the solution of Pennes' equation, including thermoregulation effects in both the blood perfusion coefficient and the metabolic heat. The numerical tool here developed has been first validated by comparison with experiments considering the acetabular cup of a real hip prosthesis placed within a phantom (implant "embedded") or thermally insulated (Fig. 1). A 3 T clinical scanner has been used with an echo planar imaging (EPI)-like sequence.

The thermal effects have been studied simulating a patient with a unilateral right hip prosthesis (the prosthesis was inserted in the "Duke" anatomical model, belonging to the Virtual Population). Different positions of the patient within the MRI scanner have been analyzed and some common sequences have been investigated. As an example, the maximum temperature increase (after 12 minutes of exposure) consequent to the application of an EPI sequence is summarized in the Table, for different configurations of the sequence (gradient coils G_x , G_y and G_z) and implant material.

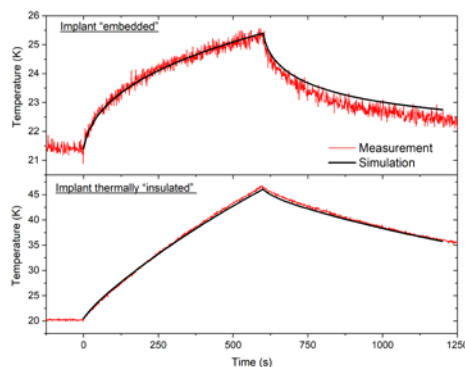


Figure 1 – Experimental validation of the computational tool.

Table I - Maximum temperature increase (after 12 minutes exposure) consequent to the application of an EPI sequence

Imaging plane	Slice selection	Phase encoding	Frequency encoding	Max temperature increase (K)	
				CoCrMo alloy	Ti6Al4V alloy
Sagittal	G_x	G_y	G_z	3.20	2.26
Coronal	G_y	G_x	G_z		
Sagittal	G_x	G_z	G_y	1.86	1.30
Transversal	G_z	G_x	G_y	3.24	2.30
Transversal	G_z	G_y	G_x		
Coronal	G_y	G_z	G_x		

[1] T. Song et al., Magn. Reson. Med. **80** (2018), 2726-2730.

[2] L. Zilberti et al., Magn. Reson. Med. **74** (2015) 272-279.

Maximizing local magnetic particle concentrations using dynamic optimization

Rikkert Van Durme, A. Coene, G. Crevecoeur, L. Dupré

Ghent University, Ghent, Belgium

In magnetic targeting, magnetic nano- or microparticles are brought inside the human body and targeted towards diseased regions for therapeutic procedures such as hyperthermia and drug delivery [1]. To non-invasively guide them through veins, membranes and tissue, current-carrying coils generating magnetic fields and field gradients are used, as they give rise to forces exerted on magnetically susceptible particles from a distance. Accurate dynamical models including these forces can be combined with sophisticated control algorithms for deep and effective magnetic drug targeting [2].

In this contribution, a dynamical model is developed relating particle concentrations in voxels in a sample to coil currents as $\dot{\mathbf{y}} = A(\mathbf{u})\mathbf{y}$, where \mathbf{y} are the concentrations and \mathbf{u} the currents. A is governed by viscous effects from the fluid surrounding the particles and magnetic forces depending on geometry and currents. Model-based dynamic optimization is then applied to calculate the currents required in the coils to maximize particle concentrations in predefined voxel(s) of interest. The problem is formulated as follows:

$$(\mathbf{y}^*, \mathbf{u}^*) = \arg \min_{\mathbf{y}, \mathbf{u}} \int_0^T -y^i(t) dt, \text{ subject to } \begin{cases} \dot{\mathbf{y}} = A(\mathbf{u})\mathbf{y} \\ |u_j| \leq I_{\max} & j = 1, \dots, n \\ \mathbf{y}(0) = \mathbf{y}_0 \end{cases}$$

We want to maximize the particle concentration in the i -th voxel, y^i , in a system with n coils of which the currents are limited by I_{\max} . The initial concentrations are given by \mathbf{y}_0 . The coils are activated over a time period T and the optimal currents are denoted by \mathbf{u}^* , yielding the concentrations \mathbf{y}^* .

In Figure 1, results are shown for a numerical experiment in 2D. The initial distribution is used to calculate the required currents in coils surrounding the sample.

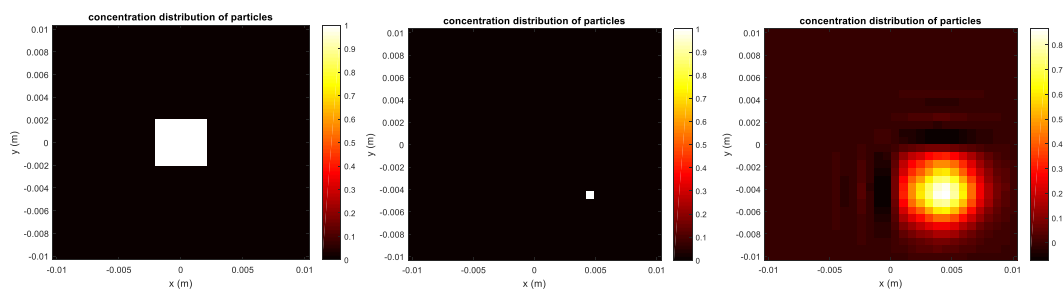


Figure 1: Left: initial distribution of particles. Center: targeted voxel. Right: distribution after dynamical optimization.

-
- [1] Pankhurst, Q. A., Connolly, J., Jones, S. K., & Dobson, J. (2003). Applications of magnetic nanoparticles in biomedicine. *J. Phys. D.: Appl. Phys.*, 36(13), R167.
- [2] Shapiro, B., Kulkarni, S., Nacev, A., Muro, S., Stepanov, P. Y., & Weinberg, I. N. (2015). Open challenges in magnetic drug targeting. *Wiley Interdisciplinary Reviews: Nanomedicine and Nanobiotechnology*, 7(3), 446-457.

Selective Magnetic Separation to concentrate bioactive compounds from microalgae

Maria G. Savvidou^{1,2}, Angelo Ferraro², Antonio Molino³, Evangelos Hristoforou²

¹ Biotechnology Laboratory, School of Chemical Engineering, National Technical University of Athens, Athens, Greece, ² Laboratory of electronic sensors, School of Electrical Engineering and Computer Engineering, National Technical University of Athens, Athens, Greece, ³ ENEA, Italian National Agency for New Technologies, Energy and sustainable Economic Development, Department of Sustainability, Portici, Naples, Italy

Abstract

Bioactive compounds from various natural sources (plants, fruits, fungi, bacteria, algae etc.) have been attracting more and more attention, owing to their broad diversity of functionalities and benefits to the human health. The extraction of bioactive compounds from plant materials is the first step in the utilization of phytochemicals in the preparation of dietary supplements or nutraceuticals, food ingredients, pharmaceutical, and cosmetic products. However, many of these compounds often exist at extremely low concentration in a mixture so that new extraction methods are required to obtain several high-quality bioactive compounds by lowering, at the same time, the cost production and the energy consumption.

In this work we present preliminary results for the extraction of astaxanthin. This molecule belongs to the family of carotenoids, which is very attractive for important industrial markets, such as food grade coloring and antioxidant agent. Our investigation is focused in the use of organic binders which present many advantages such as easy and inexpensive synthesis, the possibility of thousands of combinations that will result in at least one molecule able to bind the target compound and the fast screening. In the present work, different astaxanthin extracts preparations from *Haematococcus pluvialis* (microalgae) were used as target compounds to be bind on magnetic nanoparticles.

Thermal Noise Magnetometry of Magnetic Nanoparticle Ensembles

K. Everaert^{1,2}, J. Leliaert², B. Van Waeyenberge², F. Wiekhorst¹

¹Physikalisch-Technische Bundesanstalt, Abbestraße 2-12, D-10587 Berlin, Germany

²Department of Solid State Sciences, Ghent University, 9000 Ghent, Belgium
katrijn.everaert@ptb.de / katrijn.everaert@ugent.be

Magnetic nanoparticles are very useful in biomedical applications, where they are employed in both diagnosis (contrast agents in Magnetic Resonance Imaging, Magnetic Particle Imaging,...) and therapy (heat generator in magnetic hyperthermia). To improve the performance of these applications, the particle properties should be characterized precisely. To this end, several magnetic measurement techniques are established: static and dynamic magnetization measurements, Magnetorelaxometry (MRX), Magnetic Particle Spectroscopy. All methods have in common that they measure the magnetic response of the particles exposed to an externally applied magnetic field, which may change the magnetic state of the particles. To overcome this problem, the method of Thermal Noise Magnetometry (TNM) has been developed to characterize magnetic nanoparticle ensembles without any use of an external magnetic excitation [1].

Thermal fluctuations in the system cause the magnetic moment of the particles to change their directions. In general, two different mechanisms are distinguished: the magnetic moments of the atoms within the particle may switch direction (Néel relaxation) or the particle as a whole can rotate (Brownian relaxation). The total switching rate of nanoparticles is therefore the combination of these two mechanisms and depends on volume, anisotropy, aggregation of the particles and the viscosity and temperature of the suspension.

MRX is a particle characterization method which measures these processes by investigating the relaxation of an ensemble of magnetic nanoparticles towards zero after an initial magnetization phase. In the absence of this magnetization phase, the same switching processes still play, but result in fluctuations around the zero net magnetic moment, instead of a relaxation towards it. However, the magnetic fluctuations, which would be considered as a noise in the signal of an MRX measurement, carry the same information. Measuring the thermal noise of a magnetic nanoparticle ensemble by TNM, thus can be used as a magnetic characterization technique that does not rely on the application of an externally applied field. Such measurements have recently been proven to be feasible, and complementary to other characterization techniques due to its diminutive impact on the sample [1, 2].

Since small noise signals (a few fT/sqrt(Hz)) are to be measured, we performed simulations to determine the optimal sample configuration which takes the restrictions of the experimental setup into account. For larger sample volumes, more magnetic material is present which can contribute to the noise signal, resulting in a larger field amplitude. The ideal sample configuration is an optimum between different parameters: volume and shape of the sample, distance from the detector, costs of the material.

[1] J. Leliaert et al. Appl. Phys. Lett., 107(22):222401, 2015.

[2] J. Leliaert et al. J. Phys. D: Appl. Phys., 50(8):085004, 2017.

Numerical modelling of magnetic force on human targets in magnetic targeting applications

Serena Fiocchi^a, Marta Bonato^a, Emma Chiaramello^a, Gabriella Tognola^a, Marta Parazzini^a, Paolo Ravazzani^a

^a CNR Consiglio Nazionale delle Ricerche, Istituto di Elettronica e di Ingegneria dell'Informazione e delle Telecomunicazioni IEIIT, Milan, Italy

In the last few years, the successful use of nanoparticles (NPs) for therapeutic applications has encouraged the development of strategies to focus them in specific organs. Among them, magnetic targeting consists in the use of magnet or coils, placed close to the organ of interest, capable of producing high magnetic field gradients (and then magnetic forces) on magnetically responsive NPs, in order to increase their concentration in the target [1]. Although some experimental studies have shown the effectiveness of this technique, there are still few studies able to quantify and explain the experimental results. In this study we evaluated, by means of computational electromagnetics techniques, the attitude of different magnetic systems, optimized on anatomy, in targeting the heart of differently aged human anatomical models belonging to the Virtual Population [2,3]. Magnetic force (F_M) acting on a spherical nanoparticle can be calculated as:

$$F_M = \frac{2\pi a^3}{3} \frac{\mu_0 \chi}{(1 + \frac{\chi}{3})} \cdot \nabla(|\vec{H}|^2) \quad (1)$$

where a is the radius of the NP, $\mu_0=4\pi*10^{-7}$ N/A² is the vacuum permeability, $\chi=\mu_r-1$ is the magnetic susceptibility and ∇ is the spatial gradient operator. The magnetic field (H) produced is calculated through the magneto quasi static approximation of Maxwell's equation and then $\nabla(H^2)$, proportional to the magnetic force as in (1) was calculated (Fig. 1)

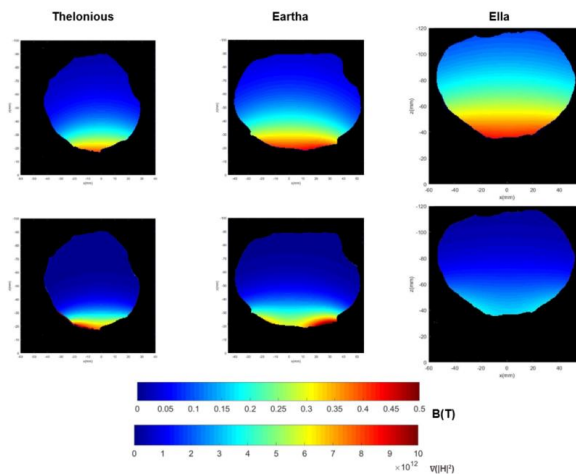


Figure 1 Example of magnetic induction B and $\nabla(|H|)^2$ distribution induced in the heart tissues by different sized magnetic systems (permanent magnets with dimension optimized on anatomy) on a transversal (x - z) slice passing to the center of both the magnetic system (origin $x,y,z=0$) and the heart of the human models.

-
- [1] B. Shapiro, J. Magn. Magn. Mater. 321(2009), 1594
 - [2] A. Christ et al. Phys. Med. Biol. 55(2010), 23-38.
 - [3] M.C. Gosselin Phys. Med. Biol. 59(2014), 5287-5303.

Advances in Magnetism 2020-21, June 13-16, 2021

**Magnetic materials for
energy applications
&
Additive manufacturing of
magnetic materials**

[Abstracts can be easily browsed through the bookmarks](#)

Structure and magnetic properties of thermodynamically predicted rapidly quenched $\text{Fe}_{85-x}\text{Cu}_x\text{B}_{15}$ alloys

Lukasz Hawelek^a, Tymon Warski^a, Adrian Radon^a, Przemyslaw Zackiewicz^a, Anna Wójcik^b, Mariola Kądziołka-Gawel^c, Aleksandra Kolano-Burian^a

^a Lukaszewicz Research Network - Institute of Non-Ferrous Metals, 5 Sowinskiego St., 44-100 Gliwice, Poland

^b Institute of Metallurgy and Materials Science Polish Academy of Sciences, 25 Reymonta St., 30-059 Krakow, Poland

^c Institute of Physics, University of Silesia, 75 Pulku Piechoty 1a St., 41-500 Chorzow, Poland

In this paper the influence of copper addition on the formation of the amorphous phase, the nanocrystallization process and the magnetic properties of $\text{Fe}_{85-x}\text{Cu}_x\text{B}_{15}$ melt-spun ribbons was described. Firstly, the prediction of chemical composition was performed by use of thermodynamic approach. Three thermodynamic parameters: enthalpy of mixing (ΔH^{mix}), configurational entropy (ΔS^{config}) and Gibbs free energy of amorphization (ΔG^{amorph}) were then calculated for Cu content from 0 to 2. The optimal value of ΔG^{amorph} , searched using evolutionary algorithms, was observed for Cu=0.6. It has been noted that two similar values of ΔG^{amorph} for alloys with Cu=0 and Cu=1.5 (see fig. 1) are observed.

Therefore, the experimental part of this work has been performed for three selected alloys: $\text{Fe}_{85}\text{B}_{15}$, $\text{Fe}_{84.4}\text{Cu}_{0.6}\text{B}_{15}$, $\text{Fe}_{83.5}\text{Cu}_{1.5}\text{B}_{15}$ (most interesting from thermodynamic point of view). Then, the formation of crystalline phases was described using differential scanning calorimetry, X-ray diffractometry, Mössbauer spectroscopy and transmission electron microscopy. It was confirmed that the addition of copper decreases the glass forming ability, while facilitating the process of nanocrystallization. Optimization of the annealing process (with heating rate $10^\circ\text{C}/\text{min}$ and subsequent isothermal annealing for 20 minutes) of toroidal cores (mass of $\sim 10\text{g}$) made from amorphous ribbons with different copper content allowed to obtain nanocrystalline, soft magnetic materials characterized by low coercivity $< 10\text{ A/m}$ and high saturation induction of above 1.6 T. Analysis of transmission electron microscope images and electron diffraction confirmed that high magnetic parameters are related to the coexistence of the amorphous and nanocrystalline phases, which was confirmed also by Mössbauer spectroscopy. Additionally, the complex permeability in the $10^4\text{-}10^8\text{ Hz}$ frequency range together with core power losses obtained from magnetic induction dependence up to the frequency of 400 kHz was successfully measured.

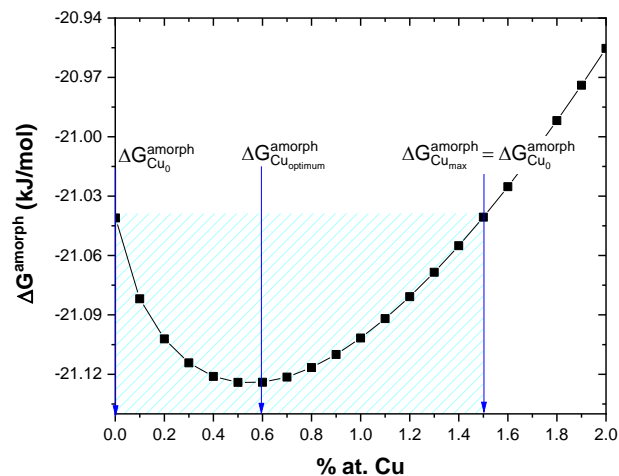


Figure 1. The influence of copper content in $\text{Fe}_{85-x}\text{Cu}_x\text{B}_{15}$ alloy on the Gibbs free energy of amorphization

Investigations on the magnetic properties of the $R_xZr_{1-x}Fe_{11-z}Co_zTiC$ ($R = Y, Gd$) alloys

D. Benea^a, R. Hirian^a, V. Pop^a, O. Isnard^{b,c}

^a Faculty of Physics, Babeş-Bolyai University Cluj-Napoca, Kogălniceanu str 1,
400084 Cluj-Napoca, Romania

^b Université Grenoble Alpes, Institut Néel, Grenoble, F-38042, France

^c CNRS, Institut Néel, 25 rue des Martyrs, F-38042 Grenoble, France

We present theoretical and experimental investigations on the electronic and magnetic properties of the $R_xZr_{1-x}Fe_{11}Ti$ and $RFe_{11-z}Co_zTiC$ ($R = Y, Gd$; $x = 0 - 0.2$; $z = 0 - 3$) alloys. The theoretical calculations describe the dependence of the magnetic properties (magnetic moments, magneto-crystalline anisotropy, exchange-coupling parameters) on the R/Zr and Fe/Co ratios [1]. The R for Zr substitution in $Y_xZr_{1-x}Fe_{11}Ti$ ($x = 0 - 0.2$) increases the calculated total magnetic moment by increasing Zr content x but the magneto-crystalline anisotropy energy shows a slight decrease. On the other hand, the improvement of the magnetic properties (total magnetic moment and magneto-crystalline anisotropy energy) for permanent magnets applications of $RFe_{11}Ti$ based alloys appears to be efficient upon partial Co for Fe substitution. The experimental measurements are in progress to test the theoretical findings.

This study may give an insight on the influence of the Zr, Co and C doping on the magnetic properties of the $R_xZr_{1-x}Fe_{11-z}Co_zTi$ ($R = Y, Gd$) alloys, aiming to obtain rare-earth free permanent magnets with enhanced magneto-crystalline anisotropy (MAE) and higher magnetization.

[1] Munich SPRKKR calculation code <http://olymp.cup.uni-muenchen.de/>

Effect of Cr addition on thermal stability, magnetic and electro-chemical properties of high induction Fe-B alloys

Tymon Warski^a, Przemysław Zackiewicz^a, Wojciech Lonski^b, Rafał Babilas^b,
Aleksandra Kolano-Burian^a, Lukasz Hawelek^a

^a Department of Functional Materials, Lukaszewicz Research Network—Institute of Non-Ferrous Metals, Gliwice, Poland

^b Department of Engineering Materials and Biomaterials, Silesian University of Technology, Gliwice, Poland

Highly inductive amorphous and nanocrystalline Fe-based materials are commonly used in power electronics, among others in industrial transformers, stator cores or induction devices. A wide range of applications is associated with high saturation induction, low coercivity H_c and core power losses P_s of materials. The high concentration of Fe and the appropriate crystal structure are mainly responsible for the useful soft magnetic properties. However, the increase in Fe content is associated with one of the most important application disadvantages - reduction of corrosion resistance. This disadvantage limits the production techniques and application possibilities. For this reason, many scientists and engineers optimize the chemical composition of Fe-based metallic glasses to increase their anti-corrosion resistance while maintaining the soft magnetic properties of the material and the glass formation ability (GFA). Research shows that the addition of small amounts of elements such as Cr, Mo or Nb increases the corrosion resistance while maintaining the magnetic properties of the material, of which Cr gives the most promising results due to the high passivation capacity of the surface layer [1-2]. However, the literature lacks research on the effect of Cr in binary alloys such as Fe-B, which necessitates additional research.

In this work the effect of substitution of Fe by Cr on the thermal stability, crystal structure, magnetic and electro-chemical properties of Fe-B binary alloys with high induction ($B_s > 1.5T$) was investigated. Firstly, Fe-B alloys with different content of Cr in the form of ribbons were obtained by melt-spinning method. The characteristic crystallization temperatures of the alpha-iron phase for the as-spun samples were determined by differential scanning calorimetry. In order to determine the optimal soft magnetic properties, the material in the form of wound cores were subjected to a controlled isothermal annealing process for 20 minutes in vacuum at the temperature resulting from the kinetics of crystallization. In addition, air annealing process was also performed to check the influence of surface oxidation on magnetic properties for different Cr content. Coercivity H_c , saturation induction B_s and core power losses at $B = 1T$ and frequency $f = 50Hz$ ($P_{10/50}$) were determined for all samples. Moreover, for the samples with the optimal magnetic properties the magnetic permeability were determined in a frequency range $f = 10^4-10^8$ Hz. The crystal structure of as-spun and annealed alloys was determined by X-ray diffraction method (XRD). Finally, electrochemical and corrosion studies were conducted on selected materials.

This work was financed by the National Science Centre OPUS14 Grant no 2017/27/B/ST8/01601

-
- [1] Z.Long, Y. Shao, G. Xie, P. Zhang, B. Shen, A. Inoue, Journal of Alloys and Compounds, **492** (2008), 52-59.
- [2] Y.Han, C.T. Chang, S.L. Zhu, A. Inoue, D.V. Louzguine-Luzgin, E. Shalaan, F. Al-Marzouki, Intermetallics **54** (2014), 169-175.

Quick characterization method for SMC materials for a preliminary selection

Emir Poskovic^{a,b}, Luca Ferraris^a, Fausto Franchini^c, Federico Carosio^c, Marco Actis Grande^c

^a Politecnico di Torino, Energy Department, Alessandria, Italy

^b Università degli Studi di Padova, Department of Industrial Engineering, Padua, Italy

^c Politecnico di Torino, Department of Applied Science and Technology, Alessandria, Italy

The conversion of energy in various industrial applications is usually performed with the use of machines equipped with functional materials. Part of these materials is represented by soft and hard magnets, which provide the magnetic quantities necessary for the operativity of the electrical machines adopted in the several industrial applications. In the electrical machines, as soft magnetic materials, the laminated steels are commonly adopted, while for the permanent magnets the sintered ferrites and NdFeB are the most common solutions. On the other hand, the growing demand for space reduction with the increment of efficiency leads to the necessity of exploring other magnetic materials able to face the challenge better than the traditional ones.

Bonded magnets have been used to replace sintered magnets obtaining the best use of space and particular magnetic properties. Instead, for the magnetic circuit, the Soft Magnetic Composites (SMC) allow to realize very complex magnetic design (3D path for flux) with iron losses reduction at medium-high frequencies, especially for the eddy currents losses contribution. On the other hand, SMC materials have some drawbacks: low mechanical properties and high hysteresis losses. For this reason, different studies considering several variables have been carried out: inorganic or organic layer to cover ferromagnetic particles, and the adoption of different production processes. For a quicker and more indicative overview, particular tests have been performed: Single Sheet Tester (SST) for magnetic properties and accurate measurement of conductivity allow immediate characteristics of the SMCS. Such approach has been followed for to obtain precisely earlier the information on the possible SMC materials. SST and conductivity measurement are faster to prepared than toroid test, which typically used to measure properties of SMC materials.

In this work, for different typologies of SMC materials electrical conductivity have been deducted and its effect analyzed on losses behaviour. Also, the effect of the compaction process and layer content has been investigated.

LCL soft ferrite filter design for grid connected three-phase 5-levels cascaded H-Bridge inverters with MC PWM modulation techniques

G. Ala^a, R. Miceli^a, G. Giglia^a, P. Romano, G. Schettino^a, F. Viola^a,
S. Quondam Antonio^b, H. P. Rimal^b

^a Università degli Studi di Palermo, Dipartimento di Ingegneria, Palermo, Italy

^b Università degli Studi di Perugia, Dipartimento di Ingegneria, Perugia, Italy

Over the last decades, the grid-connected PV plants in low and medium voltage grids raised to big numbers. For this reason, the conversion systems play an important role and, in particular, the Cascaded H-Bridges (CHB) multilevel inverters due to their higher performances with respects to the traditional ones (low harmonic content, flexibility, low voltage stress, modularity etc.). In these applications, PWM multicarrier modulation schemes with sinusoidal reference, shown in Fig.1, are growing up in the use for their easy implementation in the electronic systems.

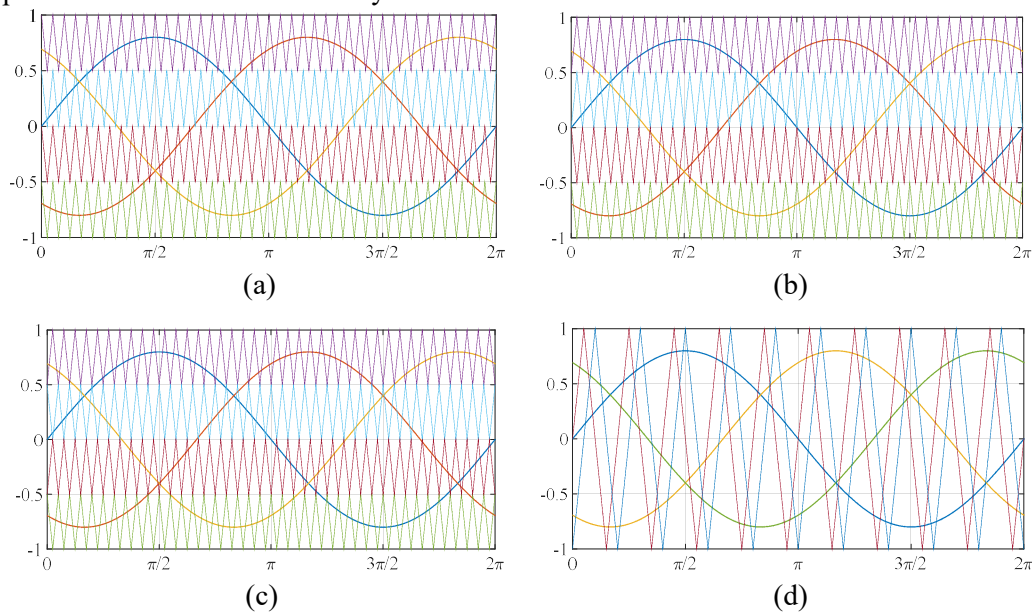


Fig.1: PWM multicarrier modulation schemes with sinusoidal reference: (a) Phase Disposition - PD; (b) Phase Opposition Disposition –POD; (c) Alternative Phase Opposition Disposition –APOD; and (d) Phase Shifted – PS.

For these systems, one of the most interesting aspect is the LCL filtering design in terms of filter requirements. Indeed, the design of the LCL power filter is influenced by the harmonic content of the output voltage and thus by the modulation schemes implemented. Moreover, also the modulation schemes influence the performance of the closed control loop. According with a step-by-step design procedure that takes into account the power rating of the converter, the line frequency and the switching frequency, in this paper after having evaluated the filter parameters for each modulation scheme, the influence of ferromagnetic material is investigated. This in order to evaluate the performance of the grid-connected system by taking into account the grid code limits IEEE 1574 and IEC 61727, in order to identify the best solution among the modulation schemes.

-
- [1] G. Ala , M. Caruso, R. Miceli, F. Pellitteri, G. Schettino, M. Trapanese, F. Viola, “Experimental Investigation on the Performances of a Multilevel Inverter Using a Field Programmable Gate Array-Based Control System,” *Energies*, vol. 12, no. 4, pp. 1-17, 2019.

Effects of fabricating conditions on the coercivity of Fe-Mn soft magnetic powders.

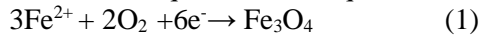
Tatsuya Kon^a, Nobuyoshi Imaoka^a and Kimihiro Ozaki^a

^aNational Institute of ADVANCED INDUSTRIAL SCIENCE AND TECHNOLOGY (AIST)

The annual world market for electric vehicles is expected to reach 15 million cars by 2020 [1]. As the market expands, the demand for the development of superior soft magnetic materials for drive motors is increasing. We have reported newly developed, high magnetization Fe-Mn powders that can easily be solidified by conventional powder-metallurgy processes [2]. The Fe-Mn powders are fabricated by reducing nano-ferrite produced by wet synthesis. In this paper, the effect of wet synthesis conditions on magnetic properties was researched.

Experimental method.

Fe-Mn powders doped with 0.2 at% manganese was fabricated by the reduction of manganese doped nano-ferrite ((Fe_{1-x}, Mn_x)₃O₄) with hydrogen gas at 950 °C. Nano-ferrite was fabricated by eq. (1) with neutralization reaction between FeCl₂ aq. and NaOH aq..



In this research, we have compared the magnetic properties of magnetic powders with different concentrations of aqueous solution and different pH during the reaction.

Table 1 shows wet synthesis conditions. Reaction pH and Oxidation-Reduction Potential (ORP) were controlled by stirring and solution feeding speed (Fig. 1). Coercivity of Fe-Mn powders was measured by Vibrating Sample Magnetometer with Helmholtz coil.

Experimental results and discussion.

The nano-ferrite under pH = 12 [-] condition was almost consisted by nano-sized spherical magnetite. On the other hand, the nano-ferrite under pH = 7 was consist spherical magnetite and coarse plate-like precipitate. Figure 2 shows coercivity of each Fe-Mn powders. Only pH = 7 was obtained high coercivity. From the above, it is pressured that the crystal shape of nano-ferrite and coercivity has something interaction.

Table 1: Wet synthesis conditions.

Concentration of FeCl ₂ and NaOH aq.	Reaction pH [-]
540mM	12
1180mM	12
1180mM	7

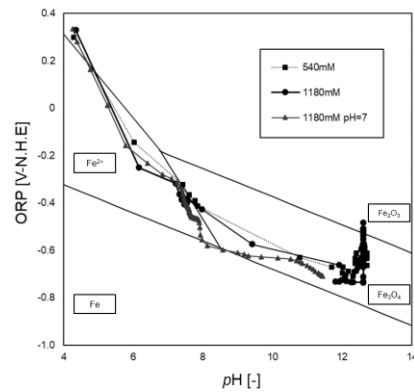


Figure 1: pH - ORP diagram with nano-ferrite fabrication.

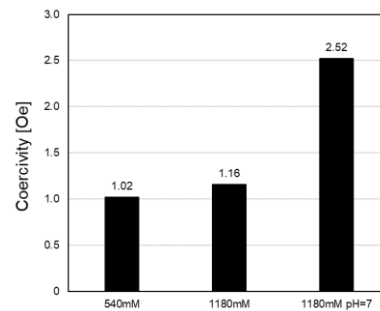


Figure 2: Relationships between coercivity and wet synthesis conditions.

[1] N. Imaoka, S. Yamamoto and K. Ozaki, Proc. IEEE International Magnetics Conference, Singapore, 2018, pp.1-7

[2] N. Imaoka and K. Ozaki, Int. Patent Appl. WO 2017/164376, 28 September 2017.

Magnetic properties and magnetocaloric effect of FeRh – an ab-initio study

Rafael Vieira^{a,b}, Olle Eriksson^{a,c}, Torbjörn Björkman^b, Heike C. Herper^a

^a Uppsala University, Sweden

^b Åbo Akademi, Finland

^c Örebro University, Sweden

The increasing interest in the application of magnetocaloric (MCE) materials for magnetic cooling devices has led to an intensive search for new materials with a more attractive performance to cost ratio. To this it is necessary to understand the relevant features that enhance the magnetocaloric effect in existing materials and in a second step based on the gained knowledge develop strategies to identify new MCE materials. FeRh, the leading material in view of magnetocaloric performance, goes through a metamagnetic transition from an antiferromagnetic to ferromagnetic phase around room temperature. This transition has piqued interest in this material, and it has been subjected to multiple studies. In this work, electronic, structural and magnetic properties of both phases have been studied from first principles aiming to find a reliable non-tailored approach to determine the entropy variation of the magnetocaloric effect [1] with very good agreement with experimental results [2].

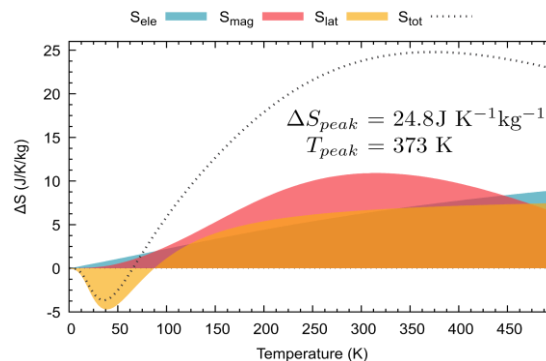


Figure 1: Total entropy variation and respective components estimated for the AFM → FM transition on FeRh [1].

In case of FeRh the electronic (S_{ele}), lattice (S_{lat}), and magnetic (S_{mag}) entropy contributions have approximately the same order of magnitude and the same sign, see Fig 1. The entropy peak of S_{mag} around the transition temperature suggests that the transition is mainly driven by magnetic subsystem, where small magnetic fluctuations may be playing an important role for the metamagnetic transition. Furthermore, it is found that the Debye model fails to predict S_{lat} when applied to FeRh, due to the existence of soft vibrational modes on the phonon spectra.

[1] Martinho Vieira, R., Eriksson, O., Bergman, A., & Herper, H. C. (2020) *Journal of Alloys and Compounds*, 157811.

[2] Cooke, D. W., Hellman, F., Baldasseroni, C., Bordel, C., Moyerman, S., & Fullerton, E. E. (2012) *Physical Review Letters*, 109(25), 255901.

Influence of cyclic magnetic field frequency on magnetocaloric effect in manganite's

Adler Gamzatov^a, A.M. Aliev, D-H. Kim^b, A.R. Kaul^c

^a Amirkhanov Institute of Physics, DFRC of RAS, Makhachkala, Russia

^b Department of Physics, Chungbuk National University, Cheongju, South Korea

^c Moscow State University, Moscow, Russia

Magnetic refrigeration machines have a number of significant advantages over conventional cooling systems. But here are many problems with creation of such. Materials with giant values of the magnetocaloric effect (MCE) are needed for the production of magnetic refrigerators and recent studies were focused on the search for new promising materials. The most of currently existing prototypes of refrigerators operate at cycle frequencies up to 4 Hz. One of the ways to improve the efficiency of cooling machines is increasing their working cycles' frequencies. But the materials for magnetic cooling technology cannot be considered as suitable, until they are tested for their magnetocaloric properties in alternating (cyclic) magnetic fields. It is due to the fact that magnetocaloric properties of materials can significantly differ at single or continues cyclic magnetic field application.

Experimental study of the frequency dependences of the MCE, when the applied field varies according to the law $\Delta H = H_0 \sin(\omega t)$ (where for our experiments the amplitude value $H_0 = 6.2$ kOe, $\omega = 0.3-30$ Hz is the cyclic frequency) have been started relatively recently [1-3] and are of great interest due to the fact, that the investigation of MCE in cyclic fields is as close as possible to the actual operating conditions of the magnetic cooling device. Depending on the phase transition nature and the type of magnetic ordering, the MCE behavior can strongly depend on the frequency of the field change [3]. In addition, the cyclic action of the magnetic field causes irreversible effects leading to MCE decrease and degradation of the magnetocaloric material [4], which requires further research also.

There are several reasons for this. Due to the various relaxation processes, the increase of the frequency of AC field can lead to a decrease of the MCE value. Effect on the MCE value in this case depends on the frequency of the field change. Measuring value of the MCE will also depend on the field frequency due to the reduction of the ability of the working material to exchange energy with heat exchanger when the frequency of cycle increases. There are also mechanisms that can affect on the MCE value, even at low frequencies the field changes. Hysteresis effects, the accumulation of structural defects, incompleteness of phase transitions at field application are some of them. These mechanisms cannot be manifested at single cycle of the field application, but can significantly effect on the MCE value at continues cycles. These mechanisms can also depend on the field frequency and the rate of the field change. So we see a growing interest in the MCE study in cyclic magnetic fields in recent years, but current studies are limited by a few cycles of field application and the frequencies of the used magnetic fields - by several hertz.

This paper presents the results of a study of the frequency dependence of the magnetocaloric effect for a number of manganites.

The research was supported by a grant of the Russian Science Foundation (Project No. 18-12-00415).

[1] A.M. Aliev, arXiv:1409.6898 (2014)

[2] T. Gottschall, K. P. Skokov, et al, Phys. Rev. Appl. **5** (2016), 024013-024020.

[3] A. M. Aliev, A. B. Batdalov, et al, J. of Alloys and Compounds **676**, (2016) 601-605.

[4] A. M. Aliev, A. B. Batdalov et al, Applied Physics Letters **109** (2016) 202407.

Structural, magnetic and electronic properties of Fe-Rh-Y (Y=Mn, Pd) compounds: ab initio study

Oksana Pavlukhina^a, Vladimir Sokolovskiy^{a,b}, Vasiliy Buchelnikov^{a,b}, Mikhail Zagrebin^{a,b}

^a Chelyabinsk State University, Chelyabinsk, Russia

^b National University of Science and Technology 'MISIS', Moscow, Russia.

Fe-Rh alloys currently attract more and more attention owing to the possibility of their application in magnetic cooling, magnetic recording, and spintronic devices [1-2]. On the one hand, equiatomic Fe-Rh alloys with CsCl structure demonstrate metamagnetic phase transition between antiferromagnetic (AFM) phase and ferromagnetic (FM) one that is accompanied by a change in the cell volume [3]. It well known, that the magnetic order in FeRh compounds depends strongly on the concentration. Theoretical research helps to describe and understand the phenomena occurring in the material. In this work, we present theoretical investigations of the structural and magnetic properties Fe_{1-x}Mn_xRh (x = 0.5-1) alloys and FeRh_{1-x}Pd_x (x=0.5- 1) alloys. The structural and magnetic properties of Mn and Pd-doped Fe-Rh alloys are investigated by using the density functional theory calculations as implemented in the VASP package. The ab initio calculations have been carried out by using the 16-atom supercell approach with different initial spin configurations. The energy calculations were performed for the supercell. Calculations were carried out for ferromagnetic, paramagnetic and three kinds of antiferromagnetic states as functions of the lattice parameter. The equilibrium lattice parameters $a = 3.009$ for Fe_{1-x}Mn_xRh (x = 0.5) up to 3.031 for Fe_{1-x}Mn_xRh (x = 1). It can be concluded that the addition of Mn atoms leads to an increase in the lattice equilibrium parameter. The equilibrium lattice parameters $a = 3.012$ for FeRh_{1-x}Pd_x (x = 0.5) up to 3.05 for FeRh_{1-x}Pd_x (x = 1). It can be concluded that the addition of Pd atoms leads to an increase in the lattice equilibrium parameter due to the larger atomic radius of Pd compared to the lower Rh value. The total and partial DOS curves for Fe-Rh-Y (Y=Mn, Pd) alloy was calculated. The calculation of the total energy for the tetragonal distortion of the cubic structure along the z axis is performed also. To accomplish this, we fixed the volume of a supercell as $V_0 = a_0^3 \approx a^2c$. Spin polarization for ferromagnetically ordered FePd, FeRh_{0.25}Pd_{0.75} alloy was found to be approximately 65%, 57%. Our calculations have shown that the substitution of Mn for Fe results in an appearance of stable body-centered tetragonal state. We also calculated the lattice constants, volume cell, partial and total magnetic moments.

This work was supported by RSF-Russian Science Foundation No. 17-72-20022.

-
- [1] S. Cumpson, P. Hidding, and R. Coehoorn, IEEE Trans. Magn. **36** (2000), 2271
 - [2] J.-U. Thiele, S. Maat, and E. E. Fullerton, Appl. Phys. Lett. **82** (2003), 2859
 - [3] M. Ibarra, P. Algarabel, Phys. Rev. B. **50** (1994), 4196

New concept of electromagnetic field source for magnetic refrigeration

Simon Nosan^a, Urban Tomc^a, Katja Klinar^a, Andrej Kitanovski^a

^a University of Ljubljana, Faculty of Mechanical Engineering, Ljubljana, Slovenia

This article reports on the latest research achievements on development of static magnetic refrigerators and heat pumps systems. In the article we present the results on the numerical investigation on the novel design of the static magnetic field source. The investigated magnetic field source represents a substantial improvement versus the solution, that concerned the use of electromagnetic field sources with the regeneration of magnetic energy and were presented by Klinar et al. [1]. The results of the study represent an important basis for the future development of static electromagnetic field sources in the domain of magnetic refrigeration and heat pumping.

Electromagnets during operation heat up due to the Joule losses in the winding. By significantly reducing the Joule heat, the electromagnet can achieve energy efficiency comparable to structures of permanent magnet assemblies with motor driven rotation, which were up-to-date applied in magnetic refrigeration or heat pumping.

Fast magnetization/demagnetization process is crucial for the compactness of device, since it defines the frequency of the operation. An instant, step-change of the magnetic flux density in the magnetocaloric material cannot be achieved with permanent magnets regardless the principle of movement. By implementing magnetic energy recovery into electromagnetic field source it is not only possible to achieve higher efficiency, but also faster field change due to accumulated electric energy in each cycle. With additional modification of previously presented electronic circuit, it is possible to ensure a constant magnetic field during magnetized state of magnetocaloric material.

We have designed 25 conceptual solutions for which we have tested the feasibility of operation and implementation. The most promising concept was evaluated using the Ansoft Maxwell software tool. Based on the obtained results, we chose a geometry for more detailed analysis, for which we made 30 iterations regarding the iron core and windings, and for each geometry several iterations to obtain the most appropriate value of the magnetic flux density in the air gap.

According to simulations, a form of magnetic structure can be achieved which allows the magnetic field alternately to be established efficiently in the air gap. This reflects as a lower input power, that needs to be provided to the electromagnet, which results in the lower electrical power consumption of a structure and lower heating of the windings.

-
- [1] Klinar K, Tomc U, Jelenc B, Nosan S, Kitanovski A. New frontiers in magnetic refrigeration with high oscillation energy-efficient electromagnets. Appl Energy 2019

Magnetostriction of Fe-Ga-Z (Z=Al, Ge, Si) alloys studying by torque method

Mariya V. Matyunina, Mikhail A. Zagrebin, Vladimir V. Sokolovskiy,
Vasiliy D. Buchelnikov
Chelyabinsk State University, Chelyabinsk, Russia

In the last two decades, the Fe-based magnetic materials have attracted considerable attention due to their unusual mechanical, magnetic and electrical properties. Among them, the iron-gallium alloy, possessing the highest saturation magnetostriction and demonstrating two peaks of magnetostriction at room temperature [1-3]. The first peak corresponds to the A2/D0₃ phase boundary, further decreasing of magnetostriction is associated with the increase of an ordered D0₃ structure and reached the minimum at about 25 at.% of Ga content [3-4]. In this work, we consider the effect of adding a third element to the Fe₇₅Ga₂₅ alloy on the elastic and magnetic properties of the crystal structure of D0₃.

The Fe₇₅Ga_{25-x}Z_x (Z=Al, Ge, Si) with a concentration of Z-element in the range 1≤x≤6 at.% were investigated using density functional theory implemented into the SPR-KKR software package [5]. To perform the crystal structure optimization, we used body-centred cubic D0₃(*Fm-3m*, #225) structure. The exchange-correlation energy was treated by the generalized gradient approximation. Using the torque method implemented into the SPR-KKR the magnetocrystalline anisotropy energy (MAE) was calculated. The magnetoelastic coupling coefficient $-b_1$ and tetragonal coefficient of magnetostriction λ_{001} were determined through the dependences of MAE from small tetragonal deformations [6]. Figure 1 (a) shows that the substitution of Ga atoms by Z elements leads to decreasing of equilibrium lattice parameters; adding of Ge atoms energetically stabilize D0₃ structure (See Figure 1 (b)).

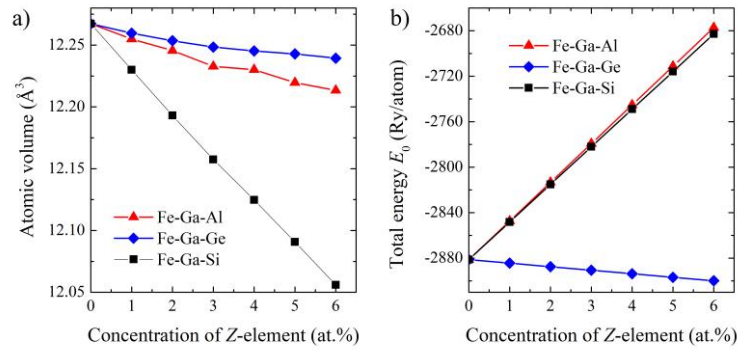


Figure 1: (a) The calculated atomic volume and (b) total energy for D0₃ structure of Fe Fe₇₅Ga_{25-x}Z_x alloys depending on Z concentration (at.%).

Acknowledgments: The reported study was funded by RFBR, project number 19-32-90138.

- [1] A.E. Clark et al., J. Appl. Phys. **93** (2003), 8621-8623.
- [2] A.E. Clark et al., J. Appl. Phys. **93** (2003), 8621-8623.
- [3] J.B. Restorff et al. J. Appl. Phys. **111** (2012), 023905-12.
- [4] I.S. Golovin et al. Physics of Metals and Metallography, **121** (2020) 937.
- [5] H. Ebert, D. Ködderitzsch, J. Minár, Rep. Prog. Phys. **74** (2011), 96501-48.
- [6] H. Wang et al., Sci. Rep. **3** (2013), 3521-5.

Insight into the magnetization process of ferromagnetic shape memory films with twinned microstructure

Francesca Casoli^a, Gaspare Varvaro^b, Simone Fabbrici^a, Milad Takhsha Ghahfarokhi^a, Federica Celegato^c, Paola Tiberto^c, Franca Albertini^a

^a IMEM-CNR, Parma, Italy

^b nM²-Lab, ISM-CNR, Monterotondo Scalo (Roma), Italy

^c INRIM, Torino, Italy

Magnetic shape memory materials show outstanding multifunctional properties, originating from the occurrence of both a martensitic transformation and magnetic order. Thin films and nanostructures of these materials have a great potential for applications such as micro- or nano-actuators, energy harvesters, valves and solid-state microrefrigerators [1].

We have demonstrated that a huge and reversible magnetization jump can be achieved in 200 nm Ni-Mn-Ga films [2, Figure 1]. This is possible when the proper microstructure is obtained: growth conditions and a stress applied to the substrate enable the proper microstructure, where differently twinned martensitic regions are aligned anisotropically. The films were epitaxially grown on Cr/MgO(1 0 0) by r.f. sputtering.

We here examine the relation between the film microstructure and magnetization process. We have simulated magnetization processes in films with different martensitic microstructures, e.g., showing different orientation and spatial organization of the martensitic twin variants. The micromagnetic simulations, realized by the OOMMF code [3], show a good agreement with the experimental results, with magnetization jumps taking place in the first quadrant of the (M,H) diagram (Figure 1). The results of the simulations will be compared with a detailed experimental investigation realized by magnetometry and vectorial magnetometry, i.e., measuring magnetization curves along different directions of the substrate crystal, simultaneously recording parallel and transverse magnetization components.

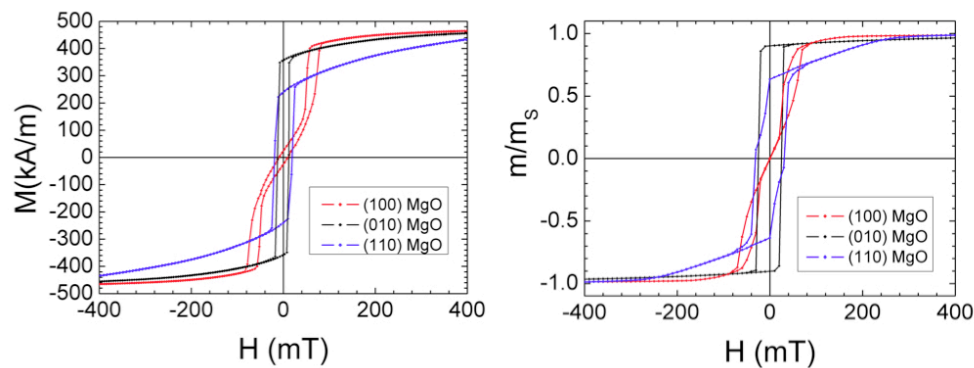


Figure 1: Experimental (left) and simulated (right) hysteresis curves, obtained applying a magnetic field along different directions of the MgO substrate.

[1] A. Backen et al., *Adv. Eng. Mater.* 14, 696–709 (2012)

[2] P. Ranzieri et al., *Adv. Mater.* 27, 4760 (2015)

[3] M. J. Donahue and D. G. Porter, *OOMMF User's Guide, Version 1.0: Interagency Report* (National Institute of Standards and Technology, Gaithersburg, MD, 1999)

Magnetostriction of A2 phase in Fe-(Ga, Ge, Al) alloys: insights from first-principles calculations

Mariya V. Matyunina, Mikhail A. Zagrebin, Vladimir V. Sokolovskiy,
Vasiliy D. Buchelnikov

Chelyabinsk State University, Chelyabinsk, Russia

The Fe-Ga alloys are successful magnetostrictive materials, which demonstrated two peaks of saturation magnetostriction λ_{001} 395×10^{-6} and 350×10^{-6} at room temperature for compositions with $x \approx 19$ at.% and $x \approx 27$ at.%, respectively [1]. After the discovery of giant magnetostriction in Fe-Ga alloys other Fe-based alloys such as Fe-(Ge, Al) have been investigated in more detail. Each of these alloys has magnetostriction of saturation that increases as more Fe atoms are substituted with solute atoms [2]. According to the experimental results for $\text{Fe}_{100-x}(\text{Ga, Ge, Al})_x$ alloys in the range of 0-10 at.% A2 phase is predominant for all these alloys [3]. Besides, the concentration dependencies of magnetostriction constant are the same for the considered alloys [4-6]. In this study, we investigate the concentration dependencies of magnetostriction in the A2 phase in $\text{Fe}_{100-x}(\text{Ga, Ge, Al})_x$ (0-9.375 at.%) alloys by means of the density functional theory.

The calculations were carried out by using the Vienna *Ab initio* simulation package (VASP) [7, 8]. For calculations, we used lattice parameters, obtained by geometry optimization of the crystal structure in an account of the atoms supercell approach with 32 atoms supercell. The generalized gradient approximation according to the Perdew-Burke-Ernzerhof parametrization [9] was used to take into account the exchange-correlation effects. In our calculations A2 crystal structure (*Im-3m* no. 229 space group, prototype α -Fe) with Fe and (Ga, Ge, Al) atoms randomly distributed is considered.

As a result, concentration dependencies of tetragonal magnetostriction λ_{001} of $\text{Fe}_{100-x}(\text{Ga, Ge, Al})_x$ (0-9.375 at.%) alloys have been obtained.

Support by Russian Science Foundation (Grant No. 18-12-00283) is acknowledged.

-
- [1] A.E. Clark et al., J. Appl. Phys. **93** (2003), 8621-8623.
 - [2] K.H.J. Buschow, Handbook of Magnetic Materials. Amsterdam: Elsevier Science B.V, 2012.
 - [3] O. Kubaschewski., Iron-binary phase diagrams. Berlin: Springer-Verlag, 1982
 - [4] A.E. Clark et al., J. Appl. Phys. **93** (2003), 8621.
 - [5] J.B. Restorff et al., J. Appl. Phys. **111** (2012), 023905.
 - [6] E.M. Summers et al., J. Mater. Sci. **42** (2007), 9582.
 - [7] G. Kresse, J. Furthmüller, Phys. Rev. B. **54** (1996), 11169-11186.
 - [8] G. Kresse, D. Joubert, Phys. Rev. B. **59** (1999), 1758-1775.
 - [9] J.P. Perdew et al., Phys. Rev. Lett. **77** (1996), 3865.

Magnetic properties of HPT Fe-Ni-Al alloys

Maxim N. Ulyanov^{a,b}, Sergey V. Taskaev^{a,b}, Dmitriy V. Gunderov^c, Dmitriy S. Bataev^a, Mikhail Yu. Bogush^a

^a Department of Physics, Chelyabinsk State University, Chelyabinsk, Russia

^b National Research South Ural State University, Chelyabinsk, Russia

^c Institute of Molecule and Crystal Physics RAS, Ufa, Russia

The China is a practically complete monopolist in the market of rare-earth elements. There are no alternatives to China in the supply of rare earth elements. Growing in recent years, domestic demand for rare-earth elements in China has led to the restriction of their supplies to the international market, so there is an urgent need to develop alternative free rare-earth permanent magnets [1-5].

The proposed project is aimed at integrating the achievements of theoretical and experimental research, which aimed at creating innovative directions for obtaining new functional materials, in particular, new types of free critical elements permanent magnets (including rare earth elements). High performance permanent magnets have become indispensable materials in many industries, ranging from data storage to small motors and clean energy devices. Thus, the reduction of the content of critical elements in the production of permanent magnets is an adequate response to the crisis of the supply of rare earth metals and their oxides and will make it possible to avoid the monopolistic dominance of China in the market of rare earth elements.

Along with rare-earth systems, some Fe-based alloys are some of the most promising candidates for rare-earth compounds for the production of permanent magnets.

In this work we report on the results of investigation of magnetic properties Fe-Ni-Al system after severe plastic deformation by high pressure torsion.

The authors gratefully acknowledge the Russian Science Foundation project #19-72-00047.

-
- [1] K. Kramer, Phys. Today, 63, 22-24 (2010).
 - [2] S Sugimoto, J. Phys. D: Appl. Phys. 44, 064001 (2011).
 - [3] R. Skomski, J.E. Shield, and D.J. Sellmyer, Magnetism Technology International, UKIP Media & Events, Ltd., p. 26-29 (2011).
 - [4] M.J. Kramer et al., JOM, 64, 752-763 (2012).
 - [5] B. Balamurugan et al., Scripta Materialia, 67, 542-547 (2012).

Variety of magnetic structures in $R(\text{Co}_{0.84}\text{Fe}_{0.16})_2$ ($R = \text{Ho}, \text{Er}$) systems with yttrium substituted for rare earth elements

Maksim S. Anikin, Evgeny N. Tarasov, Dmitry S. Neznakhin, Mikhail A. Semkin,
Nadezhda V. Selezneva, Aleksander V. Zinin

Ural Federal University, Yekaterinburg, Russia

Earlier, in the study of quasi-binary compounds $R(\text{Co}_{1-y}\text{Fe}_y)_2$ ($R = \text{Gd}, \text{Dy}, \text{Ho}, \text{Er}$), the existence of a significant magnetocaloric effect (MCE) in a wide temperature range, below the Curie temperature (T_C), was found. It arises both at the partial substitution of Fe for Co at a fixed R and at varying the R type at a fixed Fe (y) content, which the authors attributed to the weakening of the intersublattice exchange interaction between R- and 3d-magnetic sublattices [1, 2]. To better understand the role of exchange interactions between R and 3d magnetic sublattices in such systems, two series of compounds $R_{1-x}\text{Y}_x(\text{Co}_{0.84}\text{Fe}_{0.16})_2$ ($x = 0-1$, $R = \text{Ho}, \text{Er}$) were synthesized and their structure, magnetic and magneto-thermal properties was studied.

As a result of the study, it was established that when holmium or erbium is replaced by "nonmagnetic" yttrium, four types of magnetic structure are realized in turn:

- 1) $x \leq 0.40$ – ferrimagnets with a predominant magnetic moment of rare-earth sublattices in the entire temperature range of magnetic ordering of compounds;
- 2) $0.60 \leq x \leq 0.75$ – ferrimagnets having magnetic compensation points on the temperature dependence of the resulting magnetization;
- 3) $0.80 \leq x \leq 0.85$ – ferrimagnets with predominant magnetic moments of 3d-sublattices in the entire temperature range of magnetic ordering of compounds;
- 4) $x = 1$ – single-sublattice ferromagnet.

Each of these magnetic structures has its own temperature dependences of specific magnetization (σ), high-field susceptibility (χ_{hf}), and the magnetic entropy change (ΔS_m). In particular, the magnetization curves of the $R_{0.2}\text{Y}_{0.8}(\text{Co}_{0.84}\text{Fe}_{0.16})_2$ compounds exhibit metamagnetic transitions in high magnetic fields.

The crystal lattice parameter (a) increases monotonically as the yttrium content (x) increases. At the same time, the Curie temperature concentration dependence shows a general tendency to decline, with a local maximum at $x = 0.6$ for compounds with Er and $x = 0.8$ for compounds with Ho. Presumably, this $T_C(x)$ dependence can be related to the inhomogeneous distribution of R and yttrium atoms via the crystal lattice in $8b$ site (clustering).

Extrema at intermediate yttrium concentrations are also observed in the dependences of magnetizations in a magnetic field of 90 kOe ($\sigma_{f.u.}$), remanent magnetization (σ_r), and coercive force (H_c), determined at a temperature of 5 K.

In a ferromagnetic compound containing 100% yttrium, along with the magnetic contribution to the entropy at the Curie temperature, a magnetocaloric effect is also observed in the low-temperature region below T_C . Further research is required to determine its nature.

This work has been supported by Russian Science Foundation (grant № 19-72-00038).

[1] M. Anikin, E. Tarasov, et al. J. Magn. Magn. Mater. **418** (2016), 181–187.

[2] M.S. Anikin, E.N. Tarasov, et al. Met. Sci. Heat Treat. **60** (2018), 522-527.

Ab-initio study of the electronic structure and magnetic properties of $\text{Ce}_2\text{Fe}_{17}$

Alena Vishina^a, Olle Eriksson^{a,b}, Heike C. Herper^a

^a Department of Physics and Astronomy, Uppsala University, Se-75120 Uppsala, Sweden

^b School of Science and Technology, Örebro University, SE-701 82 Örebro, Sweden

$\text{Ce}_2\text{Fe}_{17}$ with its high magnetization and low cost can be considered an attractive candidate for rare-earth (RE) lean permanent magnets. The drawback of this material is its low Curie temperature (T_C) and basal plane magnetocrystalline anisotropy. A large amount of experimental work, however, has been done on increasing the T_C and improving the other magnetic characteristics by doping [1, 2, etc].

$\text{Ce}_2\text{Fe}_{17}$ and $\text{Ce}_2\text{Fe}_{17-x}\text{Zr}_x$ structures have been studied experimentally since the 1970'ies. However, the results of these studies regarding the magnetic state of $\text{Ce}_2\text{Fe}_{17}$ vary a lot and sometimes contradict each other, with ferromagnetic, antiferromagnetic, and non-collinear states observed at the low temperatures. Theoretical investigations of this compound are not only scarce but also disagree with the existing experimental magnetic data (ex. [2]). Hence, we investigated carefully the best way of describing the electronic and magnetic structure of the material to reproduce the experimental findings.

The Local Density Approximation (LDA), Generalized Gradient Approximation (GGA) as well as the LDA+U correction scheme were used to obtain the relaxed crystal structure and the ground state magnetization using Vienna Ab Initio Simulation Package (VASP) [3].

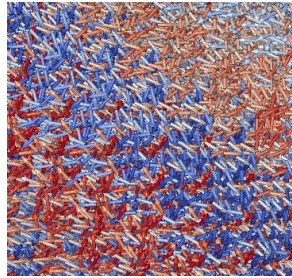


Figure 1: Non-collinear spin structure obtained for $\text{Ce}_2\text{Fe}_{17}$ with UppASD.

Different treatments of the Ce f -electron were considered as well to account for the mixed-valence state of Ce reported in several experimental works. The Curie temperature and magnetic state at the higher temperatures were determined using Monte Carlo simulations implemented within Uppsala Atomistic Spin Dynamics (UppASD) software [4] using the exchange parameters calculated with the RSPt code [5]. The results of each method were compared to experimental data.

We were able to show, that $\text{Ce}_2\text{Fe}_{17}$ ground state is noncollinear. The transition temperature of the helical state and q -vectors of the spin structure are in a good agreement with the experimental data.

-
- [1] Gary J. Long et al, JMMM **176** (1997), 217-232.
 - [2] T. Pandey and D.S. Parker, Phys. Rev. Applied. **13** (2020), 034039.
 - [3] G. Kresse and J. Hafner, Phys. Rev. B, **47** (1993), 558.
 - [4] O. Eriksson et al, "Atomistic Spin Dynamics: Foundations and Applications" (2017).
 - [5] J.M. Wills and B.R. Cooper, Phys. Rev. B, **36** (1987), 3809.

3D printing of Magneto-Responsive Polymeric Materials with Tunable Mechanical and Magnetic Properties by Digital Light Processing

Simone Lantean^{a,b}, Gabriele Barrera^c, Candido F. Pirri^{a,d}, Paola Tiberto^c, Marco Sangermano^a, Ignazio Roppolo^a, Giancarlo Rizza^b

^a Politecnico di Torino, Torino, Italy

^b CEA/DRF/IRAMIS, Ecole polytechnique, CNRS, Institut Polytechnique de Paris, Palaiseau, France

^c INRiM, Torino, Italy

^d Istituto Italiano di Tecnologia, Torino, Italy

Changing the shape of 3D printed objects is nowadays one of the most important challenges for additive manufacturing (called 4-dimensional printing). Among the different strategies, an accessible pathway to fabricate stimuli-responsive printed objects consists in magnetizing a soft-polymer by loading the polymeric matrix with ferromagnetic fillers, such as magnetite (Fe_3O_4) particles.

In this work we used Digital Light Processing (DLP) for printing magneto-responsive polymeric materials with tunable mechanical and magnetic properties. In DLP, a digital light projector illuminates a photocurable resin loaded with Fe_3O_4 particles by means of a two-dimensional pixel pattern obtaining high-resolution 3D objects with complex shapes (see fig. 1a).

Mechanical properties were tailored, from stiff to soft, by combining urethane-acrylate resins with butyl acrylate as the reactive diluent. Moreover, the magnetic response of the printed samples was tuned by changing the Fe_3O_4 nanoparticle loading up to nominal 6 wt% (see fig 1b). Following this strategy, we fabricated magneto-responsive active components with programmable complex functions using external magnetic fields gradient. Different objects were printed varying stiffness and magnetic responses, probing different kinds of movements, such as rolling, translation, stretching, shape-shifting and folding/unfolding.

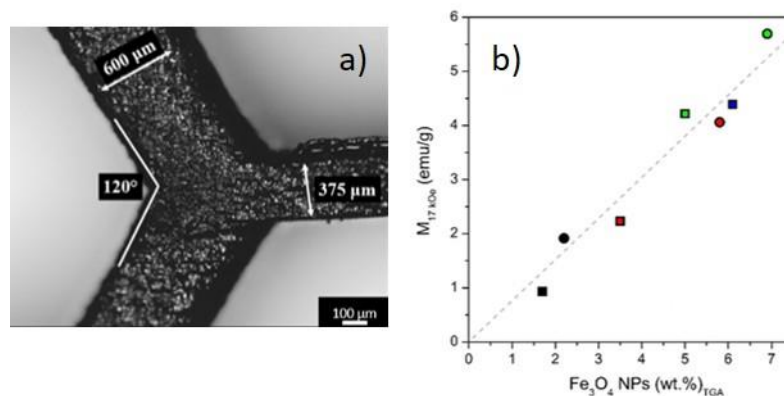


Figure 1: a) Detail of the 3D printed hexagons; b) evolution of magnetization (at $H = 17$ kOe) values for the 3D printed magnetic polymers (75Eb25BA squares and 50Eb50BA circles) as a function of Fe_3O_4 nanoparticles concentration estimated by TGA measurements (dotted line is a guide to the eyes).

Advances in Magnetism 2020-21, June 13-16, 2021

Spin waves and magnonics

Skyrmions

Abstracts can be easily browsed through the bookmarks

Spin wave beams in multilayer magnonic crystals

Sergey Odintsov^a, Evgeniy Beginin^a, Sergey Nikitov^b, Alexandr Sadovnikov^a

^a Saratov State University, Saratov, Russia

^b Kotelnikov Institute of Radioengineering and Electronics, Russian Academy of Sciences, Moscow, Russia

The study of spin-wave transport in multilayer structures of yttrium-iron garnet (YIG) films with a thickness in nanometer up to micron range and in the gigahertz and sub-terahertz frequency ranges[1,2] has been of great interest. Investigations of the transfer of spin momentum in planar and multilayer magnetic structures make it possible to reveal that spin waves(SW) could potentially be used as data carriers in low energy computing devices [3]. In this work, we combine the ideas of using the lateral and vertical spin-wave transport along with the frequency selective properties of the magnonic crystals

We investigate bi-layer four-channel spin-waveguiding structure, which we refer to as MCS. Each single magnonic crystal structure were placed one above the other and was separated with a vertical gap by the transparent mica layer.

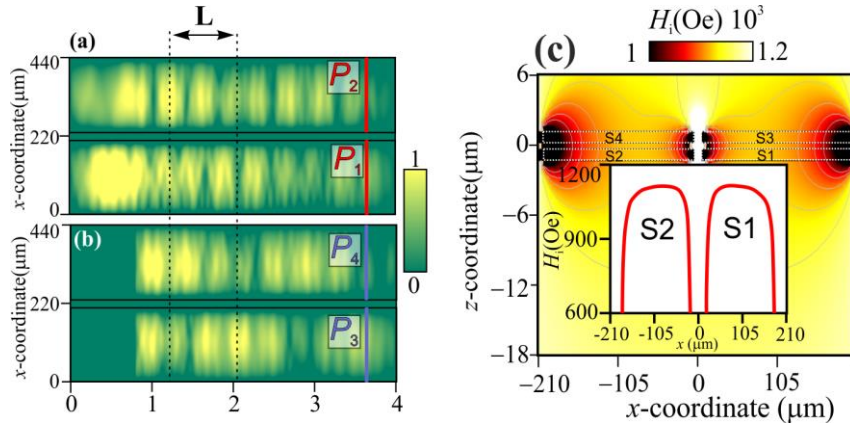


Figure 1: Maps of component m_z of dynamic magnetization in bottom layer (a), top layer (b); distribution of the internal magnetic field H_i (inset: H_{ix} profile for the lateral system of the bottom layer)(c)

The possibility of transferring the angular momentum in the lateral and vertical directions and spatial-frequency selection of the spin-wave signal has been demonstrated. It is shown that the revealed method of spin-wave transport control can find application in the fabrication of magnonic logic elements based on the principles of spatial-frequency selection of a microwave signal in multilayer topologies of magnonic networks.

This work was supported by RFBR (Grants No.19-37-90079, 18-29-27026)

[1] V. V. Kruglyak, S. O. Demokritov, and D. Grundler, J. Phys. D: Appl. Phys.43, 264001 (2010)

[2] V. E. Demidov, S. Urazhdin, A. Anane, V. Cros, and S. O. Demokritov, Journal of Applied Physics127, 170901

[3]S.A. Odincov, A.A.Grachev, S.A.Nikitov,A.V.Sadovnikov // Journal of Magnetism and Magnetic Materials. Vol. 500, 166344, 2020.

Spin-wave prorogation and spatial-frequency separation in a lateral non-identical system of coupled magnonic crystals with defect zone.

Vladislav Gubanov^a, Alexandr Sadovnikov^a.

^a Laboratory «Magnetics Metamaterials», Saratov State University, Saratov, Russia

The study of physical principles that determine the possibility of using spin waves (SW) to create information signal processing devices based on magnonics principles is of great interest [1]. Microstructures based on the iron-yttrium garnet (YIG) can be used in the processing of spin-wave signals due to the low attenuation. To control the properties of propagating SW, the method of structuring YIG films and creating irregular micro- and nanoscale waveguides, including structures with broken translational symmetry, can be used [2,3].

The structure (see fig. 1) based on film gadolinium garnet (GGG) with dimensions ($W \times D \times T$) $740 \mu\text{m} \times 10000 \mu\text{m} \times 500 \mu\text{m}$. On the surface of the GGG film, both magnonic crystals are formed an YIG film with thicknesses $t_1 = 10 \mu\text{m}$ (wide area) and $t_2 = 8.5 \mu\text{m}$ (narrow area), and magnon crystal widths $w_1 = 200 \mu\text{m}$ (narrow magnonic crystal) and $w_2 = 500 \mu\text{m}$, (wide magnonic crystal) and the gap between magnon crystals $g = 40 \mu\text{m}$. The period of the magnonic crystal λ is $200 \mu\text{m}$. The saturation magnetization of the YIG film is 139 G. Each magnonic crystal is divided into three regions: regions with segment lengths l_1 and l_3 equal to $4700 \mu\text{m}$ and a bridge region with a length $l_2 = 600 \mu\text{m}$, which corresponds to the Fabry-Perot resonance.

By the means of Brillouin light scattering technique, we obtained 2-D intensity maps of the SW propagating in the structure for case spin wave excitation on narrow magnonic crystal. The possibility of controlling the intermode coupling of SW propagating in observed structure near

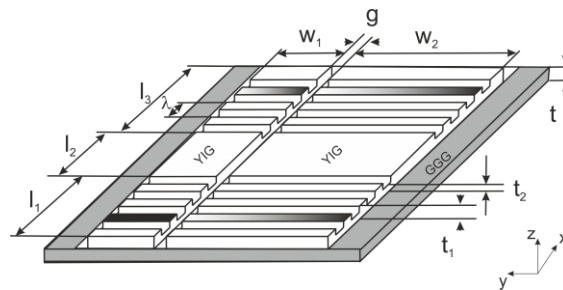


Figure 1. Scetch of lateral non-identical system of coupled magnonic crystals with defect zone.

the band gap frequency of the transmission zone is demonstrated. Based on the results of micromagnetic modeling, the mechanism that accompanies the observed mode of intermode coupling in the lateral non-identical system of coupled magnonic crystals with defect zone is determined, and the spatial-frequency signal separation modes are studied.

This work was supported by the Russian Science Foundation (project no. 20-79-10191).

-
- [1] D Sander et al 2017 J. Phys. D: Appl. Phys. **50** 363001
 - [2] A.V. Sadovnikov, A.A. Grachev, V.A. Gubanov, Appl. Phys. Lett. **112** (2018), 142402.
 - [3] A. V. Sadovnikov, V. A. Gubanov, S. E. Sheshukova Phys. Rev. Applied. **9** (2018) 051002

Anisotropy control in the meander structure of permalloy with tangential magnetization.

Vladislav Gubanov^a, Yulia Gubanova^a, Natalia Noginova^b, Alexandr Sadovnikov^a.

^a Laboratory «Magnetics Metamaterials», Saratov State University, Saratov, Russia

^b Materials Science and Engineering, Center for Materials Research Norfolk State University, Norfolk, VA, USA

One of the methods for controlling anisotropy is the structuring of ferrimagnetic films. It has recently been shown that in structures with etching, spin-wave resonances can be excited [1]. In this work, the method of ferromagnetic resonance (FMR) is used to study the effect of the shape on the properties of propagation of spin waves. When using the FMR method, oscillations of the type of uniform precession of the magnetization vector are excited, caused by an alternating magnetic field (microwave field) perpendicular to the external constant magnetic field H_0 . An experimental and micromagnetic study of FMR peaks from the bias angle was carried out.

Numerical simulation of the structure under study was carried out by the finite difference method by solving the Landau - Lifshitz equation with Hilbert damping. The structure under study is a meander waveguide made of permalloy (20% Fe + 80% Ni) with a modulation period $p = 740$ nm [2, 3]. The thickness of the permalloy layer was $h = 50$ nm. The height of the entire periodic structure is $w = 170$ nm.

When a field is applied along the x-axis (when the vertical sections are unsaturated), one peak is observed in the plot, and when a field is applied along the z-axis (all segments are saturated), several FMR peaks are observed. Plotting the dependence of the FMR peaks on the bias angle at different thicknesses of the vertical segments of the meander structure, it was found that with a decrease in the thickness of the vertical section, the low-field and high-field branches converge.

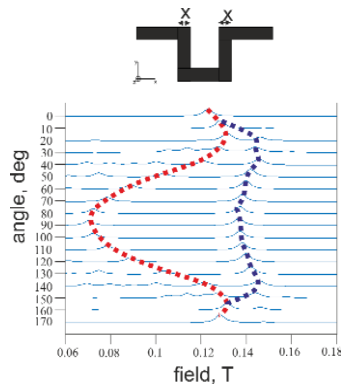


Figure 1. Dependence of FMR peaks on the bias angle

This work was supported by a grant from the Russian Foundation for Basic Research (No. 18-29-27026) and a grant from the President of the Russian Federation MK-1870.2020.9.

-
- [1] A. V. Sadovnikov, V. A. Gubanov, S. E. Sheshukova, Yu. P. Sharaevskii, S. A. Nikitov Spin-wave drop filter based on asymmetric side-coupled magnonic crystals// Phys. Rev. Applied. 9, 051002 (2018)
 - [2] Durach M, Noginova N // Phys. Rev. 2017, B 96 (19), 195411 .
 - [3] E.N. Beginin, A.V. Sadovnikov, V.K. Sakharov, A.I. Stognij, Y.V. Khivintsev, S.A. Nikitov, //JMMM, 492, (2019), 165647

Principles of Magnonic Qubit Formation

Yu. M. Bunkov

M-granat, Russian Quantum Center, Skolkovo, 143025 Moscow, Russia

Bose condensation of excited magnons has been observed in various magnetically ordered systems, such as superfluid ^3He [1, 2], antiferromagnets with coupled nuclear-electron precession [3], yttrium iron garnet (YIG) [4, 5], etc. It occurs when the density of magnons exceeds the critical one [6]. This coherent quantum state is uniquely suited to quantum computing. First, it exists at room temperature. The question of the thermal limit of using this phenomenon as a quantum qubit is open. Secondly, Bose condensate consists of a large number of particles in a single quantum state. Using part of them to read out the information does not destroy this state. Third, magnons qubits can be controlled and interacted with using photons, phonons, the Josephson effect, the Hall effect, etc. [7]. And besides, it is interference-resistant to RF noise over a wide frequency range. In general, a qubit based on a Bose condensate of magnons can combine the properties of known spin-based qubits, superconducting qubits and qubits based on atomic Bose condensation.

The review talk will consider the construction of qubits based on the interaction of two magnons condensates. The first experiments in this area have already been carried out on Bose condensates of magnons in superfluid ^3He [8] and in longitudinally magnetized YIG films [9, 10]. In our laboratory, we study the bound states of mBECs on out of plane magnetized YIG films. The first results have already been obtained for systems with two condensates coupled by means of photon, phonon, and magnons superfluid coupling. The creation of qubits on three or more interconnected mBECs will be considered. The question of entanglement of magnons condensates will also be discussed.

Financial support by the Russian Science Foundation within the Grant 19-12-00397 “Spin Superfluids” is gratefully acknowledged.

-
- [1] Yu. M. Bunkov and G.E. Volovik, *Phys. Rev. Lett.* 98, 265302 (2007).
 - [2] Yu. M. Bunkov, *Japan J. Appl. Phys.*, 26, 1809 (1987).
 - [3] Yu. M. Bunkov, et al., *Phys. Rev. Lett.* 108, 177002 (2012).
 - [4] Yu. M. Bunkov, et al., *JETP Lett.*, 111, 62 (2020).
 - [5] D. A. Bozhko, et al., *Low Temp.Phys.*, 41, 1024 (2015).
 - [6] Yu. M. Bunkov, and V. L. Safonov, *J. Magn. Magn. Mater.*, 452, 30 (2018).
 - [7] Yu. M. Bunkov, *JETP*, 131, 18 (2020).
 - [8] S. Autti, et al., *Nature materials.*, <https://doi.org/10.1038/s41563-020-0780-y> (2020).
 - [9] M. Mohseni, et al., *New J. Phys.*, 22, 083080 (2020).
 - [10] I. V. Borisenko et al., *Scientific Reports*, 10, 14881 (2020).

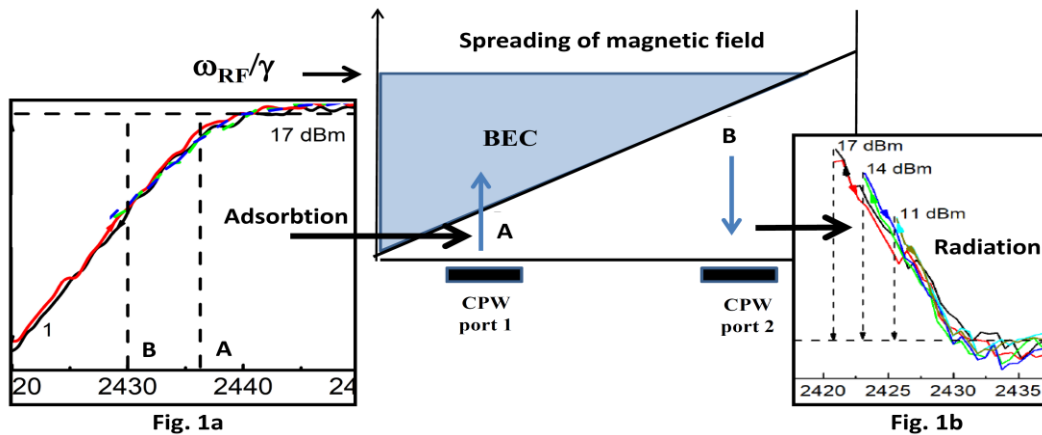
Bose condensation of magnons in a YIG film at a magnetic field gradient.

V. I. Belotelov^{a,b}, Yu. M. Bunkov^a, A.A. Kholin^b, G. A. Knyazev^a, A. N. Kuzmichev^a,
P. M. Vetoshko^a

^aRussian Quantum Center, Skolkovo, 143025, Moscow, Russia

^bCrimean Federal University. V.I. Vernadsky, 295007, Simferopol, Russia

We have investigated the formation of a Bose condensate of magnons in a perpendicularly magnetized yttrium iron garnet (YIG) film under high-frequency pumping. We used an ellipsoidal sample with dimensions of 5 mm x 1 mm and 6 μm thicknesses. We excited the magnons with a strip line located on one side of the ellipsoid, and recorded the magnon signal from the other side with the second strip line. The magnetic field gradient was directed between the stripe lines. The installation diagram can be found in [1]. We swept the magnetic field and observed the formation of the magnon state of coherent precession in the region of the first stripe line, the signal of which is shown in Fig. 1a. We also observed the formation of a state of magnon coherent precession of the second stripe line from the region of its location in a higher magnetic field (Fig. 1b). This signal appeared when the pump frequency was higher than the resonant field in this region. This experiment shows that the magnon Bose condensate (mBEC) fills the entire space in which the local magnetic field is less than the pumping frequency of magnons. We investigated the region of magnetic fields of existence of mBEC on the pump power. MBEC collapses when the supplied pump power cannot compensate for the magnon relaxation processes. In these experiments, the boson system of magnons behaves similarly to the boson-condensate of magnons in antiferromagnetic superfluid $^3\text{He-B}$, which was studied in detail earlier [2]. In conclusion, we note that the magnonic BEC forms a coherently precessing state with the properties of magnonic superfluidity [3,4].



This work was financially supported by the Russian Ministry of Education and Science, Megagrant project 075-15-2019-1934.

[1] P. M. Vetoshko, et al., JETP Letters 112, 290 (2020).

[2] Yu. M. Bunkov, J. Mag. Mag. Mat, 310, 1476 (2007).

[3] Yu. M. Bunkov, J. Appl. Mag. Res., (2020).

[4] Yu. M. Bunkov, and G. E. Volovik, "Spin superfluidity and magnon BEC" in "Novel Superfluids", eds. K. H. Bennemann and J. B. Ketterson, Oxford University press (2013).

Spin dynamics in $[\text{Co}_{60}\text{Fe}_{40}/\text{Pt}]_5$ multilayers investigated with femtosecond laser pulses

M. A. B. Tavares^a, L. H. F. Andrade^a, F. M. Matinaga^c, G. F. M. Gomes^{b,c}, M. M. Zapata^a, L. E. Fernandez-Outon^{a,c}, M. D. Martins^a

^a Nanotechnology, CDTN/CNEN, Belo Horizonte, M.G., Brazil

^b PPGMCS, Unimontes, Montes Claros, M.G., Brazil

^c Departamento de Física, UFMG, Belo Horizonte, M.G., Brazil

Using femtosecond light pulses to study ultrafast magnetization dynamics has been a fruitful approach for investigating magnetic materials and their applications [1]. It has been allowing a better understanding of magnetization dynamics at sub-picosecond timescales which is a pre-requisite for improving the speed and performance of current devices. Here we report on the ultrafast magnetization dynamics of $[\text{Co}_{60}\text{Fe}_{40}/\text{Pt}]_5$ multilayers grown with the same deposition conditions and thickness and which were synthesized over Pt buffers with varying crystallinity. The time-resolved measurements were carried out with 100 fs laser pulses from a Ti:Sapphire oscillator at low fluency (0.1 mJ.cm^{-2}) in a standard time resolved femtosecond magneto-optical setup and the results are presented in fig. 1. By fitting the experimental data with the Landau-Lifshitz-Gilbert equation, we may evaluate the effective damping parameter, α , for each sample which decreases from 0.2 to 0.05 (fig. 1a to 1d). Note that these values are higher than for single layers and may be correlated, as reported before in multilayers, to an enhanced scattering and spin pumping effects from the Pt adjacent layers.

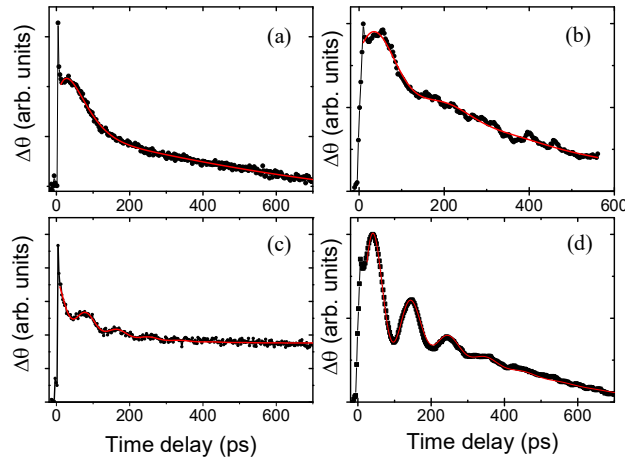


Figure 1: Damped precession of $[\text{Co}_{60}\text{Fe}_{40}/\text{Pt}]_5$ multilayers with varying structural properties (decreasing damping from (a) to (d)).

[1] A. Barman, J. Sinha, Spin Dynamics and Damping in Ferromagnetic Thin Films and Nanostructures, Springer (2017).

[2] M. A. B. Tavares et al, AIP Advances 9, 12, 125322 (2019).

Spin pumping by MSSW in YIG/n-InSb and YIG/Pt microstructures

Yuri Khivintsev^{a,b}, Yuri Nikulin^{a,b}, Valentin Sakharov^a, Michail Seleznev^{a,b}
Alexander Kozhevnikov^a, Sergei Vysotskii^{a,b}, Yuri Filimonov^{a,b}

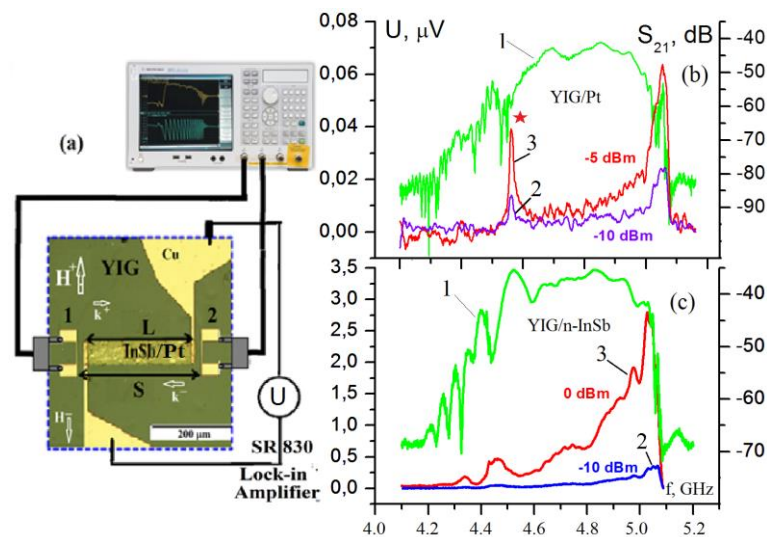
^a Kotel'nikov IRE RAS, Saratov Branch, Saratov, Russia

^b Chernyshevsky Saratov State University, Saratov, Russia

Detection of the spin waves (SW) in "conductor - magnetic dielectric" structures are interesting for information processing systems based on magnon spintronics [1]. In order to convert the spin current associated with the SW propagating in yttrium iron garnet (YIG) films into the electric current one can use Pt [2] or n-InSb [3] films. We studied and compared effects of the magnetostatic surface waves (MSSW) propagation and detection in YIG/n-InSb and YIG/Pt microstructures, see Figure (a).

Polycrystalline n-InSb and Pt films were sputtered on a top of $\approx 8 \mu\text{m}$ thick YIG film between π -shaped input (1) and output (2) antennas having length $\approx 100 \mu\text{m}$, width $\approx 10 \mu\text{m}$ and spaced at distance $S \approx 300 \mu\text{m}$, see Figure (a). Semiconductor film had thickness $\approx 500 \text{ nm}$, Hall mobility and electron concentration $\mu_e \approx 20000 \text{ cm}^2/\text{V}\cdot\text{s}$ and $n_e \approx 5.8 \cdot 10^{16} \text{ cm}^{-3}$, respectively. The Pt film had thickness $\approx 10 \text{ nm}$. Both n-InSb and Pt films have width $b \approx 100 \mu\text{m}$ and length $L \approx 200 \mu\text{m}$.

MSSW transmission (S_{21}) measurements were done using a vector network analyzer along with a microwave probe station for in-plane magnetic field $H \approx 940 \text{ Oe}$ applied along the antennas that corresponds to the excitation of MSSW (see curves 1 on Fig. (b) and (c)). DC voltage $U(f)$ generated at the edges of the InSb and Pt stripes due to the MSSW propagation was measured in carrier modulation (100 kHz) mode in order to separate the thermal voltage induced by the microwave heating of InSb and inertialess effects associated with the transfer of the MSSW impulse to the electrons of InSb. DC voltage linearly increase with incident microwave power and reached a maximal values near MSSW short wavelength cut-off frequency, see curves 2 and 3 on Fig. (b) and (c). In the YIG/Pt structure an additional peak of DC voltage was detected near long wavelength limit frequency, see asterisk on Fig. (b).



This work was supported by the RFBR grant No. 19-37-90099.

- [1] A.V. Chumak, et al *Nature Physic* **11** (2015) 453
- [2] M. Balinsky, et al. *IEEE Mag. Let.* **6** (2015) 3000604
- [3] B. Schneider *Physica Status Solidi* **23** (1974) 187

On the role of continuum models in the simulation, design and evaluation of magnetic skyrmion devices.

P. Robert Kotiuga^a,

^a ECE Dept., Boston University, Boston MA, USA

Computer gates and memory devices based on magnetic skyrmions are close to becoming a reality [1]. Skyrmion-based electronic devices are a subset of spintronic nanoscale devices based on chiral materials[2,3]. The Dzyaloshinskii-Moriya (D-M) interaction is a chiral magnetic interaction which models chiral magnetic materials showing particular promise for extending CMOS compatible Skyrmion electronics at, or below, 5 nm where silicon devices are no longer competitive[3]. This technology is a natural extension of the device physics underlying MRAM [4, 5]. The models used for nanoscale device design are phenomenological in nature and there are problems interpreting both boundary conditions and limiting conditions associated with singularities.

The purpose of this paper is to introduce a hierarchy of models for the design of such devices and to provide a solid foundation for the introduction of topological tools. The models are:

- 1) A lattice model which is a model of the physics at the atomic level. Very little analysis is performed at this level other than to observe that exchange coupling leads to an elliptic system of integro-differential equations associated with the Hamiltonian when a continuum model is made.
- 2) A continuum model which is used in the LLG equation. Regularity results about the elliptic principal symbol dictate the possibilities for topological phenomena associated with defects. It is only at this level that topological arguments can be made and a proper formulation of boundary conditions can be formulated.
- 3) Lattice systems associated with discretizations of the continuum model. Although these models can be interpreted in physical terms, they are not a substitute for the physics that can be formulated in terms of the actual quantum physics associated with the atomic lattice.

In this paper we show that the interplay between these three types of models leads to geometric and topological formulations of issues associated with defects and boundary conditions [6], a clearer understanding of the use of the LLG equation in the nanoscale devices, as well as a more geometric connection to the mathematical formalism used to describe quantum phenomena. In the process, the role of chirality emerges more cleanly and it points to the role of topology in the possibility of near reversible computing generating a minimum of entropy and heat [7, 8, 9]. Finally, by appealing to Morse theory applied to lattice systems arising from the discretization of the continuum models, the author formulates a notion of “topological frustration” which provides a framework for understanding “complexity” in the context of such systems.

-
- [1] K. Everschor-Sitte, J. Masell, R. M. Reeve, and M. Kläui, Magnetic skyrmions—Overview of recent progress in an active research field, *J. Appl. Phys.* **124**, 240901 (2018); <https://doi.org/10.1063/1.5048972>
 - [2] Kang, W., Huang, Y., Zhang, X., Zhou, Y., Zhao, W., “Skyrmion-Electronics: An Overview and Outlook”, *Proc. IEEE*, vol. 104, no.10, Oct 2016; pp 2040-2061.
 - [3] Schütte, C., Rosch, A., “Dynamics and energetics of emergent magnetic monopoles in chiral magnets”, *Phys. Rev. B*, vol. 90, 174432 (2014).
 - [4] Engel-Herbert, R., Locatelli, A., Cherifi, S., Schaadt, D. M., Mohanty, J., Ploog, J.H., Bauer, E., Belkhou, R., Heun, S., Pavlovska, A., Leo, T., Hesjedal, T., “Investigation of magnetically coupled ferromagnetic stripe arrays”, *Applied Physics A*, vol 84, 2006, pp 231-236, DOI: 10.1007/s00339-006-3619-8
 - [5] Kazemi, M., Rowlands, G.E., Ipek, E., Buhrman, R.A., Friedman, E.G., “Compact Model for spin-Orbit magnetic Tunnel Junctions.” *IEEE Trans ELECTRON DEV*, vol. 63, no. 2, FEB.2016, pp 848-855.
 - [6] Kotiuga, P. R., “Weitzenböck Identities and Variational Formulations in Nanophotonics and Micromagnetics”. *IEEE Trans. MAG*, vol. 43, no. 4, April 2007, pp1669-1672.
 - [7] Kotiuga, P.R., “The Algebraic Topology of Bloch Points”, *IEEE Trans. MAG*, vol. 25, no. 5, Sept. 1989, pp. 3476-3478.
 - [8] Kotiuga, P.R., Toffoli, T., “Potential for Computation in Micromagnetics via Topological Conservation Laws”, *Physica D*, vol. 120, 1998, pp. 139-161.
 - [9] Kotiuga, P.R., Giles, R.C., “A Topological Invariant for the Accessibility Problem of Micromagnetics”, *Journ. Applied Phys.*, vol. 67 no. 9, May 1990, pp. 5347-5349.

Nanopatterning multidimensional spin-textures: from magnetic domains to topological solitons.

Edoardo Albisetti^{a, b}, Daniela Petti^a, Giacomo Sala^a, Silvia Tacchi^c, Simone Finizio^d,
Sebastian Wintz^d, Jörg Raabe^d, Paolo Vavassori^e, Matteo Pancaldi^e,
Elisa Riedo^f, Riccardo Bertacco^a.

^aDipartimento di Fisica, Politecnico di Milano, 20133 Milano, Italy.

^bAdvanced Science Research Center, New York, NY 10031, USA.

^cIstituto Officina dei Materiali del CNR (CNR-IOM), Unità di Perugia, c/o Dipartimento di Fisica e Geologia, Perugia, Italy.

^dPaul Scherrer Institute, Forschungsstrasse 111, 5232, Villigen, PSI, Switzerland.

^eCICnanoGUNE, E-20018 Donostia-San Sebastian, Spain.

^fTandon School of Engineering, New York University, New York NY 11201, USA

Spin-textures, i.e. non-uniform spin-configurations in magnetic materials, are interesting due to their scalability, robustness and rich phenomenology. In particular, magnetic domain walls and topological solitons, such as vortices and skyrmions, are attractive both as active components in spintronic and spin-wave devices, and as information bits for data storage applications. In this framework, finding new methodologies for stabilizing and controlling the topology of nanoscale spin-textures is highly appealing.

Here, we show some strategies, based on the recently developed thermally assisted magnetic scanning probe lithography technique (tam-SPL) [1], for stabilizing and deterministically controlling the topology of spin-textures, by crafting at the nanoscale the unidirectional anisotropy landscape of exchange bias systems.

In particular, we show that 2-D magnetic domains, 1-D domain walls and 0-D vortices and antivortices with deterministic topology can be stabilized in continuous IrMn/CoFeB films magnetized in-plane (see e.g. Figure 1). [2, 3] Furthermore, we show that the same concept can be applied to synthetic antiferromagnets (SAF) [4], composed by two antiferromagnetically coupled ferromagnetic layers, for patterning tailored domain walls and vortices. Finally, we show that chiral spin-textures such as domains walls and skyrmions can be deterministically stabilized in out-of-plane magnetized IrMn/CoFeB/MgO systems characterized by perpendicular exchange bias and Dzyaloshinskii-Moriya interaction.

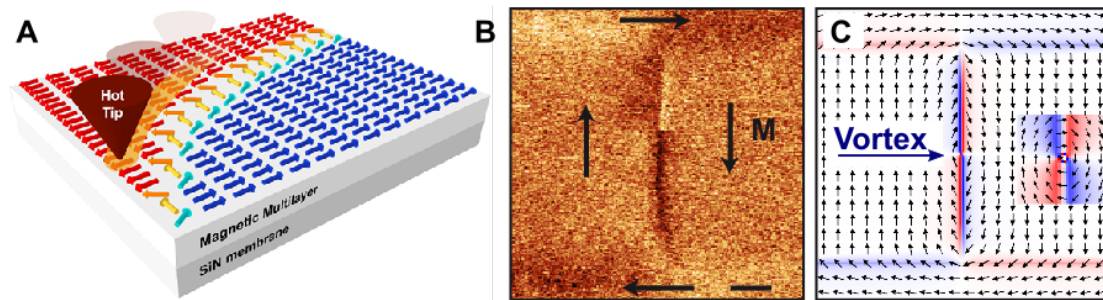


Figure 1. A. Sketch of tam-SPL patterning. B, C. Magnetic Force Microscopy (MFM) image and micromagnetic simulation of a patterned topological soliton within a Néel domain wall in a continuous CoFeB/IrMn/Ru stack. Scale bar: 3 μm .

[1] E. Albisetti et al., Nat. Nanotechnol. **11** (6) (2016), 545–551.

[2] E. Albisetti et al., App. Phys. Lett. **113** (2018), 162401.

[3] E. Albisetti et al., Commun. Phys. **1** (2018), 56.

[4] E. Albisetti et al., submitted. (arXiv preprint: 1902.09420).

The complete picture: real-space imaging of confined magnetic skyrmion tubes

Max T. Birch^{a,b}, D. Cortés-Ortuño^c, L. A. Turnbull^a, M. N. Wilson^a, F. Groß^d,
N. Träger^d, A. Laurenson^e, N. Bukin^e, S. H. Moody^a, M. Weigand^d,
G. Schütz^d, H. Popescu^f, R. Fan^b, P. Steadman^b, J. A. T. Verezhak^g,
G. Balakrishnan^g, J. C. Loudon^h, A. C. Twitchett-Harrison^h, O. Hovorka^c,
H. Fangohr^{c,i}, F. Y. Ogrin^e, J. Gräfe^d and P. D. Hatton^a

^a Department of Physics, Durham University, DH1 3LE, UK

^b Diamond Light Source, Harwell Innovation Campus, Didcot, OX11 0DE, UK

^c Engineering, University of Southampton, Southampton SO17 1BJ, UK

^d Max Planck Institute for Intelligent Systems, 70569 Stuttgart, Germany

^e School of Physics and Astronomy, University of Exeter, Exeter, EX4 4QL, UK

^f Synchrotron SOLEIL, Saint Aubin, BP 48, 91192 Gif-sur-Yvette, France

^g Department of Physics, University of Warwick, Coventry, CV4 7AL, UK

^h Department of Materials Science and Metallurgy, University of Cambridge,
Cambridge, CB3 0FS, UK

ⁱ European XFEL GmbH, Holzkoppel 4, 22869 Schenefeld, Germany

Magnetic skyrmions are topologically nontrivial particles with a potential application as information elements in future spintronic device architectures. While they are commonly portrayed as two-dimensional objects, in reality magnetic skyrmions are thought to exist as elongated, tube-like objects extending along the applied magnetic field direction. Study of this skyrmion tube state is highly relevant for investigating skyrmion metastability and for implementation in recently proposed magnonic computing. However, direct experimental imaging of skyrmion tubes has yet to be reported. Here, we demonstrate the first real-space observation of skyrmion tubes in a lamella of FeGe using resonant magnetic x-ray imaging and comparative micromagnetic simulations, confirming their extended structure. Representative results are displayed in Fig. 1. The formation of these structures at the edge of the sample highlights the importance of confinement and edge effects in the stabilisation of the skyrmion tube state, opening the door to further investigations into this unexplored dimension of the skyrmion spin texture.

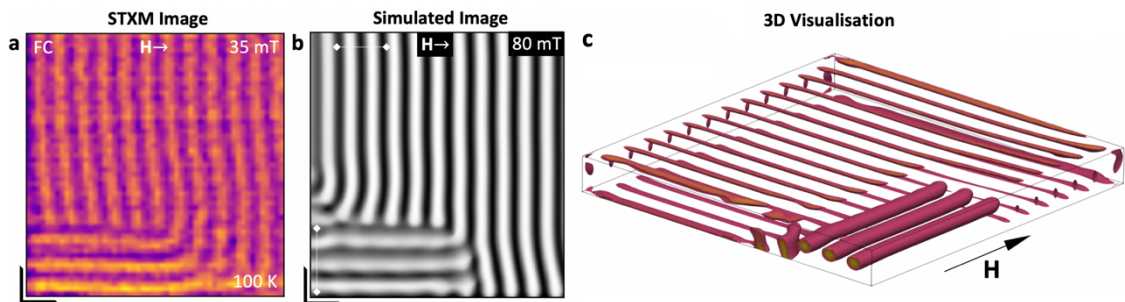


Figure 1: Experimental observation and micromagnetic simulations of skyrmion tubes. **a**, Scanning transmission x-ray micrograph of the skyrmion tube spin texture embedded in the conical state in an FeGe lamella. The colourmap plots the normalised out-of-plane magnetisation averaged through the thickness of the sample, m_z . **b**, Comparative simulated image of the skyrmion tube state. The black L-shape in **a** and **b** indicates the location of the corner of the sample. **c**, Three dimensional visualisation of the micromagnetic simulation of the skyrmion tube state, achieved by plotting all cells with $m_y < 0$.

Spin-orbit torque

Magnetic recording, magnetic memories and sensors

Magnetic levitation and bearings, electrical machines and other electromagnetic devices

Electromagnetic non-destructive testing

Numerical and analytical model of an antiferromagnetic terahertz detector

Vito Puliafito^a, Ansaf Safin^{b,c}, Israa Medlej^d, M. Carpentieri^e, B. Azzarboni^a, A. Slavin^f, G. Finocchio^a

^a University of Messina, Italy

^b Kotelnikov Institute of Radioengineering and Electronics, R.A.S., Moscow, Russia

^c National Research University “Moscow Power Engineering Institute”, Russia

^d Lebanese University, Hadeth Beirut, Lebanon

^e Politecnico di Bari, Italy

^f Oakland University, Rochester, MI, USA

Terahertz technology is attracting a lot of attention in the scientific community for the intriguing properties of that frequency gap. Spintronics, in particular, is focusing on this topic studying antiferromagnetic materials which generally host fast dynamics [1-2].

In this field of research, a full micromagnetic framework for studying magnetization dynamics of antiferromagnets (AFMs), in particular under the influence of spin-orbit-torques, has been developed and compared successfully with analytical models [3]. The magnetization dynamics of current-driven AFMs is described as dynamics of two exchange-coupled sub-lattices by solving two Landau-Lifshitz-Gilbert equations including a torque term due to the spin-Hall effect. The exchange coupling of the sub-lattices includes the inhomogeneous intra-lattice, the homogeneous inter-lattice, and the inhomogeneous inter-lattice contributions.

Within this micromagnetic framework, we performed modeling of an AFM spin-Hall oscillator [3,4]. In our numerical study, the oscillator consists of an AFM layer (40x40x5 nm³) having a uniaxial anisotropy and coupled to a layer of a heavy metal. The AFM dynamics is described as precession of two coupled sub-lattice magnetizations \mathbf{m}_1 and \mathbf{m}_2 around the polarization \mathbf{p} of the spin-Hall current, and may show a hysteretic behavior. The frequency of the generated signal shows a blue-shift with the increase of the applied current, from hundreds of GHz up to several THz, as expected [3]. In particular, the AFM oscillator demonstrates an interesting behavior in the sub-threshold regime. We studied the AFM resonance frequency (AFMR) of the oscillator, which defines the spectral “gap” of the device, as a function of different parameters. The most important result is that the AFMR frequency decreases with the increase of the direct electric current applied to the heavy metal, and converges to the self-oscillation frequency at and above the threshold current. This result, which agrees with a previous analytical model, demonstrates the possibility to use the sub-threshold oscillator as a current-tunable signal detector of a resonance type in the THz frequency range.

-
- [1] Jungwirth et al. Nat. Phys. **14** 200 2018.
 - [2] Gomonay et al. Phys. Status Solidi RRL **11** 1700022 2017.
 - [3] Puliafito et al. Phys. Rev. B **99** 024405 2019.
 - [4] Khymyn et al. Sci. Rep. **7** 43705 2017.

Mutual phase locking of the nonlinear THz-frequency antiferromagnetic spin-Hall oscillators

Ansar Safin^{a,b}, Sergey Nikitov^a, Andrei Slavin^c, Vasyl Tiberkevich^c

^a Kotel'nikov Institute of Radioengineering and Electronics, Russian Academy of Sciences, Moscow, Russian Federation

^b National research university "MPEI", Moscow, Russian Federation

^c Oakland University, Rochester, Michigan, United states

The terahertz (THz) frequency range is receiving great attention because of its many applications [1], such as ultrahigh speed communication, THz-imaging and sensing and many others. The development of the efficient and compact THz sources and detectors is one of the attractive technical problem of modern microwave and THz technology. There are many different ways to generate THz waves, such as quantum cascade lasers, free-electron lasers, superconducting Josephson junctions, etc. The majority of these THz sources cannot be made sufficiently compact and/or require low temperatures, and limits their usability in real applications.

Spintronics of antiferromagnets (AFMs) have great potential to generate THz signals [2] because of the numerous physical effects: display ultrafast dynamics, produce no stray fields, and capable of generating large magnetotransport effects. In [3] it is calculated the output radiation power of the single AFM-based spin-Hall oscillator (SHO), and it is shown that this power increases with the increase of working frequency. However, the output power of SHO-based devices needs to be improved because the THz power emitted from a single oscillator is approximately on the order of nanowatts and picowatts, which is too weak for real practical applications. One of the best ways to increase the output power of the spintronic-based THz-source is to use the effect of phase locking (synchronization). Previously in [4], [5] it was shown, that AFM SHO can be effectively phase-locked to a driving ac electrical signal at different external frequencies.

In this work, we propose and theoretically study the dynamics of a pair of mutually coupled by the common electrical current AFM SHOs. When referring to the mutual locking of the Neel phases φ_n we mean, that both average and oscillating frequencies are equal over a short time. We demonstrate numerically that in typical parameters (for nickel oxide) by variation of a DC electrical current it is possible to find the phase-locking interval for a non-identical SHOs. In the presence of an additive Gaussian noise the spectral linewidth of the output oscillations in the phase locking interval decreases. All these results could be used to construct large arrays of mutual coupled THz-frequency SHOs..

[1] Zhang X.-C., Xu J. Introduction to THz Wave Photonics. Springer, 246 p (2010).

[2] Baltz V. et al // Rev. of Mod. Phys. Vol. 90. 015005 (2018).

[3] Sulymenko O. et al. // Phys. Rev. Appl. Vol. 8. 064007 (2017).

[4] Khymyn R. et al. // Book of abstracts "Intermag – 2018". P. 795 (2018).

[5] O. Gomonay, T. Jungwirth and J. Sinova, <https://arxiv.org/pdf/1712.02686.pdf> (2017)

Local magnetization reversal in FeGa magnetic nanostructures

G. Pradhan^a, G. Barrera^a, F. Celegato^a, M. Coisson^a, P. Tiberto^a

^a Advanced materials and Life science Divisions, INRiM, Torino, Italy

The recent advances in nanofabrication techniques have given a boost to the study of artificially patterned nanostructures for future applications in catalysis, photonics, sensing and for fabricating smart, multifunctional systems. In case of magnetic nanostructures, the quest of the last two decades was to create and understand new materials and phenomena to gain advances in high density magnetic storage, sensor technology and magneto-logic devices.

Large-area arrays of nanostructures are fabricated by several methods, either top-down (laser writing) or bottom-up (self-assembly). Generally, conventional top-down methods lead to highly ordered, small area patterns due to the sequential nature of the writing process, which, together with the high cost of equipment, limits widespread applications. Alternative bottom-up techniques have been explored for the preparation of large-area patterned structures despite being less-ordered. Among the important properties that need to be investigated, magnetization processes as a function of the applied magnetic field in patterned magnetic structures are of utmost importance. In order to gain an insight on such processes in individual patterned structures, available high-sensitivity magnetometry techniques, or optical Kerr-effect microscopes lack the required sensitivity and space resolution. Magnetic force microscopy (MFM) is a technique that offers excellent space resolution but limited possibility of investigating the magnetic-field dependence of the magnetization.

In this work, different patterned magnetic structures have been produced exploiting either Laser writing lithography or self-assembling of polystyrene nanospheres. Magnetization processes have been studied by MFM in individual FeGa nanostructures having different dimensions. Nanodots fabricated using laser lithography have a diameter between 1 μm to 2 μm (Fig 1(b)) as observed by Scanning electron microscopy (SEM). With nanosphere lithography, we obtained lower dimensions of dots ($d \sim 350\text{-}400\text{ nm}$) shown in 1(e). The magnetic hysteresis measurements were performed using Alternating gradient field magnetometer (AGFM). The magnetic states are recorded using MFM as a function of applied field along the film plane (Fig (c) and (f)). The difference in phase contrast at different field reveals the change in magnetic state of the nanodots by both laser and self-assembly lithography. Also, the nanodots were prepared for different composition of FeGa (having different magnetostrictive constant) at 70:30 and 80:20 (Fe:Ga) and magnetization processes were studied.

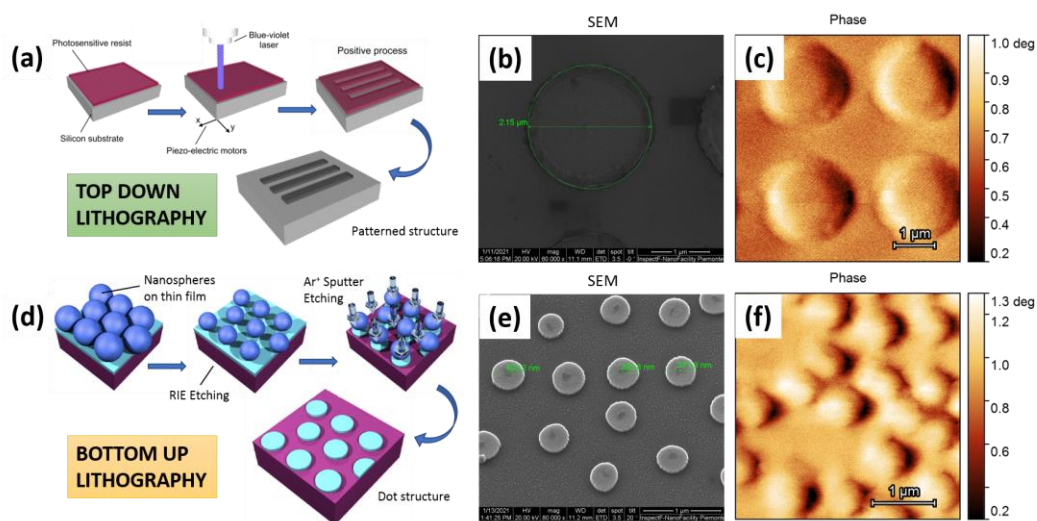


Figure 1: Schematic of Laser and Self-assembly lithography is shown in (a) and (d), respectively. (b) and (e) shows the SEM images and the MFM recordings at saturation field are represented by (c) and (f) of the nanodots fabricated by top-down and bottom-up lithography, respectively. The scale bar is 1 μm .

research on the performance of DC-DC Converter based on electrical steel sheet and ferrite mixed core for medium frequency transformer

Wang Yang^a, Chen Dezhi^a, Cao Xiongxiang^a, Zhang Shichong^a

^a Shenyang University of Technology

In order to improve the thermal stability of DC-DC converter, to reduce the vibration/noise, cost savings, based on the electrical steel piece of ferromagnetic material and ferrite material both can be complementary, this paper puts forward using electrical steel mixed with ferrite core structure, composition of DC-DC converter in the intermediate frequency transformer core, to further improve the performance of medium frequency transformer.

Firstly, based on the magnetic properties measuring device of electrical steel and ferrite, the magnetic properties of electric steel and ferrite at different temperatures and frequencies were measured respectively, and the B-H curve, B-P curve and magnetic permeability curve of electrical steel and ferrite materials at different frequencies and different temperatures were given; Secondly, based on the improved genetic algorithm with medium frequency transformer loss minimum, vibration and noise minimum, lowest cost as the optimization goal, design a based on electrical steel and ferrite core of 20 kW medium-frequency transformer, main structure as shown in figure.1, the medium frequency transformer and using 3D electromagnetic field finite element method, the three-dimensional finite element model is established, on the joint simulation of power electronic control and high-frequency transformer ontology is given of medium frequency transformer core flux density under different load conditions, core loss and winding loss and the temperature rise distribution; Finally, a prototype was developed based on the design scheme, and an experimental platform for DC-DC converter was built. Experimental research was carried out on the DC-DC converter under different load conditions to verify the performance superiority of the combined core material of electrical steel sheet and ferrite and the correctness of the proposed scheme.

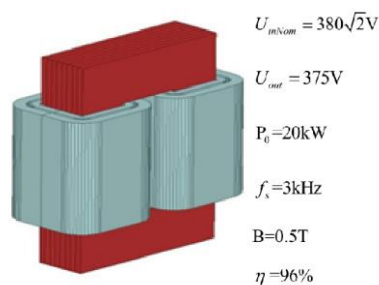


Figure 1: medium-frequency transformer main structure

It provides guidance for the design of intermediate frequency transformer. See the detailed experimental results and content in the full text.

Study on core loss of thin silicon steel medium frequency transformer

Xiongxiang Cao^a, Dezhi Chen^a, Yang Wang^a, Shichong Zhang^a, Baodong Bai^a

^a School of Electrical Engineering, Shenyang University of Technology, Shenyang, China

The calculation of core loss and winding loss is a key step in transformer temperature rise control and optimization design. This paper investigates the loss model of a 2kHz, 20kW three-winding medium frequency transformer using 0.15mm oriented silicon steel sheet. First, the magnetic properties of silicon steel wafers at 2 kHz were measured based on a single silicon steel wafer magnetic property measurement system. The B-H curve, B-P curve and excitation power curve were obtained at 2 kHz and at room temperature. Next, utilize the MSE (modified Steinmetz equation) to calculate the loss of 0.15mm silicon steel sheet under non-sinusoidal excitation[1]. And FEA simulation of an medium frequency transformer with an input of 537V to obtain core loss parameters; compare the simulation data with the theoretical calculation data. Finally, The characteristics of the medium frequency transformer under different load conditions (no-load, rated load, and overload) are experimentally studied to verify the correctness of the proposed scheme.

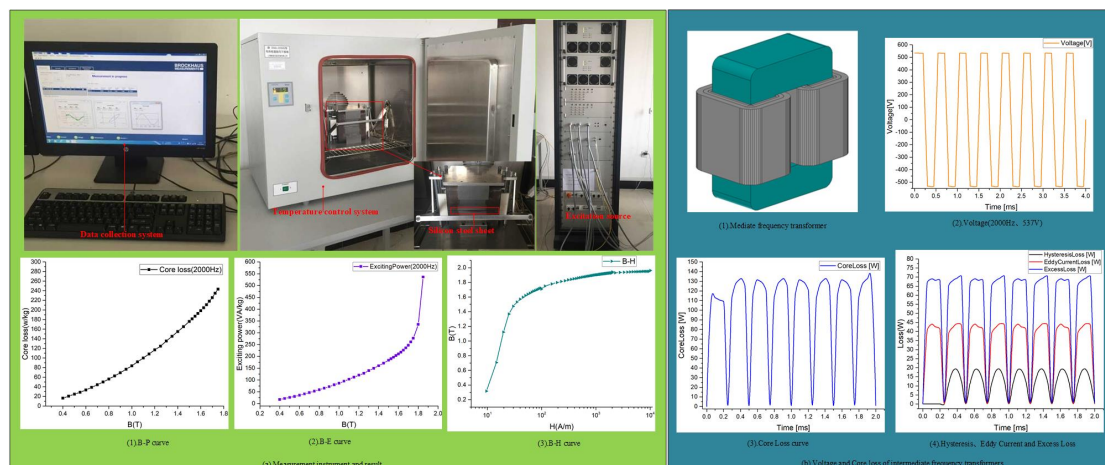


Figure 1: (a): Measurement instrument and result B-P, B-E and B-H curve (b): Voltage and Core loss of mediate frequency transformers.

This paper based on the monolithic silicon steel wafer measurement system, the test work of magnetic characteristics of silicon steel wafers at 2kHz was completed. A mediate frequency transformer 3D FEA model with electromagnetic loss field coupling was established to analyse the magnetic properties and core losses characteristics of the under different operating conditions. Detailed experimental results and comparisons are shown in the full paper.

[1] Reinert J, Brockmeyer A, De Doncker R W A. Calculation of losses in ferro-and ferrimagnetic materials based on the modified Steinmetz equation[J]. Industry Applications, IEEE Transactions on, 2001, 37(4): 1055-1061.

Analytical Design, Analysis and Experimental Validation of Planar Induction Heating Coil for Domestic Induction Cooker

Dae Yong Um, Min Jae Kim, Ho Yeong Lee, Jung Min kim, Gwan Soo Park

Pusan National University, Busan, South Korea

This paper presents an analytical design procedure for designing a planar inductor for domestic induction cookers. Induction heating technologies have been already mature, but quantitative design and analysis are still complicate due to the behaviour of eddy current and hysteresis effect [1], [2]. Therefore, each component in induction heating coil should be investigated more detailed. This paper covers planar coil, which is widely used in wireless power transfer including induction heating devices. An application for domestic induction cooker is selected because it has typical parts of wireless power transfer system [3]. A 3-D structure of the induction cooker, as shown in Figure 1, was transformed into a simple axisymmetric problem for analytical calculation. In 3-D structure, arrangement of ferrite core and end-effect of both vessels and ferrite core affecting the electromagnetic performance are analyzed by using finite element analysis (FEA). Then, a correction method to consider the 3-D geometry of induction cooker is presented. In addition, a vessel is generally ferromagnetic material so that a nonlinear calculation should be considered. To avoid the complexity due to iterative calculation, the magnetization curve was simply formulated.

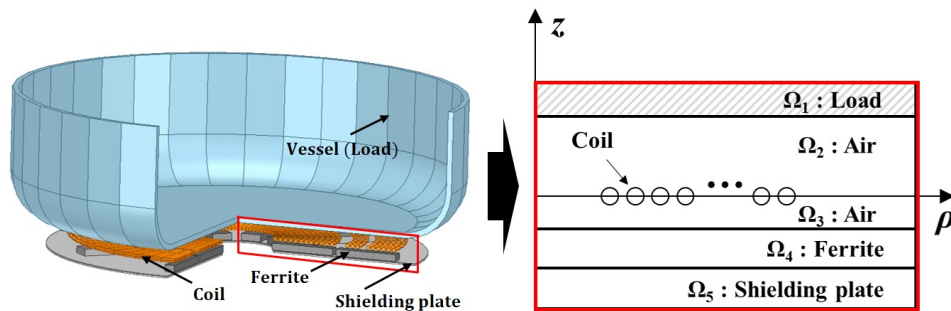


Figure 1: Schematic diagram of domestic induction cooker and an axisymmetric model for the analytical formulation of induction heating problem

Prior to an inductor design, it is necessary to predict the heat source inside a vessel and the separation of losses in the inductor accurately. In this paper, both theoretical developments and experiments were conducted to estimate the eddy current loss and hysteresis loss in vessels. Static hysteresis characteristics was measured by making specimens of typical material used in vessels. The hysteresis loss was calculated and the result was used as a look-up table for calculating the heat source more precisely. The loss in wires was also dealt in terms of a solid wire and litz wire. The eddy currents in both wires was calculated and the calculation suggests the criteria to select a wire suitable for the target operating condition.

Finally, based on the calculations for each component, several inductors was designed and manufactured as examples. The output power was measured and analyzed to discuss the estimation error. This paper can guide the design of planar-type or further innovative induction heating devices based on the proposed calculation process and analysis.

[1] C. Li et al., IEEE Access (2019), pp. 62646-62656.

[2] J. R. Garcia et al., in Proc. IEEE ASPEC (1994), pp. 302-307.

[3] O. Lucia et al., IEEE Trans. Ind. Electron (2014), pp. 2509-2520.

An electromagnetic analysis of the design of brushless DC motor

Ozturk Tosun ^a, N.Fusun Oyman Serteller^b, Vedat Topuz^c, Kenan Toker^b

^a Electrical and Electronics Engineering, Institute of Science and Technology, Marmara University, Istanbul, Turkey

^b Electrical and Electronics Engineering, Technology Faculty, Marmara University, Istanbul, Turkey

^c Vocational College of Technical Sciences, Marmara University, Istanbul, Turkey

The Brushless DC (BLDC) motors have rapidly developed over the past decade, particularly in the automotive, aerospace, electric bicycles and home appliance sectors [1]. Although they are very similar to permanent magnet synchronous motors, the main difference between them is the shape of the voltage functions in the air gap inside the motor. The shape is trapezoidal in BLDC motors, while sinusoidal in permanent magnet synchronous motors.

As in all other motors, the BLDC motor consists of a stator and a rotor fig.1 (a). The rotor is a non-winding structure on which permanent magnets (PM) are assembled. The PMs are either surface or inner mounted. The stator has a winding star or delta connected. In this study, PMs of the rotor are performed and analyzed for the inner rotor, the surface mounted PMs and the stator winding is delta connected. Motor structure and magnetic field values are based on Maxwell equations as following:

$$\nabla^2 A = -\mu J \quad (1)$$

Where $A(Wb/m)$ is vector potential and $J(A/m^2)$ is current density. In this study, the performance characteristics of BLDC motor such as efficiency, torque, cogging torque and magnetic flux density are assessed by using Ansys/Maxwell 2D (see fig.1(b) and (c)). The maximum flux density value formed in the stator is examined due to both copper losses and core losses.

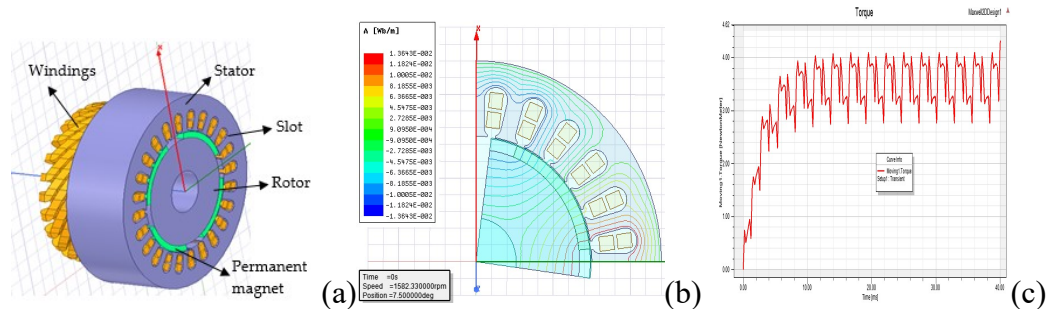


Figure 1: The BLDC motor structure(a), B analysis results (b) the torque versus time graph(c).

In this frame, the most appropriate BLDC motor dimensions are determined by using Maxwell 2 D software tools and a genetic algorithm method. Also, the related experimental studies are conducted.

[1] Morchin, W. C., and Oman, H. "Electric Bicycles-A Guide to Design and Use," IEEE Press Series on Electronics Technology, 2016.

Influence of Ferrite Sections Variation on 3D LTCC Micro-Transformer Performance

Andrea Marić^a and Ljiljana Živanov^{a,b}

^a University of Novi Sad, Faculty of Technical Sciences, Department of Electronics, Novi Sad, Serbia

^b Academy of Engineering Sciences of Serbia, Belgrade, Serbia

Implementation of passive components in wide range of various electronic modules is more than evident. They are unavoidable element in mobile telecommunication and sensor systems, filters, power converters, antennas etc. [1]. Due to diverse application range, performance improvement of passives is a necessity. Therefore component design, choice of fabrication technology, implemented materials can be seen as main factors that influence on components characteristics and performance of modules that they are integrated in.

Presented work show influence of design variation on electrical properties of 3D micro-transformer embedded inside three substrates realised as combination of dielectric and ferrite ceramic material. Transformers are fabricated implementing conventional LTCC (Low Temperature Co-fired Ceramic) technological process, using ESL 41020 dielectric and ESL 40011 ferrite tapes and adequate conductive pastes [2]. Transformer geometry is the same for all three samples. Transformer windings are embedded inside 10 of ceramic tape layers which have different ratio of dielectric and ferrite material. Primary windings are printed on the top of forth, while secondary is formed on the backside of sixth dielectric tape, with two ferrite tapes in between for all three samples. Transformer structures differ by number and position of ferrite sections that form ceramic substrate (see fig. 1). This influences on the performance of designed transformers (inductance, Q-factor, useful frequency range etc.) that are determined by electrical characterisation after fabrication (see fig. 2).

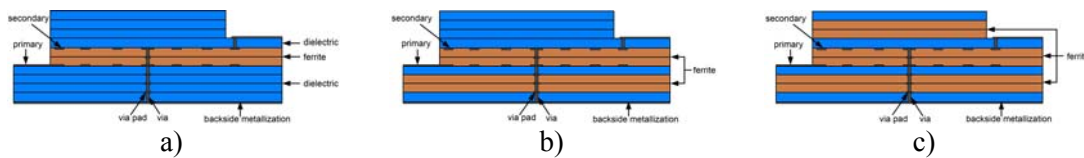


Figure 1: Schematic representation of designed 3D LTCC transformers with a) one (1fs), b) two (2fs) and c) three (3fs) ferrite sections.

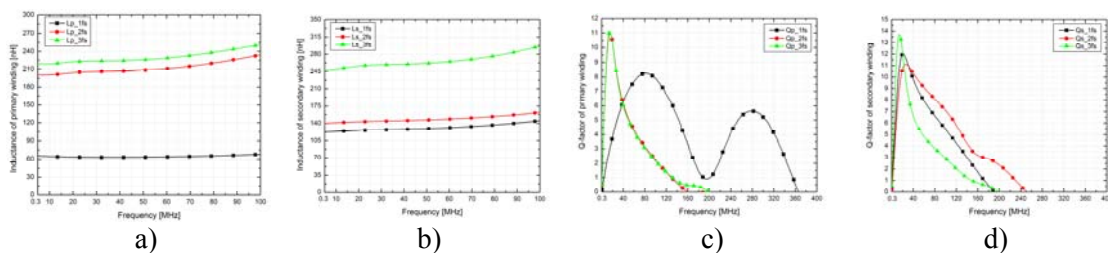


Figure 2: Frequency dependence of transformers a) and c) primary, b) and d) secondary inductance and Q-factor.

According to presented results influence of substrate configuration on 3D LTCC micro-transformers can be determined. It is evidently noticeable that number and position of ferrite sections have noticeable impact on inductance of transformer windings, while influence on Q-factor maximum and useful frequency range is less evident.

[1] X. Mi, S. Ueda, Adv. Microwave Circ. and Syst. (2010), 249-290.

[2] A. Maric, Lj. Zivanov, 42nd ISSE Conf. (2019), 1-5.

Conical coaxial magnetic gear

Iliana Marinova, Valentin Mateev

Technical University of Sofia, Sofia, Bulgaria

In this work is proposed a computational model of conical Coaxial Magnetic Gear (CMG) design. 3D time-dependent finite element model is used for operational characteristics calculation. Losses during conical magnetic gears operation are determined and compared with cylindrical one with same overall size. Special attention is focused on harmonic distortion caused by different peripheral rotor speeds due to diameter change.

Conical CMG axial cross-section and design parameters are shown in fig. 1.

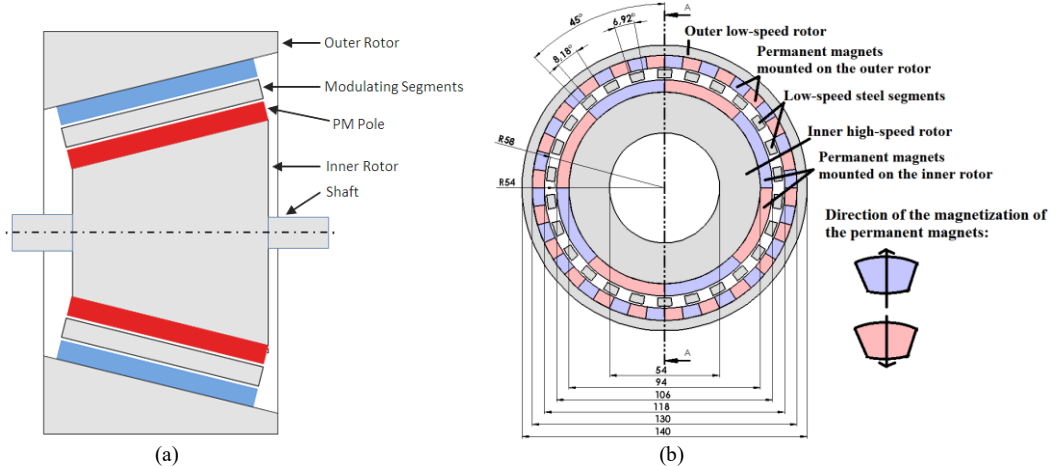


Figure 1: Conical CMG axial cross-section (a) and design parameters [1] (b).

Optimal cone angle for maximal torque density is calculated. Harmonic analysis shows significant harmonic distortion. All frequency harmonics different from main flux frequency are creating torques with none proper frequency of rotation, limiting the output of the conical CMG torque (fig. 2). Here they are increased by peripheral rotor speed variation.

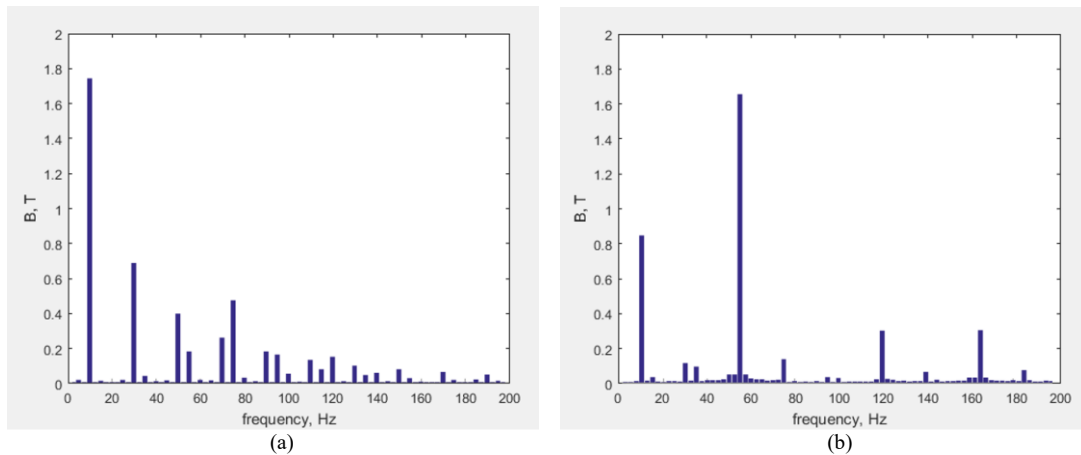


Figure 2: FFT results of the radial components of the flux density in inner (a) and outer (b) air-gaps of the CMG.

[1] V. Mateev, M. Todorova, I. Marinova, Eddy Current Losses of Coaxial Magnetic Gears, Proceedings of 23rd International Conference on Electrical Machines, ICEM 2018, pp. 1157-1162.

Big Data Analysis of Signal Transfer in Levitation System of Medium and Low Speed Maglev Train

Chen Chen^{a,c}, Junqi Xu^{b*}, Guobin Lin^b, Yougang Sun^{a,c}

^a The Key Laboratory of Road and Traffic Engineering, Ministry of Education, Tongji University, Shanghai, China

^b Maglev Transportation Engineering R&D Center, Tongji University, Shanghai, China

^c College of Transportation Engineering, Tongji University, Shanghai, China

Abstract: The levitation control system is the most fundamental foundation for the normal operation of the medium and low speed maglev train. Its levitation performance directly affects the stability and comfort of the maglev train. With the popularity of the Internet, sensor devices with monitoring function have been widely used in enterprises. The communication process of sensor equipment of medium and low speed maglev train involves many kinds of massive data such as suspension gap, control current, acceleration, time and so on. Based on the large data analysis method and the data mining of the sensor equipment of the suspension system of the medium and low speed maglev train, the anomaly detection model of signal transmission is established. In addition, by analyzing the characteristics of all kinds of data and aiming at the imbalance of sensor data acquisition, the SMOTE algorithm is improved, and the effectiveness of the improved SMOTE algorithm is verified. Combining network search and cross validation to find the global optimal solution of tree depth and Gini impurity threshold parameters, the generalization ability and diagnostic accuracy of the model are improved. Finally, the AUC values under the learning curve and ROC curve are used to evaluate the performance of the model, and the model tree is visually interpreted.

Coaxial magnetic gear with viscose ferrofluid

Valentin Mateev, Iliana Marinova

Technical University of Sofia, Sofia, Bulgaria

In this work is proposed a Coaxial Magnetic Gear (CMG) design with viscose ferrofluid between rotors. It is supposed to operate in low rotational speeds where the dynamic viscose friction is very low. Results about power and torque transmission are obtained by finite element method modeling. Effects of the viscose ferrofluid over the magnetic gear efficiency are estimated.

The present development of nano-ferrofluid materials with increased magnetic permeability could significantly decrease the magnetic reluctance of the electromagnetic systems. Ferrofluid is characterized with high magnetization saturation with very weak remanence. The electromagnetic devices working with ferrofluid have better operational characteristics, reduced energy consumption, compact in size, etc [1]. Ferrofluid in actuators increases magnetic force and thus, with such construction could be obtained greater force in smaller volume. Ferrofluid perfectly adapts to any geometry and could moves through very small channels. The presence of ferrfluid solution between rotational parts of the magnetic gear will increase dynamic friction force/torque, and in high rotational speeds output torque will be reduced and general efficiency will decrease. Because of that the ferrofluid appliance is limited only for the gap of the low speed rotor, and for very low rotational speeds (fig. 1-a).

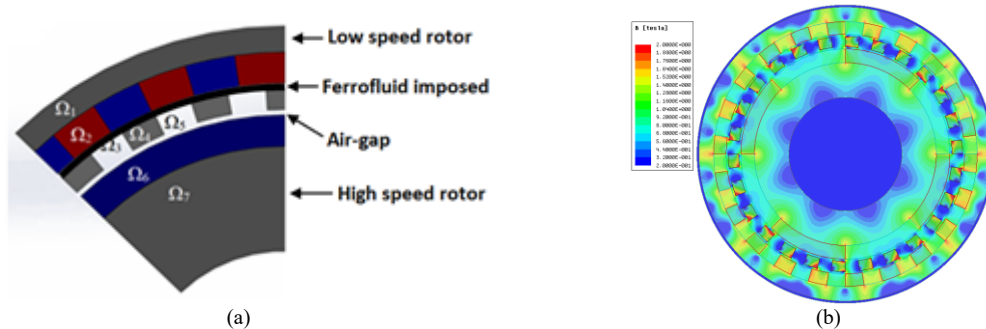


Figure 1: CMG with viscose ferrofluid, design domains (a), and modelled magnetic flux density in the CMG with ferrofluid (b).

Time dependent magnetic vector potential – scalar electric potential formulation is used for CMG modelling [2]. Ferrofluid dynamics is estimated by 3D Navier–Stokes equation with magnetic force imposed [3].

CMG magnetic field (fig. 1-b), and output torque comparison with and without ferrofluid is made. At rotational speeds below 750 rpm the presence of ferrofluid is leading to greater output torque values compared with air gap magnetic gear. Effects of the viscose ferrofluid dynamics are estimated depending on fluid properties variation in order to increase the rotational speeds range for efficient operation. Distance between rotors and modulating segments could be increased proportionally to the reduced magnetic reluctance.

-
- [1] V. Mateev, A. Terzova, I. Marinova, Design Analysis of Electromagnetic Actuator with Ferrofluid, Proceeding of XVIII-th International Symposium of Electrical Apparatus, SIELA 2014, pp. 129-132.
 - [2] V. Mateev, M. Todorova, I. Marinova, Eddy Current Losses of Coaxial Magnetic Gears, Proceedings of 23rd International Conference on Electrical Machines, ICEM 2018, pp. 1157-1162.
 - [3] V. Mateev, G. Ivanov, I. Marinova, Modeling of fluid flow cooling of high-speed rotational electrical devices, Proceedings of 16th Conference on Electrical Machines, Drives and Power Systems, ELMA 2019, art. no. 8771637.

Coaxial magnetic gear torque control

Valentin Mateev, Iliana Marinova

Technical University of Sofia, Sofia, Bulgaria

Overload of magnetic gears effects in output rotor slipping which reduce its speed and limits torque transfer. Here is presented a control system to avoid overload and keep optimal power transmission between rotors of a coaxial magnetic gear. The dynamic control model couples transient finite element magnetic model and kinematic losses model, to keep the maximal efficiency operational point in efficiency mapping charts. Input and output rotational speeds, torques and air gap magnetic fluxes will be dynamically acquired by sophisticated control system to optimize the power transmission, and avoid slipping at overload.

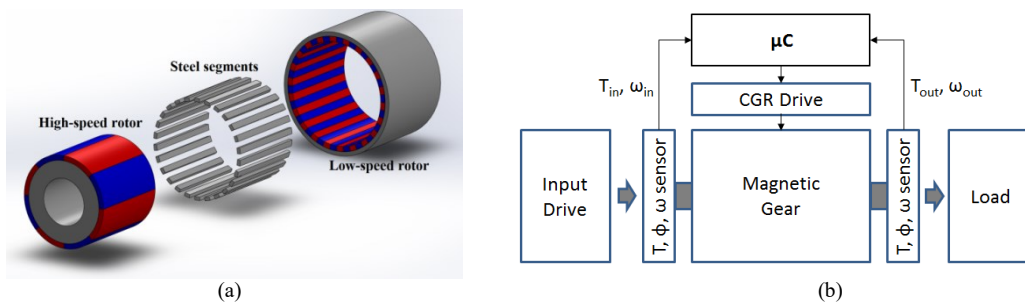


Figure 1: CMG assembly (a), and control system block diagram (b).

Considered Coaxial Magnetic Gear (CMG) design (fig. 1-a) is described in [1]. Block diagram of modelled CMG control system is presented in fig. 1-b. In Controllable Variable Transmission (CVT) mode the flux modulating segments are rotating in order to change the gear ratio. The power for this rotation must be covered by an outer source, to overcome the resistive magnetic torque over the modulating segments rotor.

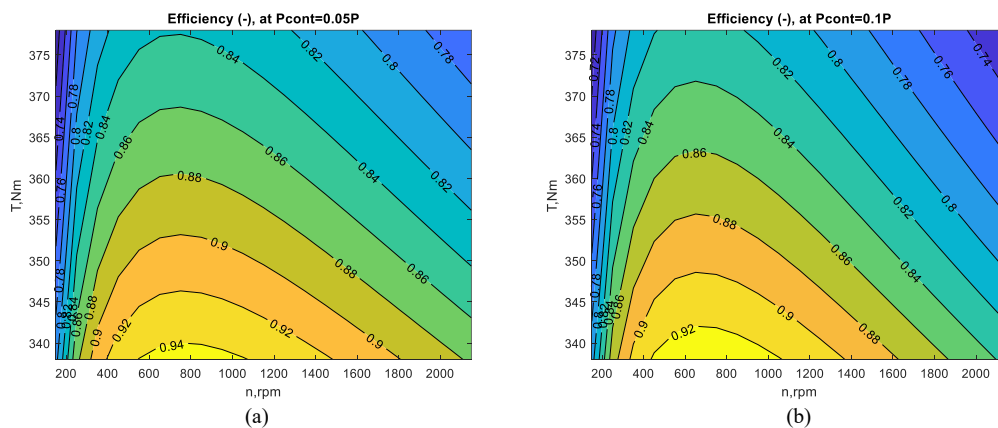


Figure 2: Efficiency of CMG control at $P_{Cont} = 0.05P_{Out}$ (a), and $P_{Cont} = 0.1P_{Out}$ (b).

According to estimated losses, efficiency mapping at CMG overload, at torques above 320 Nm, at different control power ratios, are shown in fig.2. At low speed overload efficiency is influenced mainly by rotor slipping, while in high speeds by eddy currents.

[1] V. Mateev, M. Todorova, I. Marinova, Eddy Current Losses of Coaxial Magnetic Gears, Proceedings of 23rd International Conference on Electrical Machines, ICEM 2018, pp. 1157-1162.

Levitation Robust control for magnetic levitation system of maglev vehicle with time-delay

Youngang Sun^a, Junqi Xu^a, Lijun Rong^a, Wen Ji^a, Guobin Lin^a

^a National Maglev Transportation Engineering R&D Center, Tongji University, Shanghai, China

Abstract: The time-delay in the control loop of the magnetic levitation system for maglev vehicle is inevitable. Factors such as high-speed and track irregularity will amplify the time-delay effect, present limit cycle and bifurcation dynamic phenomena, and even result in levitation failure. Aiming at the problem of airgap control of magnetic levitation system for maglev vehicle under time-delay condition, firstly establish the time-delay dynamics model of magnetic levitation system in the time-delay environment based on Newton's law and Kirchhoff's law. Then the levitation robust controller is designed based on the presented dynamic model. The stability condition of proposed levitation robust controller is obtained by constructing Lyapunov-Krasovskii function. Next, the LMI toolbox is utilized to get the corresponding control parameters of the proposed robust controller. Finally, in order to verify the performance of the proposed controller, a controller area network (CAN) communication module, which can truly reflect the uncertainty caused by network communication, is established based on MATLAB/SimEvents. The simulation results and comparison analysis are included to show the effectiveness of the proposed levitation controller.

Keywords: Magnetic levitation system, Levitation Robust control, maglev vehicle, time-delay, Lyapunov-Krasovskii method.

Thickness measurements using Eddy current techniques

L. Ferrigno^a, M. Laracca^{a,b}, A. Tamburrino^a, S. Ventre^a, A. Sardellitti^c

^a Dept. of Electrical and Information Engineering, University of Cassino and Southern Lazio,
Via G. Di Biasio, 43, Cassino, {ferrigno, m.laracca, tamburrino, ventre}@unicas.it

^b Department of Medicine and Health Science - University of Molise,
Via F. De Sanctis, 86100, Campobasso, Italy, marco.laracca@unimol.it

^c D-Solutions srl, Corso della Repubblica, 5, Cassino, alessandro.sardellitti@d-solutions.it

In recent years the concept of safety in the automotive industry is gaining increasing attention. Structural components of a vehicle need to satisfy safety ranges established by increasingly restrictive regulations. In this framework, thickness measurements play a very important role because provide information about the acceptability of components in terms of strength and elasticity.

To date, there are many methods and techniques, based on different physical principles, used to measure the thickness in the industry. One of the most used is based on ultrasound. However, this technique requires the contact to the material through a couplant gel, a proper time for sample preparation and, moreover, it relies on the operator skill.

In this work we propose Eddy Current Testing as a viable alternative to overcome these problems. The starting point is the approach proposed in [1, 2] for nonmagnetic materials. Specifically, the thickness Δ for an almost planar geometry can be found as:

$$\Delta = \frac{2\alpha_0}{2\pi f^* \sigma \mu_0}$$

where f^* is the frequency where the real part of the impedance of the probe achieves its minimum and α_0 is characteristic constant of the probe. Initial experimental tests performed out from 200Hz to 20kHz, measuring at each frequency value the impedance of the probe. The tests were carried out on two aluminium 2024T3 plates, of thickness 2mm and 10mm. The thickness was measured with an accuracy of 0.8%.

With reference to ferromagnetic materials, skin depth poses severe challenges: as the magnetic permeability increases, the sensor ability to inspect plates with typical thicknesses of the automotive field decreases. Through a simulative study based on a semi-analytical model, we studied the effect of the sensor size and operating frequency on the response of the probe. The increase of the sensor diameter is relevant for low relative permeability materials whereas the decrease of the operating frequency is relevant at high magnetic permeabilities, but signals with frequencies lower than 50 Hz are very noisy and difficult to be analyzed. In the full contribution we will discuss the design of the probe and processing method in full.

Acknowledgement: The authors would like to thank the D-Solutions s.r.l. company for its support in development and testing of presented techniques in real scenarios and its courtesy to show the activity results.

[1] W. Yin, A.J. Peyton “Thickness measurement of non-magnetic plates using multi-frequency eddy current sensors” NDT&E international, 40 (2007), 43-48

[2] Mingyang Lu, Liyuan Yin, Anthony J. Peyton, and Wuliang Yin “A Novel Compensation Algorithm for...” IEEE Transaction on Instrumentation and Measurement, Vol. 65, No. 12, December 2016

Printed magnetic needle probes sensor, embedding magnetic state monitoring

H. S. Nguedjang^a, Y. A. Tene Deffo^a, P. Tsafack^a, B. Ducharme^b, M.A. Raulet^c, L. Morel^c

^a University of Buea, Faculty of engineering and technology, Cameroon.

^b Laboratoire de Genie Electrique et Ferroélectricité – INSA

Bat. Gustave FERRIE, 8 rue de la physique, 69621 Villeurbanne cedex, France.

^c Laboratoire Ampère – Université Claude Bernard Lyon 1, Villeurbanne, France.

The use of micro-magnetic non-destructive techniques has increased exponentially in the industrial field [1][2]. The Needle-probe technique of measuring local magnetic flux in electrical steel sheets has made its way into the non-destructive testing field over the past 70 years. In spite the earlier nature of this technique, there is still a meaningful lot of development to be done as per concerning its industrial implementation for an in-situ detailed monitoring of the magnetic behavior of some electric machines.

This situation paves the way for developing a pint-sized, embedded version of the needle probe sensors which comes forth to surpass the limits of the probe due to its size. The design is tailored around Printed Circuit board technique with the use of conductive ink (silver ink). A circuit is printed on a coated electrical steel sheet (40mm x 20mm x 0.3mm) while respecting a distance of 1 cm [3][4] between the two contact point with the materials. The routes are done as close as possible: 0.1mm distant from each other; so as to reduce losses due to air [5].

Given that the electrical steel sheets making up the laminated magnetic circuit of electric machines like transformers, AC/DC machines are coated, the sensor can be embedded into the magnetic circuit with no risk of conductivity, thus an idea of homogeneity state assured.

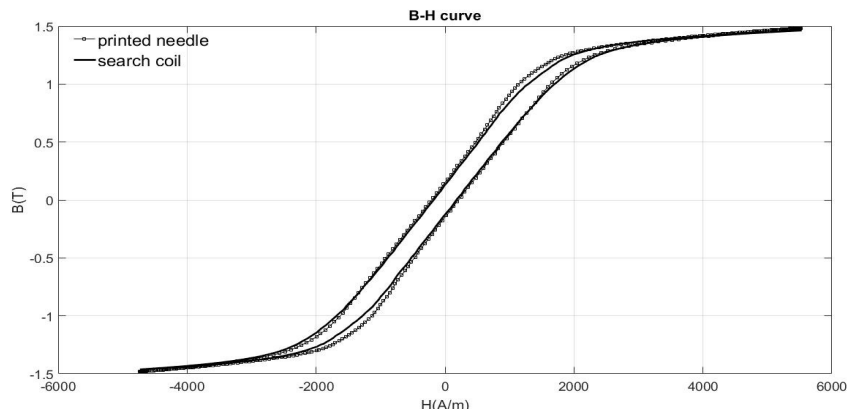


Figure 1: hysteresis loop when using printed needle and search coil.

- [1] T. Matsumoto & al., J. of Mag. And Mag. Mat., vol. 479, pp. 212-221, 2019.
- [2] B. Gupta & al., NDT & E Int., vol. 104, pp. 42-50, 2019.
- [3] K. Senda & al., Electr. Eng. Japan, vol. 126, n° 4, pp. 942-9, 1999.
- [4] Y.A. Tene Deffo & al., IEEE Trans. On Mag., vol. 55, iss. 7, 2019.
- [5] L. George & al., IEEE Trans. On Mag., vol. 37, iss. 14, p. 2756, 2001.

Effect of external metal shape and distance on signal in magnetic flux leakage type non-destructive testing

Chang Geun Heo, Gwan Soo Park

Pusan National University, Busan, Republic of Korea

Most energy sources used in industry are transported via pipelines. If there is a hole due to corrosion in the pipe, the transported energy source may leak, which may adversely affect the environment or cause an accident such as an explosion. Therefore, it is important to inspect the pipe regularly.

Non-destructive testing(NDT) is a method of inspecting pipes for corrosion, etc. without damaging the pipes. Research on NDT is primarily focused on detecting corrosion or crack in pipes. However, if you can find and eliminate the cause of corrosion rather than detecting corrosion that has already occurred, the pipe will be able to be used a little longer and reduce the cost of pipe maintenance. One of the factors that causes corrosion is the metal that exists outside the pipe. Generally, pipes are coated with a plastic material to prevent contact with oxygen. However, the external metal can penetrate the plastic coating, and when the plastic coating is peeled off by the external metal, oxygen comes into contact with the pipe, causing corrosion. If the external metal is found and removed before the plastic coating is peeled off, the pipe can be prevented from corrosion.

The magnetic flux leakage(MFL) method, one of the most representative NDT methods, uses permanent magnets to saturate the ferromagnetic pipe by applying a large magnetic field to the pipe and measure the leakage magnetic flux signal due to changes in the state of the pipe including corrosion[1]-[2]. Since most of the commonly found metals are ferromagnetic and the MFL method is sensitive to magnetic changes, it is easy to find metals outside the pipe using the MFL method. In addition, due to its high sensitivity, the shape and distance of the external metal affects the MFL signal.

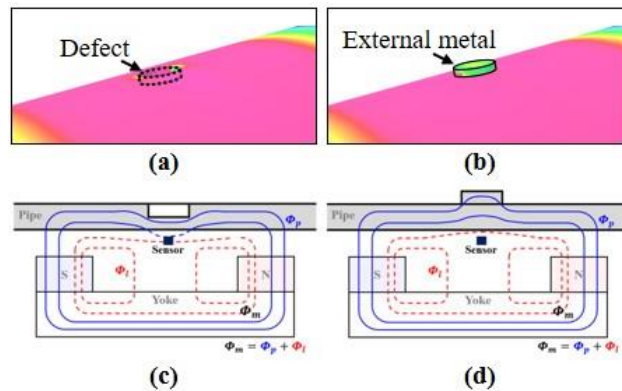


Figure 1: Distribution of magnetic flux density around (a) the defect. (b) the external metal. Diagram of magnetic flux line around (c) the defect. (d) the external metal.

This paper analyzes the effect of metals outside the pipe on the MFL signal. Furthermore, an algorithm for estimating the shape and distance of the external metal is also proposed.

[1] H. M. Kim et al., IEEE Trans. Magn., vol. 54, no. 11(2018), 1-5.

[2] X. Peng et al. IEEE Trans. Magn., vol. 56, no. 6(2020), 1-15.

Advances in Magnetism 2020-21, June 13-16, 2021

**Advanced measurement
techniques**

**FORC-based identification
techniques**

**Artificial intelligence,
optimization and inverse
problems**

Abstracts can be easily browsed through the bookmarks

Observation of field induced motions of a single diamagnetic particle to study the structure of individual nano-size particle

Chiaki Uyeda, Hiroki Fukuyama, Keiji Hisayoshi, Kentaro Terada

Institute of Earth & Space Science, Graduate School of Science, Osaka Univ., Japan

Diamagnetic magnetization (i.e., χ_{DIA} and $\Delta\chi$) of a single particle with mass below several milligrams is obtained by observing its field-induced motions without the knowledge of mass m of particle[1]. The two parameters directly reflect the spatial distribution of localized electron of a solid material, and variance of these values with respect to the published value may derive from structural deformation of the sample. Value of χ_{DIA} is obtained by observing the terminal velocity $v_{\text{T DIA}}$ of a particle that translated in a area of monotonically decreasing field; this is because v_{T} depend on χ_{DIA} and field intensity B_0 at initial position of particle, and is independent to m [2]. A similar m independent property is observed in the period of rotational harmonic-oscillation induced by a static magnetic field on various mg-size materials including amorphous-silica [3]; the oscillation was induced by an anisotropy of magnetic susceptibility $\Delta\chi_{\text{DIA}}$. Period of oscillation τ of stable axis with respect to B is described as

$$\tau = 2\pi (I / m\Delta\chi)^{1/2} / B^{-1}. \quad (1)$$

Hence $\Delta\chi$ of oscillating crystal is obtained by inserting the measured values of τ , I/m , and B in the above equation: m is unnecessary in the measurement. The $\Delta\chi_{\text{DIA}}$ values of some well-known crystals were consistently explained by a chemical bond model [1], which is based on the assumption that $\Delta\chi_{\text{DIA}}$ is derived from the spatial anisotropy of orbitals corresponding to individual chemical bonds. It is expected that χ_{DIA} & $\Delta\chi_{\text{DIA}}$ values of single nano-size particles will provide quantitative information to estimate the extent of structural transformation, and to this end, further developments are necessary to reduce the measurable size of the field-induced motions. The technical improvements realized in the measuring the mg-size crystals secure a base to detect the magnetizations of samples with smaller sizes.

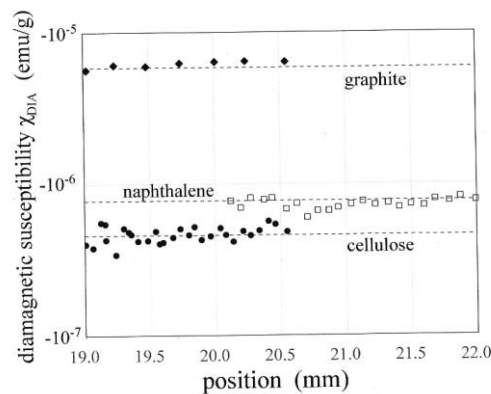


Fig. 1 Experimental χ_{DIA} values of a single particle obtained at different positions during its field-induced translation. Equation (1) is used in calculating χ_{DIA} .

- [1] C. Uyeda et al. J. Phys. Soc. Jpn. 79 (2010), 064709. [2] K. Hisayoshi et al., Sci. Rep. 6,(2016), 38431. [3] M. Yokoi et al., Planet. Space Sci. 100 (2014), 46–50.

Translation of interstellar solids induced by Nd magnetic circuit

Keiji Hisayoshi, Chiaki Uyeda, Kentaro Terada

Institute of Earth & Space Science, Graduate School of Science, Osaka Univ., Japan

Field-induced translations were observed in various diamagnetic solids in microgravity condition, which was caused by a field distribution that monotonically decreased along an x -axis [1][2]. The particles were released at a common position x_0 , and a formula was deduced from an energy conservation between x_0 and an arbitrary position x_i of the particle as,

$$v_i^2 = \chi_{\text{DIA}} (B_i^2 - B_0^2). \quad (1)$$

In the above equation, velocity of particle at position x_i is described as v_i , while B_0 and B_i denote field intensities at positions x_0 and x_i , respectively; χ_{DIA} denote the diamagnetic susceptibility of the particle per unit mass. The above equation show χ_{DIA} is obtained from a linear relationship between v_i^2 and $B_i^2 - B_0^2$ without measuring mass of particle. Furthermore, material of particle is simply identified by collating the obtained χ_{DIA} with published values without consuming the small sample as required the small sample as required. The proposed method of material analysis is effective in a remote onsite-mission to analyze mixture of heterogeneous particles immediately after collecting them. In the present report, efficiency of eq.(1) is examined for major materials that compose the interstellar solid particles, namely corundum, diamond, graphite, magnesia and silicon-carbide; the measurement is performed to practicalise the technique in a mission orientated to the solar system. The accuracy in observing v_i and B_i were considerably improved by adopting a high-speed camera (CASIO EX-F1, Japan); as shown in Fig.1, the experimental χ_{DIA} values agreed with their published values for all the measured samples. The proposed method fulfills the following qualities that are required in an apparatus designed for an on-site mission; (1) principle of analysis should be simple and well confirmed, (2) apparatus should have compact and rigid structure, (3) power consumption is low, (4) rare particles must be preserved for refined analysis. The relatively high resolution of material identification seen in Fig.1 show that the present setup is usable as a prototype to develop an apparatus for an on-site mission.

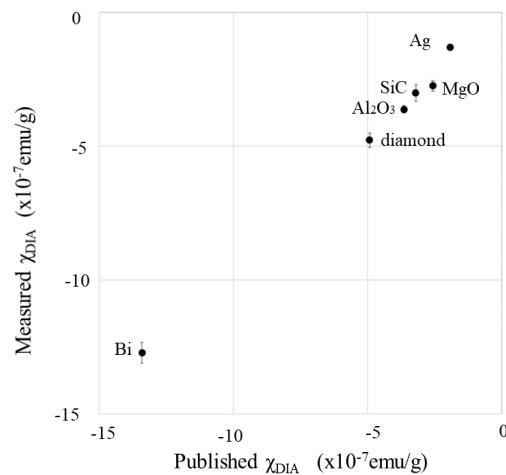


Figure 1 Experimental χ_{DIA} compared with published values.

Measurement of thin film magnetostriction using field-dependent atomic force microscopy

Marco Coisson^a, Wilhelm Hüttenes^b, Matteo Cialone^c, Gabriele Barrera^a, Federica Celegato^a, Paola Rizzi^c, Zoe Barber^b, Paola Tiberto^a

^a INRIM, Advanced Materials and Life Sciences Division, Torino, Italy

^b Cambridge University, UK

^c Department of Chemistry, University of Torino, Italy

Magnetostriction is an intrinsic property of ferromagnetic materials whose overall dimensions change when an external magnetic field is applied. Given their capability to couple electromagnetic and mechanical energy, magnetostrictive materials can be considered a basic building block for transducers and wireless control actuators. When scaling down towards the nanoscale, the reduced dimensionality introduces several challenges for the direct measurement of the magnetostriction, since the change in dimensions is in the nanometre scale. In order to measure magnetostriction of thin films, these are often mechanically coupled to a non-magnetic substrate, making a flexible bimorph. However, either custom cantilevers or measurement setups are usually required. In this work, we present a method based on standard atomic force microscopy cantilevers coated with Fe₈₁Al₁₉ films of different thickness. A commercial atomic force microscope (AFM) operating under a variable magnetic field is exploited to measure the vertical deflection of the bimorph induced by the magnetostrictive coating. The microscope is operated in fixed-point contact mode on a flat Si sample. The interplay between the magnetostrictive force, bending the cantilever up when the magnetic field is applied, and the tip-sample interaction, letting the AFM compensate for the mechanically induced upward deflection, allows the measurement of the vertical displacement of the cantilever, as a function of the applied magnetic field, as shown in Figure 1a-c. Through the measurement of the deflection of bimorphs with different coating thickness, the magnetostriction constant of the alloy can be determined (Figure 1d) with a suitable model.

The proposed method is entirely based on standard components (AFM and AFM cantilevers), and allows the measurement of the vertical deflection of cantilevers coated with magnetostrictive thin films as thin as a few tens of nanometres. The magnetostriction constant of the alloy is determined through measurements on films with different thickness.

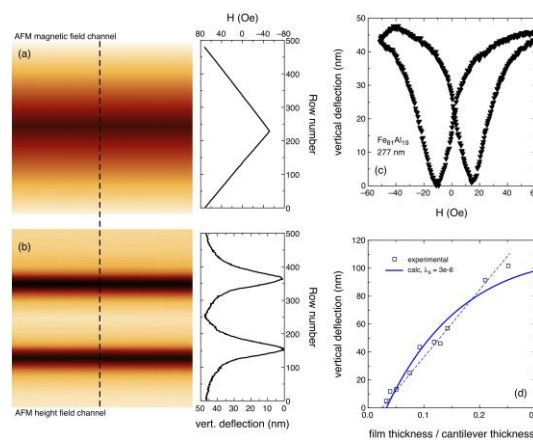


Figure 1: (a) AFM image of the applied magnetic field dependence on scan line number. (b) The same, for the cantilever vertical displacement. (c) Combination of displacement vs. applied field curves. (d) Determination of the magnetostriction constant (symbols: experimental data, line: model fitting).

Characterization of polycrystalline permanent magnets with the Singular Point Detection technique.

Riccardo Cabassi^a and Fulvio Bolzoni^a

^a Institute of Materials for Electronics and Magnetism - CNR, Parma, Italy

The determination of the anisotropy field H_A in magnetic materials can be quite problematic in the case of polycrystalline samples: the values of H_A obtained from conventional magnetometry are often ambiguous and unclear, and require long time consuming magnetization curves. In such cases, the Singular Point Detection (SPD) technique in pulsed magnetic field is the most suitable method: fast and reliable, it allows a prompt and accurate determination of H_A by means of the analysis of the successive derivatives $d^n M/dH^n$ of a quick magnetization curve. SPD was originally developed at the IMEM (former MASPEC) CNR laboratory in Parma starting from the '70s [1,2] and since then it has been extensively applied in the study of the magnetocrystalline anisotropy of several classes of hard magnetic materials. The renewed interest in the research of new materials for permanent magnets, connected with the current concerns about possible shortage in rare earth supply, make SPD a still relevant tool.

In this presentation some basic elements from theory of the magnetic anisotropy will be first recalled, then the SPD technique will be described in both theoretical and practical regards. In addition to the determination of H_A , more possible applications to the characterization of permanent magnets will be illustrated. Some examples from recent results in the field of rare-earth free or lean hard magnets will be shown.

[1] G. Asti and S. Rinaldi, Journal of Applied Physics 45, 3600 (1974)

[2] G. Asti and F. Bolzoni, J. Appl. Phys. 58, 1924 (1985)

Revealing magnetic properties of thin films utilizing polarized neutrons

S. Pütter^a, S. Mattauch^a, A. Koutsioubas^a, P. Schöffmann^a,
A. Syed Mohd^a, K. Zhernenkov^a, E. Babcock^a, Z. Salhi^a, A. Ioffe^a, T. Brückel^b

^a Jülich Centre for Neutron Science JCNS at Heinz Maier-Leibnitz Zentrum MLZ,
Forschungszentrum Jülich GmbH, Garching, Germany

^b Jülich Centre for Neutron Science and Peter Grünberg Institut PGI Quantum Materials and
Collective Phenomena JCNS-2 / PGI-4, Forschungszentrum Jülich GmbH,
Jülich, Germany

Polarized neutron reflectometry (PNR) is a versatile probe for the study of the magnetic moment with depth resolution. As self-calibrating technique, it provides independently values of the magnetic moment, its direction in the film plane, and film thickness together with its scattering length density values. It is layer selective and buried layers in multilayer systems can be analyzed [1].

In this contribution we will provide an overview of the possibilities of PNR as well as present the reflectometer MARIA [2]. It is a state of the art reflectometer at the constant neutron flux reactor in Garching, Germany. MARIA exhibits a high dynamic range of up to 7-8 orders of magnitude and a maximum Q (momentum transfer vector) higher than 0.25 \AA^{-1} . With the combination of a $400 \times 400 \text{ mm}^2$ position sensitive detector and a time-stable ^3He polarization spin filter based on Spin-Exchange Optical Pumping (SEOP), the instrument is well equipped for investigating specular reflectivity and off-specular scattering from magnetic thin films and artificially fabricated structures like nano-dots, gratings, etc. down to the monolayer regime in full spin polarization. Furthermore, the GISANS option can be used to investigate lateral correlations in the nm range. Due to the large detector and pinhole collimation of the incident neutron beam even grazing incidence diffraction measurements are possible. All the options, like GISANS, neutron polarization and ^3He polarization spin filter can be moved in and out of the neutron beam within seconds by remote controlled push button operation and do not require any realignment.

Magnetic fields can be applied up to 5 T and a low temperature sample environment (down to 3 K) is offered. Thin film samples may be fabricated in a MBE system nearby (deposition materials according to the requirements of the user). For investigation of samples which are sensitive to ambient conditions a UHV transport and measurement chamber with base pressure in 10^{-10} mbar range is provided (transfer forth and back) [3]. Typical substrate size for investigation is $10 \times 10 \text{ mm}^2$.

Examples for PNR investigation of thin films like e.g. NiO/Fe/L10-FePt, SrCoO_x, Co/W(110) Fe₄N/LaAlO₃(001) are discussed. However, the MARIA reflectometer and the MBE system are user instruments. Hence we offer measurement and sample preparation time to interested users [4]. Let's discuss your ideas!

-
- [1] J. A. C. Bland and C. A. F. Vaz, Chapter 7 in J. A. C. Bland and B. Heinrich, Eds., Ultrathin Magnetic Structures III, Springer-Verlag Berlin (2005)
 - [2] Heinz Maier-Leibnitz Zentrum. (2015). J. large-scale research facilities, 1, A8. <http://dx.doi.org/10.17815/jlsrf-1-29>; S. Mattauch, A. Koutsioumpas, et al., J. appl. Crystallography, 51, 646 (2018)
 - [3] A. Syed Mohd, S. Pütter, et al., Rev. Sci. Instrum. 87, 123909 (2016)
 - [4] www.mlz-garching.de/maria; www.mlz-garching.de/mbe

Soft and hard iron compensation without sensor motion for the compasses of an operational towed hydrophone array

Tommaso Lapucci^a, Luigi Troiano^b, Carlo Carobbi^a, Lorenzo Capineri^a

^a University of Florence, Department of Information Engineering, Florence, Italy

^b Centre for Maritime Research and Experimentation - NATO STO, La Spezia, Italy

Usually towed hydrophone arrays are instrumented with a set of compasses. Data from these sensors are utilized while beamforming the acoustic signal for target bearing estimation [1]. However, elements of the hydrophone array mounted in the neighborhood of a compass can affect the Earth's magnetic field detection. The effects depend upon the kind of elements present in the platform hosting the compass. If the disturbances are constant in time they can be compensated for by means of a magnetic calibration. This process is commonly known as soft and hard iron compensation [2].

In this paper, a solution is presented to carry out the magnetic calibration of a COTS (Commercial Off The Shelf) digital compass without unattainable sensor motion. This approach is particularly suited in applications where a physical rotation of the platform that hosts the sensor is unfeasible. In our case, the platform consists in an assembled and operational towed hydrophone array. A standard calibration process relies on physical rotation of the platform and thus on the use of the geomagnetic field as a reference during the compensation. At a variance with that, we provide to the sensor an artificial reference magnetic field to simulate the unfeasible physical rotation. We obtain this by using a tri-axial Helmholtz coil, which enables programmability of the reference magnetic field and assures the required field uniformity.

In our work the simulated geomagnetic field is characterized in terms of its best estimate and uncertainty. The analysis indicates that our method and experimental set-up represent a suitably accurate approach for the soft and hard iron compensation of the compasses equipped in the hydrophone array under test.

[1] P. Felisberto and S.M. Jesus, Towed array beamforming during ship's maneuvering, IEEE Proceedings – Radar, Sonar and Navigation, 143(3), 1996.

[2] M. J. Caruso, Applications of magnetic sensors for low cost compass systems, IEEE Position Location and Navigation Symposium, San Diego, pp. 178-184, 13-16 March 2000.

Nonmonotonic xyFORCs in two-phase magnetic systems

Alexandru Stancu^a, Laurentiu Stoleriu^a

^a Alexandru Ioan Cuza University of Iasi, Faculty of Physics, Boulevard Carol I, 11, Iasi, 700506, Romania

After the huge success of the magnetic characterization of complex magnetic systems based on the measurement of first-order reversal curves (FORC), the scientific community is at the point where the most important issue is to find new ways of using these data to improve our insight on the studied samples [1]. Also, it is important to imagine other complementary measurements that could add to the understanding on the switchings of various elements within the magnetic materials. One rather straightforward idea in improving the classical scalar FORC measurement is to use the second set of detection coils available on most commercial VSMS that are able to measure the magnetic moment on the direction perpendicular to the applied field direction [2]. We have named this type of experiment xyFORC and if one applies the field on the “x” direction, the two sets of detection coils will measure a classical FORC (named xFORC) and a FORC along the perpendicular direction, named yFORC. As from the experimental point of view this is not much more complicated than the classical FORC, our task is to understand the supplementary information given by yFORC. This work is focussed on results obtained on a sample made from a superposition of two magnetic phases with their easy axes perpendicular. The field is applied on the bisector of the angle made by the easy axes. So, in this geometry, the easy axes are at 45 degrees from both measuring directions: xFORC and yFORC.

We have observed on the yFORCs a nonmonotonical behaviour and that this can be related with the switching field of one of the two magnetic phases (see Fig.1). In this study we have used the doFORC package [3] which allows the calculation of both the first and second derivatives of the FORC data. In the presentation we show how the features observed on the yFORC can be correlated with the switchings of the two magnetic phases.

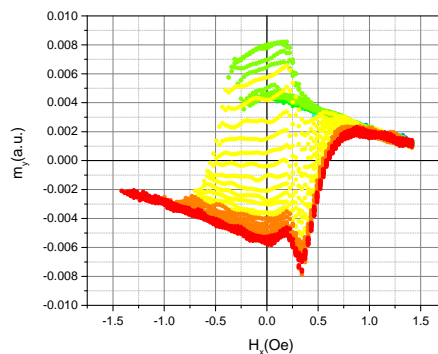


Figure 1: Experimental yFORC for a two magnetic phase system with perpendicular easy axes and the field applied along the bisector of the angle between the easy axes

-
- [1] A. Stancu et al., J. Appl. Phys. **93** (2003), 6620-6622.; A. Stancu et al., Appl. Phys. Lett. **83** (2003), 3767-3769.; C.-I. Dobrotă, A. Stancu, J. Appl. Phys. **113** (2013), 043928.
- [2] A. Markou et al., J. Magn. Magn. Mater. **445** (2018) 95-102.
- [3] D. Cimpoesu et al., J. Appl. Phys. **125** (2019) 023906.

Engineering of magnetization reversal processes in multiphase microwires by interplay of magnetostatic and magnetoelastic anisotropy

V. Kolesnikova^a, M. Rivas^b, I. Baraban^a, JC Martinez-Garcia^b, M. Gorshenkov^c, V. Rodionova^{a,c}

^aImmanuel Kant Baltic Federal University, 236004, Kaliningrad, Russia

^bDepartment of Physics, University of Oviedo, 33203, Gijón, Spain

^cNational University of Science and Technology “MISIS”, Moscow 119049, Russia

The amorphous and nanocrystalline microwires are used for logic, coding and sensing devices because of their extremely soft magnetic properties: as embedded sensors of magnetic field for technology control or tracing the health parameters, as magnetic tweezing in biomedicine [1-3]. The methods of partial or directional crystallization by heat treatments are used to reach hard magnetic properties, required for μ -magnets applications [4]. Recently, bi- and multiphase micro-scale wires are found to be useful for applications in targeting, sensing and actuating [5, 6]. Multiphase state can be achieved by the phase separation: (i) during the Taylor-Ulitovsky manufacturing process under control of the technical parameters [7] or (ii) applying the additional magnetic layers on the as-cast glass-coated microwires [5]. The first method leads to the structure of metallic nucleus composed from nanocrystals in an amorphous matrix. The second one – to the multilayered structure consisting of the amorphous or nanocrystalline nucleus and spatially separated polycrystalline shell. For effective practical application, the magnetization reversal mechanisms should be deeply understood and precisely controlled for listed systems.

In this work, a $\text{Co}_{77.5}\text{Si}_{15}\text{B}_{7.5}$ glass-coated microwire with $d/D = 12/33$ (d – diameter of the metallic nucleus, D - diameter of the wire with glass shell) was used for analysis of magnetic interactions in various types of systems: partially crystalline, and additionally covered by a magnetically soft or hard shell. In the latter, either FeNi or Co shell was deposited onto the glass using magnetron sputtering system. An initial characterization was performed by XRD and HRTEM to determine the structural features and identify the crystalline phases. For the as-cast glass-coated microwire, the fine crystals of both FCC and HCP Co modifications and amorphous Co-based phase in the nucleus were found. To understand the origin of the magnetic interaction between the different magnetic phases FORC-analysis was applied. FORC-curves and magnetic properties were measured via VSM. Differences between magnetic properties of the magnetic phases as well as clearly observed interactions were shown in the Switching Field Distribution (SFD) plots and in the FORC – diagrams. The SFD and FORC-diagram show the presence of the positive interaction in the microwire nucleus caused by the exchange coupling among the crystalline inclusions of the two phases; on the other hand, there is no trace of the residual matrix. For core/shell microwires the features that appear at FORC-pattern are due to the magnetostatic coupling between the ferromagnetic coating and the core. The relationship between magnetoelastic and magnetostatic interactions was analyzed. The interplay of the energies gives possibility to modify the magnetization process and makes it very complex with step-wise behavior. As a result, reach harmonic spectrum taken from pick-up coils during magnetization process of multiphase wires can be used for enhanced sensitivity in sensing the tags in electronic article surveillance systems [8].

[1] Sulla I. et al., J. Elect. Eng. 66.7 (2015): 161-163.

[2] Gudoshnikov S., et al. Physica status solidi (a) 211.5 (2014): 980-985.

[3] Morón C., et al. Sensors 15.11 (2015): 28340-28366.

[4] Hoshino K., et al. Lab on a Chip 11.20 (2011): 3449-3457.

[5] Torrejón J., et al. Sensor Letters 7.3 (2009): 236-239.

[6] Serrano I. G., et al. Journal of Applied Physics 115, 033903 (2014).

[7] Rodionova V. V., et al. IEEE Transactions on Magnetics 54.11 (2018): 1-6.

[8] Rodionova V., et al. Journal of Applied Physics 111, 07E735 (2012).

Machine learning estimation of the effective permeability of mixture for magnetic shielding

Salvatore Coco^a, Antonino Laudani^b

^a Università degli Studi di Catania

^b Università degli Studi Roma Tre - Dipartimento di Ingegneria

The attenuation of magnetic field at extremely low frequency (ELF) according to guidelines to define exposure limits defined by several international institutions requires some installation of shield in indoor environment, i.e. inside our buildings. An effective solution, which has a lower impact from the point of view of building construction (with respect to installation of screen made by ferromagnetic and conductive materials or wire-meshes) is to use additives for concrete or mortars in order to improve shielding effects. Recently, a solution has been proposed by the authors based on the addition of ferromagnetic particles to the mortars, usually used to refine the wall of our houses, in order to exploit their property in the attenuation of indoor magnetic field [1]. The performance of these mixtures was experimentally characterized, but at the same time several attempts have been done to achieve an effective tools/CAD for their electromagnetic analysis, which would further help the shielding design. In past works, statistical analysis were performed by starting from results of Finite Element (FE) analysis and polynomial fitting models have been proposed to build a model of the variation of effective permeability according to the mixture properties. In this work, we propose the use of a machine learning to build a simpler model. In particular, the approach is based on a supervised two-step procedure: In a first, a certain amount of FE meshes representing the same sample geometry, with different inclusions distribution, are used to compute the magnetic field. In the second phase, the data so achieved are then used to feed a neural network, able to extract the relationship, among the quantity of magnetic material used (input), its magnetic permeability (input) and the equivalent material characteristic (output). These two phases are supervised as in a machine learning approach in such a way that the estimation can be refined automatically, that is the system is settled to generate new sample and to add it to the training data set, until the established accuracy is reached. The comparison of the results with measurements are in good agreement.

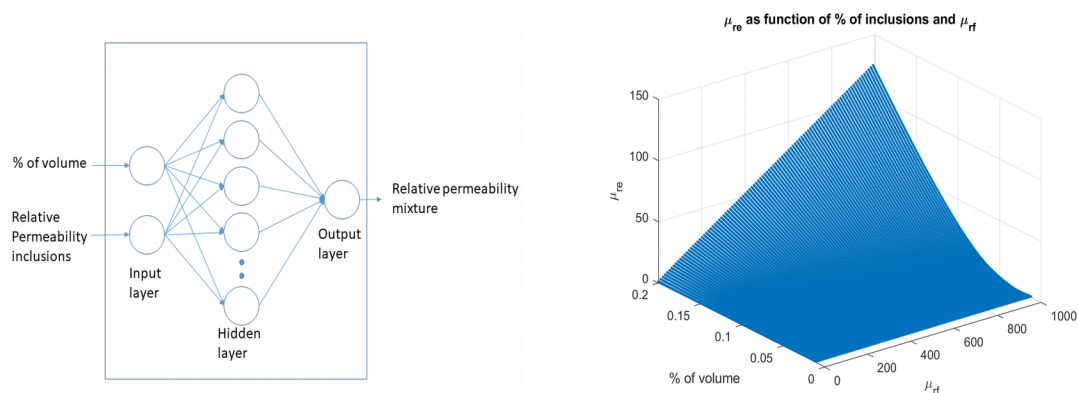


Figure 1: Schematic representation of the Neural Predictor (left) and relative permeability

[1] Laudani A., Fianchino C., Coco S., Pollicino G. - "Sistema Di Additivazione Per Malte E/O Conglomerati Schermante Ai Campi Elettromagnetici ELF". – Italian Patent N. ITCT20100011.

A neural spatial mapping of magnetic fields for exposure surveys

Salvatore Coco^a, Antonino Laudani^b

^a Università degli Studi di Catania

^b Università degli Studi Roma Tre - Dipartimento di Ingegneria

Surveys for exposure of the general public and workers to non-ionizing radiations are activities required by regulations in several countries. Regulations for such surveys set limits for exposure to electric, magnetic and electromagnetic field. Among all the field exposure surveys, the ones involving the measurement of the Extremely Low Frequency (ELF) Magnetic fields (0-3kHz) are the most time consuming due to contribution from power applications (50-60Hz) that might change during the day. To reduce the number of measurements, modelling techniques are often used to estimate the field distributions in advance. A common modelling technique is the Equivalent Source model (ES), which is very useful for outdoor environments, but can be difficult to implement in environments such as building interiors. Alternatively, it is possible to estimate the field distribution by means of a black-box approach. This involves acquiring a reduced number of measurements of the field and proceed to model the distribution by means of fitting techniques such as Neural Networks (NN). Fitting the magnetic field distribution through NN involves a difficulty related to the network generalization capabilities, which might arise when the dataset for training includes a low number of samples. To overcome this difficulty, several small NN are trained on a randomized dataset and their output are merged together creating a structure (referred as Neural Predictor, NP) that trades the increased computational cost for a higher generalization capability [1,2]. The schematic representation of the NP is shown in Fig. 1 (left) and an example of the predicted field is shown on Fig. 1 (right). Considerations on the fitting accuracy and a possible experimental setup for measurement acquisition will be discussed in the final version of this paper.

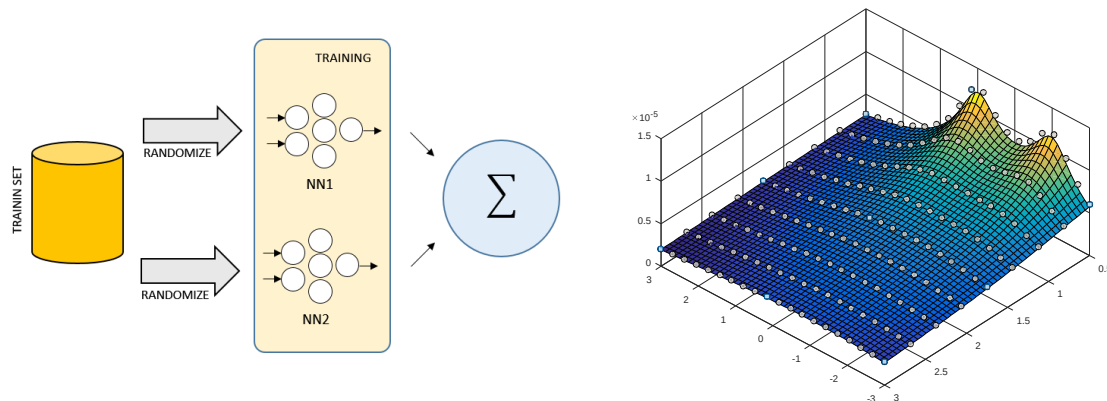


Figure 1: Schematic representation of the Neural Predictor (left) and fitting capabilities on a sample field distribution (right)

[1] Coco, S., Laudani, A., Lozito, G. M., Fulginei, F. R., & Salvini, A. (2016, October). 3D ELF magnetic field strength modeling through fully connected cascade networks. In 2016 AEIT International Annual Conference (AEIT) (pp. 1-6). IEEE.

[2] Coco, S., Laudani, A., Fulginei, F. R., & Salvini, A. (2014). A new neural predictor for ELF magnetic field strength. IEEE Transactions on Magnetics, 50(2), 69-72.

Comparative analysis between feed-forward and recurrent neural networks for simulating magnetic scalar hysteresis

Antonino Laudani, Gabriele Maria Lozito, Francesco Riganti Fulginei and Alessandro Salvini

Department of Engineering, Roma Tre University, Rome, Italy

Magnetic losses prediction is an important factor in designing complex magnetic structures for industrial applications. The scientific literature still lacks a reliable model able to represent correctly the hysteretic behaviour of magnetic materials subject to distorted and frequency-rich excitations. A possible solution lies in modelling hysteresis through Artificial Neural Networks (ANN) [1-2]. Since magnetic hysteresis is a phenomenon with memory, static artificial neural networks, such as feed-forward ANN, could not be suitable for a correct simulation. Nevertheless, on the other hand, memory based ANN are very difficult to train and show less stability. In this work a comparison between feed-forward neural networks (FFNN) and recurrent neural networks (RNN) is performed.

Using an RNN to model magnetic scalar hysteresis presents two major advantages over static FFNN models. First, since the RNN has inherently memory, there is no need for a post elaboration. Second, since inputs are sampled at a fixed rate, there is no necessity to use the magnetic permeability as output of the neural network. On the other and, RNN are more difficult to train with respect the FFNN and the problem of their stability is still an open issue. A modelling example can be seen in Fig. 1. The FFNN and RNN, both designed by using 10 hidden neurons, are trained on a training set (first order reversal curves) obtained by the static Jiles-Atherton model. As can be seen, the performances of the two kinds of ANN are quite different. In the final version of this work, a complete description of two neural systems for the estimation of magnetic losses will be presented. Performance of the systems for a wide set of excitations will be presented (both saturating and distorted fields) along with strategies to size and train a network with the best trade-off between precision and generalization capabilities.

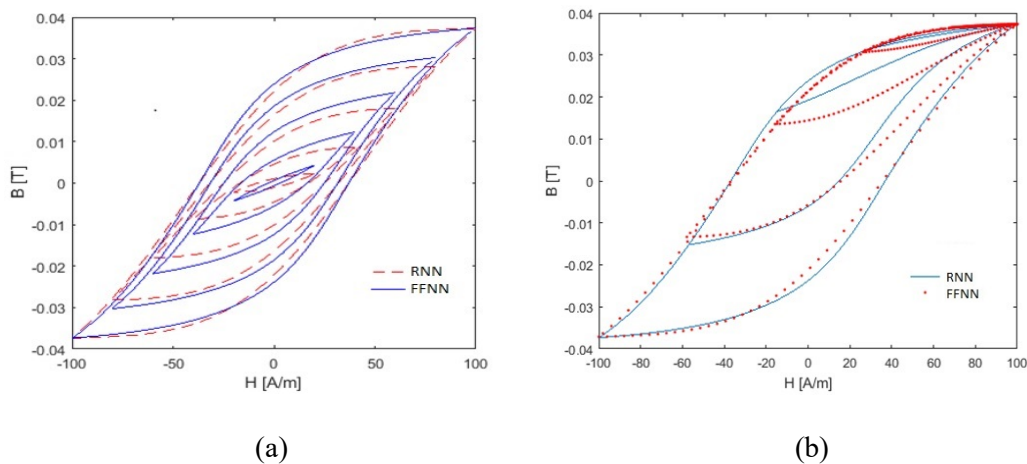


Figure 1: (a) comparison between RNN and FFNN on minor and symmetric hysteresis loops; (b) comparison between RNN and FFNN on first order reversal curves

-
- [1] F. Riganti Fulginei, et al. IEEE Trans. on Magnetics, 48(2), (2012), 307-310.
 - [2] A. Laudani, et al. RTSI 2016 IEEE 2nd International Forum.

Identification of Hysteresis Play Model from measurement data by means of Continuous Flock of Starlings Optimization algorithm

Antonino Laudani, Valentina Lucaferri, Francesco Riganti Fulginei,
Alessandro Salvini

Department of Engineering, Roma Tre University, Roma, Italy

The importance of any hysteresis model is related to two main aspects: the former is the accuracy in the reproduction of the material behaviour under different excitations; the latter is its feasibility to be implemented in a numerical code in order to be useful in the design phase of electromagnetic device. Another aspect that cannot be neglected is the identification of the model itself that usually is done starting from a number of measurements as low as possible. Among the methods that have had a discrete success in the past years there is the so-called play model. The Play Model (PM) is a kind of phenomenological model derived from the Preisach one [1]. It proposes to evaluate the magnetic flux density, B , from the applied magnetic field, H , by exploiting the weighted superposition of *play operators* that show a symmetric and rate-dependent properties. From a mathematical point of view, the PM is defined as follows:

$$\begin{cases} y(t) = \sum_{i=1}^n w_i \cdot \max\{u(t) - r_i, \min\{u(t) + r_i, y_{ei}(t - T)\}\} \\ y(0) = y_0 \end{cases}$$

where $u(t)$ and $y(t)$ are the input and the output of the model, respectively; n is the number of play operators, characterized by a threshold r_i and a slope w_i . Finally, y_{ei} represents the output of the i^{th} operators. It is clear that this model presents some advantages such as a simple mathematical formalism that allows an easy computational implementation thus reducing the processing effort. In this work, we address the identification of the play model from measurements and the problem connected to this issue. In particular, the algorithm used to solve this inverse problem is an advanced evolution of a swarm-intelligence classic algorithm, called Continuous Flock of Starling Optimization (CFSO). The basis of the CFSO is given by the well-known algorithm PSO (Particle Swarm Optimization), but CFSO adds some collective behaviour to PSO, improving the performance in exploration and refinement. Indeed, the CFSO algorithm can be configured to exhibit divergence, convergence or oscillation. Such flexibility can be exploited to create a hybrid strategy where a single algorithm can be used both for exploration and local refinement simply by adjusting the algorithm parameters. The results achieved in identification of Play Model are effective and the achieved model is in good agreement with experimental data.

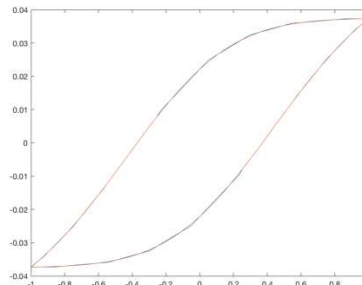


Figure 1: Schematic representation of the Neural Predictor (red line) and fitting capabilities on a sample field distribution (blue line)

An analytical formula to identify the parameters of the energy-based hysteresis model

Riccardo Scorretti^a, Fabien Sixdenier^a

^a Univ Lyon, Université Claude Bernard Lyon 1, INSA Lyon, EC Lyon, CNRS, Ampère, 69100, Villeurbanne, France

The energy based (EB) hysteresis model is a phenomenological model which respects thermodynamic laws and is inherently vectorial [1]. Henrotte et al. devised an effective numerical method to identify it, basing on the curve $H_c(H_p)$ where H_c = coercive field corresponding to the excitation $H:0 \rightarrow H_p \rightarrow -H_c$. In this work we present a different method which is less accurate, but it has the advantage of being based on an analytical formula.

The EB model is characterized by an anhysteretic magnetization function $M_{an}(h)$ and a pinning field function $\chi(\omega)$ where $\omega \in [0;1]$. $M_{an}(h)$ can be easily fitted from measured cycles. In order to determine $\chi(h)$ from the curve $H_c(H_p)$ we define an auxiliary function:

$$W(h) = \begin{cases} \chi^{-1}(h) & \text{if } 0 \leq h \leq \bar{H}_p \\ 1 & \text{otherwise} \end{cases} \quad (1)$$

where the material is saturated for $H \geq \bar{H}_p$. We demonstrate that $W(h)$ can be approximated by the following expression:

$$W(h) = \exp \left[- \int_{H_c(h)}^{\bar{H}_c} \frac{dx}{h-x} \right] \quad (2)$$

It can be observed that the property $W(h) \in [0;1]$ is enforced by construction. When $W(h)$ is known, it is easy to (numerically) compute and discretize $\chi(\omega)$. We performed measurements with a MnZn N30 Ferrite core, excited with a complex periodic signal (1st and 3rd harmonic). Measurements and simulations performed with the EB model fitted by using (2) are illustrated in figure 1. In spite of the fact that (2) is approximated, a fairly good agreement is found.

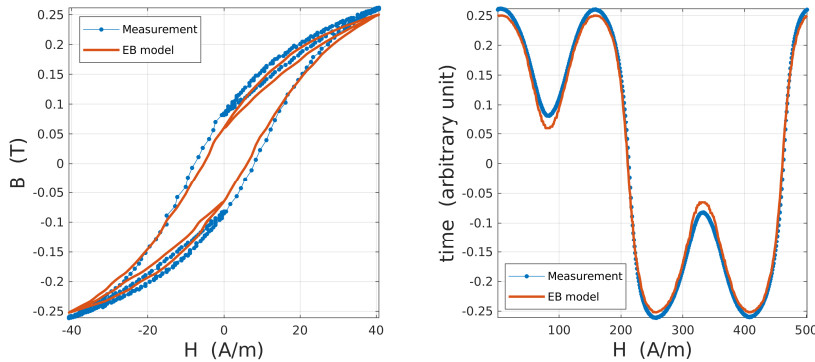


Figure 1: Left: hysteresis loop. Right: time domain signals.

[1] F. Henrotte, A. Nicolet, and K. Hameyer, COMPEL **25**, 71 (2006).

Parallel Neural Networks system for dynamic magnetic hysteresis modelling

Valentina Lucaferri ^a, Mauro Parodi ^b, Francesco Riganti Fulginei ^a, Alessandro Salvini ^a

^a Università degli Studi Roma Tre - Dipartimento di Ingegneria - Via V. Volterra 62, Roma (IT)

^b Università degli Studi di Genova - Dipartimento di Ingegneria Biofisica ed Elettronica - Via Opera Pia 11, Genova (IT)

A Neural Network (NN) based approach exploiting the properties of Singular Value Decomposition (SVD) technique for modelling dynamic hysteresis is presented. The development of static and dynamic hysteresis model is a challenging topics in the field of computational magnetism for two reasons: on one side, it is important to develop a model able to represent the behaviour of different materials and able to be identified by means of a set of measurements, regardless of the amount of computations required in the implementation; on the other hand, the model must be embeddable in simulation codes and, hence, its computational costs should be reduced as much as possible. These two requirements cannot be always satisfied, especially in the dynamic models. In such cases, the implementation of a NN represents a reasonable alternative to the use of classic models. The aim of this paper is to present a Neural Network based System able to provide the dynamic constitutive laws, preserving the low computational cost for neural networks training. This task is achieved by exploiting the Singular Value Decomposition, an efficient tool allowing the reduction both of the number of NNs needed and of the training set size. As far as the problem of hysteresis modelling is concerned, a 3D array coming from the sampling of the differential magnetic permeability, μ , for different values of the flux density, B , the magnetic field, H , and frequencies, f , is considered. Such values are collected into an array to which we refer as $\mu \in R^{m \times n \times r}$, where m is the length of B vector, n of H vector and r is the number of frequency samples, $f(x_{1,i}, x_{2,j}, x_{3,h}) = \mu(H_i, B_j, f_h)$. By applying recursively SVD, presented in [2], the magnetic permeability assumes the following reduced form:

$$\mu(B_i, H_j, f_h) = \sum_{s=1}^{\hat{p}} \sigma_s(f_s) \left[\sum_{t=1}^{p_s^\psi} \sigma_{s,t}^\psi \varphi_{s,t}^\psi(B_i) \lambda_{s,t}^\psi(f_h) \right] \left[\sum_{t=1}^{p_s^\eta} \sigma_{s,t}^\eta \varphi_{s,t}^\eta(H_j) \lambda_{s,t}^\eta(f_h) \right]$$

Where each of the unknown univariate functions can be approximated through a feed-forward Single Input Single Output, SISO, NN, as shown in Fig 1. The main advantage of this method consists in the possibility of speeding up the NN learning process, preserving the accuracy of the solution.

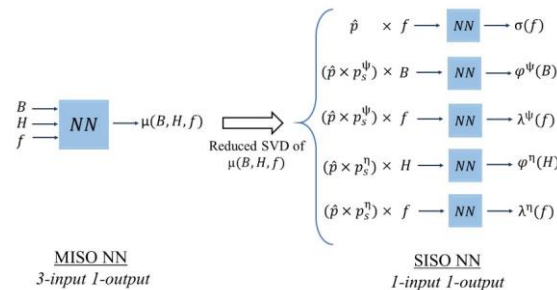


Figure 1. Transformation of a MISO NN in several SISO NNs.

[1] Z. Zhigang, L. Fugui, S. L. Ho, W. N. Fu, and W. Yan, "Modeling magnetic hysteresis under DC-biased magnetization using the neural network," *IEEE Trans. Magn.*, vol. 45, no. 10, pp. 3958–3961, Oct. 2009.

[2] Francesco Riganti Fulginei, Alessandro Salvini, and Mauro Parodi. Learning optimization of neural networks used for mimo applications based on multivariate functions decomposition. *Inverse Problems in Science and Engineering*, 20(1):29-39, 2012.

Advances in Magnetism 2020-21, June 13-16, 2021

**Spintronics, multiferroics and
voltage control of magnetism**

**Mathematical modeling and
micromagnetics**

**Macroscale modeling of
magnetic and multifunctional
materials and devices**

[Abstracts can be easily browsed through the bookmarks](#)

Comparative electric transport behavior between Co-rich soft magnetic heterostructures

E. F. Pinzón-Escobar^a, G. Alvarez^b, A. Esparza-García^a and H. Montiel^a

^a Instituto de Ciencias Aplicadas y Tecnología, UNAM, Ciudad de México, México

^b Universidad Autónoma de la Ciudad de México, Campus Cuauhtpec, CDMX, México

In this work, we present a comparative electric and magnetic study between $\text{Co}_{67}\text{Fe}_4\text{Mo}_1\text{Si}_{17}\text{B}_{11}/\text{Au}/\text{Co}_{67}\text{Fe}_4\text{Mo}_1\text{Si}_{17}\text{B}_{11}$ and $\text{Co}_{67}\text{Fe}_4\text{Mo}_1\text{Si}_{17}\text{B}_{11}/\text{Au}/\text{Ni}$ heterostructures. These Co-rich amorphous soft magnetic materials exhibit a high resistivity, low eddy current and high saturation magnetization. These heterostructures were deposited on a pyrex substrate by DC magnetron sputtering, where we have varied the $\text{Co}_{67}\text{Fe}_4\text{Mo}_1\text{Si}_{17}\text{B}_{11}$ (VITROVAC) thickness on substrate from 30 to 125 nm, holding 5 nm of Au, and 30 nm of ferromagnetic thin film in the top. The photolithography process was employed to etch line patterns from 0.1 mm to 1 mm and with 1 cm of length. Magnetic and structural properties were measured by means of vibrating sample magnetometer (VSM) and X-ray diffraction (XRD). Electrical characterization was carried out in the plane configuration (Figure 1), and the magnetoresistance measurements were carried out in all samples and we have observed a significant response. It can be observed a correlation between width of patterns with the increases in magnetoresistance, as are shown in figure 2a) and 2b).

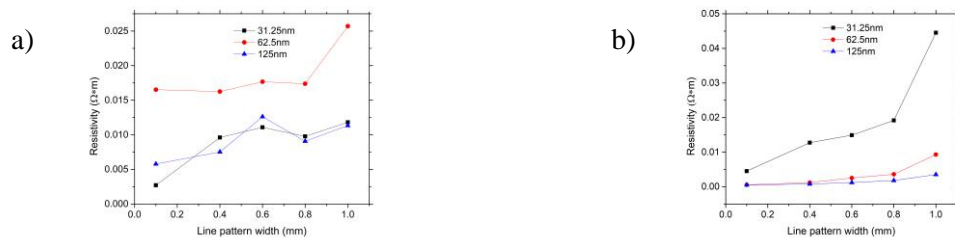


Figure 1: Resistivity of a) $\text{Co}_{67}\text{Fe}_4\text{Mo}_1\text{Si}_{17}\text{B}_{11}/\text{Au}/\text{Co}_{67}\text{Fe}_4\text{Mo}_1\text{Si}_{17}\text{B}_{11}$ and b) $\text{Co}_{67}\text{Fe}_4\text{Mo}_1\text{Si}_{17}\text{B}_{11}/\text{Au}/\text{Ni}$ vs line patterns width for three different thickness $\text{Co}_{67}\text{Fe}_4\text{Mo}_1\text{Si}_{17}\text{B}_{11}$ film on substrate.

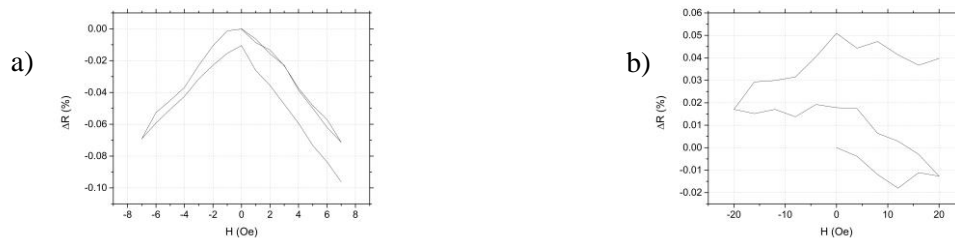


Figure 2: Magnetoresistance of a) $\text{Co}_{67}\text{Fe}_4\text{Mo}_1\text{Si}_{17}\text{B}_{11}/\text{Au}/\text{Co}_{67}\text{Fe}_4\text{Mo}_1\text{Si}_{17}\text{B}_{11}$ and b) $\text{Co}_{67}\text{Fe}_4\text{Mo}_1\text{Si}_{17}\text{B}_{11}/\text{Au}/\text{Ni}$ at 0.4 mm line width for perpendicular H (Oe) & I (A).

This work was supported by DGAPA-UNAM through the grant PAPIIT-IG100517.

Features in the field dependence of the Hall constant $\text{Mn}_{0.135}\text{Hg}_{0.865}\text{Te}$

Aleksei V. Shestakov^a, M.A. Cherosov^b, M.I. Ibragimova^a, R.M. Eremina^a

^a Zavoisky Physical-Technical Institute, FRC Kazan Scientific Center of RAS, Kazan, Russia

^b Kazan Federal University, Kazan, Russia

Narrow gap semiconductors continue to attract the attention of researchers due to the discovery of new quantum properties in the past few years. For example, Mairan fermions showed themselves in the presence of steps in the field dependence of the magnetic conductivity at the interface between Nb and a magnetic topological insulator $(\text{Cr}_{0.12}\text{Bi}_{0.26}\text{Sb}_{0.62})_2\text{Te}_3$ [1]. It has long been known about the topological properties of mercury chalcogenides. In diluted magnetic semiconductors, the strong spin-spin interactions between band electrons and localized magnetic ions lead to a host of entirely new magneto-optical physical phenomena, such as giant Faraday, giant Kerr, photoinduced magnetization effects, which was first demonstrated in monocrystals $\text{Mn}_x\text{Hg}_{1-x}\text{Te}$ by Krenn [2]. The aim of our work was to study the magnetic properties of the solid solution $\text{Mn}_{0.135}\text{Hg}_{0.865}\text{Te}$. The samples were grown by the crystallization from a two-phase mixture with replenishment of the melt from a tellurium solution 30 years ago. Now, solid solutions have been studied by X-ray fluorescence analysis (XFA). It was found that during a long storage time, mercury ions evaporated from the surface and layers formed near the surface with a high content of manganese, and at a depth – less. XFA showed that inside the sample there are regions (with medium sizes of regions $\sim 20 \mu\text{m}$) strongly depleted in manganese ions. (Figure 1). In work [3] it is shown, that Weyl points can be observed in layered structure $\text{HgTe}/\text{Hg}_{0.97}\text{Mn}_{0.03}\text{Te}$.

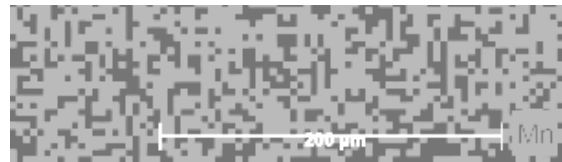


Figure 1: XFA of crystal $\text{Mn}_{0.135}\text{Hg}_{0.865}\text{Te}$.

Dependencies of Hall constant from magnetic field for crystal $\text{Mn}_{0.135}\text{Hg}_{0.865}\text{Te}$ were measured at a temperature at 5 K on the multifunctional system for measuring physical properties with superconducting magnet PPMS-9. Dependence of the Hall constant from magnetic field for $\text{Mn}_{0.135}\text{Hg}_{0.865}\text{Te}$ at a temperature 5 K show anomalous what character expressed in several aspects: there is a sign change of the Hall constant at 0.42~0.48 T (Figure 2), there are steps in the fields 0.13 и 0.33 T (Figure 2a, right insert), asymmetry in the forward and reverse fields at different speeds (10 и 1 Oe/sec).

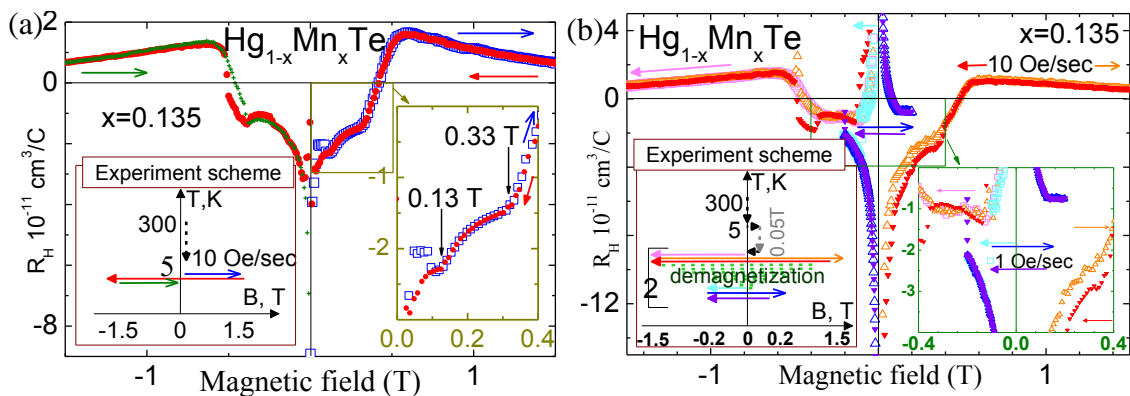


Figure 2: Magnetic field dependence of the Hall constant of $\text{Mn}_{0.135}\text{Hg}_{0.865}\text{Te}$ at a temperature 5 K under different experimental conditions: (a) 10 Oe/sec; (b) 1 Oe/sec.

[1] Qing Lin He et al. *Science* **357** (2017), 294–299.

[2] H. Krenn et al. *Phys. Rev. Lett.* **55** (1985), 1510.

[3] M. Marchewka et al. *Surface Science* **700** (2020), 121653.

Switching metal-to-half-metal behavior in Heusler alloy

Vasiliy D. Buchelnikov^a, Vladimir V. Sokolovskiy^a, Olga N. Miroshkina^{a,b,c}, Danil R. Baigutlin^{a,b}, Mikhail A. Zagrebin^{a,d}, Bernardo Barbiellini^{b,e}, and Erkki Lähderanta^b

^aChelyabinsk State University, 454001 Chelyabinsk, Russia

^bLUT-University, FI-53851 Lappeenranta, Finland

^cUniversity of Duisburg-Essen, 47057, Duisburg, Germany

^dNational Research South Ural State University, 454080 Chelyabinsk, Russia and

^ePhysics Department, Northeastern University, Boston, Massachusetts 02115, USA

Nowadays, spintronics is a rapid developing field of science and technology [1]. Ferromagnetic Heusler alloys, which are characterized by a band gap in one spin channel at the Fermi level, are interesting from this point of view [2]. In this work we propose a ferromagnetic Heusler alloy Mn_2ScSi that can switch between a metal and a half-metal. This effect can provide tunable spintronics properties.

To perform the calculations, we employed the PAW method implemented in VASP code using 16-atom supercells. The GGA for the exchange correlation functional was treated within the Perdew, Burke, and Ernzerhof (PBE) scheme. Electron correlation effects beyond GGA were included using both GGA+ U by Dudarev et al. [3] and meta-GGA SCAN by Sun et al. [4].

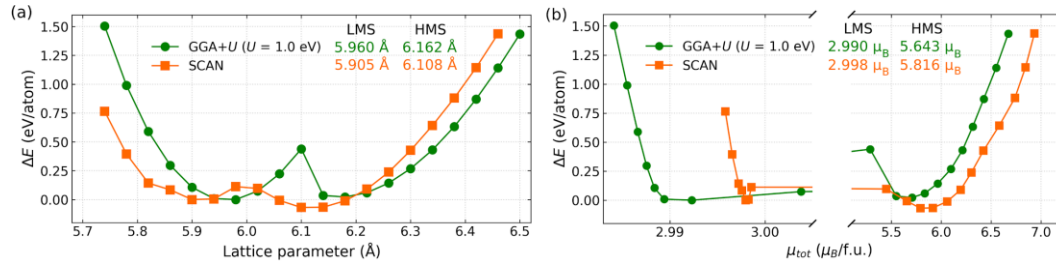


Figure. 1. The total energy difference (ΔE) as a function of (a) lattice parameter and (b) magnetic moment of Mn_2ScSi for SCAN and GGA+ U ($U=1$ eV) solutions. For each cases, the ΔE is plotted with respect to the left energy minimum.

Mn_2ScSi exhibits behavior with two energy minima, as seen in Fig. 1a. The phase at low lattice crystal volume is a low magnetic half-metallic state while the phase at high lattice crystal volume is a high magnetic metallic state. We suggest that the transition between half-metallic and metallic states can be triggered by a triaxial contraction/expansion of the crystal lattice or by an external magnetic field if we assume that the lattice is cubic and remains cubic under expansion/contraction.

The work is supported by the RFBR - Russian Foundation for Basic Research No. 20-42-740006.

-
- [1] W. Gallagher, Emerging Spintronic Memories (CRC Press, 2019) pp. 443–470.
 [2] L. Bainsla, K. Suresh, Appl. Phys. Rev. **3** (2016), 031101.
 [3] S. Dudarev, G. Botton, S. Savrasov, C. Humphreys, A. Sutton, Phys. Rev. B **57** (1998), 1505.
 [4] J. Sun, A. Ruzsinszky, J. P. Perdew, Phys. Rev. Lett. **115** (2015), 036402.

Switching of antiferromagnetic CuMnAs by ultrashort electrical pulses

Jan Zubáč^{a, b}, Zdeněk Kašpar^{a, b}, Filip Křížek^a, Vít Novák^a, Kamil Olejník^a, Tomáš Jungwirth^{a, c}

^a Institute of Physics of the Czech Academy of Sciences, Prague, Czech Republic

^b Faculty of Mathematics and Physics, Charles University, Prague, Czech Republic

^c School of Physics and Astronomy, University of Nottingham, United Kingdom

Antiferromagnetic spintronic memory devices take advantage of fast magnetization dynamics overcoming the GHz limit of their ferromagnetic counterparts used in contemporary microelectronics, e. g. in magnetic random-access memories (MRAMs).

On the other hand, manipulation of magnetic state of antiferromagnets is substantially more difficult due to the zero net magnetization and consequent low sensitivity to magnetic fields [1]. One of few proposed possibilities is to utilize the Néel spin-orbit torques induced by electrical current which can be employed for an efficient control of magnetic moments in materials meeting particular symmetry requirements [2]. Recently, a new mechanism based on controlling magnetic domain size and manipulating magnetic nano-textures has been presented [3]. Such effects has been experimentally utilized for electrical switching of epitaxially grown CuMnAs thin film samples [4] which in combination with the electrical readout may conveniently operate as memory devices [5].

In the present study, we report on electrical switching of CuMnAs memory cells with electrical pulses lengths down to a sub-nanosecond region. We investigate samples of various thicknesses grown on GaP, GaAs and Si substrates. By changing pulse parameters (length, voltage, pulse count and repetition rate) and external conditions (temperature, magnetic field), we evaluate their switching ability and efficiency and examine the underlying physical mechanisms controlling the switching process.

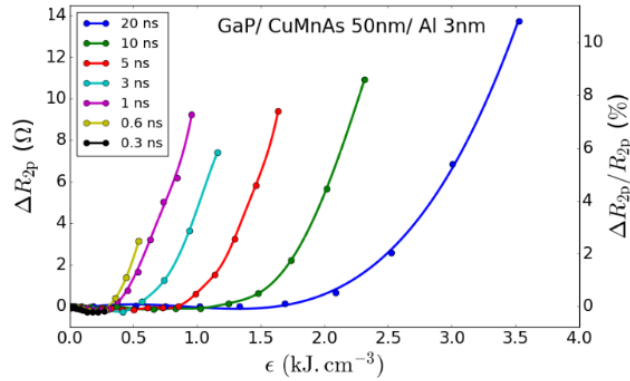


Figure 1: Readout signal of 5um CuMnAs bar as a function of energy density for different pulse widths. Relation $\epsilon = j^2 \rho \tau_p$ was used for the estimation of the energy density.

-
- [1] T. Jungwirth, Nature Nanotechnology 11.3 (2016): 231-241.
 - [2] J. Železný, Physical Review Letters 113.15 (2014): 157201.
 - [3] Z. Kašpar, arXiv:1909.09071 (2019).
 - [4] P. Wadley, Science 351.6273 (2016): 587-590.
 - [5] K. Olejník, Nature Communications 8 (2017): 15434.

X-ray resonant magnetic reflectometry (XRMR) study of the interface between ferromagnetic transition metals and MgO

Sven E. Ilse^a, Daan B. Boltje^{a,b}, Gisela Schütz^a, Eberhard Goering^a

^a Max-Planck-Institute for Intelligent Systems, Stuttgart, Germany

^b Delmic BV, Delft, South Holland, Netherlands

Multilayer systems of ferromagnetic transition metals and MgO attract a lot of attention in the last years because of their application in STT-MRAMs. Especially the interface between the magnetic transition metal and MgO is of interest since the chemical and magnetic properties at this interface are important for the performance of STT-MRAM cells. Because those properties determine for example the strength of the interfacial perpendicular magnetic anisotropy and the thickness of possible magnetic dead layers [1].

With our own reflectometer dedicated to (soft-) x-ray resonant magnetic reflectometry (XRMR) we are able to study such multilayer systems and determine the chemical and magnetic properties at the interfaces [2]. With XRMR we combine the advantages of reflectometry and X ray magnetic circular dichroism (XMCD). Thus, we are able to determine element specific chemical and magnetic depth profiles. And since, XRMR is particular sensitive to interfaces the element specific roughness of each layer can be determined as well [3,4]. To determine those depth profiles we simulate XRMR measurements using ReMagX [3-5] and fit the simulations to match actual measurements.

We performed X-ray absorption spectroscopy (XAS), XMCD and XRMR measurements on Ta|CoFeB|MgO|Al₂O₃|Au stacks. With off-resonant reflectometry measurements at different energies, we determined the chemical depth profile. Those revealed a pronounced roughness at the Ta|CoFeB interface and that especially Fe intermixes largely with other species at the interfaces. Resonant magnetic reflectometry measurements at the Cobalt and Iron L₃ edge enabled us to determine the magnetic depth profile, which revealed a 10 Å and a 4 Å thick magnetic dead layer for Fe and Co, respectively, at the CoFeB|MgO interface.

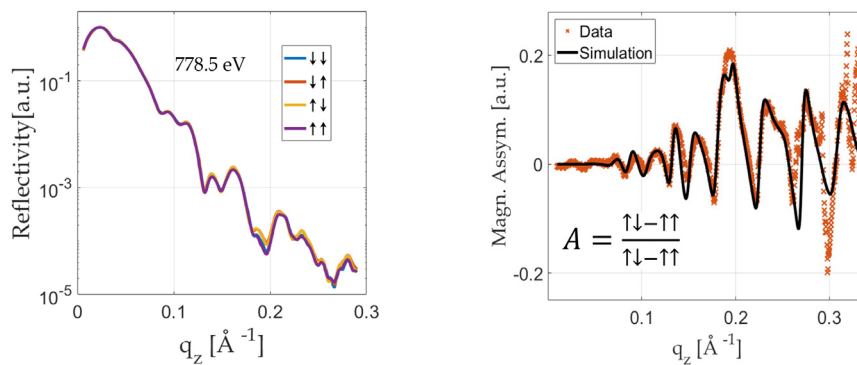


Figure 1: left: Resonant reflectivity curves measured at 778.5 eV (Co L₃ edge) with parallel (blue and purple) and antiparallel (orange and yellow) alignment of x-ray polarization and magnetization. right: Measured and with ReMagX [3-5] simulated magnetic asymmetry A at 778.5 eV (Co L₃ edge).

-
- [1] B. Dieny and M. Chshiev, Rev. Mod. Phys., 89.2, 025008 (2017).
 - [2] S. Brück, et al., Rev. Sci. Instrum., 79, 083109, (2008);
 - [3] S. Macke and E. Goering, J. Phys.: Condens. Matter, 26.36, 363201 (2014).
 - [4] S. Macke, et al., Adv. Mater., 26.38, 6554-6559 (2014)
 - [5] S. Macke, www.remagx.org

Synthesis of bismuth and cobalt ferrites nanoparticles for preparation of magnetoelectric nanocomposites

Alexander Omelyanchik^a, Liudmila Makarova^{a,b}, Irina Baraban^a, Karim Amirov^a, Marat Khairullin^b, Vladimir Rodionov^a, Nikolai Perov^b, Davide Peddis^{c,d} and Valeria Rodionova^{a,f}

^a Immanuel Kant Baltic Federal University, Kaliningrad, Russia

^b Moscow State University, Moscow, Russia

^c Istituto di Struttura della Materia – CNR, Monterotondo Stazione, Roma, Italy

^d Department of Chemistry and Industrial Chemistry, Università of Genova, Genova, Italia

^f National University of Science and Technology MISiS, Moscow, Russia

The family of magnetoelectric multiferroics is extensively developing over last decades because of its unique feature combining magnetic and electric properties in one material that makes them an irreplaceable tool, for instance, for a set of spin logic devices [1]. The Bismuth ferrite (BiFeO₃) is probably one of the most interesting materials among them, indeed in this single-phase material combined magnetic order above room temperature and large ferroelectric polarization (~90 μC cm⁻²) [2]. The next improvement of its properties, especially in the sense of control of magnetization via the electrical field and in the opposite, can be achieved in nanocomposites consisting of piezoelectric and magnetostrictive materials.

In this work, we investigate nanocomposites of BiFeO₃ nanoparticles with high ferroelectric polarization and cobalt ferrite (CoFe₂O₄) nanoparticles which are highly magnetostrictive material with well-controlled magnetic properties at the nanoscale [3]. Nanoparticles of both types were synthesized by a sol-gel auto-combustion method involving metal nitrates and citric acid. After casting, we obtained single-phase CoFe₂O₄ with inverse spinel structure confirmed with X-ray diffraction. However, when cobalt salt was replaced to bismuth, the mixture of different phases was obtained. High-temperature annealing at 600 °C was applied to homogenize phase composition of the sample and obtain single-phase perovskite structure of BiFeO₃, which was accompanied by growing of crystal size. After a composite in form of pellet was prepared by pressing and annealing of mixture of two types of nanoparticles. The magnetic properties were studied with a vibration sample magnetometer; the morphology and chemical composition were investigated with energy-dispersive X-ray spectroscopy; the thermal analysis was carried with differential scanning calorimetry, and finally, the magneto-electric properties were instigated.

The reported study was funded by RFBR according to the research project № 18-32-01016.

[1] Balinskiy, Michael, et al. "Magnetoelectric Spin Wave Modulator Based On Synthetic Multiferroic Structure." *Scientific reports* 8.1 (2018): 10867.

[2] Spaldin, N. A., and R. Ramesh. "Advances in magnetoelectric multiferroics." *Nature materials* 18.3 (2019): 203.

[3] a) da Silva, F. G., et al. "Structural and Magnetic Properties of Spinel Ferrite Nanoparticles." *Journal of nanoscience and nanotechnology* 19.8 (2019): 4888-4902;

b) Bibani, Malek, et al. "Tailoring the magnetic properties of cobalt ferrite nanoparticles using the polyol process." *Beilstein Journal of Nanotechnology* 10.1 (2019): 1166-1176.

Tracing back the interlayer thickness dependence of saturation magnetization in Co/RuFe/Co sandwiches using XMCD

Frank Schulz^a, Zach Nunn^b, Erol Girt^b, Eberhard Goering^a

^a Max-Planck-Institute for Intelligent Systems, Stuttgart, Germany

^b Simon Fraser University, Burnaby, Canada

The effect of interlayer exchange coupling in magnetic thin films has proven to be of great technological use, enabling the development of hard drives with very high storage densities [1-3]. And yet, there are aspects of this effect that are still not fully understood. Recent studies have found that the interlayer thickness of Co/RuFe/Co sandwiches does not only affect the type and strength of interlayer coupling, but also causes a non-monotonous variation of the saturation magnetization of these systems [4]. Magnetometric measurements of these samples are shown in the left part of fig. 1. In order to investigate this effect, X-ray absorption spectra have been measured in total electron yield at the L_2 and L_3 edges of both Fe and Co, as shown in the right part of fig. 1 for Co. Making use of the X-ray magnetic circular dichroism (XMCD) effect, this gives an element specific method of measuring the magnetic properties of the samples. By applying the sum rules [5,6], it was possible to determine the magnetic moment per atom coming from Co and Fe respectively. Additionally, magnetometric measurements have been performed using a superconducting quantum interference device (SQUID), which were combined with simulations using an enhanced Stoner-Wohlfarth model. It could be shown that the change in saturation magnetization does not stem from the magnetic contribution of the Fe in the interlayer, but instead can be attributed to a non-magnetic dead layer of Co near the interface of Co and RuFe. The thickness of this dead layer was estimated using a model that incorporates electron damping, as well as self absorption effects, to be approximately 0.1 nm. An effective electron mean free path is used to calculate the damping of electrons from buried layers. With this, the reduction of the saturation magnetization was successfully traced back to a reduced Co magnetic moment originating from a Co dead layer.

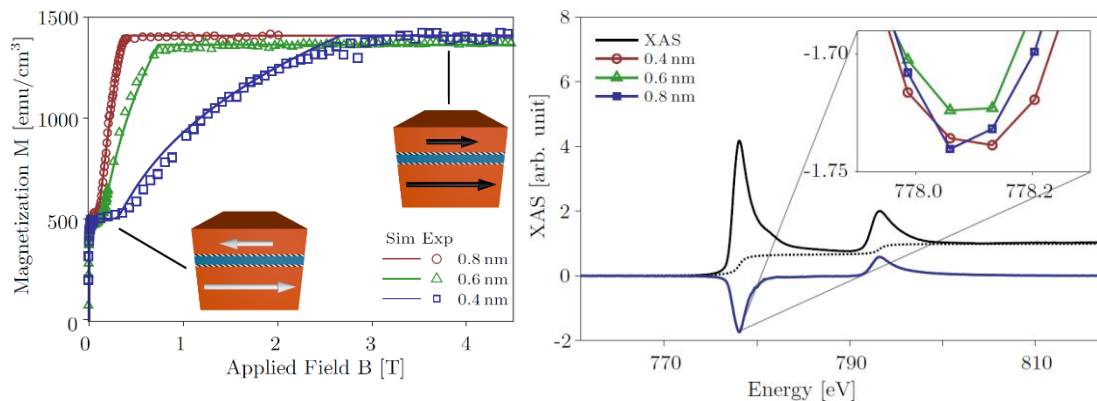


Figure 1: Left: Hysteresis loops of samples with different spacer layer thickness. Right: XAS and XMCD spectra at the Co L_2 and L_3 edges for different spacer layer thickness.

-
- [1] P. Grünberg, R. Schreiber and H. Sowers, Physical Review Letters, Vol. 57, p. 2442 (1986)
 - [2] G. Binasch, P. Grünberg and W. Zinn, Physical Review B, Vol. 39, p. 4828 (1989)
 - [3] M.N. Baibich, J.M. Broto, A. Fert and J. Chazelas, PRL, Vol. 61, 2472 (1988)
 - [4] Z. Nunn, F. Schulz, E. Goering and E. Girt, Unpublished (2019)
 - [5] B. T. Thole, P. Carra and G. van der Laan, Physical Review Letters, Vol. 68, p. 1943 (1992)
 - [6] P. Carra, B.T. Thole and X. Wang, Physical Review Letters, Vol. 70, p. 694 (1993)

Effect of Synchronized La and Al substitution on magnetic behavior of multiferroic bismuth ferrite

Deepika Tripathi¹, Rama Shanker Yadav¹, Manoj Prajapat², D. S. Rana² and Vilas Shelke^{1*}

¹Novel Materials Research Laboratory, Department of Physics, Barkatullah University, Bhopal, 462026 India

²Department of Physics, Indian Institute of Science Education and Research, Bhopal, 462066 India

*e mail: drshelke@gmail.com

Multiferroic materials have attracted worldwide attention for simultaneous use of multiple properties in single device for sensors and data storage applications. Bismuth ferrite has clear advantages of lead free composition, high ferroelectric polarization and high transition temperature. However, volatile nature of bismuth, formation of secondary phases, oxygen vacancies are the main obstacles for its synthesis [1] and low magnetization value for its applications [2,]. It is desirable to obtain single phase bismuth ferrite material with improved magnetization value [3,4]. Here, we demonstrate structural modulation using non-magnetic ion substitution as an effective strategy to improve magnetization behavior of multiferroic materials. We have prepared dual-site substituted bulk samples with compositions $\text{Bi}_{1-x}\text{La}_x\text{Fe}_{1-y}\text{Al}_y\text{O}_3$ using solid state reaction method. X-Ray diffraction patterns revealed phase purity and crystal structure modification. The Raman spectra also confirmed distortion in rhombohedral structure by shifting of modes. Magnetic measurement indicated departure from antiferromagnetic nature with high remnant magnetization values in these samples.

References:

- [1] S. Pillai, D. Bhuwal, T. Shripathi, V. Shelke, J. Mater. Sci. Mater. Electron, 24, 2950 (2013)
- [2] S. Pillai, et al., Appl. Phys. Lett. **102**, 072907 (2013)
- [3] S. Pillai, D. Tripathi, T. A. Para, A. Das, T. Shripathi, V. Shelke, J. Appl. Phys. 120, 164103 (2016)
- [4] D. Tripathi, SPillai, V. Shelke, J. Mater. Sci. Mater. Electron, 30, 2795(2019)

Micromagnetic modelling of hysteresis in permalloy thin films with impurities

Inna Lobanova^{a,b}, Stéphane Despréaux^b, Stéphane Labbé^c

^a Université Grenoble Alpes, Grenoble, France

^b Laboratoire Jean Kuntzmann, CNRS, Grenoble, France

^c Sorbonne Université, Paris, France

Micromagnetism is a model of fundamental magnetic properties of ferromagnetic materials at submicrometer scale. This scale is required to resolve domain walls and their interaction with matter - key phenomena of hysteresis understanding. The basic problem consists in finding the minimum of the magnetic energy [1] at each step of a magnetisation cycle, which allows to derive the magnetic hysteretic behaviour.

In the following work we have investigated the influence of magnetic impurities and their distribution on the hysteresis cycle of permalloy thin films. The representative volume element is a rectangular sheet with $0.64\mu\text{m} \times 1.28\mu\text{m} \times 0.01\mu\text{m}$, meshed with 8192 cubic cells.

Here we present the results of the comparison between two materials – P02 and P07 - with same magnetization at saturation ($M_s=0.8\text{MA/m}$), but different exchange stiffness ($A_{P02}=13\text{pJ/m}$, $A_{P07}=1.3\mu\text{J/m}$) and uniaxial anisotropy constant ($K_{P02}=0.5\text{kJ/m}^3$, $K_{P07}=100\text{kJ/m}^3$). The impurities were placed either in the centre, corner, and sides of the sample. The corresponding geometry and hysteresis curves are presented in Figure 1.

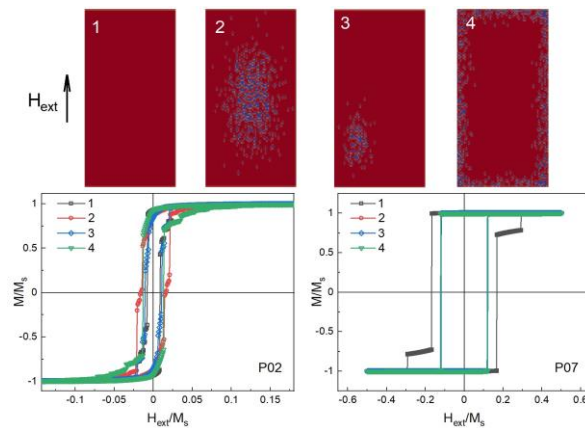


Figure 1: Top row: Samples with different position of impurities. Red – magnetic matter, blue - impurities. Bottom row: corresponding hysteresis cycles for material P02 (left) and P07 (right). Numbers in the legend correspond to numbers of geometries.

We have established that in case of a soft (P02) the impurities pin magnetic vortices and increase the coercive field. It is the strongest when the impurities are in the centre. However, in the case of material with high anisotropy and exchange constants (P07) the switching field is lower when there are impurities, as they serve as nucleation centres for the magnetization reversal, which correlates with existing theories [2]. It was additionally discovered that in the material P07 with the impurities shifted from the centre the single-domain state is energetically more favourable than the formation of domain walls.

This project has received the funding from the Research Fund for Coal and Steel of the European Union under the grant agreement No.847296, which is gratefully acknowledged.

[1] W.F. Brown Jr. “Micromagnetics”, John Wiley & Sons Inc (1963)

[2] D.S. Schmool, D. Marko, “Magnetism in Solids: Hysteresis”, Elsevier (2018)

Kinetics of phase transformations in Fe-Ga alloys

Oksana Pavluchina^{a,b}, Vasiliy Buchelnikov^{a,b}, Vladimir Sokolovskiy^{a,b}, Mikhail Zagrebin^{a,b}, Mariya Matyunina^a, Olga Miroskina^a, Danil Baigutlin^a

^a Chelyabinsk State University, Chelyabinsk, Russia

^b National University of Science and Technology MISIS, Moscow

In recent decades, the structural and magnetic properties of Fe-Ga alloys have been studied experimentally and theoretically [1–4]. The most interesting area for studying these alloys is the region of $0.18 \leq x \leq 0.30$ at. %. According to the phase diagram [2], phases A2, B2, D0₃, D0₁₉, L1₂ are observed in the indicated range. A more detailed study of phase diagrams and study of the kinetics of phase transformations in these alloys are presented in [3, 4]. The study of the kinetics of the order-disorder transition for *bcc* structures of Cu-Zn-Al alloys is presented in [5]. The Monte Carlo method is used in this theoretical work. In this work, the phase transition temperature is in good agreement with the experimental values.

Phase transformations in Fe₇₇Ga₂₃ alloys were theoretically investigated in this work. The Blume-Emery-Griffiths Hamiltonian and the Monte Carlo method were used to simulate the transitions in a three-dimensional cubic lattice with a D0₃ structure, consisting of iron and gallium atoms. For the Fe₇₇Ga₂₃ alloy, the curves of the order parameters change with temperature and cooling rate are calculated. It was found in this work that the disordered phase A2 is observed at high temperatures, which is in agreement with the available experimental data. At the next stage, a phase diagram was constructed for the Fe₇₇Ga₂₃ alloy. It was found that at the highest speed cooling, two phase transitions A2 → A2 + B2 → A2 + D0₃ are observed. At a low cooling rate, a larger number of phases are observed, which is consistent with experimental data [3].

The reported study was funded by RSF, project no. 18-12-00283, no. 17-72-20022. O.O.P., M.A.Z. and V.D.B. acknowledged NUST MISIS (project no. K2-2020-018).

-
- [1] A. Clark, J. of Appl. Phys. **93** (2003), 8621.
 - [2] O. Kubaschewski, Berlin : Springer-Verlag, 1982, 185.
 - [3] I. Golovin, Intermetallics. **114** (2019), 106610.
 - [4] A. Mohamed, Materials Letters. **279** (2020), 128508.
 - [5] F. Lanzini, Physical Review B. **77** (2008), 134207.

Self-organized critical superferromagnetic dynamics

V.N. Kondratyev ^a

^a Bogolubov Laboratory of Theoretical Physics, JINR, 141980-RU Dubna, Russia

Superferromagnetism (SFM) was invoked to specify the structures involving quantum confined objects, e.g., atomic clusters, quantum dots, nanocrystals referred for hereafter as, simply, NC, see [1] and refs. therein. Such system are of fundamental interest for a study of interactions, transport processes and phase features at fairly wide range of various parameters, e.g., coupling constants, densities, Coulomb blockade gaps etc. Such super-crystals allow for considerable benefits in '*figures of merits*' for technological, biological and therapeutic applications.

We consider magnetodynamics of NC arrays by employing the randomly jumping interacting moments (RJIM) model [1] including quantum fluctuations due to the dot discrete level structure, inter-dot coupling and disorder. Magnetic state equation of such a system is demonstrated to exhibit spinodal regions in *{disorder, magnetic field}*-plane and the critical points. In vicinity of such points of self-organized (SO) criticality the magnetization evolves as erratic jumps similar to the well-known Barkhausen effect. Exploring correlations of noise amplitudes represents then convenient analytical tool for quantitative definition, description and study of SO criticality in magnetic NC assemblies. We find strong correlations in jump amplitude distributions characterizing, thereby, a system with respect to NCs and a disorder.

[1] V.N. Kondratyev, *Phys.Lett. A* **354**, 217 (2006); *J. Phys. CS* **129**, 012013 (2008)

Evaluation of inhomogeneous mechanical residual stress distribution from the experimental needle probe method and a Jiles-Atherton-Sablik based space discretized simulation tool.

Y. A. Tene Deffo^a, P. Tsafack^a, B. Ducharne^b, E. Tanyi^a

^a Faculty of Engineering and Technology of the University of Buea, Cameroon

^b Laboratoire de Génie Electrique et Ferroélectricité, INSA Lyon, France

Hardening processes are mandatory in the fabrication of graded materials used in high performance engineering applications such as transportation, construction and energy, to resist surface wear and fatigue damage [1]. The hardness gradient profile due to the surface metallurgical treatment always matched up with a gradient of residual stress and plastic deformations. The intrinsic relationship between magnetic microstructure (magnetic domains and domain walls) and the mechanical microstructure (stress and strain fields) allows continuous evaluation and control of hardness gradient profile of steel-type ferromagnetic materials via the residual stress monitoring [2][3].

In this paper, a mixed experimental/numerical method based on the local magnetic signature is proposed to evaluate mechanical residual stress gradients in sheet metal forming process and indirectly control the viability of the hardening processes. The proposed method correlates the gradient in hardness with depth and the mechanical stress profiles (tensile and compression) of the modelled material to its equivalent magnetic signature within the bend allowance. A mechanical finite element model (FEM) is developed to generate an accurate estimation of the residual stress gradient. Sample strips of low carbon 1008-1010 steel were used as model materials and local magnetic properties measurements were carried out using the classic needle probe method. This method allows to calculate the local flux density by measuring the potential difference between two points at the surface of a ferromagnetic test material in contact with the needle probe tips [4].

This paper presents method which enables the computation of gradient of mechanical residual stress from local magnetic measurements using the needle probe method. Fig. 1 summarises the modelled and experiments results obtained.

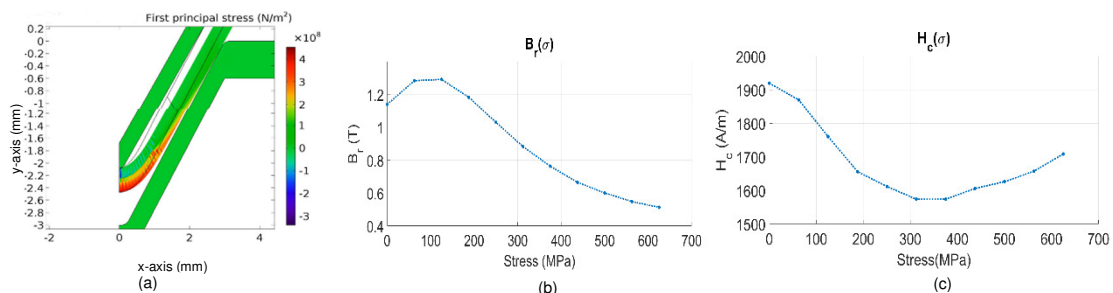


Figure 1: (a) mechanical FEM sheet forming model, (b) Remanence field tensile stress dependence (c) Coercitivity tensile stress dependence

-
- [1] Y. Miyamoto & al., New York: 1st ed., Springer, 1999.
 - [2] B. Gupta & al., J. of Mag. and Mag. Mat., vol. 486, n° 165250, 2019.
 - [3] B. Gupta & al., NDT&E, vol, 104, pp. 42-50, 2019.
 - [4] Y. A. Tene Deffo & al., IEEE Trans. Mag., vol. 55, no. 7, 2019.

Static Hysteresis modelling of NO FeSi in rolling and transverse directions by using the energy based model

Riccardo Scorretti^a, Fabien Sixdenier^a and Atef Lekdim^b

^a Univ Lyon, Université Claude Bernard Lyon 1, INSA Lyon, EC Lyon, CNRS, Ampère, 69100, Villeurbanne, France

^b LEM Tech France, 575-655-Les Allées du parc, 69800 Saint Priest, France

Vectorial hysteresis models are required in order to predict magnetic losses or magnetic waveforms in NO FeSi sheets when excited in both rolling (RD) and transverse direction (TD). One of the last developed models which has a lot of desirable properties is the energy based (EB) model of Henrotte [1], also called vector play model [2]. This model has the advantage to be intrinsically vectorial, and respects the principles of thermodynamics. Efficient identification protocols [3, 4] exist to identify its parameters.

In this model the applied magnetic field \mathbf{h} is decomposed in a reversible and irreversible part. The reversible part writes as the sum of the contribution N cells (fig. 1, left):

$$\mathbf{h}_{re} = \sum_{k=1}^N \omega_k \mathbf{h}_{re}^k \quad ; \quad \mathbf{h}_{re}^k = \begin{cases} \mathbf{h}_{re0}^k & \text{if } \|\mathbf{h} - \mathbf{h}_{re}^k\| \leq \chi^k \\ \mathbf{h} - \chi^k \frac{\mathbf{h} - \mathbf{h}_{re}^k}{\|\mathbf{h} - \mathbf{h}_{re}^k\|} & \text{otherwise} \end{cases} \quad (1)$$

In the original version each cell gives an isotropic contribution. This article presents recent developments of the EB model in order to take into account the anisotropy. In fig. 1, right are depicted two cycles of the same amplitude where the material is excited in the transverse and on the rolling directions. This first result shows that a not so complex modification of the original model is able to reproduce an anhysteretic behaviour.

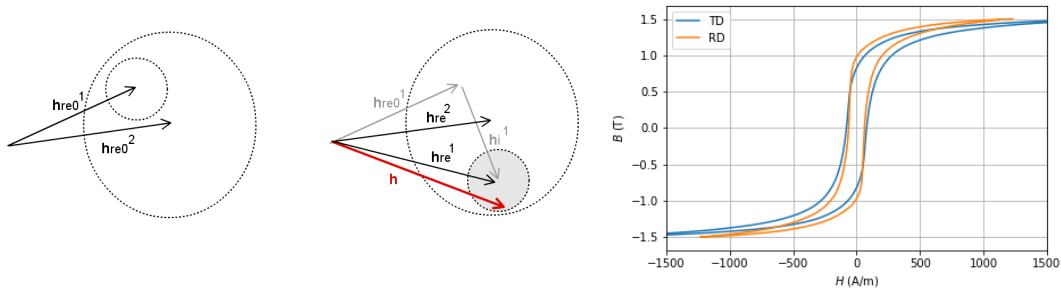


Figure 1: Left: sketch of the variation of the reversible magnetic field of a cell. Right: hysteresis loop when the material is excited in the transversal and rolling direction.

- [1] F. Henrotte, A. Nicolet, and K. Hameyer, COMPEL **25**, 71 (2006). A. Bergqvist, “Magnetic vector hysteresis model with dry friction-like pinning,” Physica B: Condensed Matter, vol. 233, no. 4, pp. 342–347, 1997.
- [2] A. Bergqvist, “Magnetic vector hysteresis model with dry friction-like pinning,” Physica B: Condensed Matter, vol. 233, no. 4, pp. 342–347, 1997.
- [3] F. Sixdenier and R. Scorretti (2017), “Numerical model of static hysteresis taking into account temperature”, International Journal of Numerical Modelling: Electronic Networks, Devices and Fields, e2221.
- [4] K. Jacques, S. Steentjes, F. Henrotte, C. Geuzaine, and K. Hameyer, “Representation of microstructural features and magnetic anisotropy of electrical steels in an energy-based vector hysteresis model”, AIP Advances, vol. 8, no. 4, p. 047602, 2018.

Modelling hysteresis phenomena in power filters: a circuit approach

Giambattista Grusso^a, Simone Quondam Antonio^b, Ermanno Cardelli^b

^a Politecnico di Milano , Italy

^b Università di Perugia, Italy

The applications of magnetic cores as power filters have always been critical from the point of view of costs, performances and dimensions. In particular, the variety of harmonics and frequencies present in the power sources of these components means that the region of their operation changes considerably due to non-linearity effects, changing the performance of the entire system. In this work we present the activity of characterization and simulation of a magnetic device used as a power filter, using a circuit model of hysteresis[1][2]. The component is a three-column transformer with two windings on the side columns, connected in series through a resistor and are powered at a frequency of 20kHz.

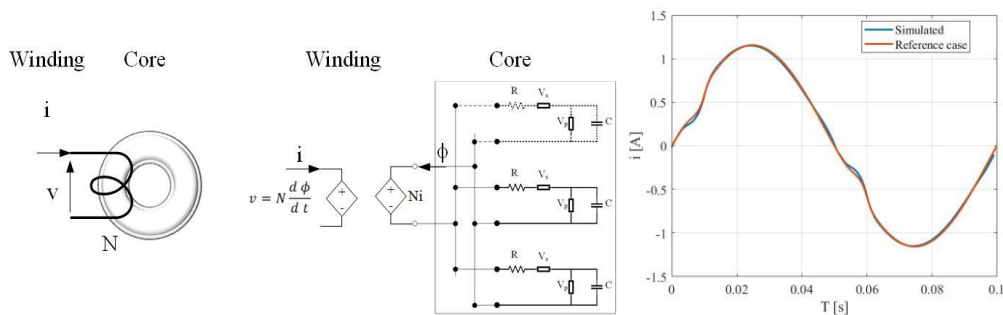


Figure 1: Representation of the equivalent model of the magnetic core and comparison

The study of magnetic devices through equivalent models, has its limits and its merits. If on the one hand they do not always allow an accurate modelling of the magnetic behaviour, especially in terms of leakage fluxes, on the other hand they have the advantage of being a good compromise when it comes to simulating a circuit in which non-linearity is taken into account. The model proposed starts from the discretization of the component in a Magnetic Equivalent Circuit (MEC) in which the magnetic non-linearities are modeled through the parallel connection of multiple hysteresis, as shown in the figure 1.

The identification process consists in the determination of the parameters of all operators of the model to obtain a best fit of the material curves

The method allows to characterize the behaviour of these devices both from the point of view of non-linearity and from the point of view of losses, as it allows the modelling of hysteresis phenomena. The model obtained is a broadband type so it can also be used to characterize the harmonic behavior.

[1] Grusso, G., Brambilla, A. International Journal of Numerical Modelling: Electronic Networks, Devices and Fields, **21** (5), pp. 309-334, 2008 10.1002/jnm.673

[2] Cardelli, E., et al IEEE Transactions on Magnetics, 53 (11), 10.1109/TMAG.2017.2698238.

Multiparameter modelling and analysis of mechanical cutting process of grain oriented silicon steel

Szymon Gontarz^a, Radoslaw Patyk^b, Lukasz Bohdal^b, Dorota Jackiewicz^c

^a Warsaw University of Technology, Faculty of Automotive and Construction Machinery Engineering, Narbutta 84, 02-524 Warsaw, Poland

^b Koszalin University of Technology, Faculty of Mechanical Engineering, Raławicka 15-17 str., 75-620 Koszalin, Poland

^c Institute of Metrology and Biomedical Engineering, Warsaw University of Technology, sw. A. Boboli 8, 02-525 Warsaw, Poland

Understanding the influence of cutting parameters for magnetic materials is a challenging task in the electrotechnical manufacturing industry, due to its multiparameters relations which refers to cut surface quality, strain and stress state after process and magnetic properties. Existing experimental methods require lots of cutting experiments and off-line tests, which may lead to high operation cost and low efficiency. In this paper mathematical, physical and numerical model of shear-slitting process and its application in Ansys/Ls-Dyna system using mesh-free method (SPH) is developed. The numerical model is used to analysis of states of stresses and strains at cut surface of material in the dependance of technological process parameters (Figure 1).

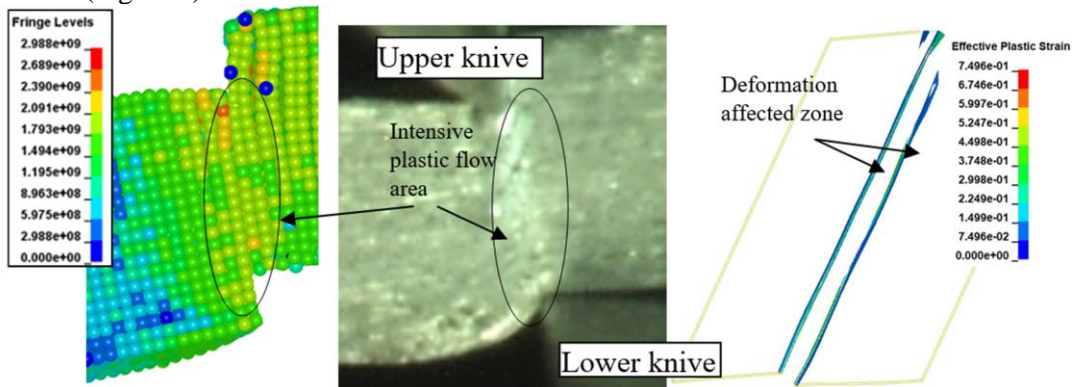


Figure 1: Example of numerical results.

To obtain knowledge of the influence of this parameters on quality of cut surface (for example burr formation) and magnetic properties of material experimental research is done. The magnetic characteristics are determined using a digitally controlled magnetic hysteresisograph HB-PL1.0. It can be observed changes in the hysteresis loops shapes related to the cutting speed settings, especially in the areas of the upper bending of the characteristic and saturation. Magnetomechanical coupling were investigated.

Examined dependent variables, as the most important operational indicators are described by regression equations from technological parameters. These equations are used in multiparameter optimization process with delivered scripts in Matlab program. A set of acceptable solutions is developed on the plane of controllable variables (of technological parameters) on account of accepted criteria (operational indicators) and limitations. Using obtained relationships, functions and results it is possible to control cutting process and obtain high cut surface quality and minimum deterioration of magnetic properties.